THE UNIVERSITY
of EDINBURGH

Effects of the PI3K pathway on neutrophil chemotaxis and swarming

Melina Michael

Doctor of Philosophy

College of Medicine and Veterinary Medicine

The University of Edinburgh

April 2022

Declaration

I declare that unless otherwise stated, the research presented in this thesis is my own work. This work has not been submitted for any other degree or professional qualification. Any published work included has been clearly referenced and cited.

Melina Michael

Acknowledgements

I am grateful for everyone who has helped me through the making of this thesis. Primarily, I would like to thank my supervisor Dr Sonja Vermeren for supporting me throughout the PhD and especially during the writing process. I appreciate her always being on hand for scientific advice, no matter how small the concern. Her passion for lab work and research was truly an inspiration. Thank you to my industry supervisor Dr Augustin Amour who went out of his way to provide help and resources to ensure I had a lovely experience at GlaxoSmithKline. I would also like to thank Dr Carsten Hansen for his advice and suggestions for reports and presentations.

Thank you to Dr Matthieu Vermeren for his help at the CRM imaging facility, but most importantly for building pipelines and writing macros for me and for teaching me everything I know about image analysis. In addition, I would like to show my appreciation to my committee chairs Prof. Ian Dransfield and Prof. Adriano Rossi for their useful comments and insightful discussions. I would also like to express my immense gratitude to BBSRC and GlaxoSmithKline for funding this work.

It has been a wonderful experience to work with the past and present members of the Vermeren group. In particular, I can't thank Julia enough for making my day to day that much more manageable, and I am grateful to Barry for his general advice and help with mouse work. Thank you to all past and present members of the w2.01 office and the regular visitors who made this a very sociable and enjoyable place to have worked, filled with cake and laughter. I

would particularly like to thank Naomi for her motivational messages during the write up, and Memo who made my PhD experience. I would also like to thank friends outside of work for ensuring a memorable few years. I am especially appreciative of the ‘original 4’ who despite living so far away have supported me by constantly checking up on the thesis progression, but most importantly, for showering me with well-timed surprises and gifts, one of the driving factors that kept me going.

Finally, I am indebted to my family, especially Khalto Huda for her endless generosity and amusing long talks, and Khalto Rima who’s support has guided me over the past decade. Myron, midnight driving and disassembling your car in the rain created the perfect distraction during the write up. Also thank you for giving me the honour of picking the tunes. Last but not least, I am extremely obliged to my parents for their continuous unwavering physical, emotional and mental support. I would not have made it this far without you.

Table of contents

Abstract

Neutrophils form part of the innate immune system, they are the most abundant circulating leukocytes in humans and play a crucial role in host defence and inflammation. Upon stimulation, neutrophils leave the blood stream and chemotax to sites of inflammation after which they employ a range of effectors functions to eliminate the threat. It is key that these functions are tightly controlled to ensure pathogen clearance and prevent a suboptimal neutrophil response, as is observed in immunosenescence, defined by the deterioration of the immune system with old age. However, it is also essential to avoid the inappropriate activation of the immune response which could lead to autoimmune diseases.

Through a range of receptors, the activation of phosphoinositide 3-kinase (PI3K) signalling regulates many aspects of neutrophil biology. Phosphatidylinositol 3,4,5-trisphosphate (PIP3), the lipid second messenger product of PI3K is subjected to dephosphorylation by several 5'phosphatases, converting it into PI(3,4)P2, a lipid second messenger in its own right. The SHIP family 5'phosphatases include the well characterised leukocyte restricted SHIP1, and the ubiquitously expressed SHIP2. SHIP1-deficient neutrophils spread extensively on the substratum, and in response to chemoattractant stimulation fail to chemotax efficiently towards a chemoattractant. Here, SHIP2 is characterised using mice with catalytically inactive SHIP2, revealing an *in vivo* recruitment defect to sites of sterile inflammation. Isolated neutrophils from catalytically inactive SHIP2 mice were also identified to have chemotaxis,

directionality, and polarisation defects *in vitro.* Several other effector functions were also tested including phagocytosis and swarming but portrayed a lack of any major defects. The effects of catalytically inactive SHIP2 are mechanistically explained by a subtle increase in PIP3 and an larger decrease in PI(3,4)P2.

The effects of immunosenescence have been well documented in the adaptive immune system, however, its effects on in the innate immune system have yet to be robustly explored. Therefore, I studied the effects of neutrophil ageing on its effector functions and identified a defect in neutrophil swarming in the absence of defects in elastase release and the formation of reactive oxygen species This is congruent with results from other groups identifying a chemotaxis defect in neutrophils from older donors.

In summary, my work identifies a non-redundant role for SHIP2 in neutrophil chemotaxis and trafficking, further enhancing our understanding of the PI3K signalling pathways in neutrophils. I also studied the phenotype of immunosenescent neutrophils, identifying a defect in neutrophil swarming.

Lay Abstract

Neutrophils are amongst the first immune cells to respond to infections. Neutrophils can attack germs in several ways, for example, they can ingest these germs by engulfing them, and they can also release cytotoxic products that can be lethal to these germs. However, before any of this is possible, neutrophils first need to travel to the sites of infection by leaving the circulation and migrating directionally towards the infected site. To do this, neutrophils follow gradients of reagents called chemoattractants that are released by the germs themselves or by their immediate environment in a process known as chemotaxis. Chemoattractants activate receptors found on the surface of neutrophils, which in turn relay the message within the neutrophil through a series of chemical changes.

An example of such a change is the activation of a cellular regulator called phosphoinositide 3-kinase (or short PI3K) which is important for chemotaxis. Activated PI3K produces PIP3 by the phosphorylation of the plasma membrane component PIP2. PIP3 is a lipid messenger and is one of the earliest cellular components to cause neutrophils to polarise, which means to direct themselves towards the chemical gradient, and to begin to chemotax up this gradient. Neutrophils contain many regulators besides PI3K that act in a signaling web; for example there are PIP3 phosphatases which will return PIP3 to PIP2, ensuring that this cellular messenger does not persist too long. SHIP1 and SHIP2 are two closely related examples of PIP3 phosphatases. Previous studies showed that in the absence of SHIP1 neutrophils stick so tightly to

surfaces that they cannot move forward. In contrast, little was known about SHIP2 function in the neutrophil. In the first part of the thesis, I found that SHIP2 is also required for neutrophil migration towards a chemoattractant. However, unlike SHIP1, SHIP2 does not regulate how much the cells stick, instead it regulates the ability of the neutrophil to sense the gradient of chemoattractant, allowing the cell to move towards the source of chemoattractant in a straight line. Interestingly, chemotaxis is the only neutrophil function that is affected by loss of SHIP2 activity.

As neutrophils move towards sites of inflammation, they follow gradients of chemoattractants which they amplify, allowing them to migrate in a coordinated fashion as swarms, named after insect swarms which they resemble. In the second part of the thesis I investigated the effects of ageing on neutrophil functions and found that neutrophils from older adults do not swarm as efficiently compared to those from younger adults.

In summary, I showed that the previously overlooked SHIP2 as well as SHIP1 both regulate separate features of neutrophil migration, and are both required for neutrophils to provide protection from infections. In addition, I also showed that neutrophils from older individuals fail to swarm efficiently towards sites of inflammation which could contribute to the deterioration of the immune response with age.

List of publications

Michael, M., McCormick, B., Anderson, K. E., Karmakar, U., Vermeren, M., Schurmans, S., Amour, A., & Vermeren, S. (2021). The 5-Phosphatase SHIP2 Promotes Neutrophil Chemotaxis and Recruitment. *Frontiers in immunology*, *12*, 671756.

Chu, J. Y., McCormick, B., Mazelyte, G., **Michael, M.**, & Vermeren, S. (2019). HoxB8 neutrophils replicate Fcγ receptor and integrin-induced neutrophil signaling and functions. *Journal of leukocyte biology*, *105*(1), 93–100.

Michael, M., & Vermeren, S. (2019). A neutrophil-centric view of chemotaxis. *Essays in biochemistry*, *63*(5), 607–618.

List of Figures

List of Tables

List of abbreviations

5-LO	5-lipoxygenase
AA	Arachidonic acid
ANOVA	Analysis of variance
APS	Ammonium persulphate
ARAP3	ArfGAP With RhoGAP Domain, Ankyrin Repeat And PH Domain 3
BAL	Bronchoalveolar lavages
BM	Bone marrow
BSA	Bovine serum albumin
$CaCl_2$	Calcium Chloride
CCL	C-C motif ligand, chemokine
CD62E	E-selectin
CD62P	P-selectin
CG	Cathepsin G
CHO	Chinese hamster ovary cells
CO_2	Carbon dioxide
COPD	Chronic obstructive pulmonary disease
CXCL	CXC motif chemokine ligand
CXCR	CXC motif chemokine receptor
DAMPs	Damage-associated molecular pattern
DFP	Diisopropylfluorophosphate
DMEM	Dulbecco's Modified Eagle's Medium
DMSO	Dimethyl sulfoxide
DNA	Deoxyribonucleic acid
DTT	Dithiothreitol
E. coli	Escherichia coli
ECL	Enhanced chemiluminescence
EDTA	Ethylenediaminetetraacetic acid
EGTA	Ethylene glycol-bis(β-aminoethyl ether)
ER	Estrogen receptor
Erk	Extracellular regulated kinase
ESL-1	E-selectin ligand-1
FACS	Fluorescence-activated cell sorting
FcγR	Fc gamma receptor
FBS	Fetal bovine serum
FITC	Fluorescein isothiocyanate
FLAP	5-LO activating protein
fMLF	N-formylmethionine-leucyl-phenylalanine
GAGs	Glycosaminoglycans
GAPs	GTPase-activating proteins
GEFs	Guanine nucleotide exchange factors
GM-CSF	Granulocyte-macrophage colony stimulating factor
GPCRs	G protein-coupled receptors
GAPs	GTPase-activating proteins
GDP	Guanine diphosphate

GEFs	Guanine nucleotide exchange factors
GTP	Guanine triphosphate
HBSS	Hank's Balanced Salt Solution
HCL	Hydrochloric acid
HEPES	4-(2-hydroxyethyl)-1-piperazineethanesulfonic acid
HI-FBS	Heat-inactivated fetal bovine serum
HLB	Hypotonic lysis buffer
HoxB8	Homeobox B8
HRP	Horseradish peroxidase
HyperLB	Hypertonic lysis buffer
ICAM	Intercellular adhesion molecules
Ig	Immunoglobulin
ILB	Isotonic lysis buffer
IMDM	Iscove's Modified Dulbecco's Medium
IP	Immunoprecipitation
JAMs	Junctional adhesion molecules
KCl	Potassium chloride
KH_2PO_4	Monopotassium phosphate
LPS	Lipopolysaccharide
LTA4H	LTA4 hydrolase
LTB4	Leukotriene B4
$MgCl_2$	Magnesium Chloride
$MgSO_4$	Magnesium sulfate
MPO	Myeloperoxidase
mTOR	Mammalian target of rapamycin
mTORC2	mTOR Complex 2
Na_2PO_4	Disodium phosphate
Na_3VO_4	Sodium orthovanadate
NaCl	Sodium Chloride
NADPH	Nicotinamide adenine dinucleotide phosphate
NaF	Sodium fluoride
$NaHCO_3$	Sodium bicarbonate
NaOH	Sodium Hydroxide
NE	Neutrophil elastase
NETs	Neutrophil extracellular traps
NH_4Cl	Ammonium chloride
NMR	Nuclear magnetic resonance
PAF	Platelet activating factor
PAMPs	Pathogen-associated molecular pattern
PBS	Phosphate buffer saline
PBST	PBS supplemented with 0.1% Tween-20
PCR	Polymerase chain reaction
PDK1	Phosphoinositide-dependent kinase 1
PECAM1	Platelet/endothelial cell adhesion molecule 1
PFA	Paraformaldehyde
PH	Pleckstrin homology
PI(3,4)P2	Phosphatidylinositol 3,4-bisphosphate
PI(4,5)P2	Phosphatidylinositol 4,5-bisphosphate

PI3K	Phosphoinositide 3-kinase
PIP3	Phosphatidylinositol 3,4,5-trisphosphate
PKB	Protein kinase B
PLA_2	Phospholipase A_2
Plat-E	Platinum-E
PLC	Phospholipase C
PMN	Polymorphonuclear leukocytes
PMSF	Phenylmethylsulfonyl fluoride
PRP	Top platelet rich plasma
PRR	Pattern recognition receptor
PSGL-1	P-selectin glycoprotein ligand-1
PTB	Phosphotyrosine-binding
PTEN	Phosphatase and tensin homolog
PVDF	Polyvinylidene difluoride
RasGRP4	Ras guanyl releasing protein 4
RIPA	Radioimmunoprecipitation assay
ROS	Reactive oxygen species
RPMI	Roswell Park Memorial Institute
RT	Room temperature
RTKs	Receptor tyrosine kinases
SAM	Sterile alpha motif
SDS	Sodium Dodecyl Sulphate
SDS-PAGE	Sodium Dodecyl Sulphate PolyAcrylamide Gel
SEM	Standard errors of the mean
SFK	Src family kinases
SHIP1	SH2 Domain-Containing Inositol 5'-Phosphatase 1
SHIP2	SH2 Domain-Containing Inositol 5'-Phosphatase 2
Syk	Spleen tyrosine kinase
TAE	Tris-acetate-EDTA
TBS	Tris-buffered saline
TEMED	T etramethylethylenediamine
TNF	Tumour necrosis factor
Tris-HCl	Tris(hydroxymethyl)aminomethane hydrochloride
Tx-100	Triton X-100
WT	Wild-type

1. Introduction

1.1 Basics of Neutrophil Biology and Functions

Neutrophils are the most abundant leukocytes in human blood, forming up to 70% of all leukocytes (though only ~20% in mouse) [1]. ~10^{11} neutrophils, also known as polymorphonuclear leukocytes (PMN), are produced per day in the bone marrow [2]. They are terminally differentiated, and upon entry into the circulation, neutrophils survive for only 10-18 hours [3, 4], although some studies show they can survive longer [3, 5]. Once in the circulation, neutrophils detect signs of microbial threat and upon detection are recruited to the sites of infection and inflammation where they deploy a range of effector functions, namely: phagocytosis, degranulation, the formation of a range of reactive oxygen species, cytokine production and the release of neutrophil extracellular traps (NETs). The homeostatic removal of neutrophils is mediated by macrophages following neutrophil homing to haematopoietic sites including the bone marrow, liver or spleen [6].

The functions of neutrophils in providing a first line immune response against infection by invading pathogens are well established and makes them key players in the innate immune system [7]. Recently, the importance of neutrophils in the development of the inflammatory response beyond these antimicrobial properties has been recognised. Neutrophils are transcriptionally active and can release cytokines [8-11] to signal to other neutrophils and neighbouring cells, either propagating or dampening the immune response for the resolution of inflammation [12]. To contribute to the efficient resolution of

inflammation, neutrophils undergo programmed cell death, also known as apoptosis, which causes them to experience characteristic changes such as the alteration of surface markers to aid other phagocytes, especially macrophages to clear them up by non-phlogistic efferocytosis [13].

The strict regulation of neutrophil turnover is important to avoid diseases. For example, a decrease in the number of neutrophils called neutropenia impairs the innate immune defense making patients particularly susceptible to bacterial and fungal infections [14, 15]. In addition, neutrophil effector functions must be tightly controlled to avoid excessive inflammation and host tissue damage as seen in chronic inflammation, autoimmune diseases and cancer progression. In contrast, a drop in neutrophil antimicrobial properties that is detected in immunosenescence may be the cause of decreased bacterial clearance observed in the elderly. Therefore, it is pivotal that the number and functions of neutrophils are tightly regulated to allow for optimal physiological conditions.

1.1.1 Recruitment to sites of inflammation

Circulating neutrophils are recruited to peripheral tissues in response to microbial invasion or sterile tissue injury in a process known as the classical leukocyte recruitment cascade. Tissue resident sentinel cells such as dendritic cells or macrophages are activated by pathogen-associated molecular pattern (PAMPs) and damage-associated molecular pattern (DAMPs) molecules causing them to release pro-inflammatory mediators and initiate the recruitment of neutrophils to these sites [16]. Adhesion molecules on the

endothelium are upregulated, including E-selectin (CD62E) and P-selectin (CD62P), and transiently bind to the constitutively expressed L-selectin, E-selectin ligand-1 (ESL-1) and P-selectin glycoprotein ligand-1 (PSGL-1) among other glycosylated ligands. This results in the tethering of neutrophils on the endothelium through reversable bonds which resist the shear stress created by blood flow [17]. Rolling on the endothelium, an early step of the leukocyte recruitment cascade, is initiated by forming new bonds at the front and breaking bonds at the rear.

While rolling over the endothelium, the neutrophil is activated after encountering a gradient of immobilised chemoattractants/chemokines leading to the site of infection or inflammation. These molecular guidance signals bind to the G protein coupled receptors which in turn through inside out signaling induce confirmational changes in cell surface integrins such as LFA1 and Mac1, increasing their affinity to their binding partners such as ICAM1 and ICAM2. This mediates slow rolling followed by neutrophil arrest. After arrest, neutrophils flatten to minimise surface exposure to blood flow and crawl towards favourable sites for transmigration, following gradients of chemoattractants/chemokines. Intraluminal crawling can happen upstream, against the flow of blood where neutrophils begin diapedesis through the interaction of ICAM1 with Mac1 among others [18]. Transmigration often occurs at cell junctions and is mediated by several adhesion molecules including platelet/endothelial cell adhesion molecule 1 (PECAM1) as well as junctional adhesion molecules (JAMs). Next, to reach the extravascular space, neutrophils traverse the basement membrane by making use of proteolytic

enzymes including gelatinase [19]. Once in the extravascular space, neutrophils directionally migrate along a gradient of chemoattractant such as IL-8 in a process known as chemotaxis to reach sites of inflammation and infection. Neutrophil chemotaxis and trafficking is discussed in further detail below in section 1.3.

Molecules on endothelium	**Molecules on neutrophil**
Tethering and rolling	
P-selectin	PSGL1, PTX3
E-selectin	PSGL1, ESL1, CD44
PSGL1, GlyCAM	L-selectin
Slow rolling	
ICAM1	LFA-1
E-selectin	PSGL1, ESL1, CD44
Arrest and adhesion	
ICAM1	LFA-1
VCAM1	VLA4
Crawling	
ICAM1	MAC1
Diapedesis and transmigration	
ICAM1, ICAM2	LFA-1, MAC1
VCAM1	VLA4
CD99	CD99
PECAM1	PECAM1
JAMA	LFA1
JAMB	VLA4
JAMC	MAC1

Table 1.1.1 Neutrophil-endothelial cell interactions during the neutrophil recruitment cascade. This is not an exhaustive list, adapted from [20].

1.1.2 Antimicrobial Functions of Neutrophils

Small invading pathogens are phagocytosed and the antimicrobial agents contained within neutrophil granules are released into the phagosome [21]. Otherwise, cytokines, chromatin to form neutrophil extracellular traps (NETs) and cytotoxic products including reactive oxygen species (ROS) can be released extracellularly. Neutrophils lie at the interface with the adaptive immune system as they aid in the initiation and propagation of inflammation by the activation and recruitment of other immune cells. All these functions rely on the ability of neutrophils to accurately migrate towards sites of inflammation by chemotaxis [22].

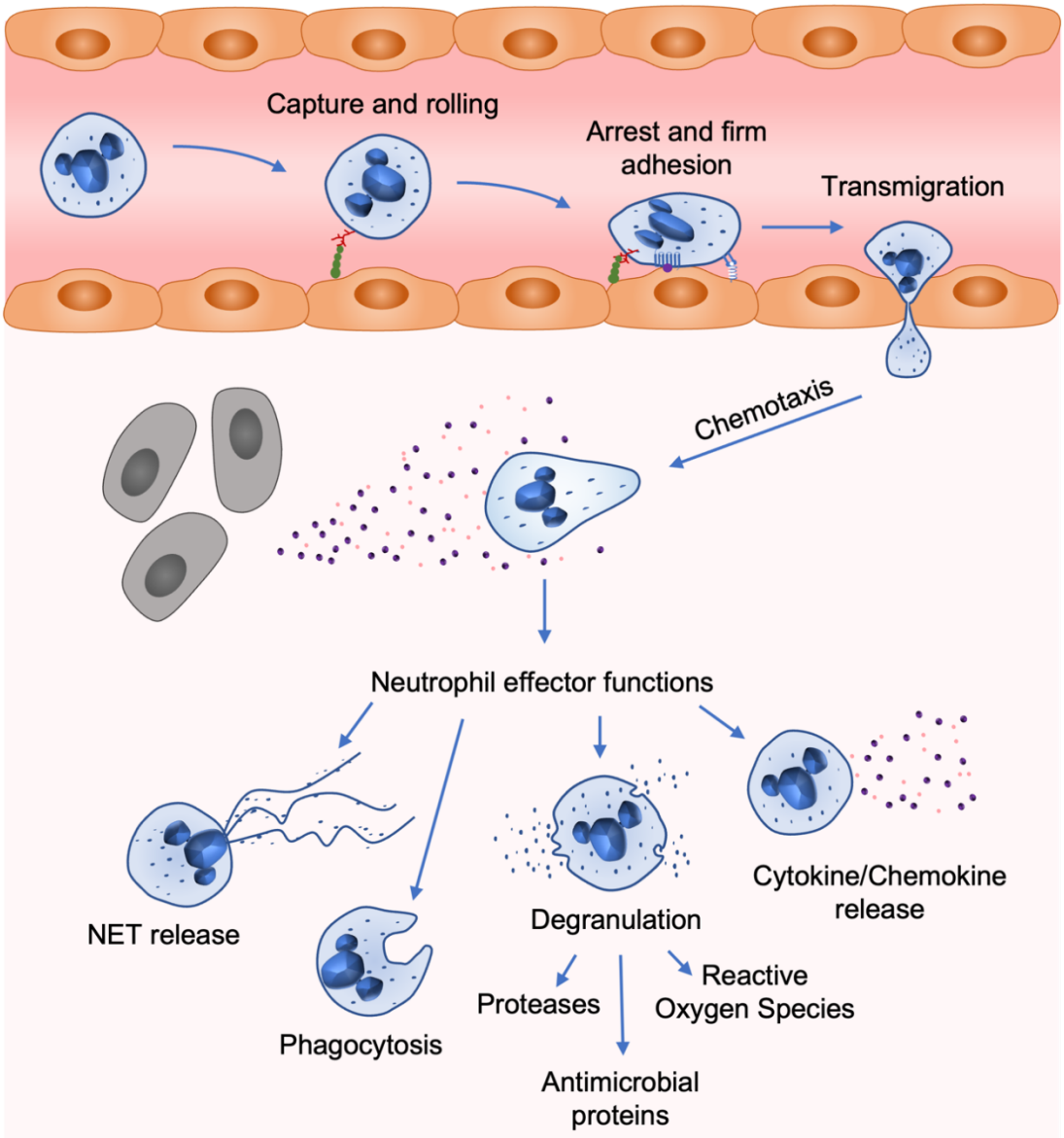

Figure 1.1.2 An overview of neutrophil recruitment and downstream effector functions dependent on accurate chemotaxis. When sentinel cells come in contact with pathogens, they release inflammatory mediators which lead to the upregulation of adhesion molecules on the endothelium surface (P and E selectin). Ligands of these receptors are found on the free moving neutrophil in the bloodstream, causing them to tether and roll along the endothelium. Chemoattractants being released from the site of infection guide the neutrophils by ligating their cognate receptors. Neutrophils express a range of G protein coupled chemoattractant/chemokine receptors with the help of which they detect, and quickly react to gradients of chemoattractants, e.g. bacterial peptides. This underpins their ability to leave the blood stream and move directionally (chemotax) towards sources of chemoattractant. Once neutrophils reach the sites of inflammation, they deploy a range of effector functions including phagocytosis, degranulation, production of reactive oxygen species (ROS), and the release of neutrophil extracellular traps (NETs) to eliminate pathogens [23]. Made with PowerPoint.

1.1.2.1 Phagocytosis

Phagocytosis is a process by which phagocytes ingest and kill invading bacterial and fungal pathogens. On the surface of the neutrophil, there are receptors that can recognize pathogens such as pattern recognition receptors (PRRs), as well as opsonic receptors which recognize the host proteins deposited onto the pathogens [24]. Opsonic receptors include complement receptors and FcγRs which engulf pathogens into a vacuole. Neutrophils are very efficient phagocytes and form pseudopod extensions to engulf IgG opsonized particles which occurs in less than 20 seconds [25]. This is followed by the fusion of the vacuole with preformed granules containing NADPH oxidase subunits and hydrolytic enzymes to form the phagosome [26]. There are several differences in phagocytosis between neutrophils and other professional phagocytes e.g. macrophages in particle uptake, speed and granule release during phagocyte maturation [27].

1.1.2.2 Degranulation

Neutrophil granules store proteinases and antimicrobial peptides making them essential organelles during the process of inflammation. These granules can either fuse with the phagosome during uptake, or fuse with the plasma membrane for extracellular release. At least four types of granules exist: the primary granules, also known as the Azurophilic granules are the largest and the first to be formed during maturation. They are the only to contain myeloperoxidase (MPO), an enzyme essential for oxidative burst as well as a range of other cargo and antimicrobial compounds including lysozymes, defensins and several serine proteases such as neutrophil elastase (NE), and

cathepsin G (CG) [28]. The specific granules, also known as the secondary granules are recognized for containing glycoprotein lactoferrin in addition to other antimicrobial compounds that are employed in extracellular killing. The gelatinase, or tertiary granules are the smallest, containing relatively few antimicrobials and also store metalloproteases, namely collagenase (MMP-8), gelatinase (MMP-9) and leukolysin (MMP-25) [29]. Finally, the secretory vesicles contain human serum albumin as they are endocytic vesicles with a reservoir of membrane receptors which mobilise at the early phases of the inflammatory response [30].

1.1.2.3 Reactive Oxygen Species

Reactive Oxygen species (ROS) are formed by a process called respiratory burst which relies on the activation of the NADPH oxidase [24]. It is an electron transfer system, the assembly of which requires the translocation of the cytosolic components $p40^{phox}$, $p47^{phox}$, and $p67^{phox}$ to the plasma and phagosomal membranes. This is where the GTPase Rac2 and the catalytic core, consisting of $gp91^{phox}$ and $gp22^{phox}$ reside. Intracellular ROS production occurs at the phagolysosomal membrane into the phagosome whereas extracellular ROS occurs at the plasma membrane to the outside.

The assembled NADPH complex then reduces molecular oxygen to superoxide initiating several downstream effectors. Superoxide can form the strong oxidant peroxynitrite when it reacts with nitric oxide at inflammatory sites, it can also dismutate to form hydrogen peroxide. After degranulation into the phagosome, the previously mentioned MPO reacts with the hydrogen

peroxide to produce the more reactive hypochlorous acid which is characterised by strong antimicrobial action in vitro [31].

1.1.2.4 Neutrophil Extracellular Traps

Upon activation, neutrophils can release chromatin fibres called neutrophil extracellular traps (NETs) [32, 33]. These fibrous structures have important functions in host defense by trapping pathogens within a sticky meshwork of decondensed chromatin with assembled cytosolic and granule proteins. This acts as a physical barrier to stop pathogens from spreading in addition to exposing them to the trapped antimicrobial peptides within [34]. Histones have great antimicrobial activity, which work together with the high local concentrations of MPO, neutrophil elastase, lactoferrin-chelating proteins among other antimicrobial peptides from secondary and tertiary granules to degrade virulence factors and disarm the pathogens. This allows NETs to kill the pathogens before it is engulfed by neutrophils or other phagocytes. NETs help to keep the noxious proteins that are potentially harmful to the host from diffusing away from the sites of inflammation and cause further damage [35]. However, tissue damage from NETs has been well documented, showing they can directly kill endothelial and epithelial cells [36, 37] as well as potentially enhance infections during chronic inflammation as identified from patients with cystic fibrosis [38].

1.1.3 Experimental models

The short lifespan of terminally differentiated mature neutrophils makes them refractory to being cultured and genetically modified by transfection or transduction. One way to address biological signalling is by using inhibitors that target specific proteins, however, off target effects can pose major limitations. Therefore, research aimed towards understanding molecular signalling cascades in neutrophils has often relied on genetically engineered mice. Mice are commonly used as experimental models to study signalling pathways that underline cellular responses since genetic studies have shown significant conservation with humans [39-41].

Research aimed towards understanding molecular signalling cascades in neutrophils has also relied on cell lines. Several human myeloid cell lines have been used to study neutrophil functions by being induced to terminally differentiate into neutrophil-like cells in vitro. Commonly used cell lines are HL-60 cells [42] which were acquired from a patient with acute myeloid leukemia and its subline PLB-985 [43], both serving as primary model systems. In addition to such cell lines, the social amoeba *Dictyostelium discoideum* is being used to interrogate the regulation of neutrophil chemotaxis and the molecular mechanisms involved.

1.1.3.1 Conditionally HoxB8-immobilised haematopoietic progenitor cells

More recently, conditionally HoxB8 immortalized neutrophil polarised mouse progenitor cells have become a useful tool in neutrophil research. 'HoxB8 neutrophils' are generated by retrovirally transducing bone marrow cells with a HoxB8-estrogen receptor (ER) fusion construct. Supplementation of the culture medium with tamoxifen or estradiol activates the transcription of the HoxB8 gene which arrests progenitor cell differentiation, rendering the progenitors immortal. The additional supplementation with GM-CSF or SCF commits these cells to the monocyte and granulocyte lineages. Studies have shown that six days after estrogen withdrawal, 81% of cells supplemented with SCF and GM-CSF differentiated into primary-like 'HoxB8 neutrophils' exhibiting their characteristic multi-lobular nuclear morphology [44]. An advantage of HoxB8 neutrophils over the other neutrophil-like cells is that they come from a non-cancerous background, meaning they undergo more physiological neutrophil differentiation [45]. Conditionally HoxB8 immortalised progenitor cells are amenable to genetic modification by retroviral and lentiviral transduction while preserving their neutrophil morphological features. Of course, it is also possible to generate HoxB8 cells from previously modified mice and stack on further genetic modifications.

Upon stimulation, HoxB8 neutrophils were shown to replicate the effector functions of freshly isolated neutrophils including ROS production, degranulation from secondary and tertiary granules, cytokine/chemokine release, phagocytosis as well as apoptosis [45]. Newer studies have also used

HoxB8 cells to study swarming and in vivo neutrophil recruitment [46-48]. In addition, chemotaxis assays using the Dunn chamber have shown that HoxB8 neutrophils are a suitable model to investigate the molecular signalling cascades involved in chemotaxis. HoxB8 neutrophils do respond to fMLP and can chemotax directionally towards this stimulus (Figure 1.1.3.1 A) just like primary neutrophils [49]. The individual tracks from these neutrophils were used to calculate the total accumulated and Euclidian distances travelled with results resembling those of freshly isolated bone marrow neutrophils (BMNs) (Figure 1.1.3.1 B). Also similar to BMNs, the time lapse images revealed a polarized morphology to these chemotaxing HoxB8 neutrophils with a leading edge and trailing end (Figure 1.1.3.1 C). This suggests that the HoxB8 cell line is a suitable model to study chemotaxis.

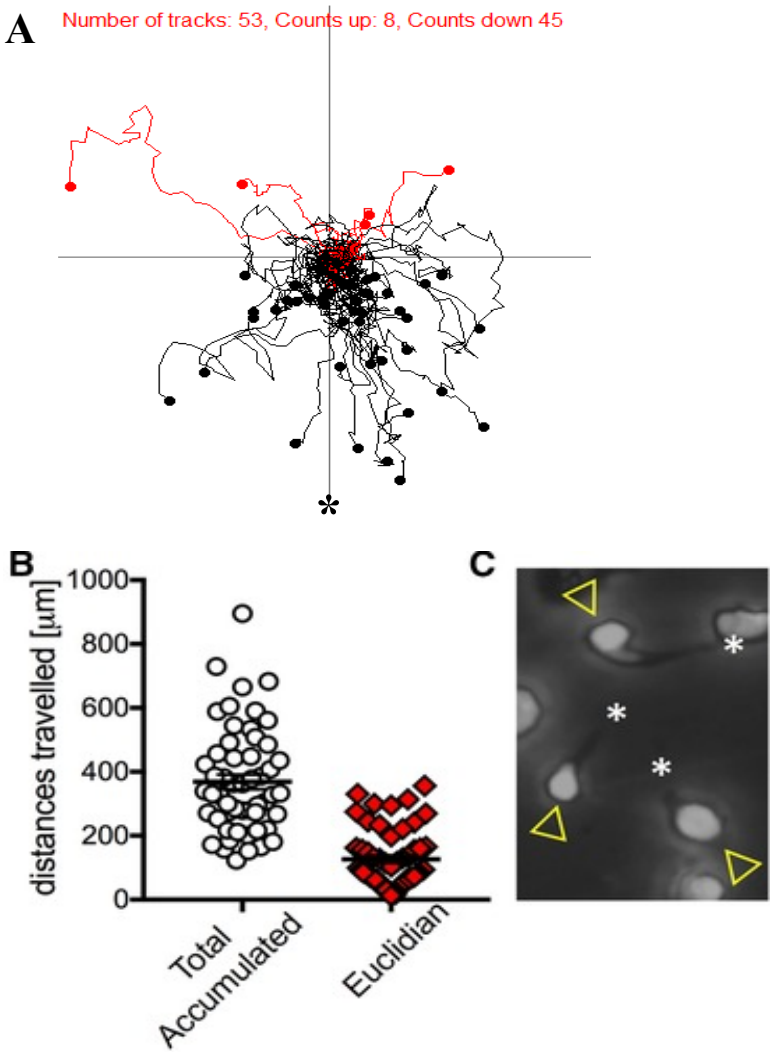

Figure 1.1.3.1 HoxB8 neutrophils can chemotax towards fMLF. (A-B) Chemotaxis assays using Dunn chambers were performed on three different days. **(A)** Spider plot showing the tracks of individual HoxB8 neutrophils chemotaxing towards fMLF, where the symbol * indicates the source of chemoattractant. **(B)** Graph of total and Euclidian distances travelled by the cells. (**C**) Image of chemotaxing HoxB8 neutrophils cropped from a time-lapse movie identifying 3 cells showing the characteristic morphology of migrating neutrophils comprising a leading edge (arrowhead) and a trailing end (asterisk). Figure from [49].

1.2 PI3K signalling

To study any of the neutrophil effector functions and the mechanisms involved in detail, it is essential to understand the underlying signalling. One of the most well-defined pathways is that of phosphoinositide 3-kinase (PI3K) signalling which is implicated in numerous neutrophil functions including spreading, chemotaxis and pathogen elimination [50]. There are eight PI3Ks found in mammals which are divided up into 3 classes: Class I (also known as 'agonist-activated') PI3Ks which are heterodimeric and subdivided into Class IA (regulatory subunit: p85 family and catalytic subunit: p110α, β or δ) and Class IB (regulatory subunit: p101 or p84 and catalytic subunit: p110γ), Class II isoforms (PI3K2Cα,β,γ), and a Class III isoform. All three classes are expressed in neutrophils and catalyse the phosphorylation of inositol phospholipids. The functions of Class II isoforms are essential for regulating endosomal trafficking in insulin signalling while Class III isoforms are crucial for regulating autophagy as well as endosome and lysosome trafficking [51]. My work however focuses mostly on Class I PI3Ks which are discussed in more depth in the next section.

		Catalytic subunit	Regulatory subunit	Lipid Substrate	Lipid Product	Expression
Class I	**A**	p110α p110β	p85	PI(4,5)P2	PI(3,4,5)P3	Ubiquitous
		p110δ				Leukocytes
	B	p110γ	p101 p87			
Class II		PI3K-C2α PI3K-C2β		PI or PI4P	PI3P or PI(3,4)P2	Ubiquitous
		PI3K-C2γ				Liver
Class III		Vps34	Vps15	PI	PI3P	Ubiquitous

Table 1.2 PI3K isoforms. The subunits, expression, lipid substrates and products are listed for each of the PI3K classes, modified from [52].

1.2.1 Class I PI3K

Class I PI3K isoforms are the most abundant in neutrophils and they can be directly or indirectly regulated by receptors including, integrin, antibody (Fc), and G protein coupled receptors as well as by GTPases such as Ras [53]. Upon activation, class I PI3Ks phosphorylate the integral plasma membrane component phosphatidylinositol 4,5-bisphosphate (PI4,5P2) to generate phosphatidylinositol 3,4,5-trisphosphate (PIP3), a membrane localised short-lived second messenger. Effector proteins bind to and are activated by PIP3 often by being recruited to the plasma membrane through conserved domains such as the well characterised PH domain. One important downstream effector of PIP3 is PKB (also known as AKT). Once recruited to the membrane by its

PH domain it can then be fully activated by 3-phosphoinositide-dependent kinase (PDK1) mediated phosphorylation of threonine 308 or by rapamycin-insensitive mTOR complex (mTORC2) mediated phosphorylation of serine 473 [54, 55]. In addition, PIP3 generation by Class I PI3Ks is antagonised by phosphatases that dephosphorylate PIP3. The 3'phosphatase phosphatase and tensin homolog (PTEN) removes the phosphate from the 3-position which converts PIP3 back to PI(4,5)P2, while 5'phosphatases including the SH2 domain containing inositol-5-phosphatases (SHIPs) dephosphorylate the 5-position which converts PIP3 to form PI(3,4)P2, a lipid second messenger in its own right.

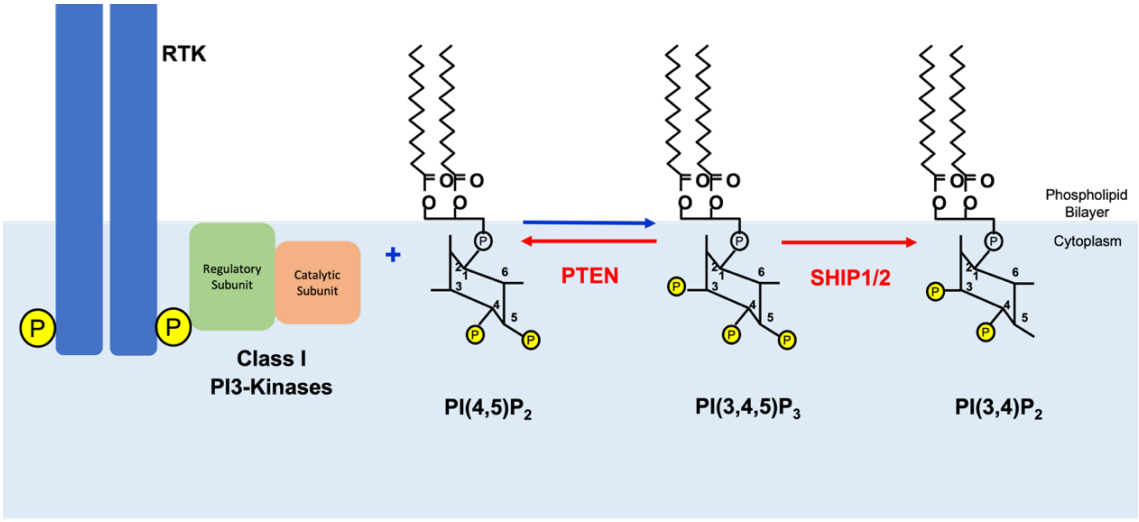

Figure 1.2.1 Inositol phospholipids in the Class I PI3K signalling pathway. In response to RTK activation, PI3K is recruited to the plasma membrane where it is allosterically activated. It can then phosphorylate PI(4,5)P2 at the D3 position of the inositol ring to produce the lipid second messenger PI(3,4,5)P3. PI3K activity is antagonised by phosphatases such as the 3'phosphatase PTEN which converts PI(3,4,5)P3 back into PI(4,5)P2 and the 5'phosphatases SHIP1/2 which convert PI(3,4,5)P3 into the lipid second messenger PI(3,4)P2. For simplicity's sake PI3Kγ is not included in this diagram. Made with PowerPoint.

1.2.2 PIP3 Phosphatases

PI3K activity is counteracted by phosphatases which hydrolyse the short-lived PIP3. Two major PI3K phosphatases in neutrophils are PTEN and the hematopoietic cell-restricted SHIP1 [56]. Global PTEN-deficiency is embryonic lethal [57], whereas SHIP1-deficient mice are viable and fertile. However, they exhibit a shortened lifespan that is thought to be due to leukocyte infiltration of the lungs [58, 59]. Both PTEN and SHIP1-deficient neutrophils have been described; PTEN knockout neutrophils are characterised by increased PIP3 [60], enhanced ROS production upon stimulated with fMLF, increased ruffling and sensitivity to chemoattractants, a minor directionality defect [61], and a lengthened lifespan [62]. SHIP1 knock-out neutrophils have elevated PIP3 levels [63], display reduced ROS production [63] and augmented apoptosis [64]. SHIP1-deficient neutrophils also spread extensively on the substratum [65].

In addition to the relatively well-studied SHIP1, several other 5' phosphatases have been identified which mostly remain poorly characterised, some of which preferentially dephosphorylate PIP3. They have different functional domains that flank the catalytic domain which consists of a conserved 300 amino acid sequence [66]. A list of human 5' phosphatases of phosphatidylinositols or inositol phosphates are shown in table 1.2.2.

5'phosphatase	**Gene name**	**No. of residues**
Type II inositol 1,4,5-trisphosphate 5-phosphatase (INPP5B)	*INPP5B*	993
Inositol polyphosphate 5-phosphatase (OCRL-1)	*OCRL/INPP5F*	*901*
72 kDa inositol polyphosphate 5-phosphatase (INPP5E)	*INPP5E*	*644*
Phosphatidylinositol 3,4,5-trisphosphate 5-phosphatase 2 (SHIP2)	*INPPL1*	1258
Inositol polyphosphate 5-phosphatase K (SKIP)	*INPP5K*	448
Phosphatidylinositol 4,5-bisphosphate 5-phosphatase A (PIPP)	*INPP5J*	*1006*
Synaptojanin 1	*SYNJ1/INPP5G*	1573
Synaptojanin 2	*SYNJ2/INPP5H*	1496
Type I inositol 1,4,5-trisphosphate 5-phosphatase (INPP5A)	*INPP5A*	412
Phosphatidylinositol 3,4,5-trisphosphate 5-phosphatase 1 (SHIP1)	*INPP5D*	1189

Table 1.2.2. 5' phosphatases. A list of human 5' phosphatases for phosphoinositides and/or inositol phosphates, adapted from [67].

1.2.2.1 Phosphatase SHIP2

SHIP2, encoded by *INPPL1* is ubiquitously expressed and belongs to the polyphosphate 5-phosphatase family. Both phosphatases SHIP2 and its isozyme SHIP1 comprise an SH2 domain at the N-terminal, a catalytic domain which is well conserved between other 5-phosphatases, a phosphotyrosine-binding (PTB) domain and a proline rich C-terminal region [68]. SHIP2 has an additional C-terminal ubiquitin interacting motif for targeted degradation. In addition, SHIP2 also contains a sterile alpha motif (SAM) domain involved in the interaction with SAM domains from other proteins such as ARAP3, for which an NMR model has been generated [69] forming heterodimers which could play a role in SHIP2 membrane translocation. Schematic of SHIP2 binding domains is shown in figure 1.2.2.1.

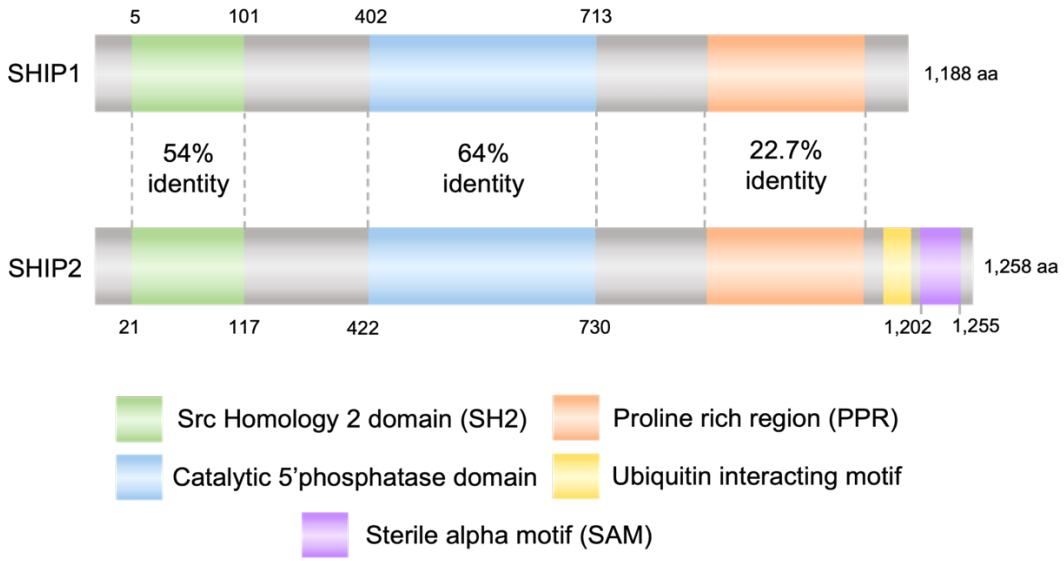

Figure 1.2.2.1 Diagram of SHIP1 and SHIP2 interacting domains. The structures of SHIP1 and SHIP2 are compared [70, 71]. Made with PowerPoint.

One study reported that due to insulin sensitivity and lethal hypoglycaemia, SHIP2-deficient mice died within three days of birth [72]. However, these SHIP2 deficient mice were genetically intact for the first 18 exons which includes the SH2 and phosphatase domains while possibly also disrupting a second gene, *Phox2a*. Another study then used a different strategy to create a total null mutation for the *Inppl1* gene and identified a distinct phenotype [73]. These SHIP2-deficient mice were characterised by normal glucose tolerance and sensitivity to insulin, however, they have a characteristically shorter snout due to an abnormality in skeletal growth. Even on a high-fat diet these mice remained lean with reduced body weight and length particularly in males. Transgenic mice overexpressing SHIP2 had increased body weight by 5% as well as a mild reduction in insulin sensitivity and glucose tolerance [74].

Unlike the hematopoietic and spermatogenetic restricted SHIP1 which was found to play a major role in immune system regulation, SHIP2 is ubiquitously expressed [67]. SHIP2 was found to regulate apoptosis in various cells. For example, the downregulation of *INPPL1* in K562 cells induced apoptosis [75], and SHIP1 deficient multiple myeloma breast cancer cells underwent apoptosis upon treatment with pan-SHIP1/2 inhibitors [76]. In gastric cancer, the opposite was determined where the overexpression of *INPPL1* induced apoptosis [77]. In addition, initial work on SHIP2 uncovered roles in diabetes and insulin signalling [78]. Although there is ongoing research in this area this is no longer considered the main pathway for SHIP2 [79].

1.2.3 Signalling downstream of PI3K

An average cell has roughly 25 PI3K downstream effectors, many of which remain poorly investigated [80]. Downstream effectors include serine/threonine kinases e.g. PDK1, tyrosine kinases e.g. BTK, signalling adaptors e.g. GAB1/2 as well as GTPase-activating proteins (GAPs) and guanine nucleotide exchange factors (GEFs) for small GTPases e.g. ARAP3. Small GTPases are molecular switches that catalyse the hydrolysis of GTP, that often cycle between their active GTP-bound and inactive GDP-bound forms (see Figure 1.2.3). GAPs activate GTPases while GEFs cause the dissociation of GDP allowing the exchange with a new GTP. Small GTPases bind to and activate several effector proteins, for example Ras can activate PI3K by activating p110α, δ and γ isoforms while Rac activates p110β [81]. In addition, many PIP3 binding proteins are GAPs and GEFs of small GTPases. For example, Vav, P-Rex, DOCK and Tiam are PIP3 activated Rac GEFs found in the neutrophil regulating different functions [82]. Although Vav was shown to regulate integrin processes, P-Rex was shown to regulate GPCR processes like ROS production [83, 84]. Interestingly however, genetic deletion of both Vav and P-Rex significantly impaired chemotaxis and in vivo recruitment to sterile inflammation [85].

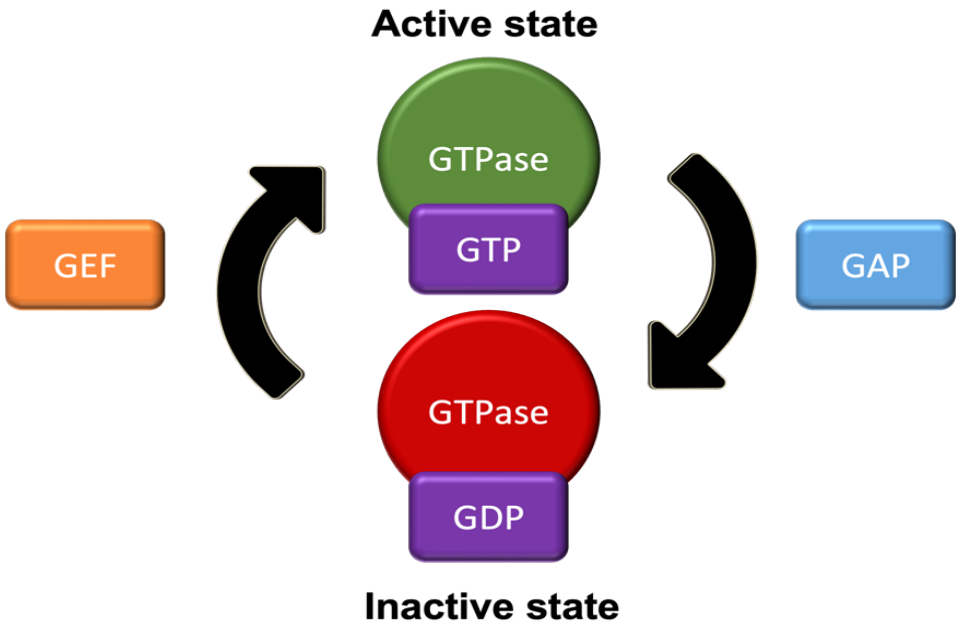

Figure 1.2.3. Cycling between the active and inactive states of small GTPases. Small GTPases are active when bound to GTP and inactive when bound to GDP. GEFs catalyse the exchange from GDP to GTP which turns on signalling, while GAPs hydrolyse GTP to GDP which terminates signalling [86]. Made with PowerPoint.

1.2.3.1 ARAP3

ARAP3 is an abundant signalling protein in neutrophils (though not restricted to neutrophils) that was identified from a screen for PIP3 binding proteins in pig neutrophils and is one of over 25 PI3K effectors [80]. It is one of three proteins in the ARAP family, and although they differ in substrate specificity and expression profile, they all have similar domain structures that include five PH domains [87, 88]. ARAP3 is a PI3K and Rap-regulated dual GAP for Arf6 and RhoA, that is found mostly in the cytosol [89]. Driven by PIP3, ARAP3 is recruited to the plasma membrane, where it is activated catalytically as an Arf GAP and where Rap-GTP can activate it as a Rho GAP. In the neutrophil, ARAP3 regulates adhesion-dependent functions including chemotaxis and

transendothelial migration [90]. ARAP3 is involved in a negative feedback loop regulating integrin inactivation downstream of PI3K [91]. First, outside in signalling initiated by binding integrin ligands causes the activation of PI3K as well as its downstream effectors. Then, ARAP3 induces the inactivation of localised integrin by negative inside out signalling. In turn, this reduces integrin-mediated PI3K activity, hence initiating the turnover of substrate adhesion.

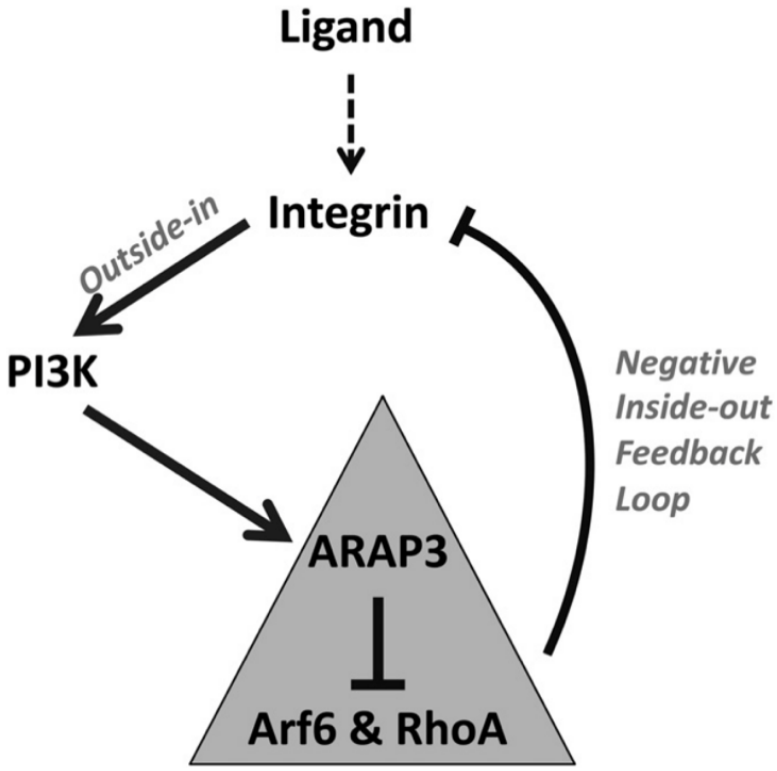

Figure 1.2.3.1. Schematic of integrin inactivation by the ARAP3 feedback loop. Integrin activation by outside in signalling in turn activated PI3K followed by ARAP3 which in a negative feedback loop regulates integrin inactivation. Figure from [91].

Similar to other signalling proteins, ARAP3 is post-transcriptionally modified to regulate its functions. The phosphorylation of serine/threonine as well as tyrosine residues are regulated upon cell stimulation. When co-expressed in cells, ARAP3 was found to be phosphorylated by Src-family kinases (SKFs) when stimulated with growth factors and with integrin binding to the extracellular matrix (ECM) substrates such as fibronectin [92]. FLAG-ARAP3 proteins analysed by Western blot show that adding selective inhibitors of PI3K and SFKs to cells plated on fibronectin suppressed adhesion induced phosphorylation of ARAP3. ARAP3 has 23 tyrosine residues and it has yet to be determined which are phosphorylated in vivo, however, Y1399 and Y1404 were both identified in a screen for SFK substrates [92]. Excitingly, cells gained the enhanced ability to form elongated membrane projections upon mutating these residues, implicating that these tyrosine residues might be negatively regulated by phosphorylation. Despite this, it is clear that other tyrosine residues are involved as the mutation of Y1399 and Y1404 decreased but didn't eliminate the adhesion dependent phosphorylation of ARAP3.

1.3 Neutrophil Chemotaxis

Perhaps the most intensely studied neutrophil function controlled by PI3K signaling is chemotaxis. Chemotaxis is a specialized form of cell migration that drives neutrophils to move directionally towards a gradient of chemoattractant, or away from a chemorepellent. There are a variety of neutrophil chemoattractants and chemokines that guide neutrophils to the sites of infection and inflammation. Neutrophils can sense gradients of chemoattractants when they bind to the uniformly distributed G protein-coupled receptors (GPCRs) at the plasma membrane [93]. This causes the PI3K product PIP3 to polarize at the leading edge. As opposed to the resting round neutrophil, polarized neutrophils adopt an asymmetric morphology with actin-rich protrusions at the leading edge forming lamellipodia and a trailing end.

The recruitment of neutrophils to sites of inflammation can occur by two different modes. They can migrate in an integrin dependent manner when breaching barriers, which occurs on a two-dimensional substrate and the cell flattens out forming integrin adhesive bonds on the substratum [94]. In vivo, integrin-dependent steps include the breaching of vessel walls. However, neutrophils can also migrate in an integrin independent manner during interstitial migration within a 3D matrix forming actin protrusions and myosin contractions to drive themselves ahead [95]. In vitro, integrin-independent migration can be analysed with cells that are embedded in a 3-dimensional collagen matrix.

1.3.1 Chemoattractant sensing

Despite some promiscuity, neutrophils have dedicated G-protein-coupled receptors (GPCRs) for each type of ligand. The large number of expressed GPCRs can detect a range of chemoattractants: formyl-peptides from bacterial or mitochondrial origin such as N-formylmethionine-leucyl-phenylalanine (fMLF) [96], complement anaphylatoxins, e.g. C5a and C3a [97], chemotactic lipids such as leukotriene B4 (LTB4) [98] and platelet activating factor (PAF) as well as classical chemokines, named after the conserved cysteine residues (CC and CXC) such as CXCR8 [99]. In addition to driving chemotaxis, many of these ligands can also trigger other neutrophil responses and/or prime them for further stimulation. Endothelial cells express extracellular glycosaminoglycans (GAGs) which bind to these chemokines to immobilise the gradient and avoid excessive diffusion [100]. The process of neutrophils moving directionally along gradients of immobilized chemoattractants is known as haptotaxis.

Receptor	Human ligands
Chemokine receptors	
CXCR1	CXCL6, CXCL8
CXCR2	CXCL1, CXCL2, CXCL3, CXCL5, CXCL6, CXCL7, CXCL8
CXCR3	CXCL4, CXCL4L1, CXCL9, CXCL10, CXCL11
CXCR4	CXCL12
CCR1	CCL3, CCL3L1, CCL4L1, CCL5, CCL7, CCL8, CCL14, CCL15, CCL16, CCL23
CCR2	CCL2, CCL7, CCL8, CCL13, CCL16
CCR3	CCL3L1, CCL5, CCL7, CCL8, CCL11, CCL13, CCL15, CCL24, CCL26, CCL28
CCR5	CCL3, CCL3L1, CCL4, CCL4L1, CCL5, CCL8, CCL11, CCL14, CCL16
Chemoattractant Receptors	
BLT1, BLT2	LTB4
FPR1, FPR2	Bacterial and mitochondrial formylated peptides, e.g. fMLF
C5aR	C5a
C3aR	C3a

Table 1.3.1 List of chemokine and chemoattractant receptors expressed in human neutrophils and their ligands. The chemokines CXCR1 and CXCR2 are abundantly expressed in circulating neutrophils while CXCR4 is enhanced upon neutrophil ageing. Others are expressed under inflammatory conditions. Adapted from [101].

1.3.2 PI3K signalling in chemotaxis

Upon ligand binding to the extracellular N-terminus, GPCRs which contain seven transmembrane α-helices undergo a confirmational change [102]. Once the signal is transduced to the intracellular domain, the heterotrimeric G protein signalling cascade is activated allowing GPCRs to act as GEFs and exchange the GDP with GTP on the Gα subunit. This also causes the release of the Gα

subunit from Gβγ dimers, allowing Gα-GTP and Gβγ to activate downstream effectors including phospholipase C (PLC) β by Gα and Gβγ, and Class I agonist-activated PI3Kγ by the Gβγ subunits [103]. Of the four agonist-activated PI3Ks in neutrophils, PI3Kγ is directly activated by Gβγ together with Ras-GTP [104, 105] which itself is activated by the Ras guanyl releasing protein 4 (RasGRP4), downstream of PLCβ [106] (for a schematic representation see Figure 1.3.2).

The localization of the PI3K lipid product PIP3 at the leading edge is one of the earliest molecular events in neutrophil chemotaxis [65, 107-110]. It is thought to be important for the neutrophil's ability to polarize and subsequently migrate directionally towards a source of chemoattractant. A polarized neutrophil has an identifiable leading edge called a pseudopod which contains membrane protrusions made of F-actin bundles called lamellipodia that propel the cell forward, and a trailing edge called the uropod characterized by the myosin light chain filaments which aid contractions at the rear. If the chemoattractant is uniform however, neutrophils polarise and migrate randomly in a process called chemokinesis. Neutrophil polarisation is also controlled by membrane tension. Membrane tensions are created by the leading-edge protrusions, preventing the formation of a secondary protrusion and preserving consistent polarisation [111].

Molecularly this is explained by the accumulation of PIP3 at the leading edge which activates regulators of small GTPases such as Rac GEFs. They then activate Rac GTPases to promote actin dependent protrusions and initiate F-

actin assembly. PIP3 at the leading edge also activates Rho GAPs such as ARAP3 which in turn inhibit the activation of RhoA [112]. The opposite holds true for the trailing end, where Rac activity is inhibited by the enriched Rho GTPase activity. Rho GTPase also activates the kinase ROCK to cause myosin II assembly at the rear of the neutrophil. Phosphatases work together with these small GTPases to keep the leading edge and trailing ends separate and maintain polarisation. Hence, PTEN which is found at the trailing domain where it is thought to dephosphorylate PIP3 to PIP2 to antagonise PI3K activity and thereby assist PIP3 polarisation at the leading edge. In the middle of the neutrophil, there is a microtubule lattice which delivers molecules to each domain of the polarised cell. Positive and negative feedback loops are believed to maintain and regulate polarisation. For example, it was determined that inhibiting PI3Ks also caused the inhibition of Rho GTPases, Rac and Cdc42 suggesting that regulators of these Rho GTPases also act downstream of PIP3. Interestingly however, inhibiting Rho GTPases (with *Clostridium difficile* toxin-B) also blocked PIP3 accumulation [113]. The fact that both PI3K and Rho GTPase inhibitors can block the accumulation of PIP3 at the leading edge suggests that cell polarity can be explained by feedback loops.

Upon chemoattractant stimulation, PI3Kγ deficient neutrophils did not produce PIP3 and hence PKB was not activated [114]. These mice displayed chemotaxis defects towards a range of stimuli both in vivo and in vitro [115, 116]. The loss of the PI3Kγ adaptor p101 also caused a reduction in PIP3 accumulation, PKB activation and cell migration [117, 118]. In humans, neutrophils from chronic obstructive pulmonary disease (COPD) patients

exhibited poor directionality when migrating towards chemoattractants. Increased PI3K activity was detected in these neutrophils [119], and inhibiting PI3Kγ and PI3Kδ restored migratory accuracy. The same was also found in neutrophils from elderly donors, highlighting the importance of PI3Kγ and PI3Kδ isoforms in chemotaxis [120].

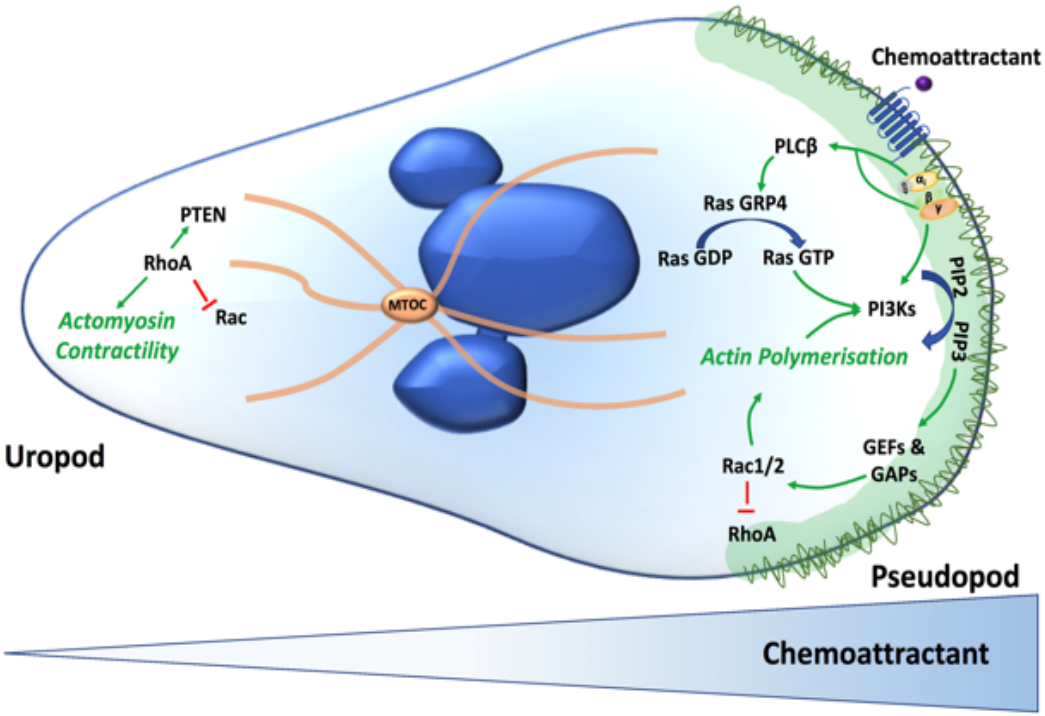

Figure 1.3.2 Molecular signalling in neutrophil polarisation and chemotaxis. Polarisation is initiated when chemoattractants bind to G-protein coupled receptors on neutrophils. This causes the accumulation of PIP3 at the leading edge where effector proteins such as Rho GEFs and GAPs lead to actin polymerisation. By acting as a 'mechanical gauge', the nucleus works together with the microtubule organising centre to propel the cell through the interstitium. The trailing end retracts by microtubule depolymerisation which in turn activates RhoA which triggers actomyosin contractility. Feedback loops at the leading and trailing edges are used to maintain polarisation, for example the inhibition of RhoA at the pseudopod. Figure reused with permission from [121].

1.3.2.1 Functions of ARAP3 in chemotaxis

ARAP3 was found to regulate neutrophil chemotaxis in a context-dependent manner. ARAP3 deficient neutrophils have a significantly reduced ability to chemotax towards fMLF in speed, Euclidean distance (shortest distance between start and finish) and total accumulated distance in 2D substrates [122]. Further analysis of ARAP3 deficient neutrophils in an integrin independent (3D substrate) context using Boyden chambers (transwells) revealed that they have a directionality defect, causing them to form a pseudopod in one direction before retracting it and extending another in a different direction. Another study used neutrophils expressing ARAP3 with a PH domain double point mutation (R302, 303A) which led to the uncoupling of ARAP3 from PI3K. Analogous to the ARAP3 deficient neutrophils, these neutrophils also showed a consistent directionality defect, however, they did not exhibit a severe integrin dependent migration defect as was previously shown with ARAP3 deficient cells [123]. This suggests the integrin dependent migration defect observed in the ARAP3 deficient cells may be due to activation by Rap-GTP rather than PI3K.

1.3.2.2 Functions of PTEN and SHIP1 in chemotaxis

PIP3 localisation to the leading edge is regulated by PTEN and SHIP1 [65]. In mouse models, PTEN and SHIP1 were both shown to have functions in initiating and maintaining neutrophil polarisation. PTEN-null neutrophils are particularly sensitive allowing low concentrations of chemoattractants which would cause little effect on wild-type neutrophils to polarise. However, after priming or upon chemoattractant saturation, this was no longer the case,

showing PTEN functions to dampen basal responsiveness [60]. This could be a way for the neutrophils to reduce inappropriate tissue damage during inflammation. PTEN was also determined to aid in distinguishing and prioritising between opposing intermediate (e.g. LTB4) and end-target (e.g. fMLP) chemoattractants [124]. Interestingly, SHIP1 deficient neutrophils were extremely spread, resembling fried eggs. They also failed to chemotax and polarised poorly forming irregular lamellae upon fMLP stimulation [65]. This suggests that PTEN and SHIP1 have non redundant regulatory functions [125].

1.4 Neutrophil trafficking

Mature neutrophils in the bone marrow undergo several processes to reach the site of inflammation, which include the following.

1.4.1 Mobilisation and Homing

Neutrophil differentiation occurs in the bone marrow, where granulocyte precursors and mature neutrophils are held. This occurs by the expression of receptor CXCR4 which binds to its ligand CXCL12 also produced in the bone marrow. When exposed to the granulocyte colony stimulating factor (G-CSF), Gr1+ bone marrow myeloid cells downregulate CXCR4 and upregulate CXCR2 while bone marrow stromal cells downregulate CXCL12 [126]. The agonists of CXCR2 are the constitutively expressed CXCL1 and CXCL2 by the bone marrow endothelium. This in turn causes neutrophil mobilisation into the circulation [127]. After one day, the neutrophils in the circulation become senescent causing the upregulation of CXCR4 which once again increases their sensitivity to CXCL12 produced in the bone marrow [128]. This causes the neutrophil to return to the bone marrow in a process known as ‘homing’ before undergoing apoptosis and their uptake by stromal macrophages [129].

1.4.2 Prioritising Chemoattractants

As laid out above, circulating neutrophils in the vasculature follow chemokines secreted from sentinel cells which lead them to the general vicinity to the site of inflammation. Once they reach the vicinity, neutrophils prioritize and chemotax towards the ‘end target’ attractants which include fMLF and C5a

[124]. Several experiments have established that chemoattractants exist in a hierarchy where ‘end target’ attractants are prioritized over intermediary chemoattractants such as LTB4 or IL-8, even in the presence of high concentrations of host derived intermediary chemoattractants [130]. This was proposed to be achieved by employing different signalling pathways for end target and intermediary attractants [131].

1.4.3 Swarming

Intravital imaging studies of inflamed animal tissues have shown that once the circulating neutrophils transmigrate to reach the extravascular space, they begin to form swarms towards the site of inflammation [132]. Neutrophil swarming is a highly coordinated accumulation of cells leading to the formation of clusters at the site of infection or tissue injury. Clustering occurs when ‘pioneer’ early arriving cells cause the large scale migration and recruitment of cells further away [133]. Neutrophil swarming occurs in 5 steps: (i) swarm initiation, involves the pioneer cells close to the site of damage migrating towards the injury. It is believed that signalling occurs through various chemoattractants in these cells, as genetically depleting single receptors of N-formyl peptide, inflammatory lipid, complement fragment, and chemokine still displayed initial recruitment [134]. As little as 2-3 pioneer cells can induce (ii); swarm amplification by neutrophil death in the developing cluster which engages a second wave of neutrophils from distant regions [135]. However, the chemotactic factors released to initiate this are yet to be determined. In (iii), swarm amplification occurs through signal relay where neutrophils amplify the

chemotactic gradient by releasing intermediate chemoattractants such as the notable LTB4. They can rapidly produce LTB4 in response to end target chemoattractants, and this autocrine-paracrine signal amplification loop enhances chemotaxis even in shallow gradients of fMLF [136]. The generation of LTB4 from the leading neutrophil prompts the activation of BLT1 from following neutrophils which allows for the further generation of LTB4 [137]. To avoid excessive inflammation, resident macrophages were shown to shield microlesions, preventing the neutrophil swarming response which could potentially lead to host injury [138]. (iv) involves the accumulation of cells at the site of injury where they form aggregations. These aggregates rearrange the extracellular tissue to displace collagen fibres by proteolysis which is enhanced by LTB4 with studies showing that LTB4 can induce the secretion of neutrophil elastase [139]. This isolates the wound from the surrounding tissue, forming a tight seal around it. After tissue remodelling, neutrophil clusters dissolve as they undergo swarm resolution in (v). The mechanism for this remains to be defined although several potential mechanisms are hypothesised, such as the antagonism of LTB4 signalling [134].

In vivo mouse models using intravital microscopy have shed important insights into neutrophil swarming and interstitial neutrophil recruitment [132]. However, there are challenges associated with studying swarming *in vivo*, for example, these experiments are low throughput and difficult to translate to study swarming in humans [140]. To overcome this, the use of microscale and microfluidic in vitro assays have become more prevalent recently. These assays can be used on human neutrophils to observe several swarms

simultaneously, and in addition, are useful tools to investigate signalling molecules from enriched supernatants [141].

As the first secondary chemoattractant found at the site of inflammation [142-144], both in vivo and in vitro studies have identified LTB4 as a key mediator in swarming [47, 136]. Stimulation by primary chemoattractants cause cytosolic phospholipase A_2 (PLA_2) to translocate to the nuclear envelope where it forms arachidonic acid (AA) by hydrolysing membrane bound lipids [145]. Concurrently, increased intracellular levels of calcium upon stimulation causes 5-lipoxygenase (5-LO) to translocate to the nuclear envelope where it associates with 5-LO activating protein (FLAP) to act on AA and generate leukotriene A4 (LTA4) [146]. Finally, LTA4 hydrolase (LTA4H) converts LTA4 into LTB4 which is secreted from the neutrophil where it can bind to the G protein-coupled receptors BLT-1 and BLT-2. Monocytes, macrophages and granulocytes produce the most LTB4 [147].

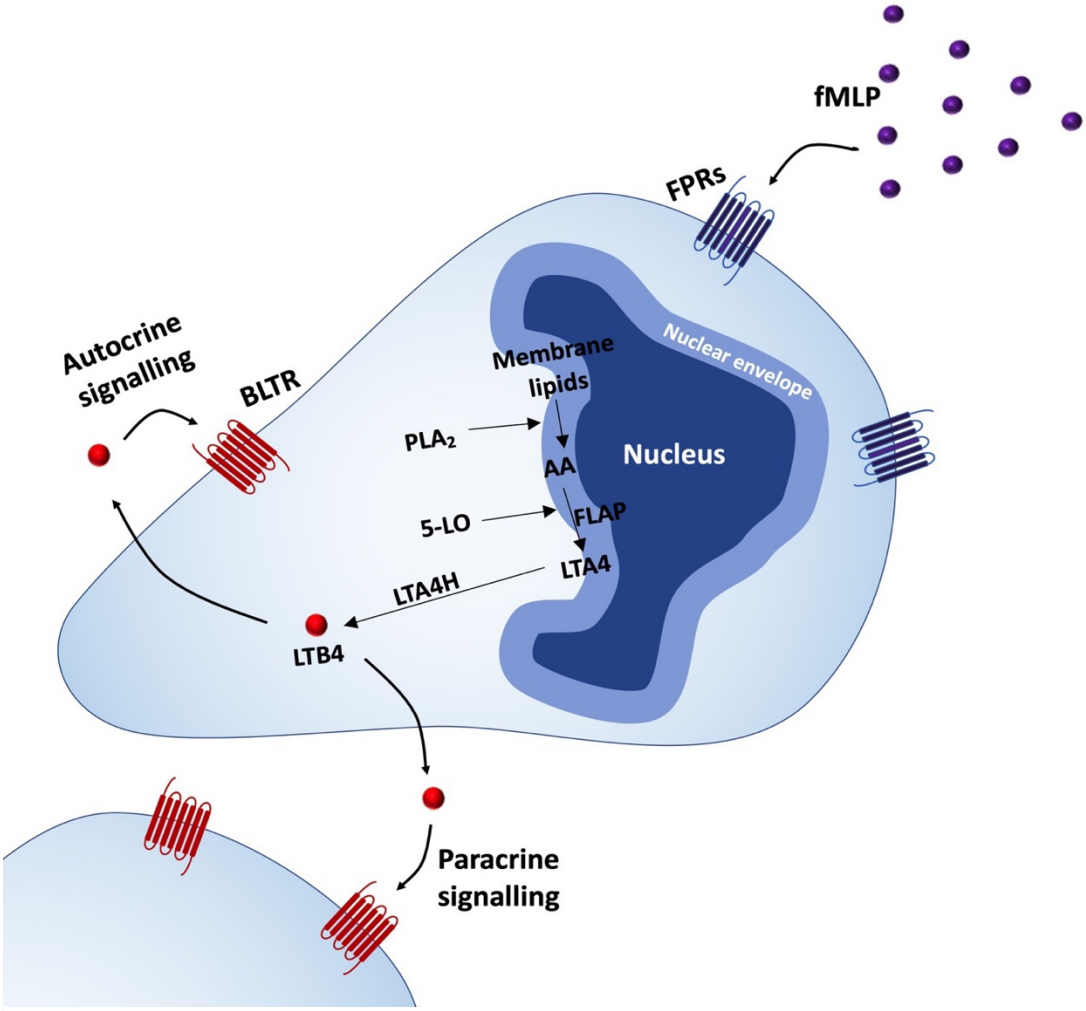

Figure 1.4.3 Neutrophil swarming towards an fMLF gradient by LTB4 relay. Neutrophil stimulation by primary chemoattractant causes PLA_2 translocation to the nuclear envelope where it hydrolyses membrane bound phospholipids to form AA. Simultaneously, increased calcium levels causes 5-LO to translocate to the nuclear envelope where it associates with FLAP to generate LTA4 which is then converted to LTB4 by LTA4H. LTB4 is then secreted from the neutrophil where it can bind to BLT receptors and act in an autocrine manner by sensitising the neutrophil towards fMLF, or in a paracrine manner as a molecular beacon for other cells. Made with PowerPoint.

1.4.4 Atypical chemokine receptors

As well as G-protein couple receptors, neutrophils also express atypical chemokine receptors known as ACKRs [148]. They are scavenger or decoy receptors as they do not support the directional movement of neutrophils and therefore do not exhibit conventional signalling functions. Nonetheless, these receptors have high affinity ligand binding in addition to ligand degradation [149]. For example, ACKR2, also known as D6 is a CC chemokine receptor which can compete with and degrade CCR1 ligands upon internalisation, protecting tissues from excessive inflammatory damage.

1.4.5 Reverse migration

Once the neutrophils carry out their functions, they are cleared from the sites of injury to avoid excessive inflammation. One way this occurs is by undergoing apoptosis after which they are efferocytosed by the resident macrophages [86, 150], however, another method is by migrating away from the wounds and re-entering the vasculature in a process known as reverse migration [151]. Inflammation increases endothelial permeability by damaging endothelial junctions. For example, neutrophil elastase release, mediated by LTB4, is responsible for cleaving the endothelial junctional adhesion molecule C (JAM-C) [152]. This allows for chemokines such as CXCL1 to escape from the site of inflammation into the circulation which drives the neutrophils to enter the circulation [153]. Intravital microscopy to observe the movement of neutrophils during a localised burn to the liver showed that neutrophils used proteases to enter the circulation by reverse transendothelial migration. They then made a

pit stop in the lungs to upregulate CXCR4 prior to homing by entering the bone marrow for clearance [154]. However, the molecular mechanisms involved in reverse migration remain to be fully understood.

Figure 1.4.5 Neutrophil trafficking and chemotaxis. The journey of neutrophils from bone marrow to sites of inflammation and back for clearance. From top left: *Mobilisation and Homing,* CXCR2 signalling causes the mobilisation of neutrophils from the bone marrow and into the circulation; senescent neutrophils up-regulate CXCR4 which initiates homing back to the bone marrow. *Leukocyte adhesion cascade*, Sentinel cells release pro inflammatory mediators and hence promote selectin-mediated interactions with the endothelium. Rolling neutrophils along the endothelium are guided by GAG-immobilised chemokines through GPCR signalling which regulates integrin mediated firm adhesion and extravasation. *Atypical chemokine receptors,* they aid neutrophils to fine tune chemokine driven responses during chemotaxis. *Swarming,* Neutrophils release LTB4 in response to some end target chemoattractants forming a feedback amplification loop that causes the directional migration of neutrophils in a 'swarm'. *Chemoattractant cascades,* a hierarchy of chemoattractants allows neutrophils to prioritise 'end-target' chemoattractants over intermediate chemoattractants. *Reverse migration,* By transendothelial migration to re-enter the circulation, neutrophils have been shown to reverse migrate by the release of proteases such as neutrophil elastase to degrade endothelial junctions such as JAM-C. Figure reused with permission from [121].

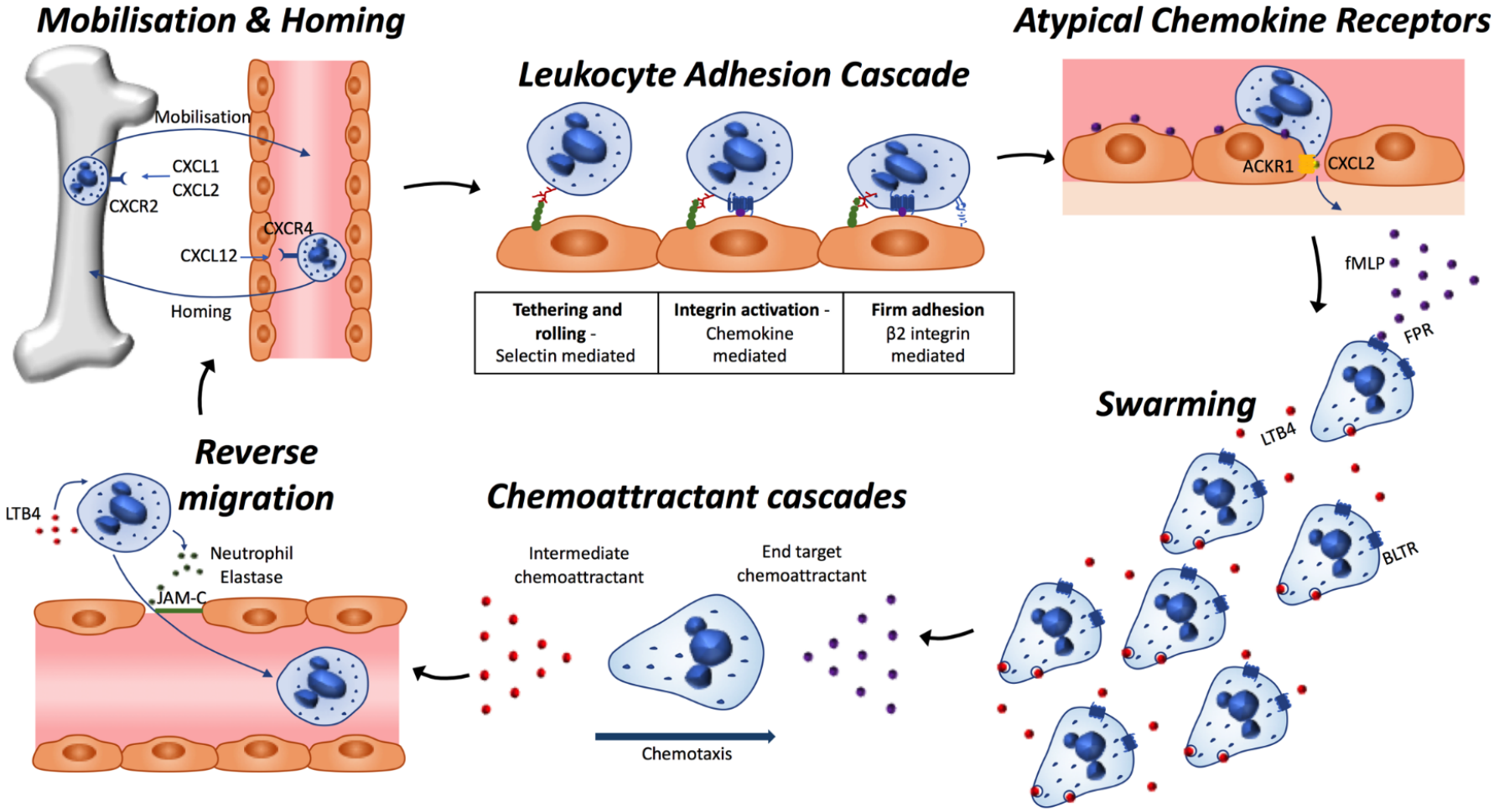
Mobilisation & Homing
Mobilisation
CXCL1
CXCL2
CXCR2
CXCR4
CXCL12
Homing
Leukocyte Adhesion Cascade
Tethering and rolling - Selectin mediated
Integrin activation - Chemokine mediated
Firm adhesion β2 integrin mediated
Atypical Chemokine Receptors
ACKR1
CXCL2
fMLP
FPR
Swarming
LTB4
BLTR
Chemoattractant cascades
Intermediate chemoattractant
End target chemoattractant
Chemotaxis
Reverse migration
LTB4
Neutrophil Elastase
JAM-C

1.5 Immunosenescence

As humans grow older, they become frail and experience higher rates of morbidity and mortality. The elderly are more susceptible to infections, tumours and autoimmune diseases, making aging one of the most complex and challenging biological phenomena. The decline in human health in the elderly occurs due to a range of factors, at the centre of which is the immune system. The deterioration of the immune system with old age, termed immunosenescence, has been well studied, with the most prominent effects recorded in the adaptive immune system. As a result of epigenetic changes, the differentiation of the hematopoietic stem cells is favoured towards the myeloid lineage over the lymphoid lineage [155]. The biggest changes to the adaptive immune system include a drop in the number of naïve T cells due to the involution of the thymus [156] leading to a decrease in the T cell receptor repertoire, whereas the number of memory T cells increases [157]. This means that although the elderly remain protected from common infections, the response to novel antigens or infections from highly mutating pathogens is weakened. Similar to the T cells, the number of B cells decline with age [158], while the memory B cells also increase [159]. Clinically, this explains the reduced responses to vaccinations noted with the elderly.

Although not as prominent as the defects in the adaptive immune system, the innate immune system also undergoes changes with ageing [155]. For example, there is a drop in the effectiveness of physical barriers which lowers the threshold for the number of bacteria required to initiate infection [160]. The

thin and dry skin attributed to the elderly contain fewer antimicrobial defences which aids bacteria to settle on the skin. The elderly also have decreased cilia function making it more challenging to export bacteria which in addition to a decreased cough reflex makes them more prone to pneumonia [161]. With age the pH of the gastric acid decreases, leaving the elderly more prone to gastrointestinal infections. As a result of decreased diuresis, bacteria can easily adhere to the bladder surface leaving the elderly more susceptible to bladder infections. Looking more specifically at the immune cells, the number and percentages of basophils and eosinophils decrease significantly [162]. Although research on these immune cells remains scarce, they both have altered functions with age, with the latter showing reduced chemotaxis, degranulation, and ROS production. This could explain why the protection against parasites and fungi decreases in the elderly.

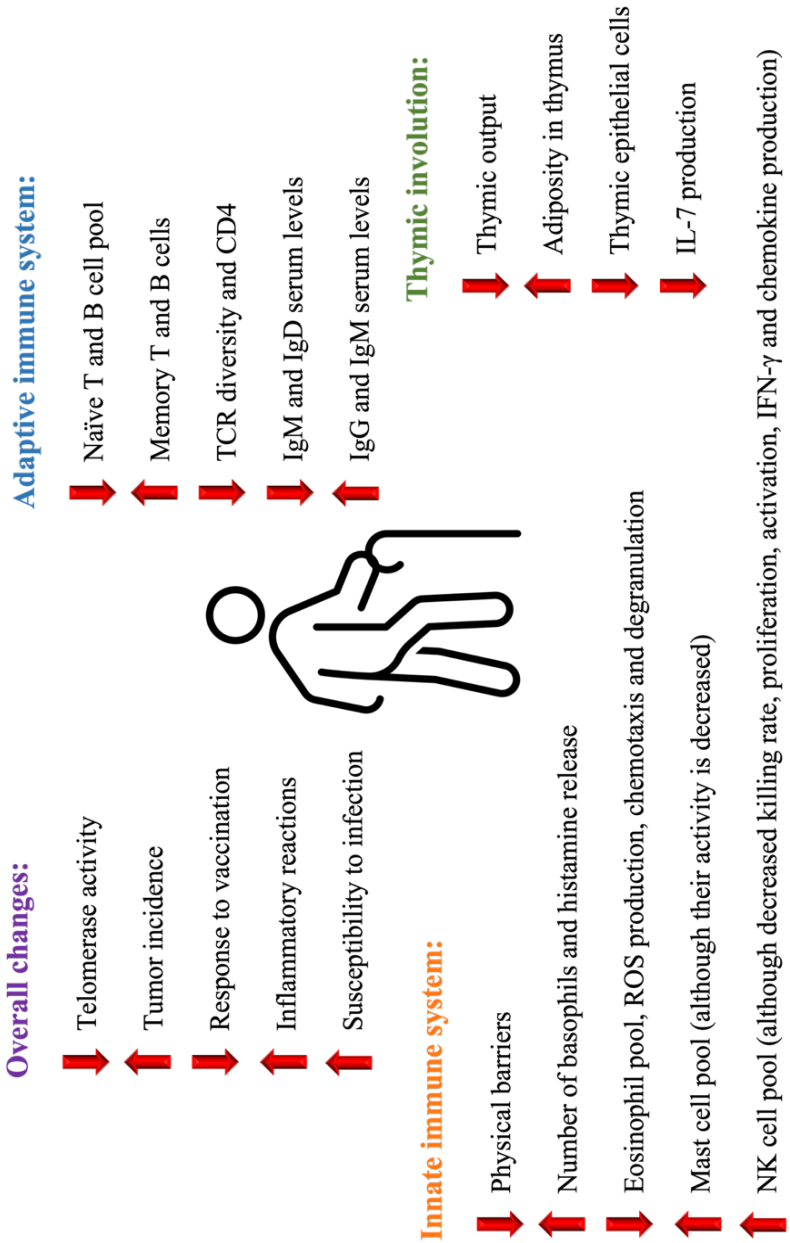

Figure 1.4 Changes that occur during aging. Adaptive immune system, innate immune system, thymic involution, and overall changes that occur during aging. Adapted from [163].

1.5.1 Neutrophil Numbers and Recruitment in Ageing

In the elderly, the number of neutrophils circulating in the blood is not altered, and neither is their rate of production in the bone marrow [164]. Infection-induced upregulation of neutrophils however is strikingly decreased [162], partly owing to the reduced responsiveness to G-CSF which would normally impede apoptosis during infection. Hence, the lower production rate and the shortened lifespan both could explain the reduction in infection induced neutrophilia in the elderly.

Neutrophils from elderly donors in the circulation have increased adhesion molecules such as CD15 (the selectin binding sialyl Lewis X) [155]. This means neutrophil tethering and rolling along the endothelium is elevated in the elderly which can be damaging to the endothelium. In addition, chemotaxis has also been shown to decrease in neutrophils from healthy elderly donors in response to a range of stimuli [120]. Aberrant neutrophil migration is associated with increasing age with the chemotaxis defect gradually increasing after the age of 30. Further investigation revealed that these neutrophils had increased PI3K activity and inhibiting PI3K class 1 δ and γ isoforms improved migratory accuracy. Interestingly, another study found a chemotaxis defect between young (25-35 years) and elderly donors (65-75 years) towards fMLF, however, no statistical difference was identified in chemotaxis between young donors and centenarians (100-102 years) [165]. This highlights the importance of chemotaxis in the immune response of aged persons.

1.5.2 Neutrophil Antimicrobial Effects in Ageing

It can be expected that a decrease in bactericidal activity would also compromise the efficiency of neutrophils for the resolution of infections. Studies focusing on the antimicrobial functions of neutrophils from elderly donors showed a significant reduction in their ability to phagocytose opsonized bacteria and yeast [166]. The phagocytic index of neutrophils from the elderly group (mean age 76) dropped by about 50% compared to the younger group (mean age 36) [167]. Further studies identified that the same percentage of neutrophils showed phagocytic ability and that this reduction is instead due to a decrease in the number of microbes phagocytosed per neutrophil. Upon stimulation with fMLF, degranulation was also shown to decrease in neutrophils from elderly donors [168]. This may lead to decreased neutrophil bactericidal properties towards certain pathogens. ROS production in response to fMLF however, has revealed contradicting results between different groups, some showed no difference between the ages [169] while others showed decreased [170] ROS production in the elderly. In contrast, significantly reduced ROS production was observed in the elderly when neutrophils were stimulated by Fc receptor ligation [171]. Hence, it is concluded that Fc mediated functions might decline in old age as observed in ROS production and phagocytosis. Finally, NET release in response to IL8 and LPS stimulation was reported to significantly decline with age as well [172].

Number in circulation	
Number of precursor in bone marrow	
Precursor activation with G-CSF	
Inhibition of apoptosis after stimulation with G-CSF	
Chemotaxis	
Expression of CD15	
Expression of Fcγ-receptor RIII (CD16)	
ROS production	
Intracellular killing	
Ca^{2+} release after fMLF stimulation	
Intracellular Ca^{2+} in resting cells	

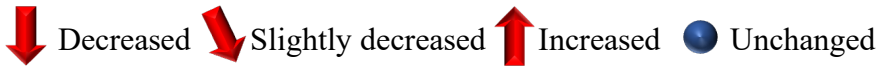

Table 1.4.2 Changes that occur to neutrophils during aging. Adapted from [155].

1.6 Hypothesis and aims

The regulation of neutrophils is pivotal for an appropriate and effective immune response. Given that PI3K signalling is implicated in many neutrophil functions, it is important to understand the functions of the different players involved. The hypothesis that I originally aimed to address was that changes in ARAP3 post-translational modification might be responsible for the decline in chemotaxis observed in old age. For technical reasons however, this project was abandoned (see chapter 3). Therefore, the main hypothesis addressed in this thesis was that the 5'phosphatase SHIP2 regulates neutrophil functions. In addition, given that neutrophils from the elderly exhibit a range of decreased neutrophil functions including a chemotaxis defect, it was also hypothesised that neutrophil swarming from elderly donors is impaired.

The major aim of my work was to investigate which neutrophil functions are regulated by SHIP2 in neutrophils to unravel the molecular mechanisms underpinning this. In addition, I aimed to examine the effects of aging on neutrophil swarming in vitro.

2. Materials and Methods

2.1 Isolating primary neutrophils

Here the isolation of human and mouse neutrophils are described using various methods. All neutrophil preps were carried out in an MSC (microbiological safety) class II cabinet, and the buffer compositions used are listed in table 2.1 below.

Buffers and Solutions	**Composition**
Geyes A	1 M NH_4Cl, 1M KCl, 1 M Na_2PO4, 1 M KH_2PO_4 and Glucose
Geyes B	1 M $MgCl_2.6H_2O$, 196 mM $MgSO_4.7H_2O$ and 1 M $CaCl_2.2H_2O$
Geyes C	1M $NaHCO_3$
Geyes solution	20% Geyes A, 5% Geyes B and 5% Geyes C, 70% $dH2O$
HBSS $^{++/--}$	HBSS modified without Ca^{++} and Mg^{++}, and supplemented with 0.25% bovine serum albumin (BSA, fatty acid and endotoxin-free) and 14 mM Hepes (pH 7.4 at RT)
PBS^{++}	Dulbecco's PBS +$CaCl_2$, +$MgCl_2$, supplemented with 4 mM Sodium bicarbonate and 1 g/L Glucose
Percoll/HBSS	90% Percoll, 10% of 10x HBSS, diluted with HBSS + Na_3CO_3 to desired final Percoll concentration
Percoll/PBS	90% Percoll, 10% of 10x PBS, diluted with 1x PBS to desired final Percoll concentration

Table 2.1 Buffer compositions used for isolating primary neutrophils.

2.1.1 Isolation of human neutrophils

2.1.1.1 Discontinuous Percoll gradient

This technique involves the standard 2-step method of erythrocyte sedimentation by dextran, followed by a discontinuous Percoll gradient to isolate polymorphonuclear neutrophils (PMNs), as described [173]. In detail: ~ 36 ml of peripheral venous blood from healthy donors was collected into 50 ml falcon tubes (BD Biosciences) containing 4 ml of 3.8% Sodium citrate, and gently mixed by slowly inverting the tube to prevent the blood from coagulating. The tubes were then centrifuged at room temperature for 20 mins at 300 g, after which the top platelet rich plasma (PRP) layer was removed and placed into a thin 10 ml glass vial. 220 µl of 1 M $CaCl_2$ was then added to the PRP and mixed by inverting the vial, and then incubated at 37°C for 1 hour to allow for clotting to produce serum. For the sedimentation of erythrocytes, 6 ml of 6% dextran T500 (Sigma-Aldrich) was added to the remaining cell layer, and the tube topped up to 50 ml with prewarmed 0.9% sterile saline (Baxter). The tube was mixed by gently inverting the contents and any air bubbles formed were removed using a pastette, and the cap was replaced. After 20-25 minutes, the leukocyte rich upper layer was cautiously removed and transferred into a new 50 ml falcon tube, and made up to 50 ml with saline and centrifuged at room temperature for 6 minutes at 350 g. In the meantime, Percoll (Sigma-Aldrich, GE17-0891-01) and PBS (Gibco) were used to create a discontinuous cation gradient by carefully layering 3 ml of 63% Percoll/PBS onto 3 ml of 72% Percoll/PBS in a 15 ml Falcon tube (compositions in table 2.1). After centrifugation, the supernatant was removed and the pellet

resuspended in 3 ml of 49.5% Percoll/PBS, which was then overlayed onto the Percoll gradient. This was then centrifuged at room temperature for 20 minutes at 720 g, with low acceleration and no brake. The 49.5% layer was removed and the monocytes at the interface with 63% Percoll was discarded, next, the granulocytes were harvested at the interface between the 72% and 63% layers, placed into a 50 ml Falcon tube and washed twice by centrifugation with PBS at room temperature for 6 minutes at 230 g. Once isolated, the neutrophils were resuspended in PBS^{++} ready to be used in functional assays. >95% purity was determined by cytocentrifuge preparations using the Reastain Quick Diff reagents (Reagena).

2.1.1.2 Further Processing with a Negative Selection Kit

For some experiments, human neutrophils were further isolated to improve purity. This was achieved using a negative selection kit, the EasySep Human neutrophil isolation kit (STEMCELL technologies, Catalog #11957) as suggested by the manufacturer's instructions. Cytocentrifuge preparations using the Reastain Quick Diff reagents and flow cytometry analysis with the Sysmex XT-2000iV revealed 100% neutrophil purity as shown in chapter 6 (Figure 6.2.1).

2.1.2 Isolation of Mouse Bone Marrow Derived Neutrophils

2.1.2.1 Bone marrow derived neutrophil prep

The hind legs of mice were dissected to collect the femurs and tibiae, and the flesh scraped off the bones. The ends of the bones were then cut off and the bone marrow (BM) flushed out into a 50 ml falcon tube with $HBSS^{++/--}$ using a 2 ml syringe (BD Plastipak) with a 25 g needle (TERUMO). BM cells were then gently resuspended to remove clumps, topped up to 40 ml with $HBSS^{++/--}$ and centrifuged at room temperature for 10 minutes at 300g (with maximal acceleration and brake). In the meantime, a discontinuous Percoll gradient was prepared in a 15 ml falcon tube by gently pipetting 4 ml of 55% Percoll/HBSS onto 6 ml of 62% Percoll/HBSS. After centrifugation, pelleted BM cells were resuspended in 3 ml of $HBSS^{++/--}$ and added onto the discontinuous Percoll gradient. The cells were then centrifuged for 30 minutes at 1300g (with gentle acceleration and without break), the top lymphocyte layer discarded, and the neutrophils harvested at the interface between the Percoll layers and placed into a 50 ml falcon tube. They were then washed by topping up with $HBSS^{++/--}$ and centrifuged for 10 minutes at 300g. Next, the cells were resuspended in Geyes solution for 2.5 minutes to lyse the erythrocytes, washed twice with $HBSS^{++/--}$, counted and resuspended in PBS^{++}, ready to be used in functional assays. Purity of mouse neutrophil preparations was determined by cytocentrifuge preparations using the Reastain Quick Diff reagents (Reagena) as 70-80%.

2.1.2.2 Bone Marrow Derived Neutrophils for Chemotaxis Experiments

For chemotaxis experiments, mouse neutrophils were prepared on ice using a variant of the above. The femurs and tibiae of mouse hind legs were flushed out into a 50 ml falcon tube with ice cold $HBSS^{++/--}$. BM cells were then gently resuspended to remove clumps, made up to 25 ml with $HBSS^{++/--}$ and left to settle. In the meantime, the gradient was prepared by carefully layering 10 ml of ice cold 60% Percoll/HBSS onto 10 ml of 70% Percoll/HBSS in a 50 ml falcon tube. Next, the supernatant was extracted into a fresh tube and made up to a final volume of 30 ml, and then overlayed onto the discontinuous Percoll gradient. The cells were then centrifuged at 4°C for 30 minutes at 1300g (with gentle acceleration and without break) after which the top lymphocyte layer was discarded using a glass pasteur pipette (Hirschmann). Subsequently, a fresh glass pipette was carefully inserted to the bottom of the tube to extract the clumps until the neutrophil layer at the interface between the 60% and 70% Percoll layers was 5ml away from the bottom. The neutrophils were then placed into a new 50 ml falcon tube, washed 3 times with 50 ml $HBSS^{++/--}$ by centrifuging at 4°C for 10 minutes at 1300 rpm (acceleration 3, brake 3), counted and resuspended in $HBSS^{++/++}$ ready to be used in chemotaxis assays. ~50% purity was determined by cytocentrifuge preparations using the Reastain Quick Diff reagents (Reagena).

2.1.2.3 Further Processing with a Negative Selection Kit

For some experiments, mouse neutrophils were subjected to further enrichment using a commercially available kit that relies on negative selection, the EasySep mouse neutrophil enrichment kit (STEMCELL technologies, Catalog #19762) as per manufacturer's instructions. The purity of neutrophils isolated solely by the Percoll prep alone, enrichment kit alone, or both combined was assessed by manually counting 500 cells from cytocentrifuge preparations, revealing 83%, 77% and 99.1% purity respectively. Figure 2.1.2.3 A shows representative cytospin images. The purity of neutrophils was also tested by flow cytometry (Attune NxT) by analysing CD11b and Ly6G (see Figure 2.1.2.3 B). Next, the activation status of each condition was tested by measuring L-selectin by flow, histogram in Figure 2.1.2.3 C. The activation status was further investigated by a ROS assay (Figure 2.1.2.3 D) as described in section 2.4.3

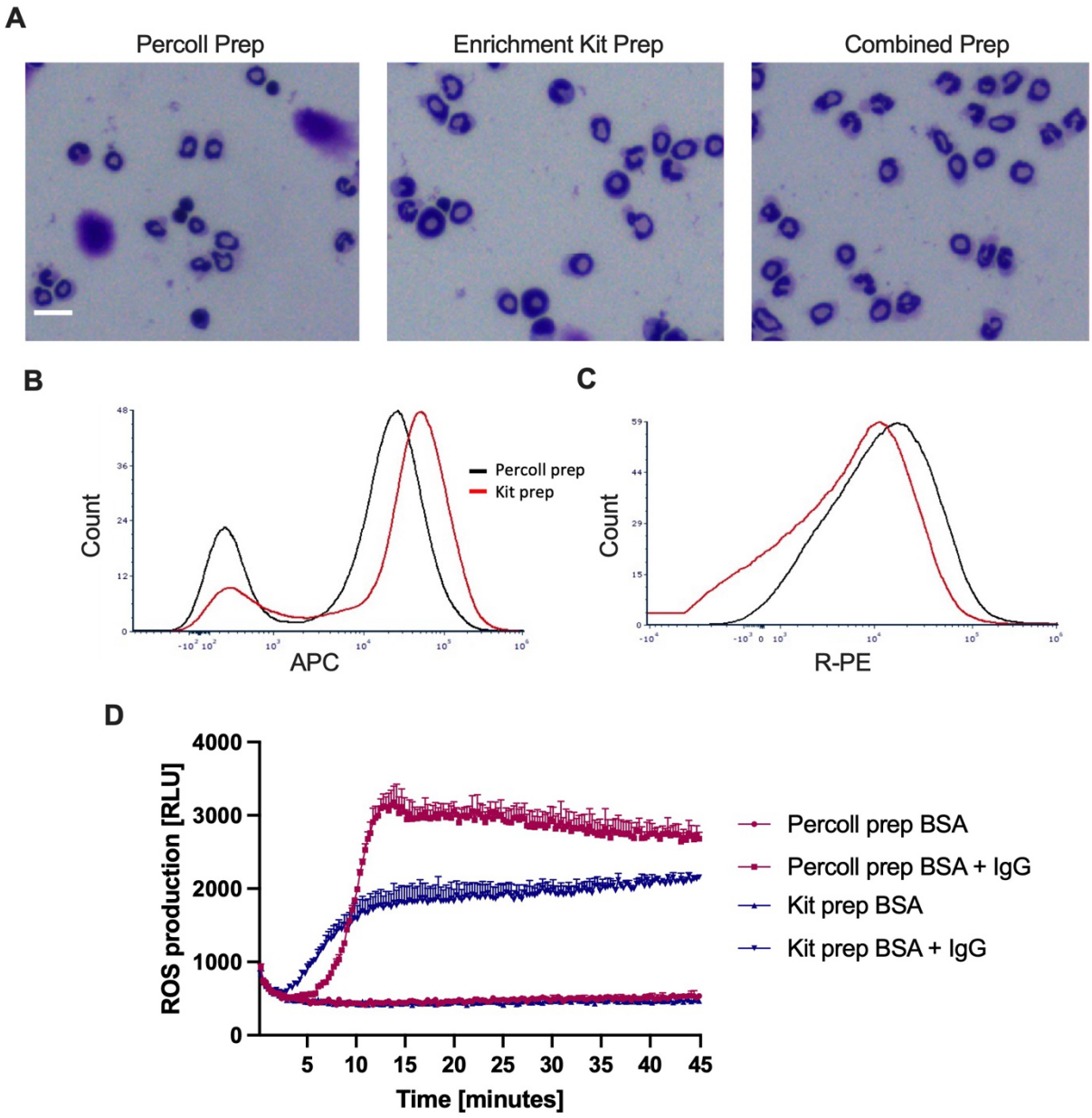

Figure 2.1.2.3 Purity of mouse neutrophils. (A) Representative cytocentrifuge preparations of Diff Quick stained neutrophils obtained from a Percoll prep, EasySep Mouse enrichment Kit, and combined Percoll prep followed by the EasySep Mouse enrichment Kit. Scale bar 20 µm. **(B)** Histogram of flow cytometry analysis showing normalised data for CD11b (APC) and Ly6G (PB). **(C)** Histogram of flow cytometry analysis of L-selectin comparing the Percoll prep to the EasySep Mouse enrichment Kit. **(D)** ROS assay to measure ROS production with and without IgG immune complex stimulation comparing the Percoll prep to the EasySep Mouse enrichment Kit.

2.2 Molecular Biology

In this section, the molecular biology techniques used for mouse genotyping as well as plasmid preparations are described, table 2.2 shows a list of the buffers used.

Buffers and Solutions	Composition
Lysis Buffer for Mouse Biopsies	50 mM Tris-HCl (pH8.0), 100 mM NaCl, 10 mM EDTA, 0.2% SDS
TE	10 mM Tris-HCl (pH8.0), 1 mM EDTA

Table 2.2 Buffer compositions for Molecular Biology techniques.

2.2.1 Mouse DNA Extraction and Ship2$^{\Delta/\Delta}$ Genotyping

To extract DNA from mouse ear notches in Eppendorf tubes, 500 µl of lysis buffer (for recipe see table 2.2) supplemented with 100 µg/ml proteinase K (Roche) was added to each tube. This was incubated at 55ºC for 4 hours (or 2.5 hours if shaking) after which the tubes were vortexed briefly and allowed to cool down at room temperature. Next, 350 µl of isopropanol was added and the tubes mixed by inversion 5-6 times. The precipitated DNA was then spun down, washed with 70% ethanol and allowed to dissolve in TE.

To genotype the samples, polymerase chain reactions (PCR) were carried out with the HotStartTaq DNA Polymerase (QIAGEN) as per manufacturer's instructions. Two PCR reactions were prepared for each mouse, one for the wild-type (WT) allele and one for the Δ allele. The forward and reverse primers used include 5'-cat tgg gag gga ggt ttg ta-3' + 5'-ggt agg tgg gtg gga aag at-3'

for the WT allele (300bp) and 5'-cat tgg gag gga ggt ttg ta-3' + 5'-ccc aaa cac agg aga atg gt-3' for the Δ allele (400bp for Δ and 1kb for the wt allele), respectively. Cycling conditions were 94°(3min)/40 cycles of 95°(30 sec)-58°(30 sec)-72°(30 sec)/72°(10min) and upon completion the PCR products were analysed by gel electrophoresis on a 1% TAE agarose gel containing GelRed (Biotium) for DNA visualisation. Images were acquired using the UVP GelDoc-It^{e} imaging system (Jena Analytik). An example is shown in Figure 2.2.1.

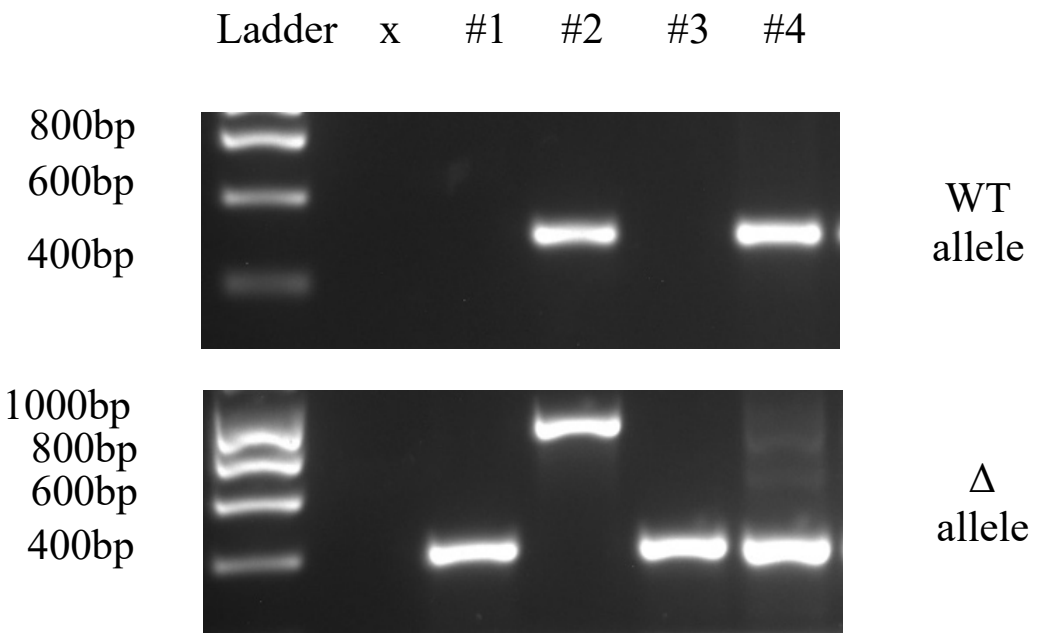

Figure 2.2.1 Genotyping Ship2$^{Δ/Δ}$ mice. A representative DNA gel showing samples from 4 ear notches, the WT allele samples found in the top row (~400bp in WT) and Δ samples at the bottom (~400bp in Δ, and occasionally an additional band at 1kb for WT allele). To the left is the ladder, hyperladder I (Bioline), followed by the no template control (x) and the samples. Mice 1 and 3 are homozygous mutants, mouse 2 is WT, and mouse 4 is heterozygous.

2.2.2 Transformation of Competent E.coli

For the transformation of *E. coli,* 5µl of plasmid were added onto 100 µl of cloning-grade competent cells (NEB) and left on ice for 30 minutes. This was followed by heat shock for 45s at 42°C. They were then placed on ice for a further 2 minutes before diluting with 900 µl of room temperature LB broth and incubating at 37°C for one hour with vigorous shaking at 250 rpm. Next, they were plated onto LB agar plates with the appropriate antibiotic for selection (100 µg/ml carbenicillin). These plates were incubated at 37°C overnight after which individual colonies were chosen and inoculated into antibiotic containing LB overnight (100 µg/ml ampicillin for pLKO.1 plasmids).

2.2.3 Plasmid Purification and Assessment

Small-scale plasmids were purified by GeneJet mini prep (Thermo Scientific) while larger scale purifications were carried out by midi prep (Qiagen) according to manufacturer's instructions. A nanodrop spectrophotometer (Thermo Scientific) was used to detect the concentration of purified plasmid. To further assess the plasmids, test digests were performed with suitable restriction enzymes (Promega) with digested DNA analysed by agarose gel electrophoresis, and stained with GelRed (Biotium) and detected using a UVP GelDoc-It^{e} imaging system (Jena Analytik).

2.3 Biochemical assays

The biochemical assays are described here, table 2.3 shows the buffers used.

Buffers and Solutions	**Composition**
2x Modified Laemmli buffer	62.5 mM Tris-HCL (pH 6.8), 4% SDS, 5% β-mercaptoethanol, 8.5% Glycerol, 0.025% Bromophenol blue, 2.5 mM Na_3VO_4, 10 µg/ml Leupeptin, 10 µg/ml Aprotinin
4x Sample Buffer	160 mM Tris-HCl (pH 6.8), 0.4M DTT, 8% SDS, 50% Glycerol, 0.012% Bromophenol blue
Coomassie staining solution	0.1% Brilliant Blue, 50% MeOH, 10% Acetic acid
Gel destain solution	10 % Methanol, 7% Acetic acid
Lysis Buffer	20mM Tris-HCl (pH 7.5), 150mM NaCl, 1mM EDTA, 1mM EGTA, 1% Triton X-100, 2.5mM Na pyrophosphate, 1mM β-glycero-phosphate, 1mM Na orthovanadate, 0.1mM PMSF and 10µg/ml of each Antipain, Aprotinin, Pepstatin A and Leupeptin
Resolving Buffer	1.5 M Tris-HCl (pH8.8), 0.4% SDS
Running Buffer	250 mM Tris-HCl, 1.92 M Glycine, 1% SDS
Stacker Buffer	0.5 M Tris-HCl (pH6.8), 0.4% SDS
Transfer Buffer	25 mM Tris-HCl (pH8.3), 192 mM Glycine and 10% Methanol

Table 2.3 Buffer compositions used in Biochemical Assays.

2.3.1 DFP treatment

Prior to treating cells with diisopropylfluorophosphate (DFP), a solution of 2% aqueous Sodium Hydroxide was prepared and placed into a fume hood where the inhibitor treatment was carried out. Next, freshly isolated primary neutrophils suspended in PBS^{++} were placed into 2 ml Eppendorf tubes at a concentration no higher than $2x10^7$/ml. DFP to a final concentration of 7mM or PBS^{++} for mock treated cells was then added and the cells and incubated for 10 minutes at room temperature. The cells were then washed twice with PBS by centrifuging at 9,500 g for 30s at room temperature to remove traces of the DFP. Cells were then considered DFP-free and used for experiments. To safely dispose of the DFP, supernatants and any waste including pipette tips were placed into the 2% aqueous NaOH and left overnight for deactivation.

2.3.2 Protein Extraction

Unless otherwise stated in chapter 3, neutrophils were lysed with ice-cold lysis buffer (recipe in table 2.3) for 5 minutes and the lysates clarified by centrifugation at 13,500 g for 15 minutes at 4°C.

2.3.3 Mouse Neutrophil Stimulation for Analysis of Signalling Events

2.3.3.1 fMLF and Fibrinogen Stimulations

For fibrinogen and fMLP co-stimulation, $5x10^6$ neutrophils per condition were pre-warmed in 0.5 ml PBS^{++} for 5 min at 37°C and plated onto fibrinogen coated (150 µg/mL) prewarmed 6 cm cell culture dishes (Corning) +/- 1 µM fMLP. The cells were incubated at 37°C for 19 minutes, after which the non-adherent cells were transferred to an Eppendorf tube and centrifuged at 4°C for 1 minute at 12,000 rpm. During the spin, the adherent cells were scraped in 500 µl of ice-cold lysis buffer and added to the pellets of the centrifuged non-adherent cells. After incubating on ice for 5 minutes clarified lysates were separated by SDS-PAGE and Western blotting (see 2.3.7).

For fMLP stimulation only, 10 µM fMLP was added to $2x10^6$ prewarmed neutrophils for each condition and gently mixed in a test tube. The cells were then pelleted, and the supernatant aspirated before being lysed with 100 µl of ice-cold lysis buffer. After incubating on ice for 5 minutes and centrifuging to clarify the lysates, samples were run on an SDS-PAGE gel.

2.3.3.2 Time Course Assay for Lipid Mass Spectrometry

To prepare samples for PI(3,4,5)P3 mass spectrometry, $1x10^6$ neutrophils were resuspended in 135 µl PBS^{++}. This was then added to 865 µl of prewarmed (37°C) 10 µM fMLP in $dPBS^{++}$ (or the $dPBS^{++}$ alone control). They were then incubated together for the specified times before terminating the reaction by adding 5 ml of the initial organic mix (CHCL3:MeOH,

1:2, v:v), vortexing and storing overnight at -80°C. The next day the samples were sent to Dr Karen Anderson, the Babraham Institute, Cambridge, for lipid extraction and mass spectrometry analysis using a QTRAP 4000 (AB Sciex) mass spectrometer, as previously described [174].

2.3.4 Immunoprecipitation

Protein G sepharose beads were equilibrated with corresponding immunoprecipitation (IP) buffer (schematic representation in Figure 3.2.3.1 B). Next, the appropriate antibody was added to each tube (anti-ARAP3 sheep polyclonal 1:400, rat monoclonal 1:1, see table 2.3.7) and allowed to couple for 90 minutes with slow end over end rotation at 4°C. In the meantime, cells of interest were lysed on ice and lysates clarified by centrifugation. After repeated washing of the beads, the clarified lysates were added. The tubes were topped up with IP buffer and left to IP for 90 minutes at slow end over end rotation at 4°C. After this, the beads were washed five times with fresh IP buffer and the supernatants carefully aspirated. Then beads were then boiled in sample buffer for 5 minutes prior to separation of proteins by SDS-PAGE.

2.3.5 Protein Gel Preparation and SDS-PAGE

Sodium Dodecyl Sulphate PolyAcrylamide Gel Electrophoresis (SDS-PAGE) was carried out on 6 or 8% polyacrylamide handcast gels (Biorad Protean II). To prepare this, the resolving gel was made with Acrylamide/Bis-acrylamide (Sigma-Aldrich, 30% stock solution, 37.5:1 ratio) in resolving buffer. To induce polymerisation, TEMED (0.1%) and ammonium persulphate (APS, 0.05%) were added right before pouring the gel between glass plates separated by

1mm spacers. The gel was overlaid with 1 ml of water-saturated Butanol for an even finish and left to polymerise. Once polymerised, the butanol was removed and the stacking gel was added on top, made with Acrylamide/Bis-acrylamide at a final concentration of 3.75% in stacker buffer supplemented with the polymerisation agents TEMED (0.1%) and APS (0.05%). A 1 mm thick Telfon comb was then inserted to create wells for loading samples after which the gel was left again for polymerisation.

Samples were prepared by boiling the lysates in sample buffer (5 minutes) or whole cells in modified Laemmli buffer (7 minutes) on a heat block. For SDS-PAGE, the gels were then set up into the electrophoresis cell, immersed in running buffer, the samples were loaded into the wells and a current applied (voltage and duration dependent on size of gel) until the loading dye front had moved to the bottom of the gel.

2.3.6 Protein Staining with Coomassie

To stain proteins with Coomassie stain, the gel cassette was carefully disassembled and the gel placed into a clean plastic container containing the Coomassie stain solution and allowed to rock on a low speed at room temperature. After 1 hour, the gel was allowed to destain in several changes of destain. Destained gels were scanned and dried down for storage.

2.3.7 Western Blot

Following SDS-PAGE, proteins on the gel were wet transferred onto a polyvinylidene difluoride (PVDF) membrane (Millipore) using ice-cold transfer buffer in a mini transfer tank (Biorad) at 100V with cooling.

For the detection of proteins, the membrane was first blocked with PBS supplemented with 0.1% Tween-20 (PBST) and 5% non-fat milk powder on a slow-moving rocker. Next, primary antibodies (see table 2.3.7) made up in PBST, 1% BSA and azide were applied typically for 1 hour at room temperature (RT). The membranes were then washed in PBST on a fast-moving rocker for 15 minutes (x3-5), and incubated with the corresponding secondary antibodies conjugated to horseradish peroxidase (HRP) in PBST supplemented with 1% BSA for 30 minutes at RT. For the sheep polyclonal anti-ARAP3 antibody PBST was supplemented with additional 1% non-fat milk in the wash buffer for 10 minute washes (x5). The membranes were washed a further 3x in PBST before incubating with an enhanced chemiluminescence (ECL) substrate (Millipore) for 5 minutes at RT. A Photon Ecomax Automatic developer was used to detect chemiluminescence with an x-ray film.

Films were scanned, and for a quantitative analysis, densitometry measurements were determined for the bands of interest using ImageJ.

Primary Antibody	Clone/Type	Dilution	Supplier
anti-ARAP3	Sheep antiserum	1:3000 (1:400 for IP)	Home-made (Krugmann et al Mol Cell 2002)
anti-ARAP3	Rat monoclonal	1:500 (1:1 for IP)	Home-made (Gambardella & Vermeren unpublished)
anti-Erk Thr202/Tyr204	Mouse monoclonal clone E10	1:1000	Cell Signaling Technology (London, UK)
anti-HSP90	Mouse monoclonal clone 3H3C27	1:4000	BioLegend (London, UK)
anti-PKB	Rabbit monoclonal clone 11E7	1:1000	Cell Signaling Technology (London, UK)
anti-PKB S473 biotinylated	Rabbit monoclonal clone D9E	1:3000	Cell Signaling Technology (London, UK)
anti-PKB T308	Rabbit monoclonal clone D25E6	1:1000	Cell Signaling Technology (London, UK)
anti-PTEN	Rabbit monoclonal clone D4.3	1:1000	Cell Signaling Technology (London, UK)
anti-SHIP1	Mouse monoclonal clone PICI-A5	1:1000	BioLegend (London, UK)
anti-SHIP2	Sheep polyclonal AF5389	1:500	R&D Systems (Abingdon, UK)
Secondary Antibodies and Conjugated Streptavidin			
anti-Sheep HRP-conjugated		1:3000	Bio-Rad
anti-Mouse HRP-conjugated		1:2000	Bio-Rad
anti-Rabbit HRP-conjugated		1:3000	Santa Cruz Biotechnology
anti-Rat HRP-conjugated		1:2000	Invitrogen
streptavidin HRP-conjugated		1:3000	BioLegend

Table 2.3.7 A table of the antibodies used for Western blot analysis.

2.4 Neutrophil Functional Assays

In this section, the different methods used to analyse neutrophil functions are described. The buffers and solutions are shown in table 2.4.0.1 while the inhibitors used are shown in table 2.4.0.2.

Buffers and Solutions	**Composition**
5x Paraformaldehyde	4% PFA, 100 mM PIPES (pH 6.8), 2 mM EGTA, 2 mM $MgCl_2$
$HBSS^{++/++}$	HBSS with Ca^{++} and Mg^{++} supplemented with 15mM HEPES (pH7.4) and 0.05% fatty acid and endotoxin-free BSA

Table 2.4.0.1 Buffer compositions used in neutrophil functional assays.

Inhibitor	**Target**	**Final Concentration**	**Supplier**
CZC24832	PI3K γ	2 μM	Sigma
IC87114	PI3K δ	1 μM	Sigma
MK-886	LTB4	100 nM	Cayman
SF1670	PTEN	250 nM	Cayman Chemical Company

Table 2.4.0.2 A table of the inhibitors used in the functional assays.

2.4.1 Chemotaxis Assays

Mouse BM neutrophils were resuspended in $HBSS^{++/++}$ with TNF-α (R&D systems, 1000 U/mL) and GM-CSF (BioLegend, 100 ng/μL) for priming at a concentration of $15x10^6$ cells/ml. The cells were then pipetted into Eppendorf tubes and placed into a dark zip lock bag to slowly rotate at 4°C for 45 minutes. Next, a collagen gel mixture was prepared by gently mixing: 2.5 μl sodium

bicarbonate buffer (Sigma S7861), 5 µl of 10 x HBSS including Ca^{++} and Mg^{++} (Gibco), and 37.5 µl of collagen (from rat tail, Roche, 10 mg in 3.3 ml 0.2% acetic acid) while avoiding the formation of bubbles. The cells were resuspended in $HBSS^{++/++}$ (at $15x10^6$ cells/ml) with either PI3K γ inhibitor CZC24832, PI3K δ inhibitor IC87114, or DMSO for vehicle controls (table 2.4.0.2). 17.5 µl of neutrophils were added to the gel mixture, which was gently pipetted up and down to mix.

Subsequently, an Ibidi chemotaxis chamber (Ibidi, µ-slide) was set up by plugging the outer ports, and a wide P20 filter tip (Greiner Bio) was used to apply 6 µl of the gel mixture into filling port A which is connected to the channel. Immediately after, the same pipette tip was placed tightly into port B to aspirate the air allowing the gel mixture in port A to be sucked homogeneously into the channel. The plugs on the outer ports were removed, and 2 new ones placed into ports A and B. The chamber was then incubated at 37°C for 20 minutes in a humidified, CO_2-controlled incubator for polymerisation to occur. 65 µl of $HBSS^{++/++}$ was used to fill the first reservoir by injecting port C while keeping the chamber at an angle and slightly elevated at the top to prevent the formation of air bubbles. The same was carried out for the second reservoir which contained fMLP (300 nM). The chamber was then placed into a 37°C preheated Evos FL Auto 2 cell imaging system for the simultaneous time lapse imaging of all 3 slots per slide. Images were taken every 15 s for 30 minutes. Figure 2.4.1 is a diagram of the µ-slide and a visual representation of the chambers and ports.

The images from each sequence were stacked using ImageJ and the cells tracked using the ‘manual track’ plugin into ImageJ. Tracks were analysed using the chemotaxis tool plugin into ImageJ (Ibidi)

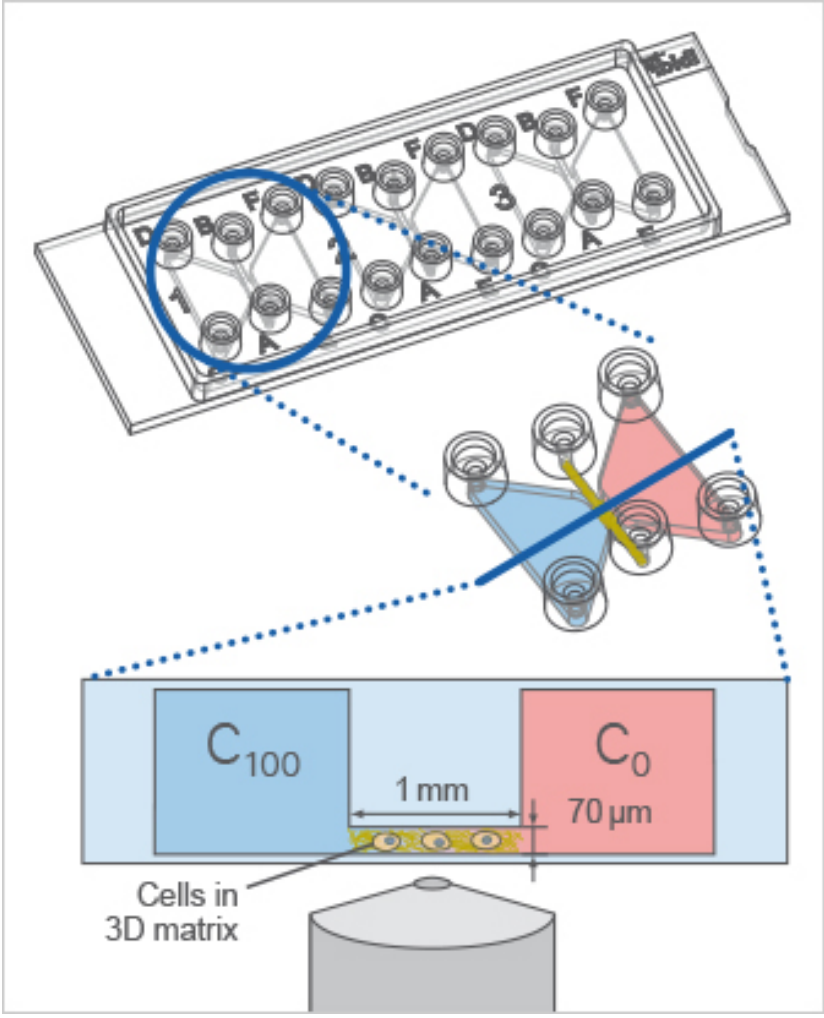

Figure 2.4.1 IBIDI µ-slide chemotaxis. A diagram showing the layout of the IBIDI µ-slide, image from [175].

2.4.2. Total ROS Production Assays by Chemiluminescence

Reactive oxygen species (ROS) production was measured by chemiluminescence in luminescence-grade 96-well plates (Nunc). For this, neutrophils were incubated in PBS^{++} with or without the appropriate inhibitors for 10 minutes in a water bath at 37˚C. For the measurement of total ROS production, luminol (150 µM) and HRP (18.75 U/ml) were added, and 180 µl of the mixture then pipetted into wells containing a stimulus of interest in a total volume of 20ul PBS^{++} for a final amount of $5x10^5$ neutrophils per well. A Cytation plate reader (BioTek) was used to record the light emission at the highest interval frequency.

To coat the wells with immobilised immune complexes (IgG-BSA), the wells were coated with fatty-acid and endotoxin-free BSA (100 µg/mL) overnight at 4˚C. The following day, they were blocked with 1% non-fat milk for 45 minutes, washed with PBS (x3), incubated with anti-BSA antibody (Sigma B7276, 1:2000) for 1h and washed again with PBS (x2). Finally, for fMLP stimulation (1 µM), the neutrophils were primed or mock primed with TNF-α (R&D systems, 1000U/mL) and GM-CSF (BioLegend, 100 ng/µL) for 1h prior to incubating with inhibitor.

2.4.3 Internal ROS Production and Elastase Release Measurements by Fluorescence

Freshly isolated neutrophils were resuspended at $1x10^6$/ml in RPMI supplemented with 10% FCS. 50 µl of neutrophils were added to wells in black 96 well plates (Greiner FLUOTRAC Microplate), followed by another 50 µl of media for mock priming or LPS (O26:B6, Sigma) at 50ng/ml for priming. The plate was sealed with adhesive sealing tape and incubated at 37°C, 5% CO_2 for 30 minutes. 50 µl of media was then added to the unstimulated conditions or 50 µl of 3 µM fMLF was added to the stimulated conditions. This was followed by another 50 µl of the Dihydrorhodamine 123 substrate (Sigma Aldrich) to all wells measuring internal ROS production, or 50 µl of the elastase substrate (CBZ-Ala-Ala-Ala-Ala)2-R110 (Invitrogen) to all wells measuring elastase release. A Molecular Devices SpectraMax i3 plate reader was used to monitor fluorescence (485nm excitation and 535nm emission wavelengths for ROS measurements, or 485nm excitation and 535nm emission wavelengths for elastase measurements) kinetically taking readings every 30 s for 30 minutes with a 5 s mix before the first read. Results were plotted and the gradients of the slopes determined for each condition.

2.4.4 Internalisation Assays

First, the neutrophils were primed in PBS^{++} with TNF-α (R&D systems, 1000 U/mL) and GM-CSF (BioLegend, 100 ng/µL) for 45 minutes at 37˚C. Rabbit IgG-opsonised 0.8 µm latex beads (both Sigma) were then added to $0.5x10^6$ neutrophils (ratio of 5:1) in 2 ml Eppendorf tubes for each condition for a final

volume of 100 µl. The tubes were pulse spun in a minifuge for 15 seconds to bring the cells into close contact with the beads, kept for 40 seconds in a 37℃ water bath, and then resuspended by gentle pipetting. Cells were then further incubated for 20 minutes at 37˚C. Cells were allowed to adhere onto electrostatically coated coverslips for 1h on ice, gently washed with PBS^{++}, fixed with 2% paraformaldehyde (PFA) for 10 minutes, and washed a further 3 times. Next, the samples were stained with anti-Rabbit Alexa Fluor 568 (see table 2.4.5.2) for 30 min at room temperature to stain uninternalised beads. After washing, cells were permeabilised with 0.1% Triton X-100 for 10 minutes, and stained again with anti-Rabbit Alexa Fluor 488 (see table 2.4.5.2) for 30 min at RT to stain all the beads. The slides were washed, mounted with ProLong Gold antifade mount (Invitrogen, thermo scientific) and finally imaged at ×20 magnification with an Evos cell imaging system (AMG) to manually record the percentage of cells that had internalised as well as the number of internalised beads per cell.

2.4.5 Immunofluorescence

2.4.5.1 Stimulations of Adherent and Suspension Neutrophils

For adherent cells, $1x10^6$ neutrophils were allowed to attach onto glass coverslips for 10 minutes at RT. In some cases, this step was performed in the presence of the inhibitor SF1670 (see table 2.4.0.2) or its vehicle in a humidified CO_2 -controlled incubator. Cells were then stimulated with PBS^{++} that did or did not contain fMLP (1 µM final concentration). After 5 minutes the

stimulus was aspirated and the cells fixed in 2% PFA for 10 minutes and washed three times.

Cells in suspension (50µL neutrophils (at $20x10^6$/mL) in Eppendorf tubes) were stimulated with 50µL PBS that did or did not contain fMLP (1µM final) and incubated for 10 minutes. The stimulation was terminated with 100µL of 2% PFA, and after a further 10 minutes the cells were washed three times by centrifugation in a minifuge and careful aspiration.

2.4.5.2 Immunocytochemistry

For PI(3,4)P2 staining, neutrophils were permeabilised with 0.5% Saponin for 15 minutes (or 10 minutes for cells in suspension), washed twice with PBS and then incubated with primary antibody (Z-B034 Echelon) in PBS supplemented with 1% BSA for 1h at room temperature. Afterwards, the samples were washed three times in PBS, and streptavidin Alexa Fluor-647 combined with AF488-conjugated phalloidin in PBS supplemented with 1% BSA was added for 30 minutes. For GR1 labelling, neutrophils were permeabilised with 0.1% Triton X-100 for 10 mins, washed twice in PBS, and incubated with FITC conjugated anti-mouse Ly-6G/Ly-6C (Gr-1) in PBS supplemented with 1% BSA for 45 mins at room temperature. Next, the samples were washed three times in PBS and a secondary antibody was added to enhance the FITC signal with anti-Rat Alexa Fluor 488 combined with AF568-conjugated phalloidin for 30 minutes, followed by a further 3 washes.

Adherent cells were then counterstained for 5 minutes with Hoechst, washed and mounted with ProLong Gold antifade mount. Fixed cells in suspension

were placed onto electrostatic slides (Superfrost plus, Thermo Scientific) for 1h first for adhesion and then treated similarly. Slides were stored in the dark at 4˚C until they were imaged, after which they were stored long term in -20˚C. Figure 2.4.5.2 is a table of the antibodies used for immunofluorescence.

Primary Antibody	Clone/Type	Dilution	Supplier
biotinylated anti-PI(3,4)P2	z-B034	1:150	Echelon Biosciences (Salt Lake City, UT, USA)
FITC-conjugated anti-mouse Ly-6G/Ly-6C (Gr-1)	RB6-8C5	1:300	BioLegend (London, UK)
Fluorescently conjugated secondary antibodies and fluorescent dyes			
AF488-conjugated phalloidin		1:40	Thermo Fisher Scientific (Loughborough, UK)
AF568-conjugated phalloidin		1:40	Thermo Fisher Scientific (Loughborough, UK)
streptavidin-AF647		1:1500	Thermo Fisher Scientific (Loughborough, UK)
Hoechst 33342		1:10,000	Thermo Fisher Scientific (Loughborough, UK)
anti-Rabbit Alexa Fluor 568		1:400	Thermo Fisher Scientific (Loughborough, UK)
anti-Rabbit Alexa Fluor 488		1:400	Thermo Fisher Scientific (Loughborough, UK)
anti-Rat Alexa Fluor 488		1:1000	Thermo Fisher Scientific (Loughborough, UK)

Table 2.4.5.2 A table of the antibodies used for immunofluorescence.

2.4.5.3 Microscopy

Once slides had cured, images at randomly selected positions were acquired using an inverted widefield Zeiss Observer or Nikon TiE microscope, keeping the settings constant between the conditions. For cells in suspension, stacks

were taken. In addition, images of representative cells were captured as single slices or stacks with the Leica TCS SP8 confocal microscope.

2.4.5.4 Image Analysis

Images were processed using the image analysis software CellProfiler, and all pipelines used were built and provided by Dr Matthieu Vermeren. A pipeline was built to measure fluorescence intensity of PI(3,4)P2 signal for n>175 neutrophils. Another pipeline was built to measure cell size and cell shape for n=50 neutrophils. Stacks of cells in suspension were first deconvolved by Huygens software before processing them through the CellProfiler pipeline. Confocal images were processed with ImageJ.

2.4.6 Swarming Assays

Freshly isolated neutrophils were resuspended in IMDM (Gibco, no phenol red) with 20% FBS (Gibco, A3160801, non-heat inactivated). Cells at a final concentration of $2.5x10^6$/ml were incubated at 37°C, depending on the condition some were incubated with Hoechst and/or MK886 inhibitor (see table 2.4.0.2). A multi-chamber dish was assembled from a glass slide containing immobilised Texas red-labelled zymosan clusters using a clip-on 16 well slide module (Grace Bio-labs) as described in detail [176]. All slides used in this thesis with immobilized zymosan clusters were kindly provided by Dr Alex Hopke (Harvard Medical School, Boston, USA). Chamber slides were placed into a humidified, temperature (37°C) and CO_2-controlled heated stage, either using a Zeiss observer or the Nikon TiE microscope. The microscope was set up for time lapse imaging (x20 magnification) in brightfield, or fluorescent

detection of Hoechst at 480 nm at 5-minute intervals for 2 hours, acquiring images of 10 separate swarms per well (and per condition) by making use of the multipoint functionality. 200µL of cells were then carefully pipetted into the appropriate wells and time lapse imaging was initiated within seconds. To analyse the images, a macro was created in ImageJ to measure fluorescence signal intensity of the swarm, indicative of the relative amount of cells present. For brightfield images, another macro was written by Dr Matthieu Vermeren to measure swarm size. Upon completion of the time lapse imaging, supernatants were collected, clarified by centrifugation, snap frozen and stored at -80°C for cytokine analysis.

2.4.6.1 Cytokine Analysis

Cytokine analysis was carried out using a human magnetic Luminex assay kit (Catalog #LXSAHM-09) as per manufacturer's instructions and read with a Bio-Rad analyser. Only cytokines with values above the lower limit of quantification (LLOQ) were further analysed. Figure 2.4.6.1 shows 2 examples: Galectin-3 with all values within detection range, and GCSF with all values below the LLOQ.

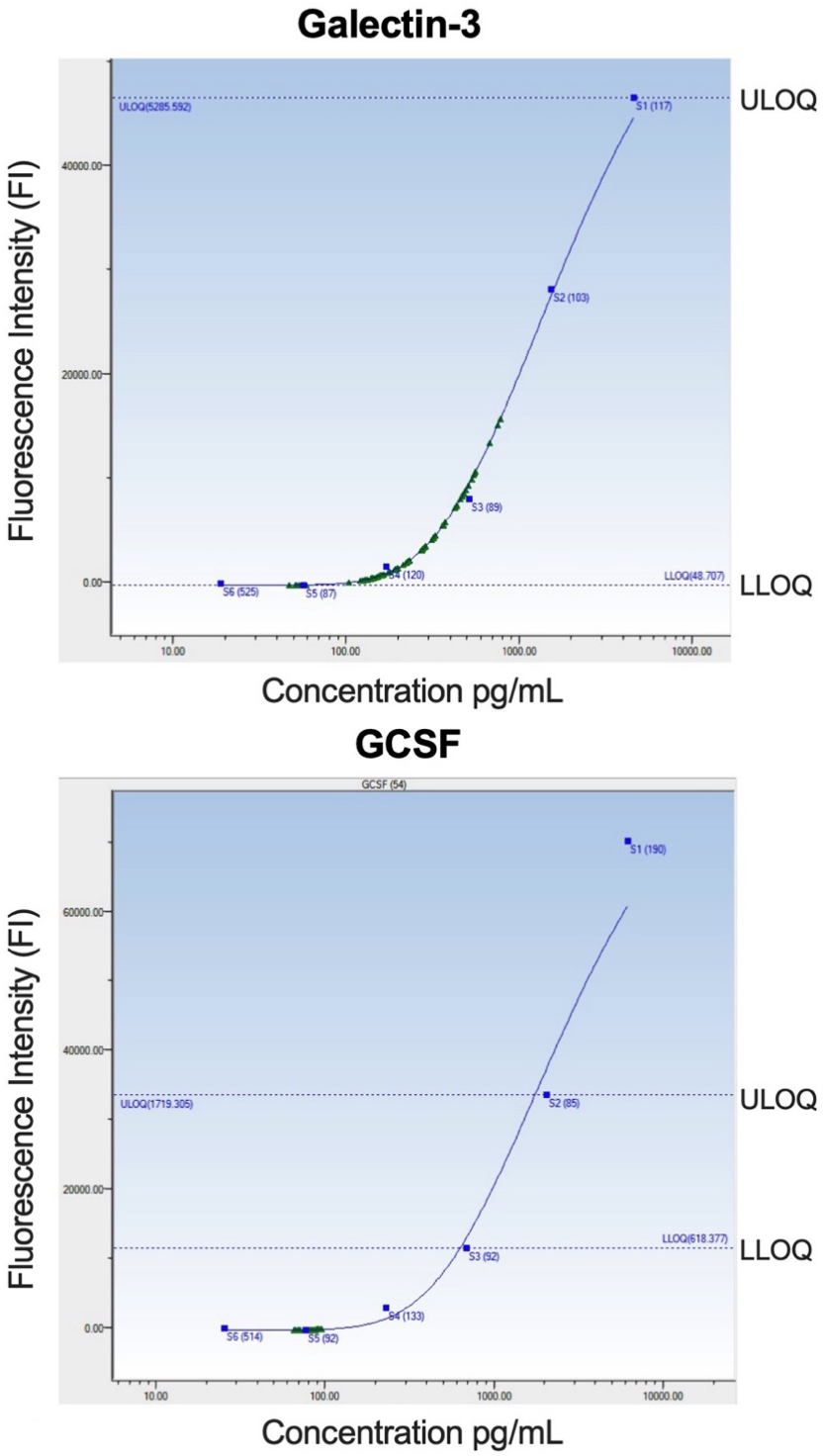

Figure 2.4.6.1 Standard curves for Luminex cytokine analysis. Standard curves for Galectin-3 and GCSF, individual values plotted. Unlike GCSF, all values for Galectin-3 were within the detection range.

2.5 Mammalian Cell Culture

Unless otherwise stated, all culture medium and supplements were purchased from Gibco and the cell culture plastics were from Corning. To wash the cells or to pellet for resuspension, they were centrifuged at 300 g for 5 minutes at room temperature.

2.5.1 Thawing and Freezing Down Cells

Cells in cryovials were brought up from liquid nitrogen on dry ice and allowed to thaw in a 37˚C water bath. Cells were washed in 15 ml falcon tubes with 10 ml of the corresponding prewarmed medium and finally resuspended in the final required volume of fresh culturing medium.

To freeze down cells, pre-cooled freezing medium was used (90% FBS and 10% Dimethyl sulfoxide) to resuspend pelleted cells. 500 µl aliquots containing $1x10^7$ cells were pipetted into prelabelled cryovials on ice, placed into a polystyrene box (Eprak) such that they were spaced out and did not touch the wall of the box and allowed to freeze slowly in a -80˚C freezer. Cryovials were moved to liquid nitrogen for long-term storage.

2.5.2 Culturing and Passaging of Adherent Cells

The Plat-E retroviral packaging cell line was cultured in complete Dulbecco's Modified Eagle's Medium (DMEM) supplemented with 10% HI-FBS, 1% glutamine and 1% Penicillin/Streptomycin, in T75 flasks at 37℃ in a humidified cell culture incubator with 5% CO_2. 60-80% confluent cells were passaged

using trypsin-EDTA (Gibco). Prior to being transfected, cells were cultured for a minimum of one week.

2.5.3 Culturing and Inducing HoxB8 Cells

HoxB8 progenitor cells were cultured in complete Roswell Park Memorial Institute (RPMI-1640) medium supplemented with 10% HI-FBS, 1% glutamine and 1% Penicillin/Streptomycin, 1 µM β-estradiol and 10 ng/ml GM-CSF as described [177], in cell culture dishes kept at 37℃ in a humidified cell culture incubator with 5% CO_2. The cells were split 1:4 every other day and cultured for at least one week before inducing differentiation or transduction. To induce granulocytic differentiation, 2 ml of progenitor cells were washed twice with D-PBS and left undisturbed in the incubator for 5 days in T75 flasks with 25ml of complete RPMI medium lacking β-estradiol. The percentage of differentiated neutrophils was determined by staining cytospins with the Reastain Quick Diff kit.

2.5.4 Transfection of PLAT-E to Generate Retroviruses

To generate retroviruses, $3x10^6$ Plat-E cells were seeded in 10 cm dishes in 15 ml medium. The following day two solutions were prepared for the transfection according to manufacturer's instructions (CalPhos 631312, Clontech). Solution A contained 15 µg plasmid DNA (mCherry-SHIP2) and 62 µl 2M Calcium solution made up to 500 ml with sterile H_2O. Solution B consisted of 500 µl of 2x HBS. Solution A was gently vortexed with solution B added dropwise, and the mixture left at RT (room temperature) for 10 minutes. Next, the transfection mixture was added to the dish, evenly distributed and

incubated overnight. The next morning (~14 hours later), retroviruses were harvested.

2.5.5 Transductions of HoxB8 Cells

Non-tissue culture treated 6 well plates were coated with 12.5 µg/ml retronectin (Clontech) for 2 hours at 37℃. The wells were then blocked with 2% fatty acid free BSA for 10 minutes at room temperature and 10 minutes at 37℃ before washing twice with PBS. In the meantime, HoxB8 cells were resuspended at $2x10^6$/ml in complete HoxB8 medium supplemented with a final concentration of 5 µg/ml polybrene. In each well, 500 µl of cells were combined with 1500 µl of lentiviral or retroviral supernatant and spinoculated at 1000g for 40 minutes at room temperature. Next, the medium was carefully removed, replaced with fresh complete HoxB8 medium and incubated for 2-3 days before selection.

2.5.6 Generation of mCherry Tagged SHIP2 HoxB8s

WT and *Arap3*$^{-/-}$ HoxB8 progenitors were generated from WT and *Arap3*$^{-/-}$ mice respectively (Figure 2.5.6 A). To generate HoxB8 progenitors, bone marrow cells from hind legs were flushed using PBS (without Mg^{2+} or Ca^{2+}) and centrifuged at 300g for 5 minutes at room temperature. Pelleted cells were then resuspended in PBS at 40µl/10^7 cells and the Lin^+ cells stained for negative selection as per manufacturer's instructions (Lineage Cell depletion Kit, Miltenyi Biotech 130-090-858). Using a magnetic column (LS, Miltenyi Biotech 130-042-401), Lin^- cells were collected, pelleted and resuspended at $1x10^6$ cells/ml in IMDM + 15% HI-FCS + 10 ng / ml IL-3 + 20ng / ml IL-6 + 25 ng / ml SCF. $1x10^6$ cells were placed in a 6 well plate and left to incubate for 3

days to grow. The cells were then transduced with the ER-HoxB8 retrovirus as detailed in 2.5.5. On the second day following transduction, the cells were selected by adding G418 (0.6 mg/ml) to the HoxB8 growth medium for 6 days after which the G418 was removed.

WT and *Arap3*$^{-/-}$ HoxB8 cells were then retrovirally transduced and mCherry expression cells enriched by fluorescence-activated cell sorting (FACS) (Figure 2.5.6 B). Once the pooled sorted cells had recovered and started rapidly dividing, the progenitors were scanned for clones expressing detectible mCherry by fluorescence microscopy. Clones that produced the highest percentages of HoxB8 neutrophils upon estradiol withdrawal were selected for imaging.

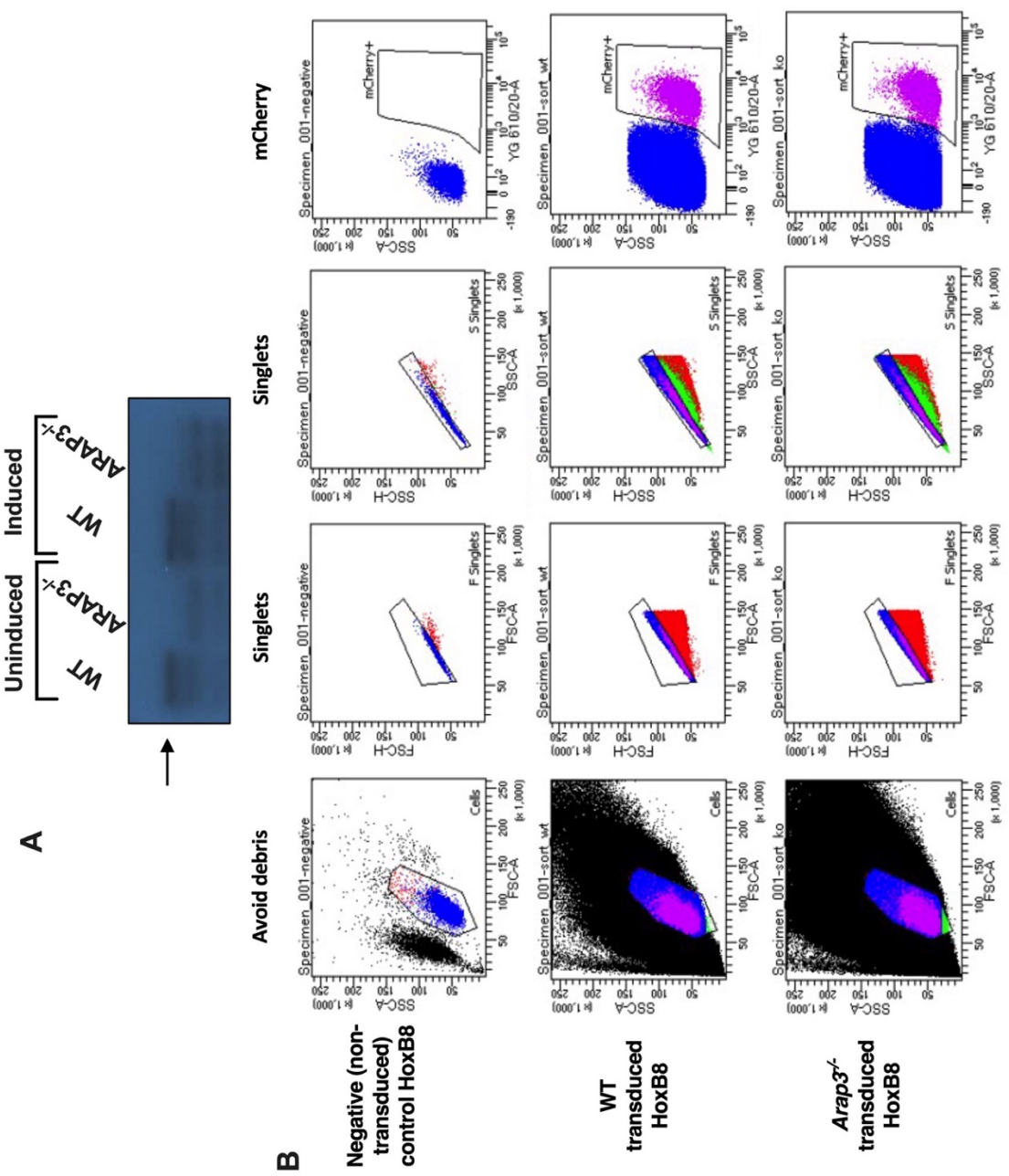

Figure 2.5.6 Generating HoxB8 cells with mCherry tagged SHIP2. (A) anti-ARAP3 Western blot comparing WT control to ARAP3 deficient HoxB8 progenitors and HoxB8 neutrophils. **(B)** Selection of HoxB8 progenitor populations that had been transduced to express mCherry-SHIP2 analysed by FACS sorting (gating was done by cell sorting facility).

2.6 Statistical Analysis

If assumptions for a parametric test were met, two-tailed Student's t-tests, paired t-tests, one-way or 2-way ANOVAs with multi-comparison post-hoc tests were applied. If not, then non-parametric Mann-Whitney tests or Kruskal-Wallis tests were performed. For kinetic experiments, the area under the curve was analysed. All statistical analysis was carried out in Graph Pad Prism 9, and p values less than 0.05 was considered statistically significant.

3. Results - Analysis of PI3K Dependent Control of Immunosenescence in the Neutrophil

3.1 Introduction

As part of the innate immune system which forms the first line of defence against pathogens, it is important that neutrophils reach the sites of infection efficiently. Having decreased migratory accuracy means that neutrophils are less likely to achieve this and ultimately eliminate invading pathogens. In addition, meandering neutrophils with decreased migratory accuracy might also promote inflammation and widespread tissue damage since neutrophils are known to release proteases into the extracellular milieu and mobilise neutrophil elastase to the cell surface at the pseudopod, which cleaves matrix proteins as they migrate [178]. Neutrophils from elderly donors were shown to migrate less accurately towards a range of stimuli [120, 179, 180], which could (at least partially) explain why the elderly have increased susceptibility to infections, as well as increased tissue injury and systemic inflammation. One study suggested that dysregulated PI3K signalling in the neutrophils from elderly donors was responsible for the poor directionality since this was improved upon inhibiting PI3K delta/gamma [120], however, which proteins downstream of PI3K might be responsible remains to be shown.

The Vermeren lab has previously demonstrated that ARAP3, a PI3K effector protein, is an important regulator of several neutrophil functions [122]. One example was directionality in chemotaxis determined by using ARAP3-

deficient neutrophils, or those in which ARAP3 was uncoupled from activation by PI3K, both of which were characterised by meandering/ non-persistent polarisation [123]. The resemblance between the chemotaxis phenotypes of ARAP3 deficient and immunosenescent neutrophils led us to hypothesise that ARAP3 might be involved in the inaccurate migration of neutrophils from elderly donors.

Unlike the majority of PIP3 binding proteins, ARAP3 has five PH domains (Figure 1A). None of the PH domains can bind to PIP3 separately, and the minimum requirement for PIP3 binding comprised the N-terminal linking sequences and two PH domains [181]. Strong binding to PIP3 however required the whole N-terminus which includes the SAM domain. Like other signalling proteins, ARAP3 is subject to regulation by post-translational modifications such as phosphorylation. Both serine/threonine and tyrosine residue phosphorylation sites have been identified, with some found to be phosphorylated in a stimulation-dependent fashion [182]. Figure 3.1B summarises the reported phosphorylation sites on ARAP3, some of which map to the PH domains.

The aim of my original project was to characterise ARAP3's phosphorylation status, comparing stimulated to unstimulated samples by immunoprecipitation followed by phospho-proteomics. Next, I planned to compare stimulated and unstimulated samples from young vs elderly donors and infer the putative functions of ARAP3 in the chemotaxis defects observed in immunosenescent neutrophils. To complement this, I also intended to uncover the effects of the

individual phosphorylation sites on the PIP3-regulated catalytic activities of ARAP3 by site-directed mutagenesis combined with transient transfection experiments. Eventually, to detect catalytically active ARAP3, phosphospecific antibodies were to be raised to the uncovered biomarkers. Unfortunately however, in this chapter I show that despite all my efforts, I was unable to successfully isolate ARAP3 from human neutrophils.

Hypothesis

I hypothesized that the phosphorylation status of ARAP3 differs between neutrophils from young and elderly donors, thereby differentially regulating ARAP3 activity and neutrophil functions in these cells.

Chapter-specific aims

The aim of this chapter was to determine and compare the phosphorylation status and individual phosphorylation sites of ARAP3 in neutrophils isolated from young and elderly donors. I further aimed to determine the catalytic effects of individual phosphorylation sites on ARAP3. Specific initial aims include:

1) To detect ARAP3 from human neutrophils isolated from peripheral blood

2) To immunoprecipitate ARAP3 from these neutrophils

3) To determine ARAP3 phosphorylation sites by mass spectrometry, with and without neutrophil activation with fMLF and other chemoattractants

e.g. CXCL8/IL-8 and LTB4 with neutrophils isolated from young and elderly donors.

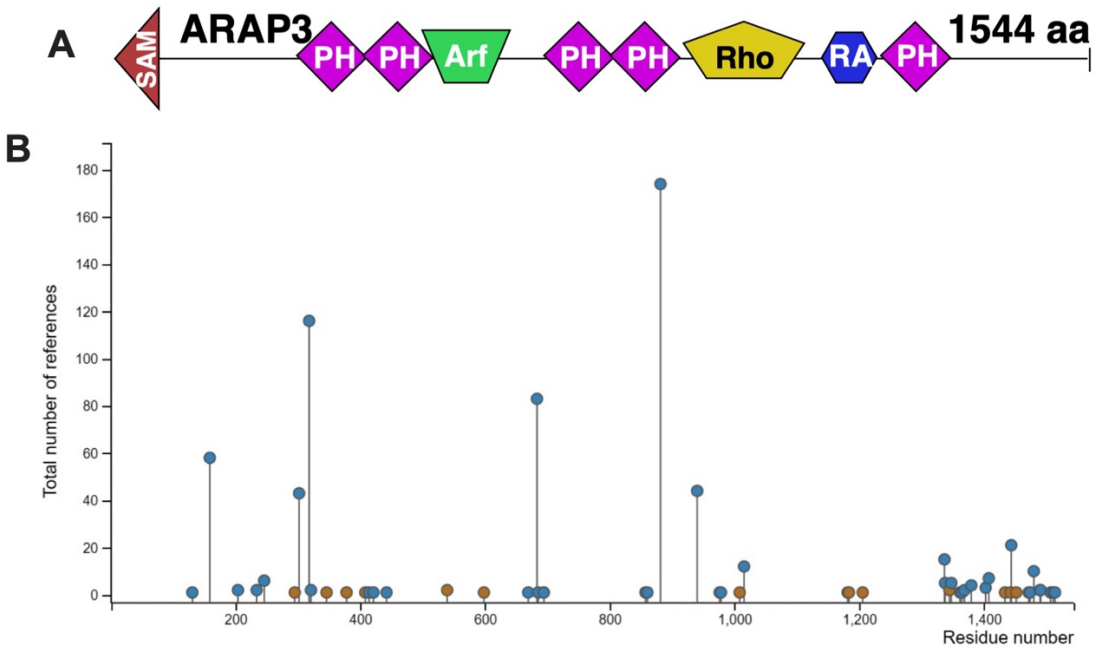

Figure 3.1 Determined phosphorylation sites of ARAP3. (A) Schematic diagram of the domain structures of ARAP3, adapted from [181]. **(B)** Graph showing reported phosphorylation sites (blue) and ubiquitination sites (orange) of ARAP3, including the number of references generated for each residue in the literature [183].

3.2 Results

3.2.1 Detection of ARAP3 in Human Neutrophils

Constituting a large proportion of the circulating leukocytes in humans, neutrophils are key players in the elimination of invading pathogens and microbial threats. To carry out their roles as the body's first line of defense, neutrophils generate antimicrobial peptides and potent proteases which can be released from granules in a controlled manner [28]. When the neutrophils are lysed for the detection of proteins within, the powerful proteases are released, degrading the contents of the lysate and making the biochemical analysis of these proteins, in particular those that are susceptible to proteolysis, very challenging. ARAP3 is a protein that is very susceptible to proteolysis (data not shown).

My first aim was to detect ARAP3 in human neutrophils. Three different methods were employed (see figure 3.2.1). The first is a standard method in the CIR which involved neutrophil lysis in the presence of a large amount of antiproteases [184]. The second method involved resuspending a pellet or neutrophils in boiling sample buffer and using a syringe to shear the DNA. The third method entailed boiling cells in hot modified Laemmli sample buffer (including extra β-mercaptoethanol and antiproteases) [185]. These methods were compared with fresh samples and snap frozen samples, with and without subjecting the cells for treatment with DFP, a powerful serine protease inhibitor [186].

A

Lysis Buffer (1)	4x Sample Buffer (2)	2x Modified Laemmli Buffer (3)
780 µl 1x TBS	160 mM Tris-HCl (pH6.8)	62.5 mM Tris-HCl (pH 6.8)
10 µl 10% NP-40	8% SDS	4% SDS
20 µl Protease cocktail	0.4M DTT	5% β-mercaptoethanol
20 µl AEBSF	50% Glycerol	8.5% Glycerol
20 µl Aprotinin	0.012% Bromophenol blue	0.025% Bromophenol blue
20 µl Leupeptin		2.5 mM Na3VO4
20 µl Benzamidine		10 µg/ml Leupeptin
20 µl Na3VO4		10 µg/ml Aprotinin
40 µl Pepstatin A		
20 µl Levamisole		
60 µl β-Glycerophosphate		

B

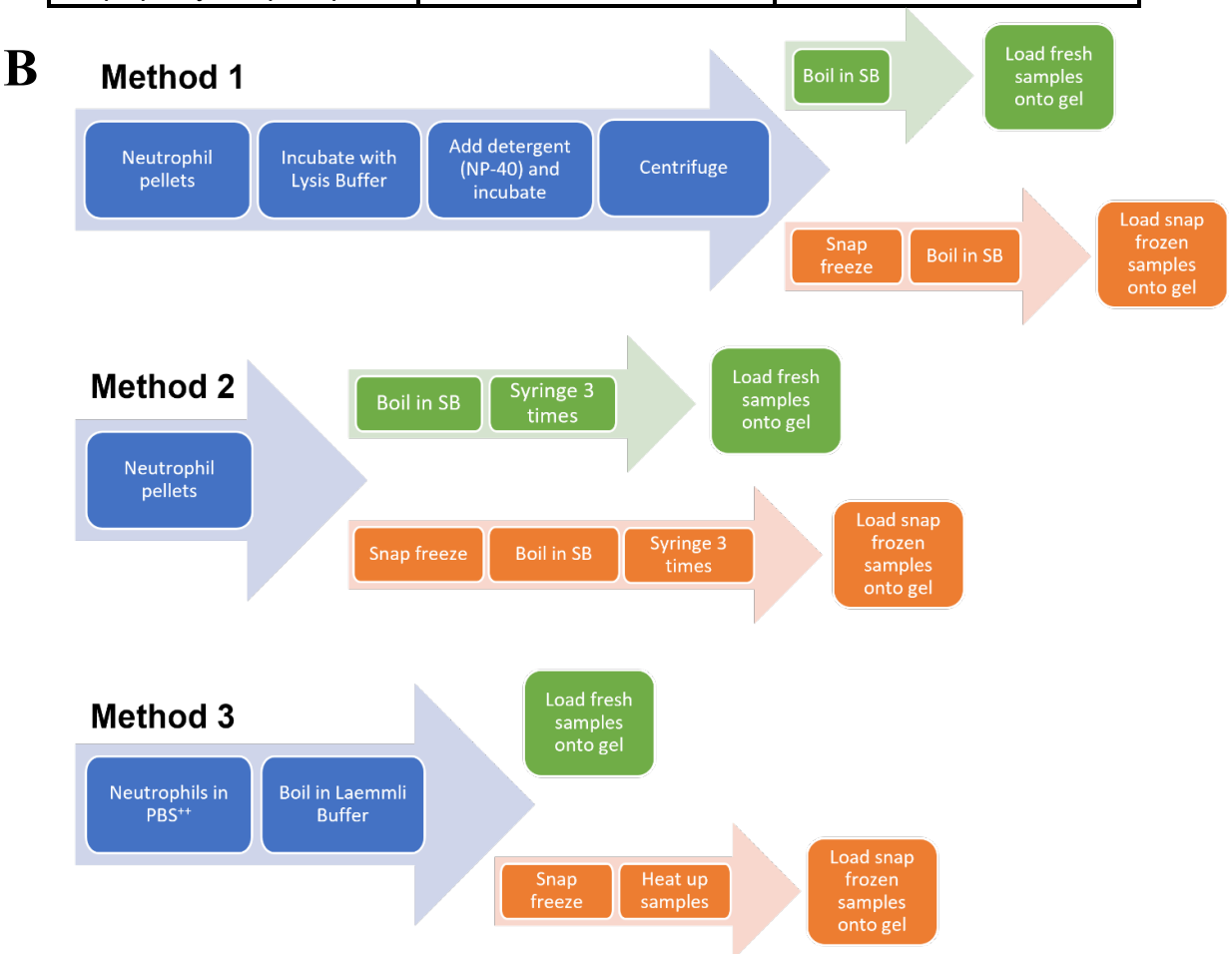

Figure 3.2.1.1 Optimisation of the detection of ARAP3 using 3 different methods. (A) Table of buffer compositions to make up the lysis buffer, sample buffer and the 2x modified Laemmli buffer and **(B)** a flow chart of the experimental protocol to prepare fresh (green) and snap frozen (orange) samples for each method.

Figure 3.2.1.2 shows that the first method was the least effective for the preservation of ARAP3 in human neutrophils, leading to complete loss of all protein in the absence of DFP even without prior snap freezing of the cells. This is likely due to the long incubation and centrifugation times employed which inadvertently allow for the degradation of ARAP3 by the proteases. While boiling fresh neutrophil pellets in sample buffer was successful, the second method led to the loss of most protein when the cells had been snap frozen in liquid nitrogen. Only the third method which involved boiling intact cells with additional reducing agent allowed recovery of ARAP3 after snap freezing of the cells. The experiment demonstrated that DFP aids the preservation and detection of ARAP3 in all methods. Although most ARAP3 was detected in fresh samples, pre-treatment with DFP in method 3 preserved a thick band even with snap frozen samples.

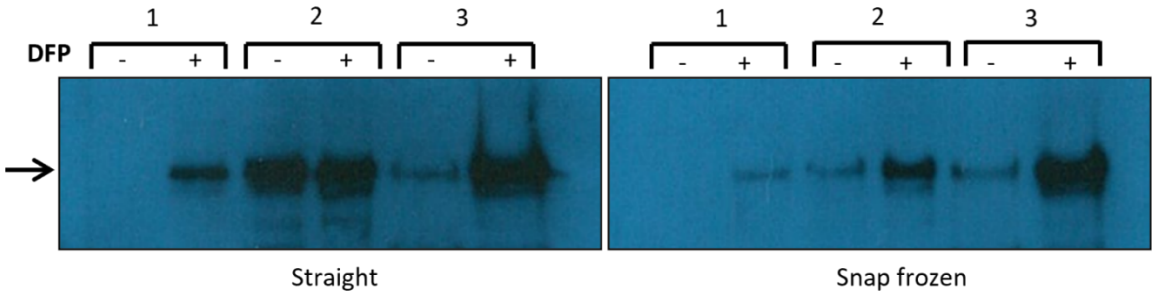

Figure 3.2.1.2 Detection of ARAP3 in human neutrophils by Western blot using the 3 methods. Isolated human neutrophils were or were not incubated with 7mM DFP for 5 minutes at RT prior to it being washed out. Cells were subsequently prepared for SDS-PAGE using 3 different methods (method 1- incubation in buffer containing antiproteases prior to adding detergent, method 2 – pellet resuspended in boiling DTT-containing sample buffer and shearing of DNA while boiling cells, method 3 – boiling of suspension cells in modified Laemmli buffer). The experiment was carried out in duplicates and half of the samples were snap frozen in liquid nitrogen. Fresh and snap frozen samples were then subjected to SDS-PAGE with $5x10^5$ cells loaded per lane followed by Western blotting with affinity-purified ARAP3

3.2.2 Comparing lysis buffers for the isolation of ARAP3

Having determined that ARAP3 from human neutrophils can be detected by Western blotting, I next aimed to isolate the protein by immunoprecipitation (IP). To optimise this, after treating all cells with DFP, three different lysis buffers were tested to establish which is best at preserving ARAP3 during IP (Figure 3.2.2.1 A). Each condition was tested with and without fMLF stimulation, and in duplicates, one was loaded straight after lysis and the other left on ice for 2 hours, corresponding to the time necessary for an IP. In addition to ARAP3, phospho-PKB, phospho-ERK and HSP90 were also detected. The Western blot in Figure 3.2.2.1 B shows that unlike phospho-PKB and phospho-ERK which showed strong bands upon stimulation, only a trace of ARAP3 could be detected, with buffer C preserving the largest amount. As expected, less ARAP3 was detected after incubating the samples on ice.

A

Lysis Buffer A	Lysis Buffer B	Lysis Buffer C
25 mM Hepes (pH 7.4)	20 mM Hepes (pH 7.4)	30 mM Hepes (pH 7.4)
0.1 M NaCl	150 mM NaCl	100 mM NaCl
0.25% NP-40	1% Tx-100	1% Tx-100
2.5 mM EDTA	5 mM EDTA	1 mM EGTA
2.5 mM EGTA	5 mM EGTA	Protease Inhibitor cocktail
2.5 mM Na_3VO_4	1 mM Na_3VO_4	Phosphatase inhibitor cocktail
25 mM β-Glycerophosphate	3 mM β-Glycerophosphate	10 µg/ml Aprotinin
25 mM NaF	30 mM NaF	10 µg/ml Leupeptin
10 µg/ml Aprotinin	10 µg/ml Aprotinin	10 µg/ml Pepstatin A
10 µg/ml Leupeptin	10 µg/ml Leupeptin	10 µg/ml Antipain
10 µg/ml Pepstatin A	10 µg/ml Pepstatin A	0.1 M PMSF
10 µg/ml Antipain	10 µg/ml Antipain	
0.1 M PMSF	0.1 M PMSF	

B

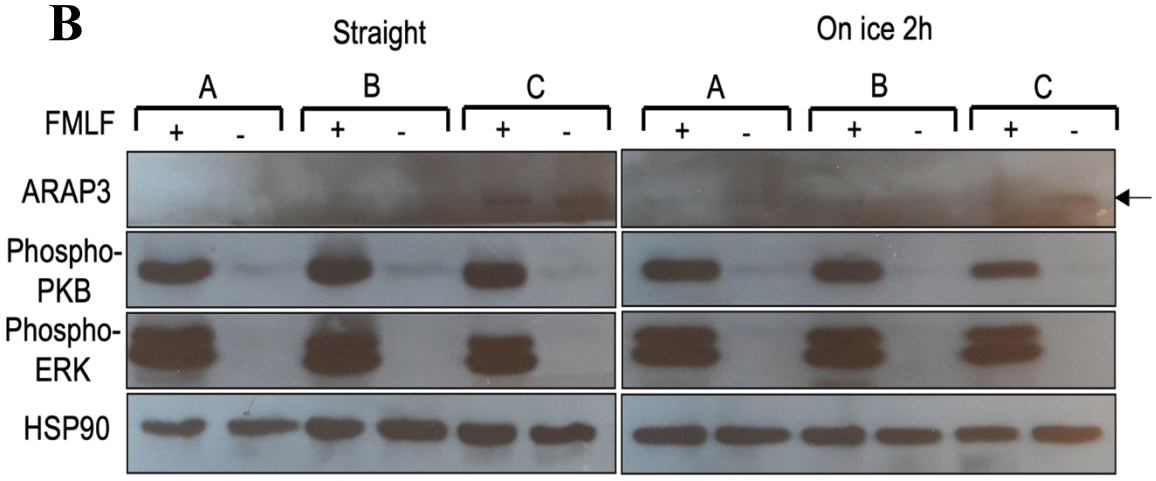

Figure 3.2.2.1 Preservation of ARAP3 with different lysis buffers. (A) Table of buffer compositions to make up the 3 different lysis and IP buffers used. **(B)** Isolated human neutrophils were treated with DFP, stimulated or mock stimulated with fMLF and lysed with ice-cold buffers A, B or C before clarifying the lysates by centrifugation. Half the samples were subjected directly to SDS-PAGE, loading $5x10^5$ cells per lane while the other half were left on ice for 2 hours before loading the gel. This was followed by Western blotting with an affinity purified sheep polyclonal anti-ARAP3 antibody [89].

Next, mouse endothelial cells were used which also express ARAP3, but contain fewer proteases than human neutrophils to IP ARAP3 using buffer C. Two antibodies were used to IP ARAP3 for comparison, namely, the sheep polyclonal and a rat monoclonal that had previously been shown to recognise native mouse ARAP3 protein (Gambardella & Vermeren, unpublished). The Western blot with either of the antibodies contained a band of ARAP3 (not shown), however, on the Coomassie-stained gel a band was only detected in samples that had been subjected to IP with the rat monoclonal antibody as shown in Figure 3.2.2.2, suggesting the rat antibody would be better suited for my purposes.

This showed that buffer C was suitable for the isolation of ARAP3 from mouse endothelial cells by IP, however, my experiments indicated that further optimisation would be required to determine the ideal conditions to prepare stable lysates and IP ARAP3 from human neutrophils while preserving tyrosine phosphorylation.

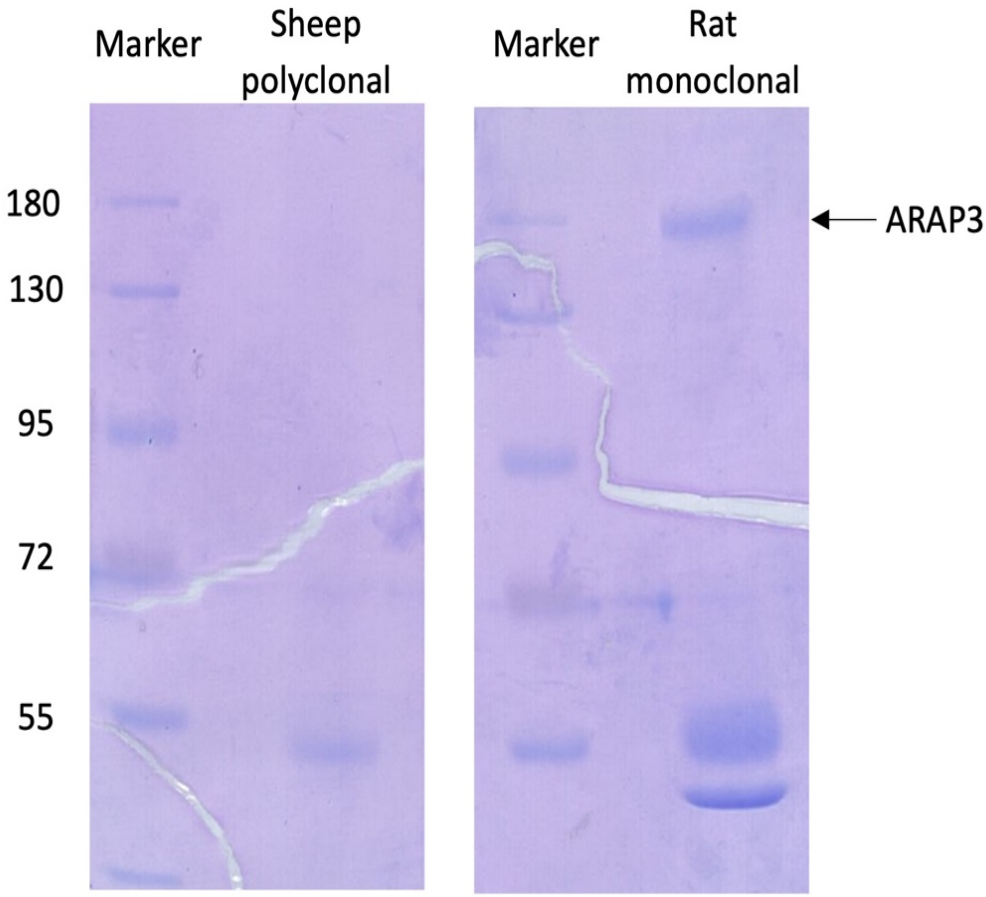

Figure 3.2.2.2 IP of ARAP3 from mouse endothelial cells detected by Coomassie stain. 1x10^7 cells were used to IP ARAP3 with sheep polyclonal and rat monoclonal antibody from mouse endothelial cells. The samples were subjected to SDS-PAGE and the gel was then Coomassie stained. ARAP3 band expected at ~170kD.

3.2.3 Immunoprecipitation of ARAP3 with Denaturing Buffers

Having established that typical lysis buffers (e.g. Figure 3.2.2.1 A) were ill suited for the preservation of ARAP3 from human neutrophils, two denaturing lysis buffers (as described in this study [187]) were investigated next. Naccache and co-workers had shown that lysing DFP-treated neutrophils in hot buffers that contain denaturing and reducing agents, namely SDS and β-mercaptoethanol, prevented the rapid degradation of Cbl, an adaptor that is very susceptible to proteolysis by proteases while preserving its stimulation-induced tyrosine phosphorylation, and allowed this protein to be immunoprecipitated after renaturing. Instead of using detergents Triton X-100 or NP40, buffer D contains 1% SDS and 0.6% β-mercaptoethanol while buffer E contains 3% SDS and 1.5% β-mercaptoethanol, respectively (full buffer compositions shown in Figure 3.2.3.1 A). After cell lysis, the lysates were passed through a desalting column to remove the high concentrations of SDS and β-mercaptoethanol using an elution buffer with antiproteases. The lysates were then used to IP ARAP3, following the experimental scheme shown in Figure 3.2.3.1 B

A

Denaturing Buffer D	**Denaturing Buffer E**	**Elution Buffer**
50 mM Tris HCL pH 8.0	62.5 mM Tris HCL pH 6.8	30 mM Hepes pH 7.4
150 mM NaCl	3% SDS	100 mM NaCl
2mM EDTA	1.5% β-mercaptoethanol	1% Tx-100
50 mM NaF	8.5% Glycerol	1 mM EGTA
20 mM NaP_2O_4	2.5 mM Na_3VO_4	Cocktail Inhibitor (100x)
1% SDS	10 µg/ml leupeptin	Phosphatase inhibitor (100x)
0.6% β-mercaptoethanol	10 µg/ml aprotinin	10 µg/ml Aprotinin
2 mM Na_3VO_4		10 µg/ml Leupeptin
10 µg/ml leupeptin		10 µg/ml Pepstatin A
10 µg/ml aprotinin		10 µg/ml Antipain
1 µM Pepstatin A		0.1 M PMSF
1 mM PMSF		
1 mM *N*-ethylmaleimide		

B

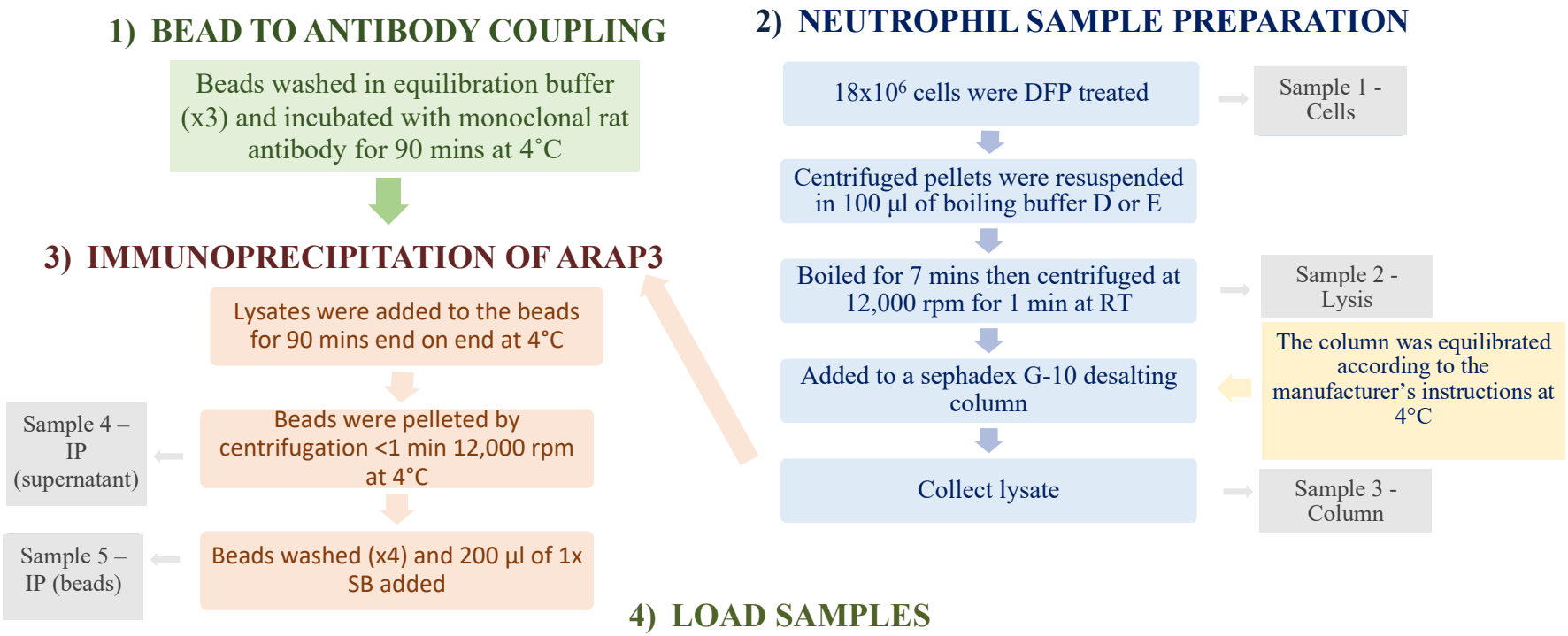

Figure 3.2.3.1 Lysing neutrophils with denaturing buffers to IP. (A) Table of buffer compositions to make up the denaturing buffer D and E. **(B)** Experimental scheme of neutrophil sample preparation and IP using denaturing buffers.

Figure 3.2.3.2 shows a representative Western blot comparing buffers D and E for the IP of ARAP3 using the rat monoclonal antibody from mouse endothelial cells. Although ARAP3 was detected after lysis and after exchanging buffers through the column, the protein was mostly lost or degraded with only extremely faint bands detected in the supernatant after IP and on the beads themselves.

The lysates prepared with buffer D were very gloopy. Some of the ARAP3 protein may have gotten stuck on the desalting column, explaining why the IP was not successful. The failure of buffer E may be due to the inability of the antibody to recognise ARAP3 after being denatured, or the inability to renature ARAP3. This hypothesis is corroborated when comparing the band from cells before lysis ('cells') to the faint band of cells after lysis ('lysis').

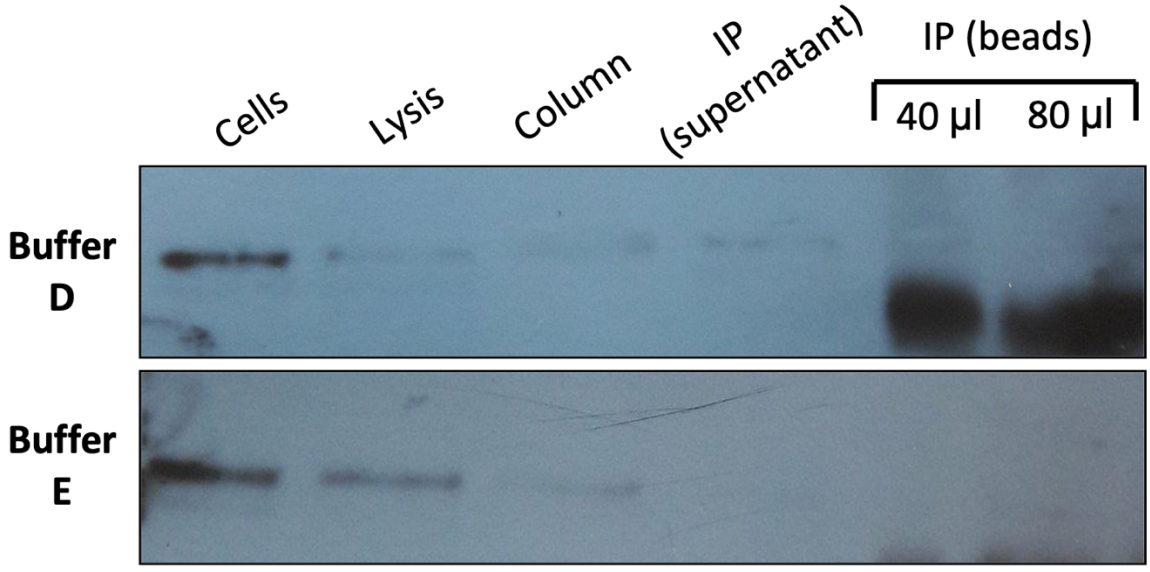

Figure 3.2.3.2 Lysing neutrophils with denaturing buffers before IP does not preserve ARAP3. $5x10^5$ cells from each of the samples were subjected to SDS-PAGE followed by western blotting with anti-ARAP3 antibody. This is one representative blot from 3 separate repeats performed on different days.

3.2.4 Immunoprecipitation of ARAP3 by sequential lysis with buffers of increasing tonicities

A later paper published by the Naccache group describes another method that was successfully used to isolate tyrosine phosphorylated Syk, another protein that is highly susceptible to proteolytic degradation from DFP-treated neutrophils [188]. The authors argue that most studies analyse only the soluble fractions and therefore discard the insoluble fractions after cell lysis with a classical lysis buffer such as RIPA. However many tyrosine kinase activities are found in the insoluble fractions [189, 190], and ARAP3 was shown to be phosphorylated by protein tyrosine kinases [182].

This approach employs three different lysis buffers for the sequential lysis of neutrophils. These include a hypotonic lysis buffer (HLB), an isotonic lysis buffer (ILB; commonly known as RIPA buffer), and a hypertonic lysis buffer (HyperLB), which only differ in their salt and NP-40 detergent concentrations (compositions shown in Figure 3.2.4.1 A).

The experimental scheme of the sequential lysis to determine the solubility of ARAP3 is described in Figure 3.2.4.1 B. In short, I first carried out an initial lysis step with HLB which was shown to preserve the overall tyrosine phosphorylation profile of Syk to a large extent [188]. After lysing the cells on ice and clarification of this lysate, the soluble fraction was then directly analysed by Western blot, while the insoluble fraction was processed by a further lysis step with ILB. The lysates were clarified once more and the soluble fraction analysed by Western blot, while the insoluble fraction was further

processed with HyperLB. The lysate was then sonicated and centrifuged, after which the soluble fraction was analysed by Western blot and the insoluble fraction resuspended in HLB then analysed by Western blot.

A

Hypotonic Lysis Buffer	Isotonic Lysis Buffer	Hypertonic Lysis Buffer
10 mM NaCl	137 mM NaCl	400 mM NaCl
0.1% NP-40	1% NP-40	1% NP-40
20 mM Tris–HCl (pH 7.5)	20 mM Tris–HCl (pH 7.5)	20 mM Tris–HCl (pH 7.5)
1 mM EDTA	1 mM EDTA	1 mM EDTA
2 mM Na_3VO_4	2 mM Na_3VO_4	2 mM Na_3VO_4
50 mg/ml trypsin inhibitor soybean	50 mg/ml trypsin inhibitor soybean	50 mg/ml trypsin inhibitor soybean
10 mg/ml aprotinin	10 mg/ml aprotinin	10 mg/ml aprotinin
10 mg/ml leupeptin	10 mg/ml leupeptin	10 mg/ml leupeptin
2 mM PMSF	2 mM PMSF	2 mM PMSF

B

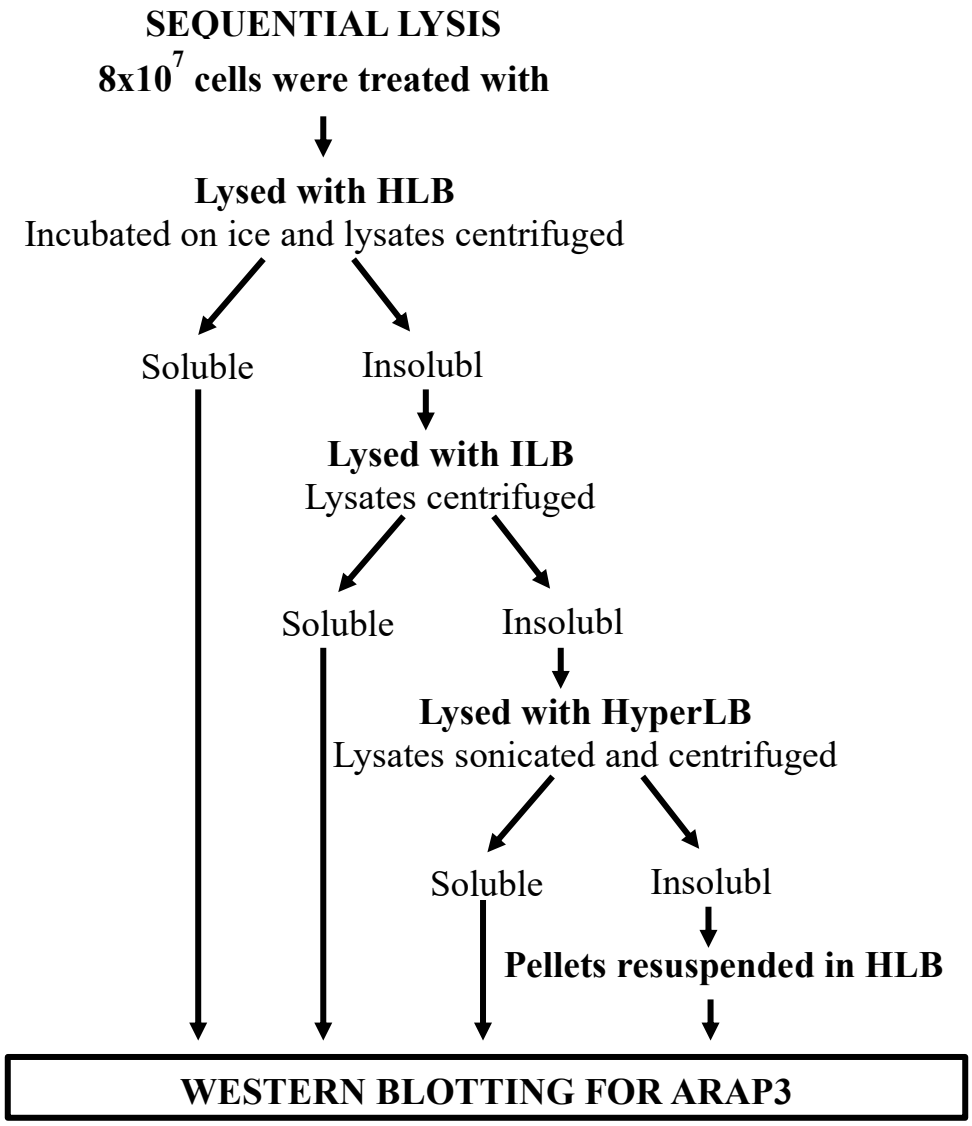

C

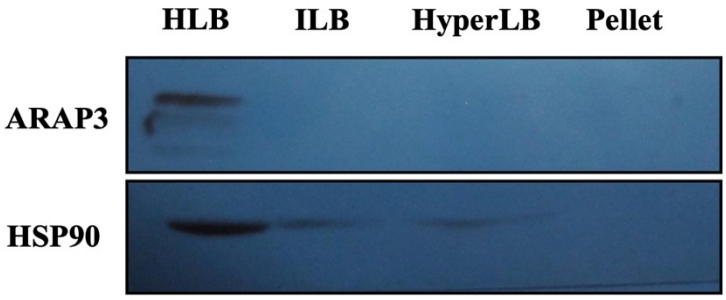

Figure 3.2.4.1 ARAP3 is soluble in Hypotonic lysis buffer. (A) Table of buffer compositions to make up the buffers of increasing tonicities. **(B)** Experimental scheme for using buffers of increasing tonicities to determine the solubility of ARAP3. **(C)** $1.2x10^6$ cells worth of lysates per condition were subjected to SDS-PAGE followed by western blotting with anti-ARAP3 antibody.

As shown in Figure 3.2.4.1 C, my experiments identified that ARAP3 was preserved in the soluble fraction of the HLB. Therefore, IPs were carried out for the isolation of ARAP3 from human neutrophils with the HLB. Western blots revealed that although both anti-ARAP3 antibodies could IP ARAP3, once again, IPs were more efficient with the rat monoclonal antibody (not shown). Figure 3.2.4.2 A shows an anti-ARAP3 blot (blotting with sheep antiserum) after ARAP3 IP with rat mAb in HLB as well as cells immediately boiled in the modified Laemmli buffer, proving that the HLB is suitable for IP of ARAP3. However, although IPed ARAP3 could be detected by Western blot, the amount of protein isolated was insufficient for it to be detected by Coomassie staining (Figure 3.2.4.2 B). This suggests that that less than 0.1 µg of ARAP3, the detection limit for Coomassie staining, was present in the sample.

To address whether poor immunoprecipitation of ARAP3 under these conditions could be due to suboptimal conditions created for the antibody by the hypotonic buffer, the conditions were converted from hypotonic to isotonic during the IP for more physiological conditions for antibody binding. For this, cells lysed in HLB were kept on ice for 5 mins, and clarified lysates were placed into a separate tube where more NaCl and NP-40 was added to a final concentration of 137 mM and 1% respectively. Figure 3.2.4.2 C shows that when the lysate is converted to isotonic conditions, ARAP3 can no longer be detected from the sample after incubating on ice for 2 hours, indicating that while these conditions may have been favourable for the immunoprecipitation of ARAP3, these physiological conditions were also more favourable for the proteases which efficiently degraded ARAP3. This suggests that adjusting the

tonicity of the buffer alone is insufficient for preparing neutrophil ARAP3 by efficient immunoprecipitation from lysates.

To further optimise the procedure, in addition to pre-treating the cells with DFP, further DFP was added to the HLB along with soybean trypsin inhibitor. Under these conditions, coomassie stained gels of mouse bone marrow neutrophils presented IPed bands of ARAP3 (Figure 3.2.4.2 D). Next, this was tested in human neutrophils lysed with HLB with added DFP and trypsin soybean inhibitor (Figure 3.2.4.2 E). Amongst a series of bands, some faint bands were detected in the ~170kDa area with the weaker HLB wash, while this was not the case with the ILB wash.

Obtaining a band with mouse bone marrow neutrophils but not human neutrophils is likely to be the consequence of having more potent proteases in human neutrophils compared to mouse, however it could also be due to the antibodies being more efficient at recognising mouse ARAP3.

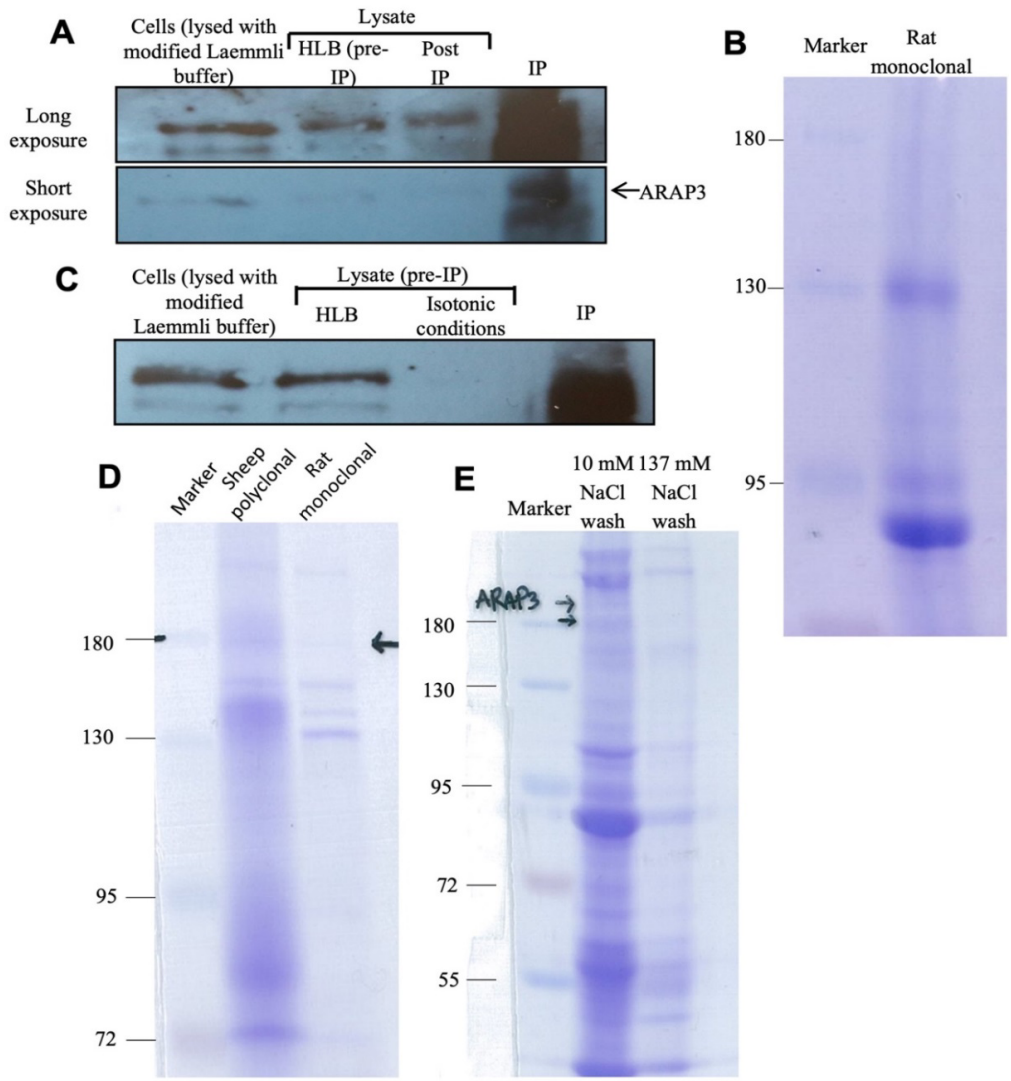

Figure 3.2.4.2 Hypotonic lysis buffer is not sufficient for immunoprecipitation of ARAP3 from human neutrophils. (A) Samples were lysed and IPed with HLB as described in the methods. $5x10^5$ neutrophils per lane were loaded or IPed using anti-ARAP3 rat monoclonal antibody followed by SDS-PAGE and Western blotting with the sheep anti-ARAP3 antibody. **(B)** $4x10^7$ cells were used to IP ARAP3 with rat monoclonal antibody from human neutrophils with HLB. The samples were subjected to SDS-PAGE and the gel was then Coomassie stained. ARAP3 band expected at ~170kD. **(C)** Western blot analysis comparing lysates from HLB before and after conversion to isotonic conditions, $5x10^5$ neutrophils were loaded per lane. **(D)** Coomassie stain of $4x10^7$ mouse bone marrow cells used to IP ARAP3 that were lysed with HLB with additional DFP and trypsin soybean inhibitor converted to isotonic conditions for IP using the sheep polyclonal antibody or the rat monoclonal. The beads were then washed with ILB. **(E)** Coomassie stain of $4x10^7$ human neutrophils used to IP ARAP3. Cells were lysed with HLB with added DFP and trypsin soybean inhibitor converted to isotonic conditions for IP. The beads were then washed either with HLB or ILB. Representative experiments are presented.

3.2.5 Mass Spec Analysis

Since isolating ARAP3 from human neutrophils was proving to be so difficult, it was decided to attempt mass spectrometry analysis without first isolating the ARAP3 protein. For this I prepared neutrophils, treated the cells with DFP, boiled the cell suspension with modified Laemmli buffer and ran the sample on a precast protein gel. The appropriate band was sent off for mass spectrometry analysis to Dr Andy Howden, University of Dundee. The aim was to ensure that ARAP3 protein could be detected from the gel slice.

Samples were run on a commercial minigel in parallel to a homemade large gel, which would tolerate a larger amount of lysate per well without being overloaded. fMLF and mock stimulated human neutrophils from 3 different donors were processed and run on both gels, and the bands were processed for mass spec analysis by our collaborators. They also attempted to enrich for phosphorylated proteins and identify phosphorylation sites. Unfortunately the peptide material corresponding to ARAP3 was insufficient for analysis of phosphorylation sites. Having spent in excess of one year attempting to isolate ARAP3 from human neutrophils and ultimately failing to do so, we decided it would be safer and more fruitful to pursue a different project.

3.3 Discussion

In this chapter I tried to isolate ARAP3 from human neutrophils. After successfully detecting the protein, I attempted to isolate the protein by IP with commonly used IP buffers. Although these classic buffers are effective for many proteins in a range of cell types, they were not sufficient for the IP of ARAP3 from neutrophils which have a large arsenal of proteases. Consulting the literature for neutrophil specific techniques to approach this, I then attempted using denaturing buffers and sequential lysis with buffers of increasing tonicities, both of which also were unsuccessful even with the addition of potent protease inhibitors such as DFP. The final endeavour was to send off the samples without isolating by IP, however there was too little peptide to carry out the required phosphopeptide enrichment to look at the phosphorylation status of the protein. My work suggests that the isolation of ARAP3 is particularly difficult in human neutrophils.

The size and charge of a protein define its structure and flexibility which in turn determine the susceptibility of a protein to degradation by proteases. Therefore, the relatively large size of ARAP3 is likely to contribute to the substantial proteolysis I observed. In addition, ARAP3 is comparatively difficult to isolate even when transiently expressed in cell lines , suggesting this protein may be subjected to particular degradation pathways as part of its physiological function.

Although challenging, we had numerous ideas and new potential avenues to investigate. One example is the nitrogen cavitation method which involves

using a pressure vessel. Nitrogen gas is dissolved in the cytoplasm of neutrophils under pressure. When the pressure is released, the nitrogen within the cells causes the disruption of the cell membranes [191]. When the pressure is kept low, this is considered a gentle method of cell disruption as only the plasma membrane and ER are disrupted while other organelles and granules remain intact. However, given how much time I had already lost, we decided the best way to approach was to cut our losses and move onto a new project.

Taking a synoptic view of the above, the focus of my project was then shifted from the GAP ARAP3 and to the 5-phosphatase SHIP2. A previous study had shown that SHIP2 and ARAP3 were able to form heterodimers through their SAM domains [192, 193] while a later study using PIP3-conjugated beads showed that SHIP2 alone could not interact with PIP3 [181]. However, immunoprecipitated heterodimers of SHIP2 with the ARAP3 fragment SAM–PH1–PH2 were able to bind to PIP3 in the bead binding assay. This sparked the idea that ARAP3 and SHIP2 heterodimers could play a role in SHIP2 membrane translocation, leading to the hypothesis that the polarisation defect of ARAP3-deficient neutrophils [91] was due to SHIP2 not being recruited to the plasma membrane. By this point, work on SHIP2 in the neutrophil had already commenced in the lab and some promising data had been obtained which suggested that this would be a fruitful direction to pursue.

4. Results - SHIP2 Regulates Neutrophil Chemotaxis and Directionality

4.1 Introduction

Previous studies have shown that global PTEN-deficiency is embryonic lethal [194], while SHIP1-deficient mice are viable and fertile. However, SHIP1 deficient mice exhibit a shortened lifespan which is thought to be partly due to leukocyte infiltration of the lungs [58]. Both PTEN and SHIP1-deficient neutrophils were previously described; PTEN knockout neutrophils exhibit enhanced ROS production when stimulated with fMLF, increased ruffling and sensitivity to chemoattractants, a minor chemotaxis directionality defect [195], and a lengthened lifespan [196]. SHIP1 knock-out neutrophils display altered ROS production [63] and augmented apoptosis [64]. SHIP1-deficient neutrophils also spread extensively on the substratum, and in response to chemoattractant stimulation fail to polarise and chemotax efficiently towards a chemoattractant [65].

Research on SHIP2 has mainly focused on insulin signalling and resistance to weight gain in SHIP2-deficiency. In contrast, the role of SHIP2 in the immune system and more specifically neutrophils largely remains to be explored. In this chapter I used mice which express catalytically dead SHIP2 in the germ-line (so-called $Ship2^{\Delta/\Delta}$ mice) to characterise the functions of SHIP2 in neutrophils.

Hypothesis

It was hypothesized that as with other phosphoinositide phosphatases, SHIP2 has an impact on neutrophil effector functions.

Chapter-specific aims

Pilot experiments performed before I moved to this project suggested that SHIP2 is a regulator of chemotaxis. Therefore, the aim of this chapter was to examine this in more detail and determine which other neutrophil functions are controlled by SHIP2. More specifically, I aimed to study the function of SHIP2 in neutrophil:

1. Spreading
2. Polarisation
3. Swarming
4. Internalisation

4.2 Results

4.2.1 Ship2$^{\Delta/\Delta}$ deletion to study functions of SHIP2 in mouse neutrophils

4.2.1.1 Ship2$^{\Delta/\Delta}$ mice

SHIP2-deficient mice (with a deletion of the *Inppl1* gene) were characterised by normal glucose tolerance and sensitivity to insulin [73]. They remain lean even on a high-fat diet, have a small stature, and have a characteristically shorter snout. For my work, I used mice carrying catalytically dead SHIP2 (catalytically inactive Ship2$^{\Delta/\Delta}$ mice) which carry a 57 amino acid deletion in their catalytic domain.

To create this, floxed Ship2 mice were derived by Dubois et al [79] who flanked the *Inppl1* exons 18 and 19 by LoxP sites. They were then crossed with PGK-Cre mice to remove exons 18 and 19 as described [79] to create Ship2$^{\Delta/+}$ mice (Figure 4.2.1.1 A). The Ship2$^{\Delta/+}$ mice were provided to us by Professor Stéphane Schurmans (Liège University, Belgium) on a mixed background. They were backcrossed for 8 generations with C57Bl/6 mice and intercrossed to form Ship2$^{\Delta/\Delta}$ at the expected Mendelian frequency. Ear notch samples from each mouse were used for genotyping by PCR as described in the methods (chapter 2.2.1). Ship2$^{\Delta/\Delta}$ mice exhibited the same phenotype as the SHIP2-deficient mice [73], displaying a small stature, leanness and a shorter snout as shown in figure 4.2.1.1 B. Ship2$^{\Delta/\Delta}$ and the Ship2$^{+/+}$ wild-type littermate controls were used throughout this chapter.

Over 50% of Ship1-deficient mice die by week 10 [58, 59], and these mice were identified to have substantially increased peripheral blood myeloid cells and develop bone marrow myeloid cell hyperplasia from a young age. In addition, they also develop sterile inflammation and lung infiltration consisting of neutrophils and macrophages. Ship2$^{\Delta/\Delta}$ mice however, were shown by other lab members of the Vermeren lab to survive for over 18 months without any signs of disease or distress [73, 79]. Blood cell counts were non-distinguishable from wild-type controls and flow cytometry analysis of lung digests showed no noticeable infiltration of immune cells in lungs or splenomegaly.

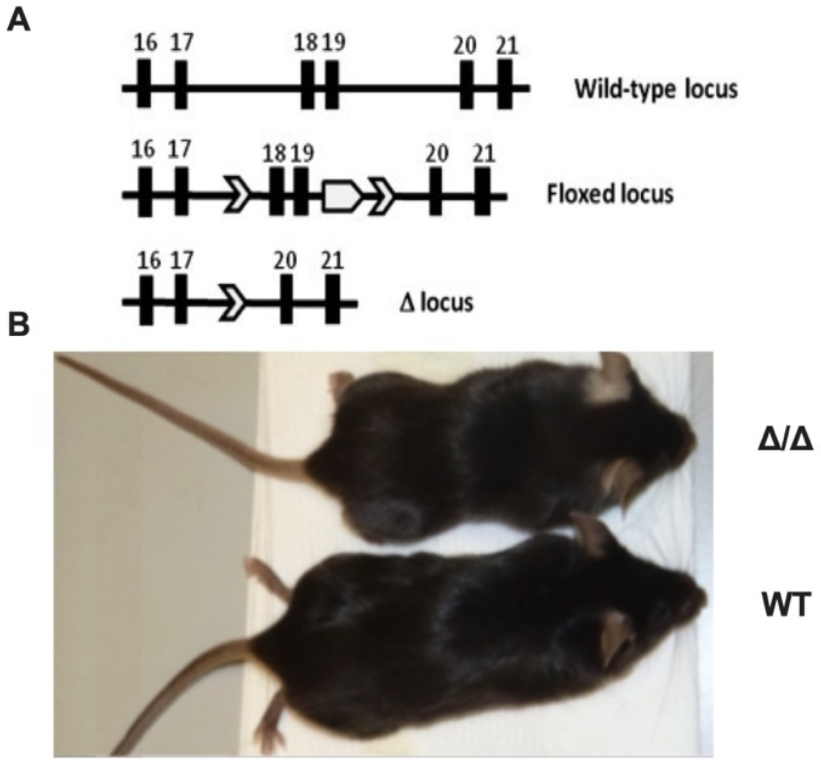

Figure 4.2.1.1 The catalytically dead Ship2 mouse. (A) Schematic drawing of the wild-type, floxed and Δ loci where the exons are represented by numbered black bars, modified from [79]. **(B)** A representative image of a Ship2$^{+/+}$ and a Ship2$^{\Delta/\Delta}$ mouse. Photo taken by Dr Sonja Vermeren.

4.2.1.2 Ship2$^{\Delta/\Delta}$ neutrophils

In order to determine the functions of SHIP2 in neutrophils, I first isolated neutrophils from Ship2$^{\Delta/\Delta}$ mice by flushing the bone marrow and harvesting the neutrophils as detailed in the methods (chapter 2.1.2). The Ship2$^{\Delta/\Delta}$ neutrophils were matched with Ship2$^{+/+}$ wild-type controls, and the expression of PIP3 phosphatases SHIP1, SHIP2 and PTEN as well as the protein kinase PKB (otherwise known as Akt) was compared between the genotypes. Despite carrying a small deletion, Ship2$^{\Delta/\Delta}$ protein did not run noticeably faster on protein gels, perhaps because of the large molecular weight of SHIP2 (160kDa approx.). Moreover, unlike in the previous report that analysed adipose and muscle tissue, I did not detect reduced expression of Ship2$^{\Delta/\Delta}$ protein [79], as shown in Figure 4.2.1.2.

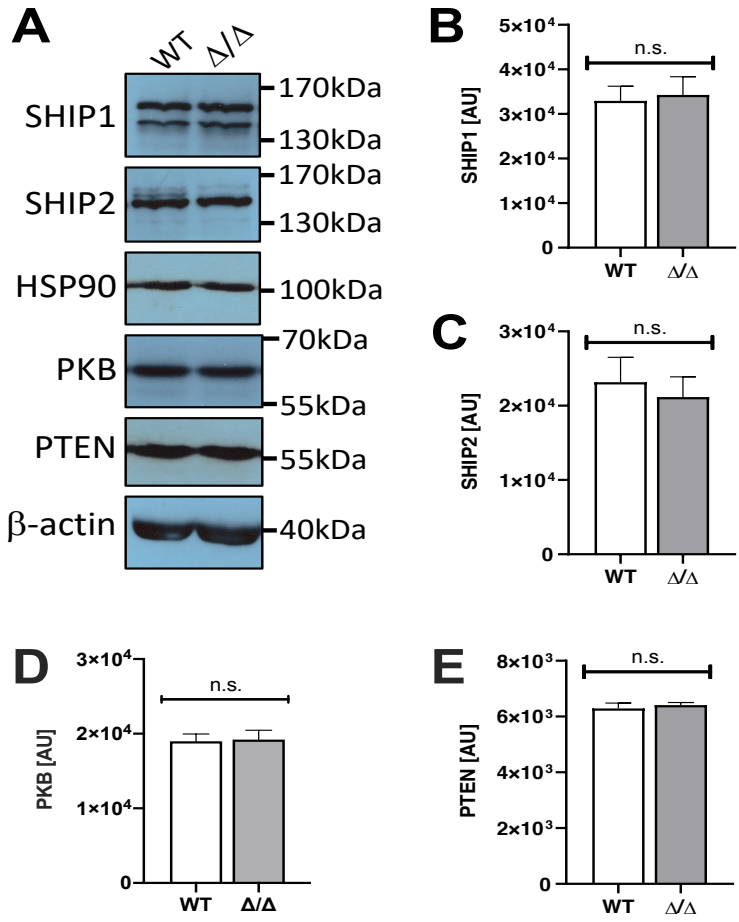

Figure 4.2.1.2 Expression of SHIP1, SHIP2, PTEN and PKB remains the same in Ship2$^{\Delta/\Delta}$ neutrophils. Neutrophils from WT and Ship2$^{\Delta/\Delta}$ mice were tested for the expression of SHIP1, SHIP2, PKB, PTEN and loading controls, HSP90 and β-actin by Western Blotting. **(A)** Representative blots and **(B-E)** densitometry measurements performed in ImageJ for 4 (PKB, PTEN, HSP90) and 5 (SHIP1, SHIP2, β-actin) separately performed experiments. Unpaired two-tailed t tests were used to determine significance.

4.2.2 SHIP2 regulates neutrophil recruitment and chemotaxis

Please note that the work described in this section was carried out by other group members and is included here solely for the sake of completeness.

4.2.2.1 SHIP2 regulates in vivo neutrophil recruitment to sites of inflammation

To examine if SHIP2 regulates the recruitment of neutrophils to sites of inflammatory challenge, members of the Vermeren lab generated bone marrow chimeras by isolating bone marrow cells from wild-type and $Ship2^{\Delta/\Delta}$ donors for reconstitution of lethally irradiated recipient wild-type mice as indicated in Figure 4.2.2.1 A. First, neutrophil recruitment was measured in response to LPS-induced acute lung injury (ALI). A significantly decreased number of $Ship2^{\Delta/\Delta}$ neutrophils was recovered compared to wild-type controls from bronchoalveolar lavages (BAL) as well as the total lung neutrophils determined in single cell digests of PBS-perfused lungs by flow cytometry. Recruitment to sites of inflammation can vary depending on the site of inflammation and the type of stimulus. Therefore, neutrophil recruitment was also analysed in response to thioglycollate-induced peritonitis in $Ship2^{\Delta/\Delta}$>WT and WT>WT bone marrow chimeras. Once again, this showed a substantial recruitment defect of $Ship2^{\Delta/\Delta}$ neutrophils compared to the wild-type as presented in Figure 4.2.2.1 D. Hence it can be concluded that $Ship2^{\Delta/\Delta}$ neutrophil recruitment to sites of inflammation is substantially impaired.

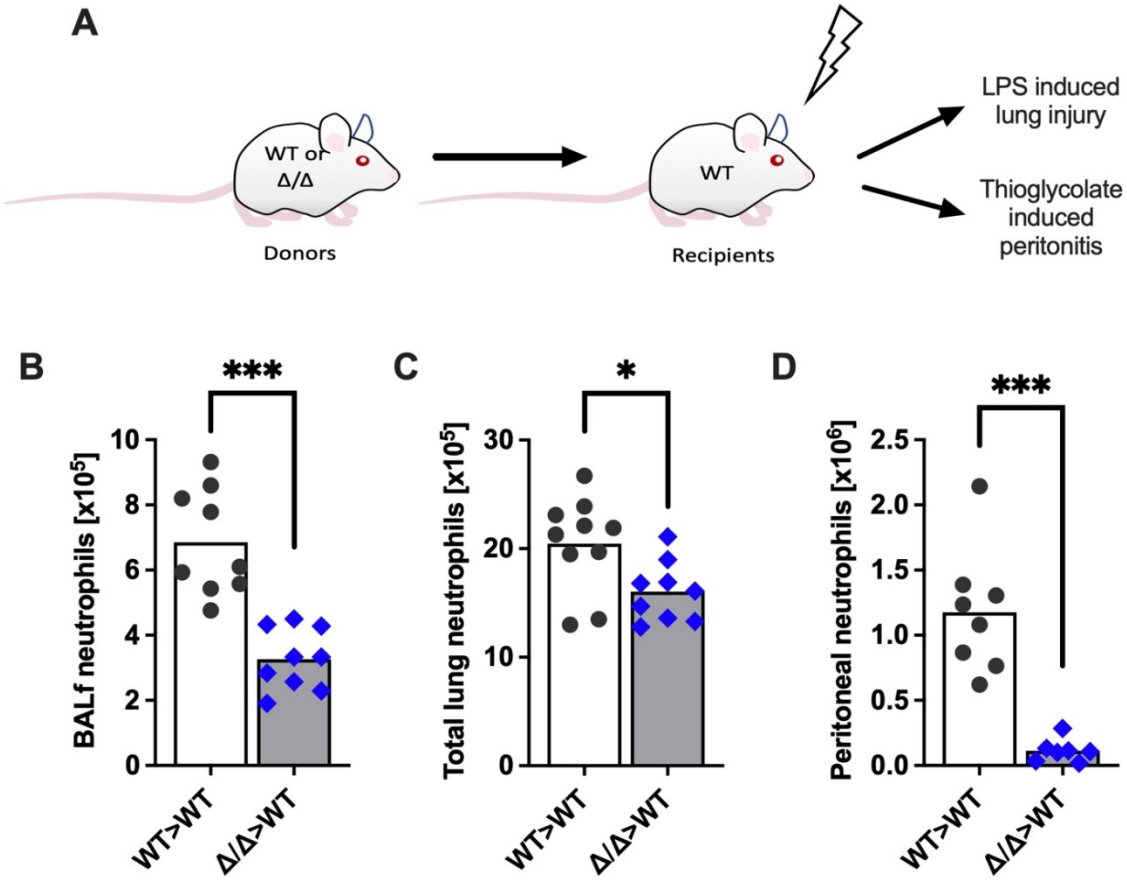

Figure 4.2.2.1 SHIP2 aids in the recruitment of neutrophils to sites of sterile inflammation. (A) Schematic diagram of the generation of bone marrow chimeras. **(B-D)** Recruitment of WT and Ship2$^{\Delta/\Delta}$ cells in acute lung injury (ALI), induced by adding 50 µl sterile saline with 1 µg LPS intratracheally into 9 bone marrow chimeras from each genotype (from 4 bone marrow donors) 4 hours prior to being sacrificed. Results of neutrophils retrieved were plotted for **(B)** bronchoalveolar lavages and **(C)** lung single cell digests. **(D)** Recruitment of WT and Ship2$^{\Delta/\Delta}$ cells in thioglycollate peritonitis induced by administering 20 ml/kg broth containing thioglycollate into 8 WT and 7 Ship2$^{\Delta/\Delta}$ bone marrow chimeras. 2.5 hours later, the peritonea were flushed and the neutrophil numbers plotted. **(B-D)** Experiments were carried out on two separate days, the graphs show pooled results with each mouse represented by a symbol. p values were determined by unpaired t-tests, *$p < 0.05$; ***$p < 0.001$. Experiments and analysis were performed by Dr Barry McCormick [197].

4.2.2.2 SHIP2 regulates in vitro neutrophil chemotaxis and directionality

Due to the substantial recruitment defect observed in these *in vivo* experiments, the involvement of SHIP2 in neutrophil chemotaxis *in vitro* was investigated next. To examine this, cells were allowed to migrate through a linear concentration gradient of fMLF in a 3D collagen matrix and their tracks represented in a spider plot (Figure 4.2.2.2 A). The tracks were analysed as detailed in the methods (section 2.4.1) which identified that the Euclidian distances (defined as the shortest distance between the start and end point) covered by $Ship2^{\Delta/\Delta}$ neutrophils were smaller than the wild-type controls. The total accumulated distances however remained the same indicating that directionality, but not the ability to migrate nor the speed of $Ship2^{\Delta/\Delta}$ neutrophils was reduced (Figure 4.2.2.2 B-D). SHIP2 was therefore determined to be a regulator of neutrophil chemotaxis, and in contrast to SHIP1 which was shown to be required for neutrophil de-adhesion during migration [63, 65], SHIP2 appears to regulate chemotactic directionality.

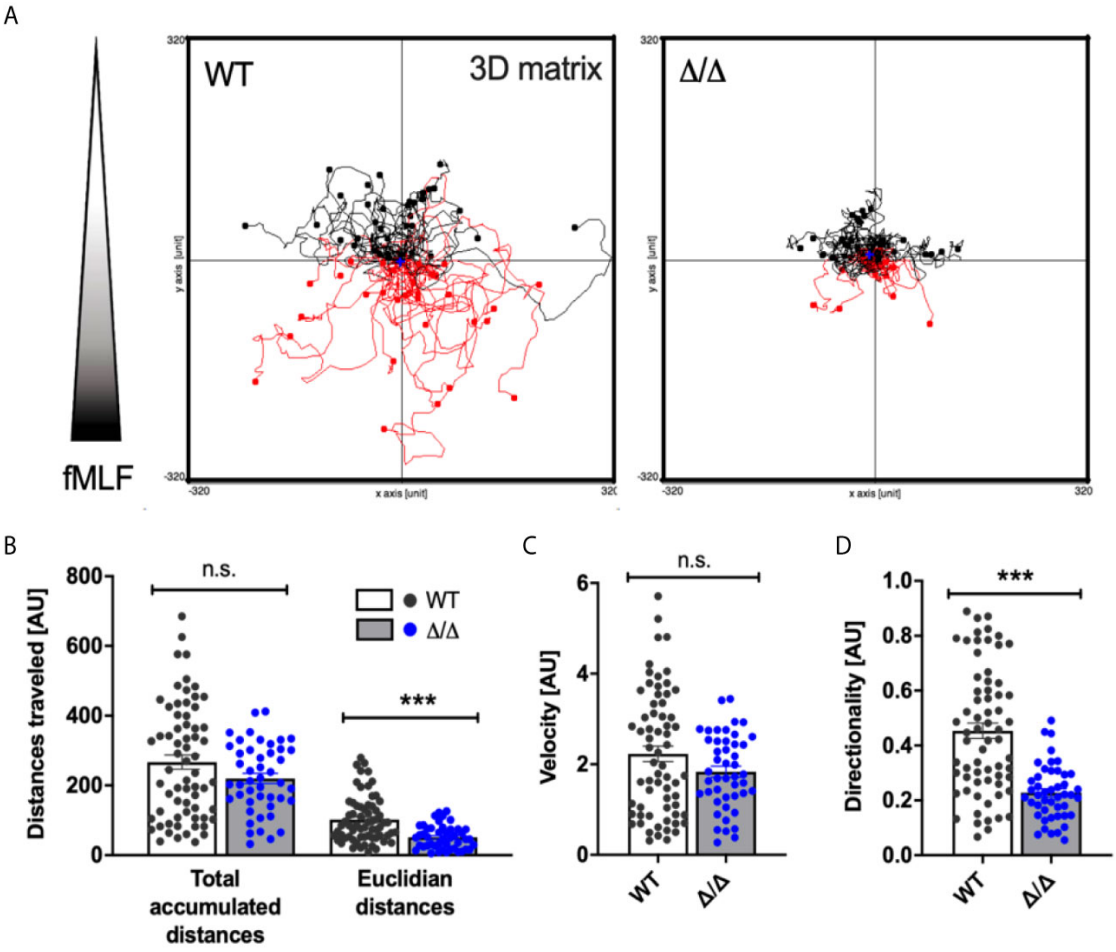

Figure 4.2.2.2 SHIP2 aids in the chemotactic directionality in vitro. WT and Ship2$^{\Delta/\Delta}$ bone marrow neutrophils were allowed to chemotax towards an fMLF stimulus (300 nM) from three separate experiments. Chemotaxis was measured by time lapse imaging for neutrophils embedded in a collagen matrix using Ibidi chemotaxis μ-slides. **(A)** Spider plots showing the tracks of individual neutrophils and the gradient of fMLF stimulus indicated to the left. The tracks were analysed using the Ibidi chemotaxis tool and the **(B)** accumulated and Euclidean distances, **(C)** velocity and **(D)** directionality were plotted. p values were calculated using the Mann-Whitney U test, ***$p < 0.001$. Experiments and analysis performed by Dr Sonja Vermeren [59, 197].

4.2.3 SHIP2$^{\Delta/\Delta}$ neutrophils fail to polarise efficiently

There are three distinct processes involved in chemotaxis which allow for neutrophils to move directionally towards a stimulus, namely: gradient sensing, polarisation, and motility [198]. As mentioned in the previous subheading, chemotaxis assays of Ship2$^{\Delta/\Delta}$ neutrophils revealed a directionality defect. In attempt to study this Ship2$^{\Delta/\Delta}$ chemotaxis defect in more detail, I carried out polarisation assays. When neutrophils polarise, they break their symmetry by forming a leading and trailing edge and adopting a more elongated shape. Figure 4.2.3 A is an image of isolated BMNs stained for GR1, these images were then run through a CellProfiler pipeline to determine two parameters, cell compactness (defined as the mean squared distance of the object's pixels from the centroid divided by the area, and where a full circle is attributed a value of 1 and larger values are given to irregular shapes) and eccentricity (defined as the ratio of the distance between the foci of the ellipse and its major axis length, where 0 is a perfect circle, and 1 represents a straight line). Neutrophils were analysed with and without stimulation, and with both parameters, stimulated Ship2$^{\Delta/\Delta}$ cells did not polarise as efficiently as the wild-type controls (Figure 4.2.3 B).

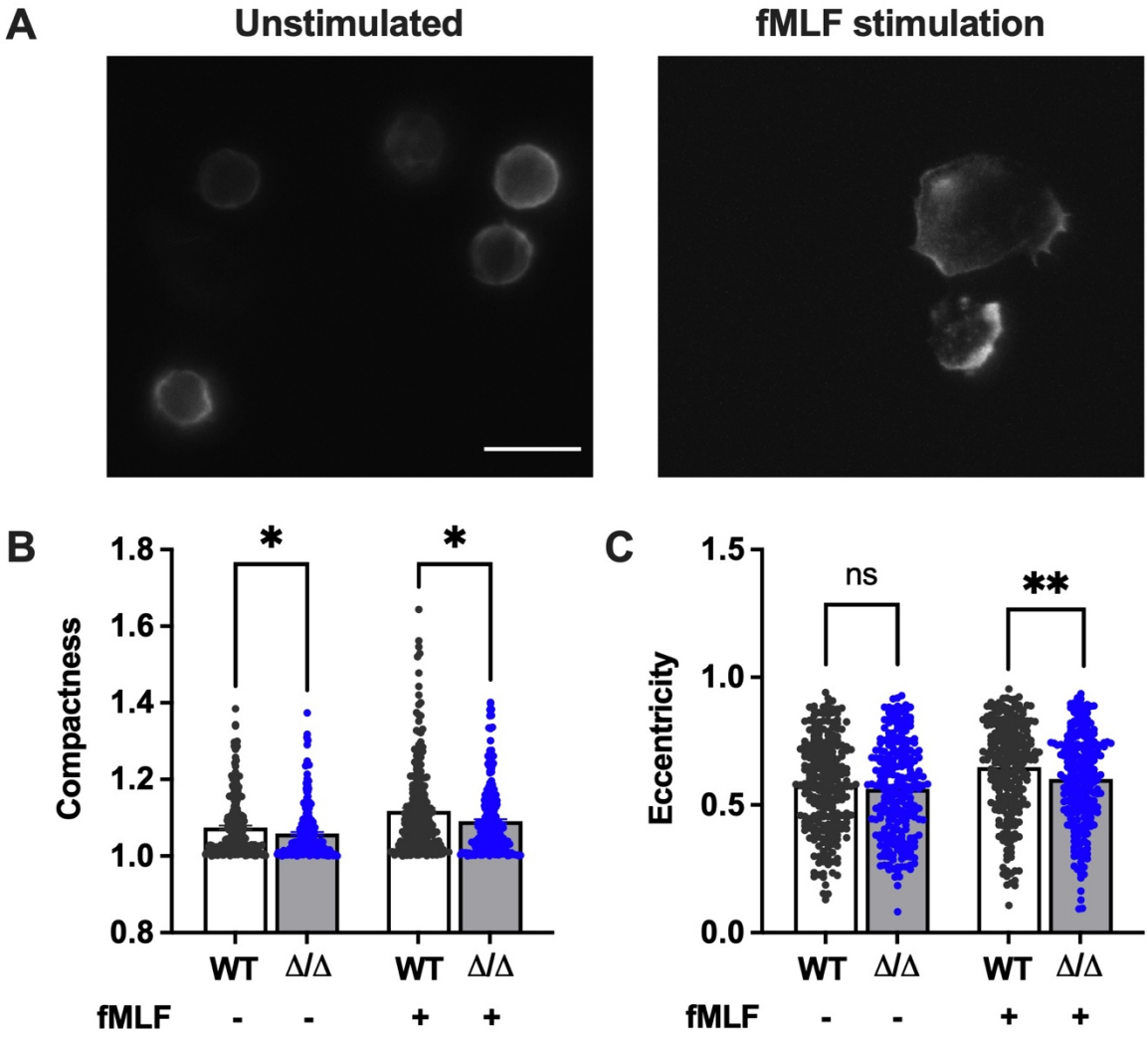

Figure 4.2.3 Ship2$^{\Delta/\Delta}$ neutrophils have a polarisation defect. BMNs were isolated, adhered onto glass coverslips, stained for GR1 and imaged. **(A)** Representative images of unstimulated and fMLF stimulated (1 μM) WT neutrophils stained for GR1, 10 μm scale bar. Polarisation in Ship2$^{\Delta/\Delta}$ neutrophils was compared to WT controls by processing acquired images of adhered neutrophils in a CellProfiler pipeline for parameters **(B)** compactness and **(C)** eccentricity with and without 1 μM fMLF stimulation for 5 minutes; higher values represent a more polarized shape. 5 experiments were performed on separate days, with n= 50 cells scored from each experiment, each of which showed the same trend. p values were determined using the Mann-Whitney U test, *p < 0.05, **p < 0.01 figure from [197].

4.2.4 SHIP2 does not regulate neutrophil swarming

Neutrophils have in recent years been shown to amplify chemotactic gradients, in particular using the lipid mediator LTB4, leading to formation of swarms. To further inspect the in vivo neutrophil recruitment defect detected earlier with Ship2$^{\Delta/\Delta}$ neutrophils, we next decided to study neutrophil swarming. Since swarms are somewhat hard to detect in the context of in vitro assays, and we are not set up for intravital imaging in Little France, I used a robust method developed by the Irimia group [141] in which neutrophils are allowed to migrate towards zymosan clusters that were immobilised on poly-L-lysine patches that had been immobilised on glass slides. With zymosan not being a chemoattractant per se, this system is dependent upon chemoattractants generated by pioneer neutrophils which are stimulated by the zymosan and which induce followers to chemotax after, causing the formation of swarms. The development and growth of neutrophil swarms on these slides were imaged and measured. For a deeper understanding of the cytokines released during swarming I also planned to perform a cytokine analysis to ultimately compare cytokines released in Ship2$^{\Delta/\Delta}$ compared to wild-type neutrophils in the event that a swarming defect was observed in these experiments.

4.2.4.1 Obtaining pure mouse neutrophils

Leukocytes release a range of cytokines, with certain leukocytes (e.g. monocytes, macrophages, T cells) being particularly strong at releasing cytokines. To accurately measure what is secreted from neutrophils it is therefore key to have a pure population of neutrophils. The importance of this has also been highlighted in previous studies, showing that insufficient purity of neutrophils can lead to misinterpretation of neutrophil-derived cytokines [199]. The best understood chemoattractant secreted during swarming is the lipid mediator of inflammation LTB4. In addition to being secreted from neutrophils, it is also largely secreted by mast cells, macrophages and monocytes [200]. When stimulated with the ionophore A23187, neutrophils produce 50 ng/10^6 cells of LTB4 whereas macrophages produce 200 ng/10^6 cells [200]. Hence, the first step was to isolate a highly purified population of neutrophils.

This was achieved by performing 2 preps back-to-back, first a prep with a discontinuous percoll gradient followed by the EasySep commercially available immunomagnetic negative selection kit which resulted in 99.1% purity as described in the methods (section 2.1.2.3). The activation status of neutrophils from each prep was tested by flow cytometry by analysing L-selectin shedding and by performing ROS assays (Figure 2.1.2.2 C,D) with experiments suggesting that both isolation methods produced neutrophils that were not activated.

4.2.4.2 SHIP2$^{\Delta/\Delta}$ neutrophils form similar sized swarms to wild-type controls

Initially, BMNs from wild-type mice were used to test the swarming assays and images were acquired in brightfield as shown in Figure 4.2.4.2.1, which consists of time lapse still images of neutrophils swarming towards a zymosan cluster. Within the first 5 minutes, only a few pioneer neutrophils were observed in the field of view but more accumulated over time, and after 2 hours a big swarm was observed around each zymosan cluster.

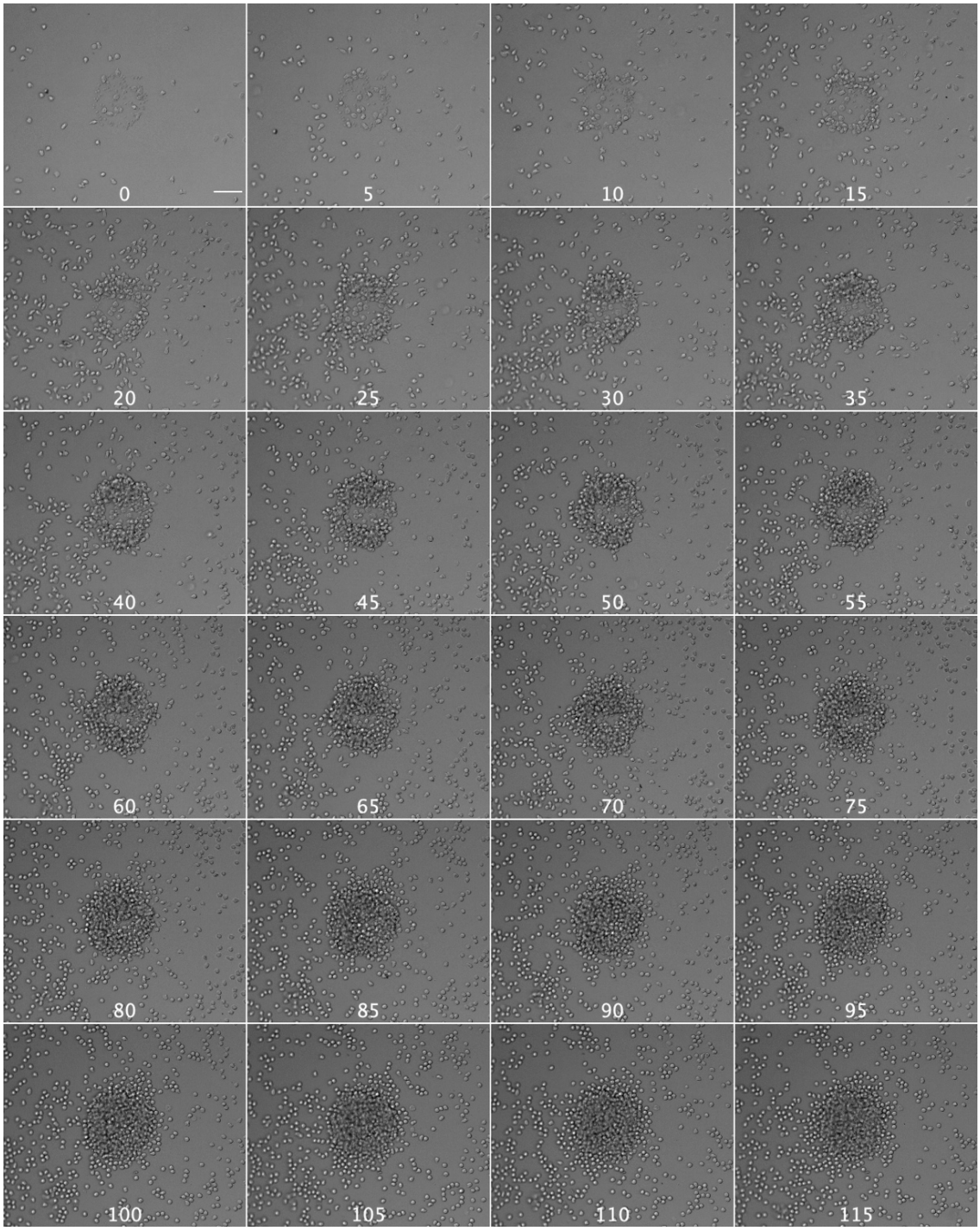

Figure 4.2.4.2.1 Time lapse movie of neutrophil swarming. $5x10^5$ BMNs were placed into wells on a glass slide containing clusters of zymosan. Time lapse images were acquired every 5 minutes, represented by each panel, for 155 minutes in brightfield, showing neutrophil swarms being formed around the zymosan. Scale bar is 50 μm.

The time lapse images were processed in Fiji and the swarm sizes as well as signal intensities were measured for each time point for 9 different zymosan clusters per well. Plotting these results in Figure 4.2.4.2.2 A,B confirmed that both the size of the swarm and the number of neutrophils within the cluster increased with time, eventually reaching a plateau at approx 2 hrs.

Neutrophils from each genotype were isolated and swarming assays performed to identify whether swarm sizes and signal intensities were regulated by SHIP2. The area under the curve for these parameters are presented in Figure 4.2.4.2.2 C, D, revealing no difference between the genotypes.

Since there were no observed differences in the size and intensity of the swarms between the genotypes, I did not, in the end, perform any cytokine analysis. I had planned to do this during my placement at GSK, however, since there was no quantifiable effect on swarming I decided to focus on human cells instead.

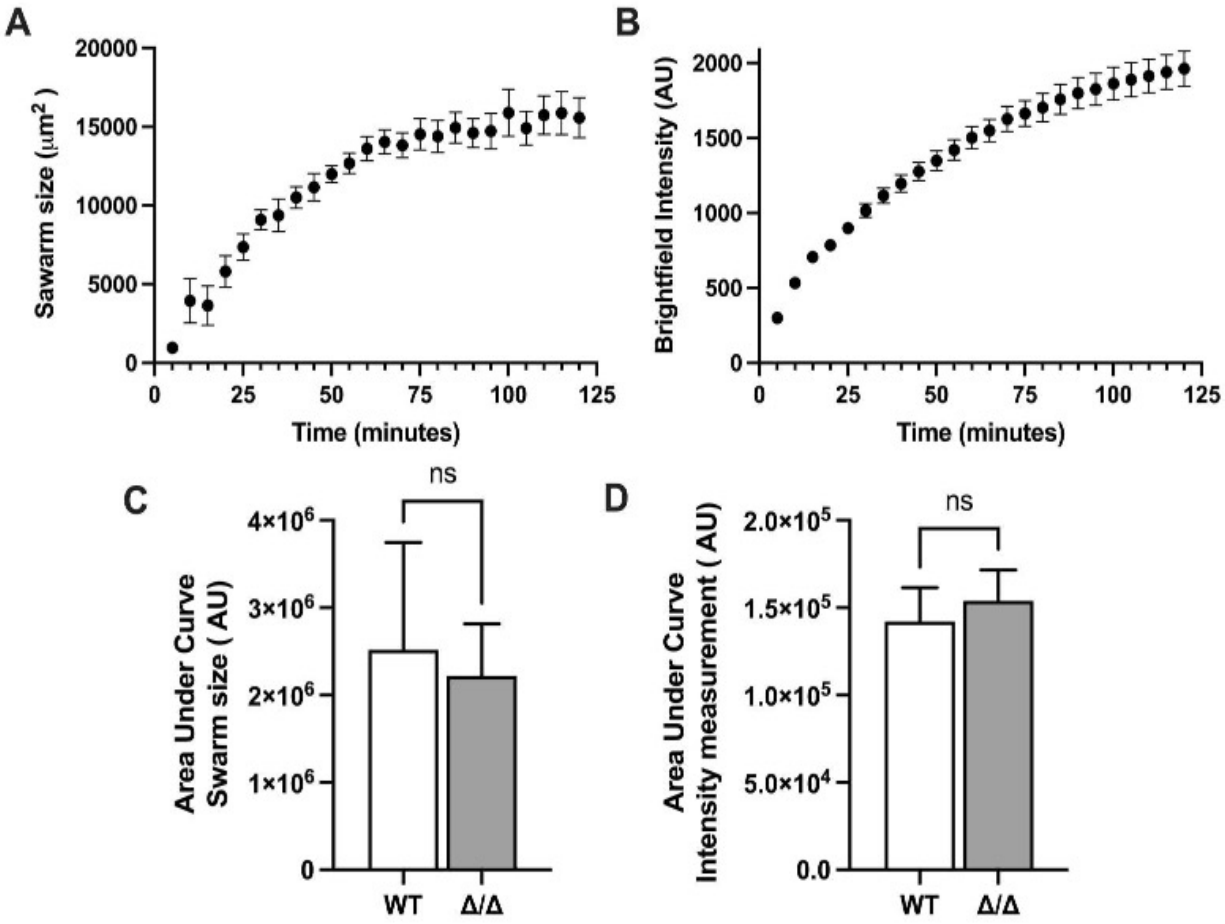

Figure 4.2.4.2.2 SHIP2 is dispensable for swarming. 5x10^5 BMNs were placed into wells on a glass slide containing clusters of zymosan. Time lapse images were acquired with multipoint functionality to simultaneously image several swarms at once, every 5 minutes for 2 hours in brightfield. To optimize the assay, the images of WT neutrophils from 9 different swarms were analysed using 2 Fiji macros to identify **(A)** swarm sizes and **(B)** the intensity of the swarm. WT neutrophils were compared to Ship2$^{\Delta/\Delta}$ neutrophils and the area under the curve was calculated and plotted for each genotype for **(C)** swarm sizes and **(D)** the intensity of the swarm from 3 separate experiments, with 9 swarms per genotype for each; *p* values were determined with an unpaired two-tailed t-test; error bars show SEM.

4.2.5 Ship2$^{\Delta/\Delta}$ neutrophils have a defect in fMLF-induced spreading and firm adhesion

Previous unpublished experiments in our lab which tested neutrophil adhesion had shown that under static conditions Ship2$^{\Delta/\Delta}$ neutrophils adhere to glass as well as the wild-type controls. To build on this and identify if SHIP2 regulates integrin dependent processes like SHIP1, I examined cell spreading which is the first step in motility, where neutrophils change from a rounded morphology in suspension to a flattened shape as they anchor onto the substrate [201]. I acquired images of GR1 stained cells as previously carried out to measure polarisation, and run them through a CellProfiler pipeline to calculate their area and measure the extent of neutrophil spreading. Interestingly, Figure 4.2.5 A shows that Ship2$^{\Delta/\Delta}$ neutrophils failed to spread as efficiently as wild-type controls upon stimulation with fMLF, suggestive of integrin-dependent functions of SHIP2.

To further understand the integrin dependent roles of SHIP2, I investigated if there is an adhesion defect under conditions of flow in collaboration with Dr Barry McCormick who had previously optimized this experiment [91]. Adhesion under flow is more representative of physiological conditions than static conditions, as neutrophils adhere to the vessel wall in blood flow. Therefore, parallel plate flow chambers coated with ICAM-1, E-selectin, and CXCL-1 were used to analyse neutrophil adhesion. Figure 4.2.5 B shows a graph that depicts the number of firmly adhered neutrophils represented for each genotype per field of view over time. Consistent with my cell spreading experiment, there were fewer firmly adhered Ship2$^{\Delta/\Delta}$ neutrophils compared to wild-type controls.

Lightly adhered and rolling cells were also analysed (data not shown) but no difference was detected between the genotypes. These results suggest that SHIP2 has a subtle effect on the regulation of neutrophil adhesion and spreading which intensifies under conditions of flow.

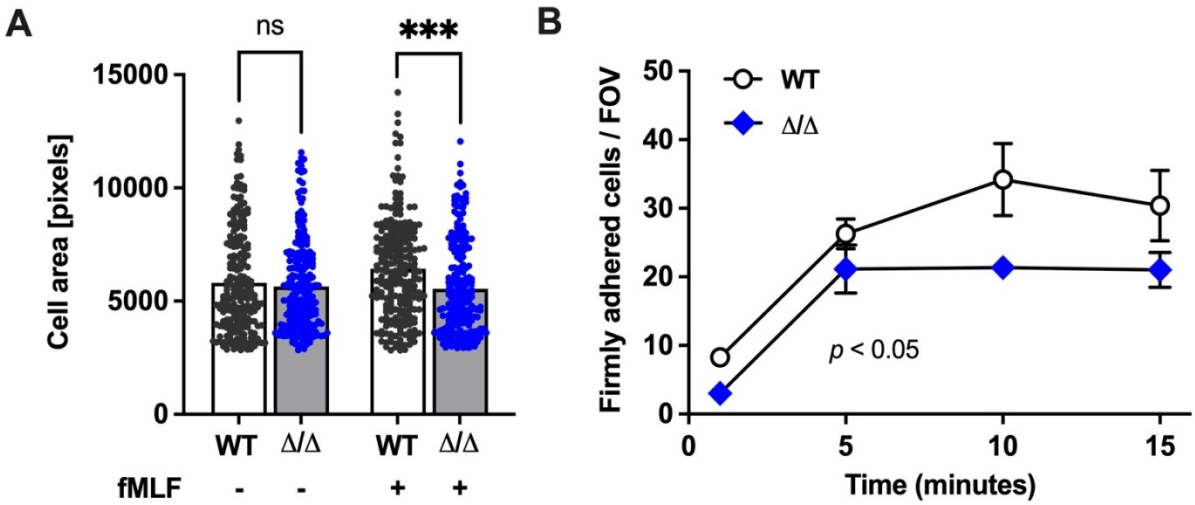

Figure 4.2.5 Ship2$^{\Delta/\Delta}$ spreading and firm adhesion defects. (A) BMNs were isolated, allowed to adhere onto glass coverslips, stained for GR1 and imaged. Ship2$^{\Delta/\Delta}$ neutrophils were compared to WT controls by processing acquired images in a CellProfiler pipeline for cell area with and without 1 μM fMLF stimulation for 5 minutes. n = 250 total obtained from 5 separate experiments. *p* values were determined using the Mann-Whitney U test. **(B)** Ship2$^{\Delta/\Delta}$ BMNs were compared to WT controls after being perfused in Ibidi VI$^{0.4}$ flow chambers coated with ICAM-1, rmE-selectin and rmCXCL1 at a constant sheer stress of 1 dyne. The graph represents results from a minimum of 3 different experiments, *p* values were determined by an unpaired, two-tailed t test of the area under the graphs (performed and analysed in collaboration with Dr Barry McCormick). ****p* < 0.001, error bars show SEM, figure from [197].

4.2.6 SHIP2 does not regulate neutrophil phagocytosis

Several studies have addressed the importance of PI3K in Fcγ-receptor mediated macrophage phagocytosis, where PIP3 was found to accumulate at the membrane of the phagosomal cup [202-204]. In addition, the knockdown of SHIP2 specifically enhanced macrophage phagocytosis, highlighting the inhibitory effects of SHIP2 on phagocytosis in the macrophage [205]. To determine if neutrophils behave similarly, internalisation experiments were carried out using IgG-opsonized latex beads, comparing $Ship2^{\Delta/\Delta}$ neutrophils to wild-type controls by immunofluorescence as detailed in the methods (section 2.4.4) with an example shown in Figure 4.2.6 A. This was repeated with five mice of each genotype examining the percentage of total internalised cells as well as the number of internalised beads per cell. Neither parameter showed a statistically significant difference between the genotypes (Figure 4.2.6 B). My result is congruent with results from our lab [206] and another study [207] where PI3K inhibitors were used to show that internalisation of antibody-opsonised beads by human neutrophils is independent of PI3K.

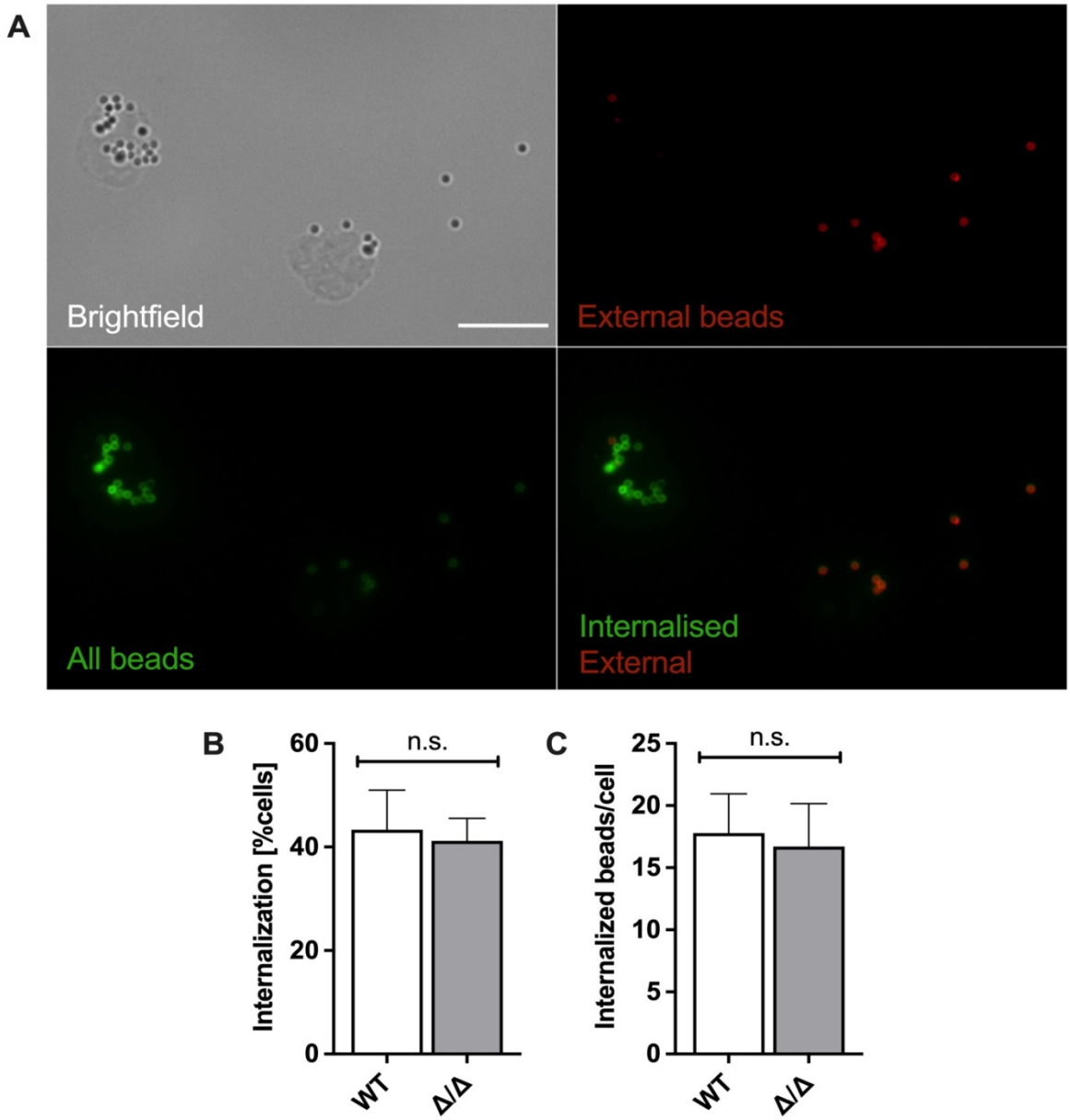

Figure 4.2.6 Ship2 is expendable for phagocytosis. BMNs were isolated and assayed for the phagocytosis of rabbit IgG opsonized latex beads. **(A)** A representative image showing attached and internalized beads. Top left panel, brightfield image of neutrophil and beads, scale bar 5 µm; top right panel shows attached beads from neutrophils stained with Alexa Fluor 568 coupled anti-rabbit IgG; bottom left panel shows labelling of all beads with Alexa Fluor 488-conjugated anti-rabbit IgG after permeabilisation; bottom right shows a merged image with internalised beads appearing green and external appearing orange. WT and Ship2$^{\Delta/\Delta}$ neutrophils were compared for the percentage of internalised beads **(B)** and number of internalized beads per cell **(C).** 100 cells were counted from 5 different experiments performed on separate days, *p* values were determined using the Mann-Whitney U test, error bars show SEM, figure partly from [197].

4.3 Discussion

In this chapter I isolated neutrophils from Ship2$^{\Delta/\Delta}$ mice rather than using SHIP2 deficient mice. Using Ship2$^{\Delta/\Delta}$ mice allowed me to identify functions that are dependent solely on the catalytic activity of SHIP2, excluding any potential scaffolding effects. Nonetheless, one possible limitation of these Ship2$^{\Delta/\Delta}$ mice is that compensatory events may have decreased the severity of the observed phenotype. Generating an inducible Ship2$^{\Delta/\Delta}$ mouse might have led to a more striking phenotype than the one observed with the constitutive mouse.

I unraveled how the 5-phosphatase SHIP2 regulates neutrophil recruitment to sites of sterile inflammation *in vivo* as well as chemotaxis and directionality *in vitro* using functional experiments. When stimulated with a chemokine, immobilized integrin ligand and selectin, SHIP2 was found to regulate firm adhesion under flow. In addition, SHIP2 was identified to regulate neutrophil spreading and polarisation when a uniform stimulus was added. Conversely, comparing wild-type to Ship2$^{\Delta/\Delta}$ neutrophils revealed no significant defect in phagocytosis or swarming. Further experiments performed by members of the Vermeren lab (not shown) had also identified that there were no significant regulatory effects of SHIP2 in degranulation and ROS production upon integrin stimulation or in response to formylated peptide stimulation.

Rather than scoring cells manually, I instead analysed randomly taken images computationally using an image analysis software in an attempt to avoid bias. The polarization graphs in Figure 4.2.3 B show 50 neutrophils plotted for each condition, and since this experiment was repeated five times, this allowed for

a total of 250 cells to be analysed. A lower power analysis with just 10 randomly chosen cells per condition also showed significance for each of the parameters plotted here. Still, it is worth noting that although significant, the polarization defect observed with the Ship2$^{\Delta/\Delta}$ neutrophils that were stimulated with uniform fMLF is only a subtle change. It is possible that analysing shape change using flow cytometry, or analysing directional polarization, e.g. by subjecting the neutrophils to a gradient of fMLF might have resulted in a more pronounced difference. We were planning to carry out a 96-well plate based experiment that had been developed by Dr Amour's colleague at GSK to test polarization in response to directional stimulation of neutrophils with fMLF using the Operetta imaging system (Perkin Elmer) and Perkin Elmer image analysis software in early 2020. I did not revisit this after the lengthy COVID-19 imposed break to my labwork, and instead finalised my work on phosphoinositides (see chapter 5) along with other experiments, notably swarming, which was optimized with mouse BMNs in Edinburgh, and further elaborated upon with human neutrophils during my placement at GSK (see chapter 6).

5. Results - SHIP2 alters global 3-phosphorylated phosphoinositide species in neutrophils

5.1 Introduction

In the previous chapter I identified the roles of SHIP2 in neutrophil effector functions. I showed that SHIP2 regulates neutrophils polarisation, chemotaxis, adhesion under conditions of flow and in vivo recruitment to sites of inflammation. To build on this, here I set out to understand the molecular mechanisms involved in the observed $Ship2^{\Delta/\Delta}$ defects to explain how SHIP2 regulates these functions.

Hypothesis

The functional defects observed in Ship2$^{\Delta/\Delta}$ neutrophils is linked to a change in PIP3 and PI(3,4)P2 levels.

Chapter-specific aims

The aim of this chapter was to understand the molecular mechanisms underpinning the observed Ship2$^{\Delta/\Delta}$ neutrophil phenotype. More specifically, I aimed to:

1) Identify if there is a change in PIP3 or PI(3,4)P2 levels in Ship2$^{\Delta/\Delta}$ neutrophils compared to wild-type controls

2) Determine the localisation of SHIP2 in neutrophils that do and don't express ARAP3

3) Investigate if inhibiting PI3K γ and δ can rescue the previously identified chemotaxis defects in Ship2$^{\Delta/\Delta}$ neutrophils

5.2 Results

5.2.1 Stimulation-induced PKB phosphorylation is not affected in SHIP2$^{\Delta/\Delta}$ neutrophils

Upon agonist stimulated activation of PI3K, the lipid second messenger PIP3 is produced at the plasma membrane, recruiting PI3K effectors to the plasma membrane where they can be further activated, e.g. by phosphorylation [50, 80]. PKB is the best understood of all PI3K effectors, and its phosphorylation status is often used as an indirect readout of PI3K activity. PKB Thr-308 is phosphorylated by the direct PI3K effector PDK1 and Ser-473 is phosphorylated indirectly via mTORC2 [208-210]. In adherent, SHIP1-deficient neutrophils, PKB is hyperphosphorylated, while PTEN-deficient neutrophils are characterized by PKB hyperphosphorylation in response to fMLF stimulation [63]. Therefore, to understand the mechanisms underlying the effector function defects in SHIP2$^{\Delta/\Delta}$ neutrophils, PKB phosphorylation levels were compared to wild-type controls. I determined Thr-308 and Ser-473 phosphorylation of neutrophils in suspension that had or had not been stimulated with fMLF for up to 5 minutes by western blotting (Figure 5.2.1 A). Densitometrical analysis of my blots indicated that there were no differences in PKB activation between the two genotypes (Figure 5.2.1 B, C).

Due to the previously detected regulatory function of SHIP2 in chemotaxis, adhesion and spreading (where cells were stimulated with a chemoattractant in the context of adhesion), I also combined stimulations by allowing the neutrophils to adhere onto fibrinogen coated tissue culture plastic while being

co-stimulated with fMLF (Figure 5.2.1 D). Again, no differences were observed between the genotypes which was confirmed with densitometry measurements (Figure 4E, F). It was therefore concluded that SHIP2 had no major effect on agonist-stimulated PKB phosphorylation.

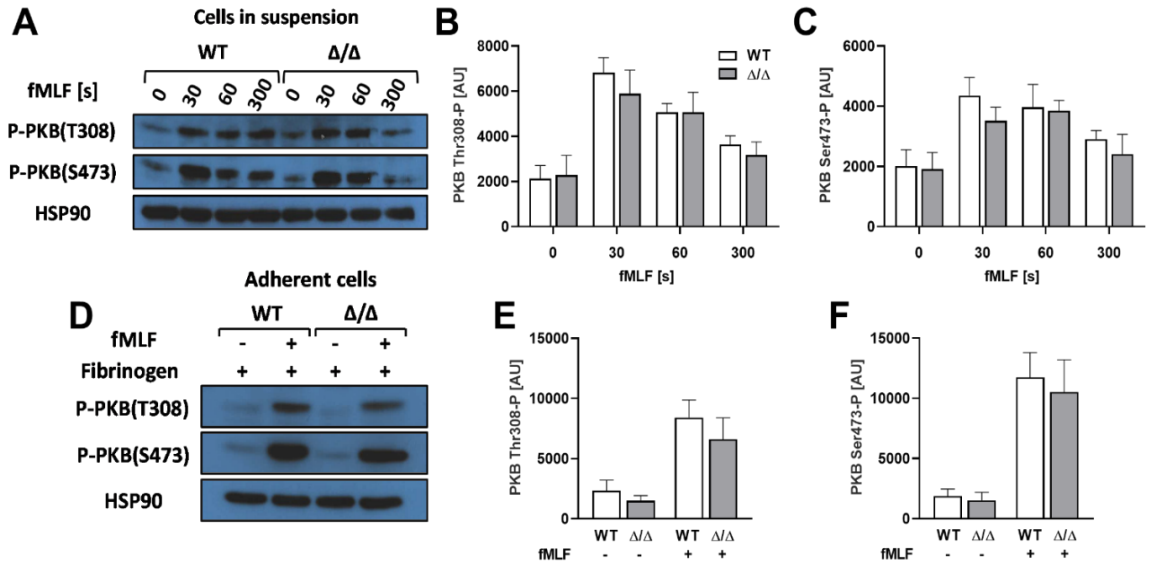

Figure 5.2.1 Similar PKB phosphorylation in WT and Ship2$^{\Delta/\Delta}$ neutrophils. (A-F) Western blot analysis of bone marrow-derived WT and Ship2$^{\Delta/\Delta}$ neutrophils stimulated and analysed for PKB phosphorylation. **(A-C)** Time course assay of cells in suspension stimulated with 1 μM fMLF at 37°C or **(D-F)** neutrophils were plated onto 150 μg/mL fibrinogen-coated surface and co-stimulated with 1 μM fMLF at 37°C for 19 minutes. **(A, D)** show representative blots probed for phospho-PKB Thr 308, Ser 473 and HSP90 as a loading control while **(B-C, E-F)** show the densitometry analyses of 5 and 4 separate experiments respectively. p values were determined by 2-way ANOVA with Sidak's multiple comparisons test post-hoc test (B, C, E, F). Figure from [197].

5.2.2 Ship2$^{\Delta/\Delta}$ neutrophils are characterised by subtly increased PIP3 in response to fMLF stimulation

PKB can be recruited to the plasma membrane by PIP3 for phosphorylation by PDK1 [208, 209], but like the majority of PI3K effectors, it can also be recruited by the second messenger PI(3,4)P2 [211, 212]. This means that the similar PKB phosphorylation I observed earlier between the genotypes could theoretically be obtained even if the ratio of these two lipid second messengers had changed. To determine levels of PIP3 in our samples more directly, I collaborated with Dr Karen Anderson at the Babraham Institute, Cambridge to use lipid mass spectrometry, a more sensitive and direct method to quantitate PIP3 production [174, 213].

Neutrophils from each genotype were stimulated with fMLF or its vehicle for up to 5 minutes prior to mass spectrometry analysis, showing a peak in PIP3 production after 10s stimulation (Figure 5.2.2 A). In every repeat, we observed subtle but consistent significantly increased PIP3 levels in Ship2$^{\Delta/\Delta}$ neutrophils at the 60s stimulation timepoint (see Figure 5.2.2 B).

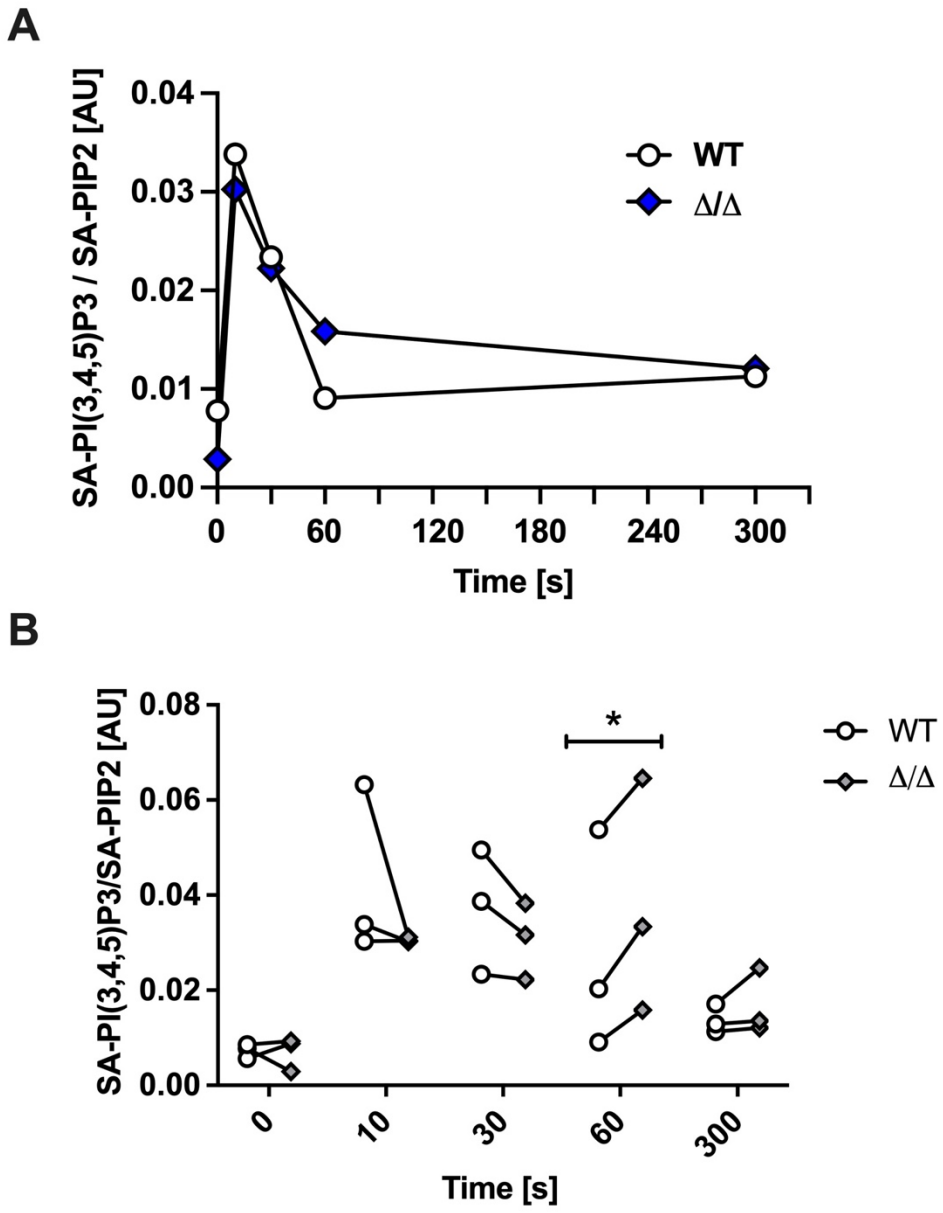

Figure 5.2.2 Subtle increase of quantified PIP3 in Ship2$^{\Delta/\Delta}$ neutrophils. Mass spectrometry analysis of PIP3 generated by fMLF stimulated and unstimulated samples. **(A)** One representative experiment of stearoyl/arachidonoyl (SA) PIP3 divided by SA-PIP2. **(B)** Reproducibility of PIP3 changes at different timepoints with all 3 experiments in Ship2$^{\Delta/\Delta}$ neutrophils. *p* values were determined by a paired t test, *p<0.05, error bars show SEM.

5.2.3 Ship2$^{\Delta/\Delta}$ neutrophils contain different levels of PI(3,4)P2 compared to controls

Effector function differences between the wild-type and Ship2$^{\Delta/\Delta}$ neutrophils described in chapter 4 could be due to the subtle increase in PI(3,4,5)P3 levels that was detected by mass spectrometry. However, another possibility for these differences could be a change in the SHIP2 product, PI(3,4)P2, which is itself a second messenger [214]. To test this, I collaborated further with Dr Karen Anderson at the Babraham institute who tried to also quantify PI(3,4)P2 by mass spectrometry using a new method that was developed by members of the Babraham Institute, Cambridge under guidance by Dr Phillip Hawkins [215]. Unfortunately, the approach was not sensitive enough to detect PI(3,4)P2, although the extraction/ozonolysis were successful, as indicated by the standards and the PI(4,5)P2 signals which were strong. This is in keeping with prior unpublished observations that neutrophils generate very little PI(3,4)P2 (Dr Phillip Hawkins, The Babraham Institute, personal communication). Instead, we therefore resorted to immunofluorescence, making use of an antibody that had previously been validated to detect PI(3,4)P2 [215].

5.2.3.1 Adherent Ship2$^{\Delta/\Delta}$ neutrophils generate less PI(3,4)P2 compared to controls

Due to the previously detected regulatory function of SHIP2 in adhesion and spreading, I wanted to see if allowing the cells to adhere onto a surface would affect PI(3,4)P2 levels in Ship2$^{\Delta/\Delta}$ neutrophils. To test this, neutrophils were allowed to adhere to glass coverslips with or without fMLF stimulation. Following fixation, cells were stained with the anti-PI(3,4)P2 antibody, images were acquired and intensity measurements carried out using CellProfiler. Figure 5.2.3.1 A shows that as with the unstimulated cells in suspension, adherent Ship2$^{\Delta/\Delta}$ neutrophils produced significantly less PI(3,4)P2 than wild-type controls. Interestingly, stimulating these cells with fMLF further decreased PI(3,4)P2 in the neutrophils.

I also compared the localisation of PI(3,4)P2 in both genotypes with and without fMLF stimulation microscopically (Figure 5.2.4.2 B). In keeping with it being the only phosphoinositide associated with clathrin mediated endocytosis [216-218], PI(3,4)P2 was consistently found on endomembranes in all conditions I examined.

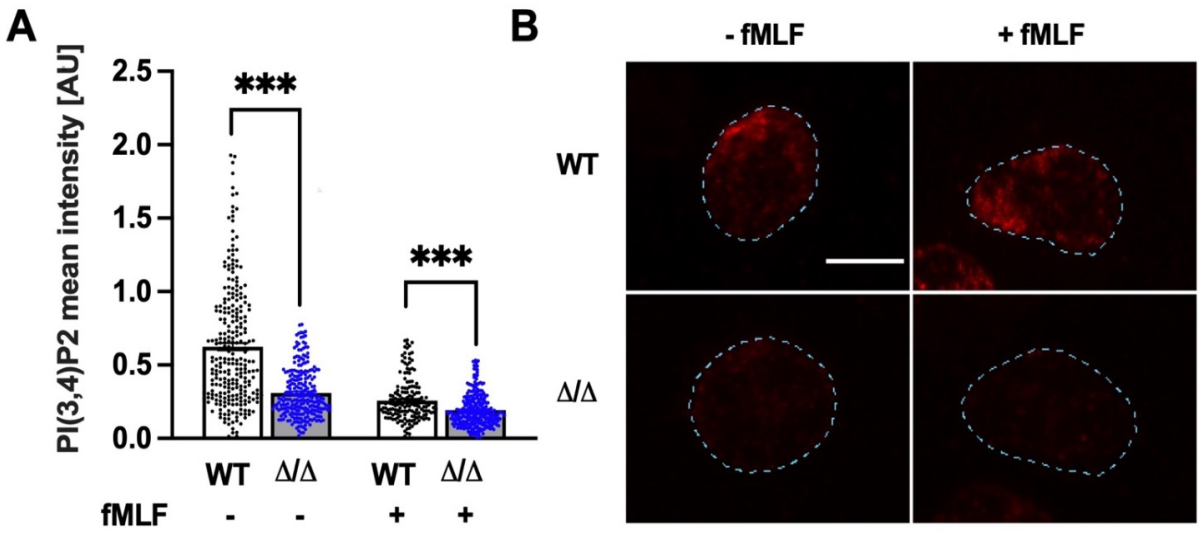

Figure 5.2.3.1 Ship2$^{\Delta/\Delta}$ neutrophils have less PI(3,4)P2. fMLF stimulated (1 μM) and unstimulated neutrophils were stained for PI(3,4)P2. **(A)** Images were acquired and analyzed automatedly using CellProfiler to quantify signal intensities which were plotted for each condition. Each point representants a neutrophil, which were prepped and stained on 3 separate days; *p* values were analysed by Mann-Whitney U test, ***p <0.001. **(B)** Confocal images were acquired of representative examples for each condition. Cell outlines are indicated by broken lines, scale bar is 5 μm. Figure from [197].

5.2.3.2 Ship2$^{\Delta/\Delta}$ neutrophils in suspension generate different levels of PI(3,4)P2

Allowing neutrophils to adhere onto glass slides is in itself a form of (integrin) stimulation. Having identified differences in PI(3,4)P2 levels in adherent neutrophils between the genotypes with and without fMLF stimulation, I then wanted to determine if the same applied to cells in suspension. To do this, I stained fixed, unstimulated and fMLF stimulated neutrophils (10s, 60s and 300s) in suspension with the anti-PI(3,4)P2 antibody and allowed them to settle on electrostatically coated slides before acquiring images comparing the two genotypes. To quantitate the observed differences in PI(3,4)P2 levels between the timepoints and genotypes, intensity measurements were performed using Cell Profiler as detailed in the methods chapter.

The first 2 repeats identified that unstimulated Ship2$^{\Delta/\Delta}$ neutrophils had weaker PI(3,4)P2 signal than wild-type controls, but no differences were detected between the genotypes at 60s and 300s of stimulation. Interestingly, there was an increase in PI(3,4)P2 levels in Ship2$^{\Delta/\Delta}$ neutrophils after 10s of stimulation. Unfortunately, at this point the directly conjugated PI(3,4)P2 antibody that we had been using was discontinued by the manufacturer and our stock ran out. For the final repeat, I prioritised the 60s timepoint where we observed less PIP3 in Ship2$^{\Delta/\Delta}$ neutrophils with the mass spectrometry analysis (to ensure consistency during analysis, all experiments were imaged on the same occasion using the same settings). Figure 5.2.3.2 shows PI(3,4)P2 intensity measurements confirming that resting Ship2$^{\Delta/\Delta}$ neutrophils have less

PI(3,4)P2 than controls, but after 60s stimulation, PI(3,4)P2 levels are similar between the genotypes.

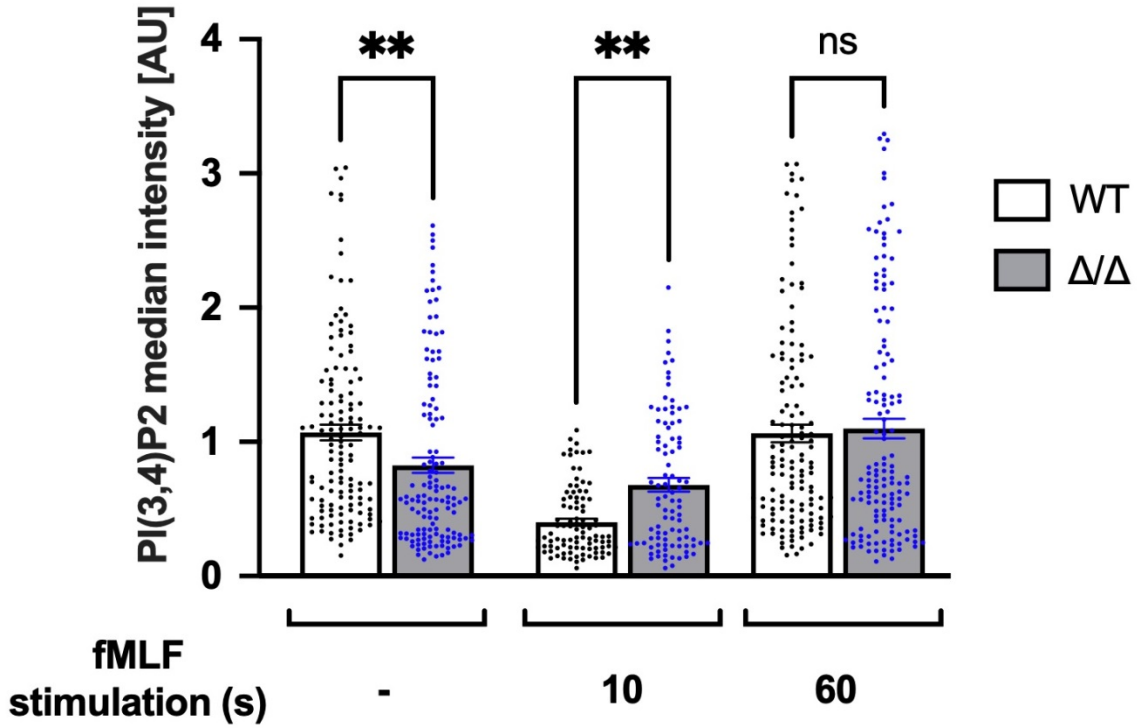

Figure 5.2.3.2 Ship2$^{\Delta/\Delta}$ neutrophils in suspension generate different levels of PI(3,4)P2 compared to wild-type controls. PI(3,4)P2 levels for cells in suspension were compared between WT and Ship2$^{\Delta/\Delta}$ neutrophils. Images were acquired of PI(3,4)P2 stained neutrophils and analyzed automatedly using CellProfiler to quantify median signal intensities. Intensity measurements from unstimulated and 60s fMLF stimulated neutrophils were obtained from 3 separate experiments. Measurements for 10s fMLF stimulated neutrophils were obtained from 2 separate experiments. Median intensities of 50 cells were plotted for each condition of every experiment and the *p* values analysed by a Kruskal-Wallis test, **p <0.01, error bars show SEM.

5.2.4 mCherry tagged SHIP2 is perinuclear and cytosolic

In fibroblasts, SHIP2 localisation was reported to be cytosolic, perinuclear and at the leading edge of the cell [219], however, this has yet to be determined in neutrophils. To address this, I retrovirally transduced HoxB8 progenitors with an mCherry-tagged SHIP2 construct. HoxB8 progenitors derived from *Arap3*$^{-/-}$ mice were also transduced with mCherry SHIP2 to determine whether ARAP3 might be involved in the localisation of SHIP2 to the plasma membrane. This had been suggested by experiments performed by Helen Craig, who found that SHIP2 was unable to associate with PIP3 beads unless in a heterodimeric form with ARAP3 [181]. To test this, *Arap3*$^{-/-}$ HoxB8 progenitors were generated from *Arap3*$^{-/-}$ mice. Wild-type and *Arap3*$^{-/-}$ HoxB8 cells were then transduced and single cell sorted by fluorescence-activated cell sorting (FACS) for mCherry as presented in the methods (Figure 2.5.6). Once the sorted cells had recovered and started to divide rapidly, the progenitors were scanned for clones expressing detectible mCherry by fluorescence microscopy. Of these, clones that produced the highest percentages of HoxB8 neutrophils upon estradiol withdrawal were allowed to adhere onto coverslips, fixed, counterstained, mounted and imaged (Figure 5.2.4). As with the fibroblasts, SHIP2 in wild-type HoxB8 neutrophils was predominantly perinuclear and cytosolic; the same was confirmed in *Arap3*$^{-/-}$ HoxB8 cells. This suggests that despite the ability of SHIP2 and ARAP3 to form heterodimers through their SAM domains, ARAP3 is not essential for SHIP2 localisation at least in unstimulated neutrophils.

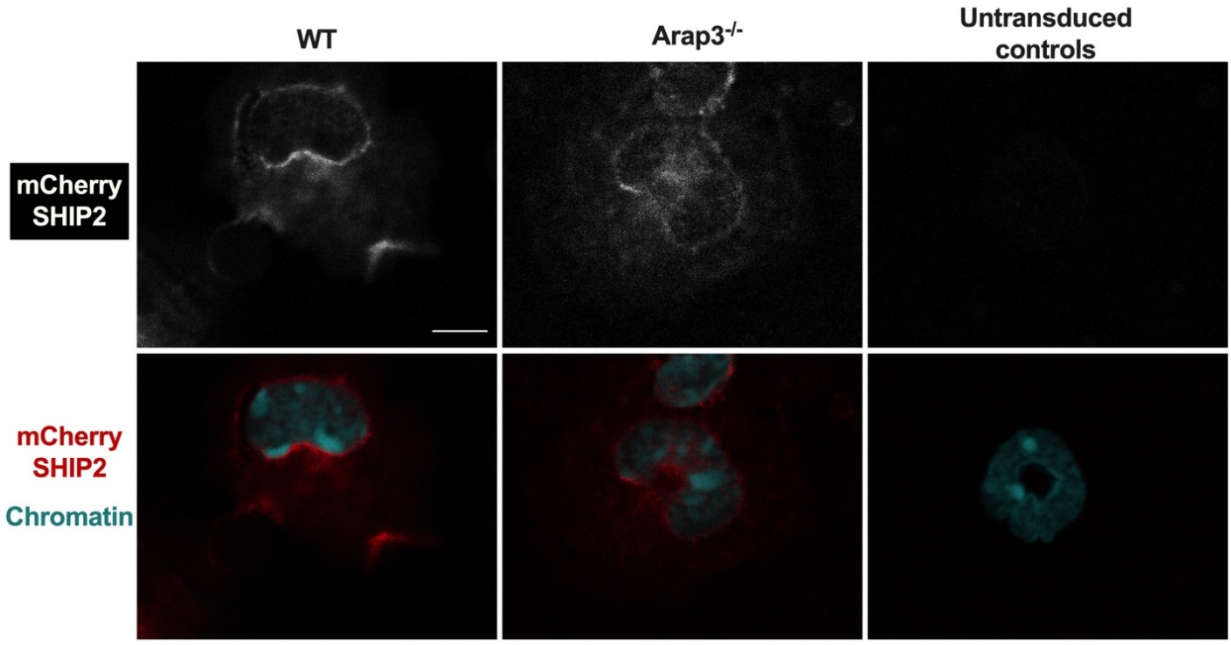

Figure 5.2.4 HoxB8 cells with mCherry tagged SHIP2. Representative examples of the localisation of SHIP2 in Hoechst-stained wild-type and *Arap3*$^{-/-}$ HoxB8 neutrophils, scale bar, 5 μm.

5.2.5 Inhibiting PI3K δ slightly improves the Ship2$^{\Delta/\Delta}$ chemotaxis directionality defect

A study on neutrophil chemotaxis in the elderly reported they exhibit a migratory defect towards a range of chemoattractants, and inhibiting PI3K γ and δ restores their migratory accuracy [120]. Having identified SHIP2 as a regulator of neutrophil chemotaxis and directionality (chapter 4.2.2.2), I hypothesised that SHIP2 is responsible for the migratory defect observed in the elderly. Therefore, to determine if the same applies to Ship2$^{\Delta/\Delta}$ neutrophils, I performed chemotaxis assays in a 3D matrix using an IBIDI chamber while inhibiting PI3K γ and δ to check if the chemotaxis defects that were previously

identified could be rescued. Chemotaxing neutrophils from the time lapse movies were then manually tracked and the Euclidian distances and directionality measured and plotted comparing wild-type and Ship2$^{\Delta/\Delta}$ neutrophils. While neither of these inhibitors improved the Euclidean distances of Ship2$^{\Delta/\Delta}$ neutrophils (Figure 5.2.5 A), interestingly, inhibiting PI3K δ subtly improved the directionality of Ship2$^{\Delta/\Delta}$ neutrophils [120] as shown in Figure 5.2.5 B.

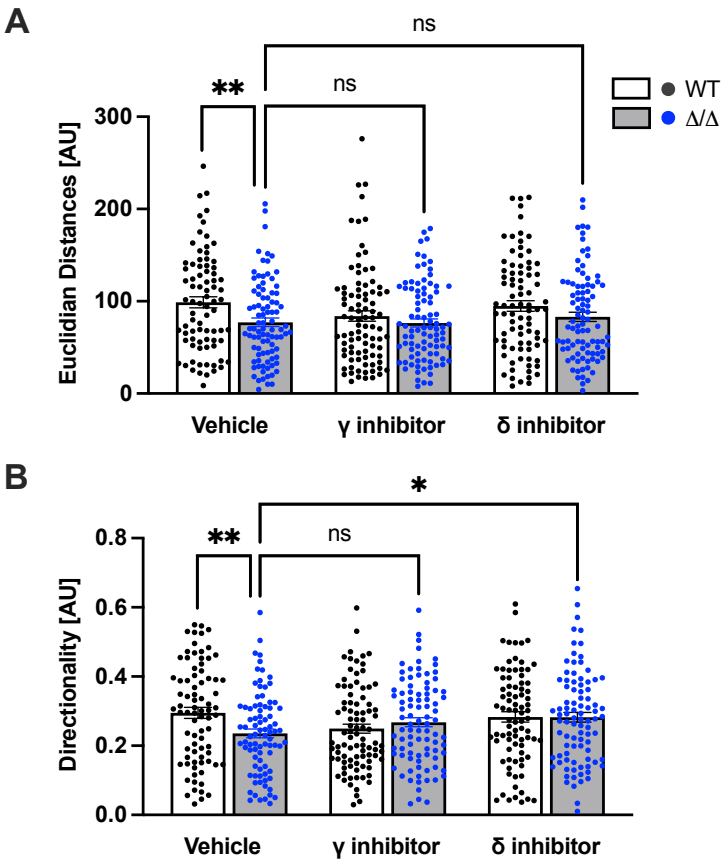

Figure 5.2.5 Inhibiting PI3Kdelta improves chemotaxis of SHIP2-deficient neutrophils. Chemotaxis assays in IBIDI chambers of primed neutrophils (TNF-α, 4.55 ng/mL and GM-CSF, 100 ng/μL) towards 300 nM fMLF were performed on wild-type and Ship2$^{\Delta/\Delta}$ BMNs incubated with PI3K γ inhibitor CZC24832 (2 μM) or PI3K δ inhibitor IC87114 (1 μM). Their paths were then tracked manually and the **(A)** Euclidean distances and **(B)** directionality calculated with the IBIDI chemotaxis and migration tool software. The values were plotted for neutrophils obtained from 3 separate experiments, 30 neutrophils per condition for each experiment, and the *p* values analysed by Mann-Whitney U test, *p =0.027, **p <0.01.

5.3 Discussion

This chapter describes the molecular mechanisms behind the functional differences observed between the Ship2$^{\Delta/\Delta}$ neutrophils and the wild-type controls. Mechanistically, the Ship2$^{\Delta/\Delta}$ neutrophil phenotype seems largely due to decreased cellular PI(3,4)P2 rather than increased PIP3. Stimulated and unstimulated neutrophil lysates from SHIP1-deficient mice are characterized by enhanced PKB Thr-308 and Ser-473 phosphorylation which signifies a hyperactivated PKB signalling pathway attributed to substantially increased PI(3,4,5)P3 production [59]. In contrast, we observed no striking difference in PI3K activity in Ship2$^{\Delta/\Delta}$ neutrophils with only a subtle increase in PIP3 after fMLF stimulation for 60s. Instead, we observed considerably reduced intracellular PI(3,4)P2 in both adherent and suspension neutrophils. It is worth noting however, that after 10s stimulation with fMLF an increase of PI(3,4)P2 was identified in suspension Ship2$^{\Delta/\Delta}$ neutrophils compared to the controls.

In keeping with previous descriptions [216-218], PI(3,4)P2 was largely located in endomembranes. PI(3,4)P2 in endomembranes is attributed to both, the phosphorylation of PI4P by Class II PI3K 2a in clathrin-dependent endocytosis and the 5-dephosphorylation of PIP3 in clathrin-independent endocytosis where SHIP2 is involved [220]. I used transduced HoxB8 neutrophils to show that SHIP2 in neutrophils is perinuclear and cytosolic. I had planned to repeat this experiment with fMLF stimulated HoxB8 neutrophils from each genotype to determine if like fibroblasts, SHIP2 in neutrophils localises to the plasma membrane of the leading edge [219]. This could explain the defective

polarisation observed in Ship2$^{\Delta/\Delta}$ neutrophils (see Chapter 4). This is particularly interesting since PI(3,4)P2 was not preferentially distributed in stimulated mouse neutrophils. I had also started working on other HoxB8 genotypes to study spatiotemporal PIP3/PI(3,4)P2 dynamics in real time, unfortunately however, due to lockdown the cells were frozen down and my work shifted focus from transduced reporters in HoxB8s to using antibodies in freshly isolated BMNs.

I was unfortunately unable to address potential redundancy between SHIP1 and SHIP2 since I did not have access to a suitable genetic model and SHIP inhibitors are not very specific. In addition, there are many other 5' phosphatases that don't use PIP3 as their major substrate which to date remain poorly characterised, and may potentially be involved in compensation [66].

Inhibiting PI3K δ subtly improved the directionality defect observed in neutrophils lacking SHIP2 catalytic activity. A previous study using a PI3K δ inhibitor in human neutrophils identified that PI3K δ plays a selective role in PIP3 amplification in neutrophil polarisation and directional migration [221]. Another similar study showed that unlike PI3K γ which is required for chemokinetic migration, PI3K δ is essential for both chemokinetic and chemotactic migration [222]. In contrast, analysis of neutrophil migration in a p110 δ$^{-/-}$ mouse in vivo, suggested that PI3Kδ deficiency alone does not interfere with neutrophil migration in response to fMLF, while resulting in subtly improved migration of neutrophils to inflammatory sites [223]. Further

experiments would need to be performed to establish whether the improved directionality observed in Ship2$^{\Delta/\Delta}$ neutrophils is due to these cells having an excess of PI3Kδ activity. Given that we did not observe increased PKB phosphorylation nor PIP3 production this seems somewhat unlikely. An alternative possibility might be that inhibiting PI3Kδ for a reason which remains to be established improves directionality at least in some contexts. Interestingly, inhibiting PI3Kδ/γ was also shown to improve directionality of neutrophils from aged donors [120]. However, this study analysed PI3K activity in a rather unusual fashion, by measuring phosphorylation of the p85 subunit of PI3K, making it difficult to conclude with certainty that the reason for the poorer directionality of neutrophils from elderly donors was indeed excessive PI3Kδ/γ activity.

6. Results - Effects of Immunosenescence in Neutrophil Effector Functions

6.1 Introduction

Immunosenescence is the deterioration of the immune system with old age. As described in the introduction, the effects of age-related changes on the adaptive immune system have been well characterised. Contrastingly however, the effects of immunosenescence in the innate immune system has yet to be thoroughly investigated.

As part of the first line of defence, it is pivotal that the appropriate number of neutrophils reach the sites of infection to clear the invading pathogens. There is currently a lack of reported studies examining this in the elderly in vivo, however, some in vitro studies have shown that despite mounting normal neutrophilia during infection [168], a chemotaxis defect is observed in neutrophils from elderly donors towards a range of stimuli [120, 179, 180] which could lead to decreased neutrophil recruitment to sites of infection. In addition, it was shown that inhibiting PI3K δ and γ restored this migratory defect, highlighting the importance of the PI3K pathway in the neutrophil immunosenescence phenotype [120]. Therefore, despite my work on ARAP3 in the context of neutrophil immunosenescence leading to a dead end, for my placement at GSK I decided to explore the effects of aging on neutrophil swarming and neutrophil functions that are thought to underpin this. This would also link well to my work on SHIP2 in the previous chapter (chapter 5.2.6)

which showed that the inhibition of PI3K δ slightly improved the directionality of Ship2$^{\Delta/\Delta}$ neutrophils.

During this 3 month placement, I isolated neutrophils from young (<25 years) and old (>60 years) donors to explore neutrophil swarming and the associated cytokines released, elastase release and ROS production. To link this to my SHIP2 work, I aimed to investigate SHIP2 expression in neutrophils from donors of these different ages as well as measure the associated phosphatase activity of SHIP2 in neutrophils from each donor as shown in the plan outline in Figure 6.1.

Hypothesis

The hypothesis tested in this chapter was that neutrophils from elderly donors are characterised by reduced swarming compared to those from young donors due to a defect in PI3K/SHIP2 signalling.

Chapter-specific aims

The aim of this chapter was to compare neutrophil swarming from young and old donors. More specific chapter aims include:

1. To determine if there is a swarming defect in neutrophils from elderly donors and investigate the consequences of inhibiting LTB4 production from each donor.

2. To establish any differences in neutrophilic cytokine release during neutrophil swarming.

3. To study neutrophil elastase release and ROS production for each age group.

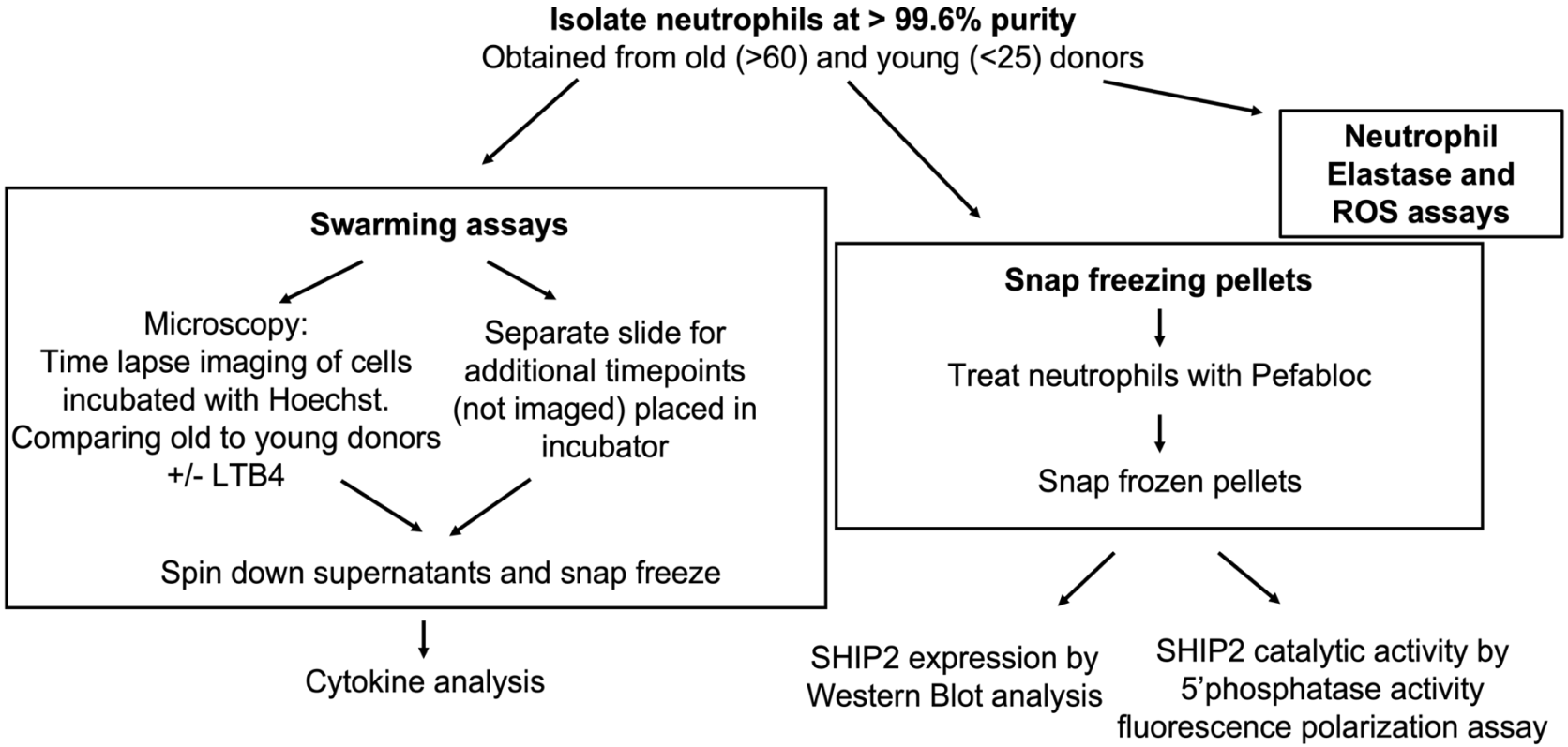

Figure 6.1 Experimental scheme of the work planned at GSK. I planned to isolate peripheral blood neutrophils from a young and elderly donor for each experiment. Once obtained, the neutrophils from each donor would be compared on the same day by performing swarming assays, elastase assays, ROS assays as well as snap freezing pefabloc treated samples. In addition, cytokine contents of the supernatants from the swarming assays would be analysed and the snap frozen cell pellets analysed for SHIP2 expression and SHIP2 phosphatase catalytic activity.

6.2 Results

6.2.1 Obtaining neutrophils at high purity

As discussed already in chapter 4, a pure preparation of neutrophils is required to study cytokine release by neutrophils. To achieve this with human peripheral blood, a two-step purification method was optimised to yield pure human neutrophils as described in the materials and methods (chapter 2.1.1). The purity and the activation of these neutrophils were compared to those isolated solely by the one-step purification method (involving dextran sedimentation and a discontinuous Percoll gradient) which I had performed in previous experiments in chapter 3. Images of cytocentrifuge preparations stained with Quick Diff reagents as well as analysis by flow cytometry showed an improvement from 97.4% purity by the one-step purification method to 100% purity with the two-step purification method as shown in Figure 6.2.1 A and B. Next, to check the activation status of these neutrophils, ROS and Elastase assays was performed both of which showed no difference between the purification methods when unstimulated or primed with LPS as shown in Figure 6.2.1 C and D.

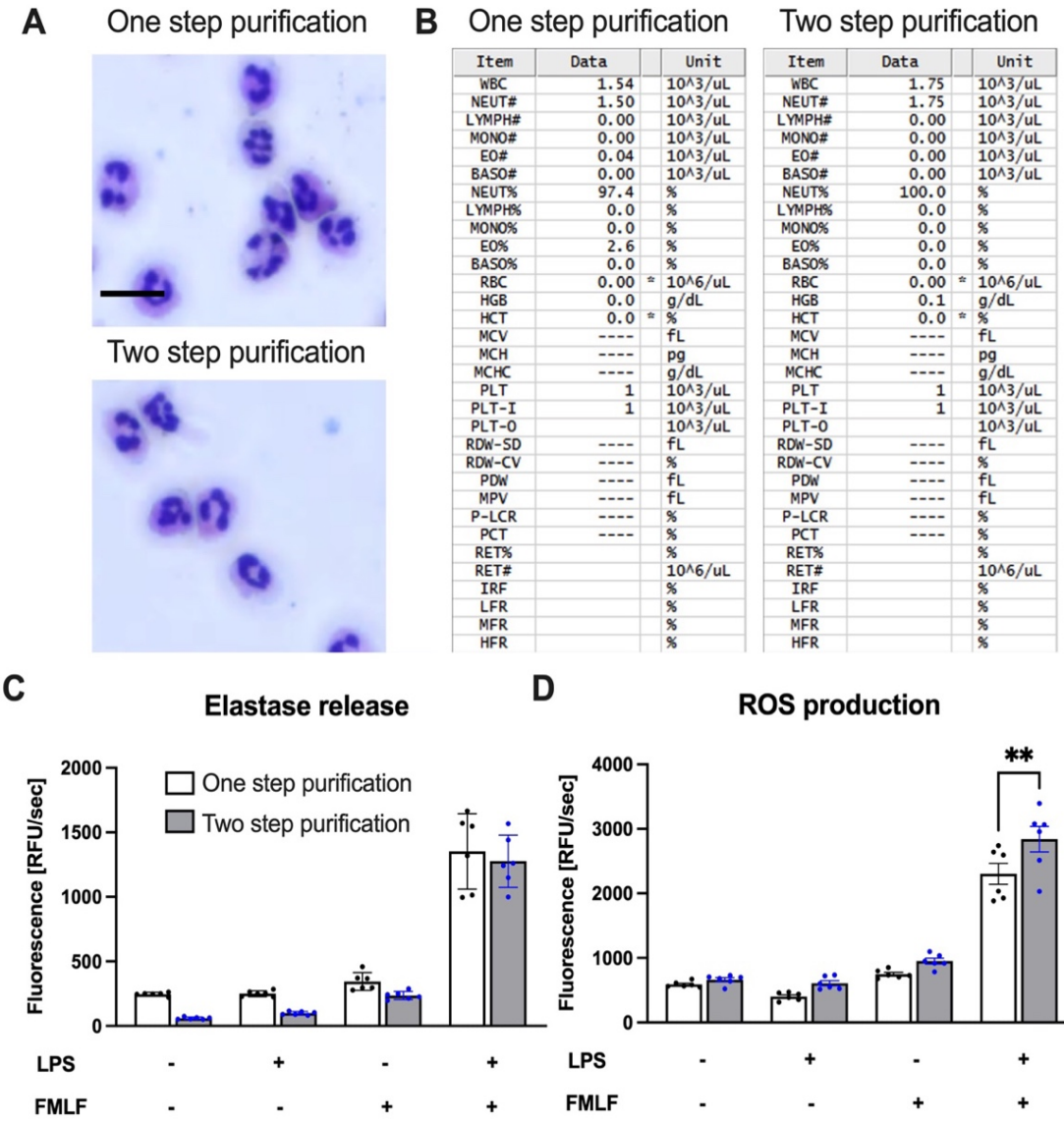

Item	Data		Unit
WBC	1.54		10^3/uL
NEUT#	1.50		10^3/uL
LYMPH#	0.00		10^3/uL
MONO#	0.00		10^3/uL
EO#	0.04		10^3/uL
BASO#	0.00		10^3/uL
NEUT%	97.4		%
LYMPH%	0.0		%
MONO%	0.0		%
EO%	2.6		%
BASO%	0.0		%
RBC	0.00	*	10^6/uL
HGB	0.0		g/dL
HCT	0.0	*	%
MCV	----		fL
MCH	----		pg
MCHC	----		g/dL
PLT	1		10^3/uL
PLT-I	1		10^3/uL
PLT-O			10^3/uL
RDW-SD	----		fL
RDW-CV	----		%
PDW	----		fL
MPV	----		fL
P-LCR	----		%
PCT	----		%
RET%			%
RET#			10^6/uL
IRF			%
LFR			%
MFR			%
HFR			%

Item	Data		Unit
WBC	1.75		10^3/uL
NEUT#	1.75		10^3/uL
LYMPH#	0.00		10^3/uL
MONO#	0.00		10^3/uL
EO#	0.00		10^3/uL
BASO#	0.00		10^3/uL
NEUT%	100.0		%
LYMPH%	0.0		%
MONO%	0.0		%
EO%	0.0		%
BASO%	0.0		%
RBC	0.00	*	10^6/uL
HGB	0.1		g/dL
HCT	0.0	*	%
MCV	----		fL
MCH	----		pg
MCHC	----		g/dL
PLT	1		10^3/uL
PLT-I	1		10^3/uL
PLT-O			10^3/uL
RDW-SD	----		fL
RDW-CV	----		%
PDW	----		fL
MPV	----		fL
P-LCR	----		%
PCT	----		%
RET%			%
RET#			10^6/uL
IRF			%
LFR			%
MFR			%
HFR			%

Figure 6.2.1 Improving the purity of human neutrophils. (A) Representative cytocentrifuge preparations of Diff Quick stained neutrophils obtained from a Percoll prep (One step purification, top image) and combined Percoll prep followed by a negative selection human enrichment Kit (two step purification, bottom image), scale bar 10 µm. **(B)** Purity of neutrophils from each sample was analysed on the Sysmex XT-2000iV. **(C-D)** Neutrophils with or without LPS priming (50 ng/ml) were either stimulated or mock stimulated with 0.75 µM fMLF to compare those isolated by the one or two step purification process, measuring **(C)** elastase release or **(D)** ROS production by fluorescence. *p* values were determined with a one-way ANOVA using Sidak's multiple comparisons test, **p<0.01, error bars show SEM.

6.2.2 Neutrophils from elderly donors are characterised by a swarming defect towards zymosan particles compared to those from young donors

To test the swarming by human neutrophils, time lapse video microscopy was performed to detect Texas Red-labelled zymosan clusters and neutrophils stained with Hoechst as shown in Figure 6.2.2.1. In the first 5 minutes, only a few neutrophils were observed in the field of view but more accumulated over time, and within 30 minutes a dense neutrophil swarm could be observed around each zymosan cluster.

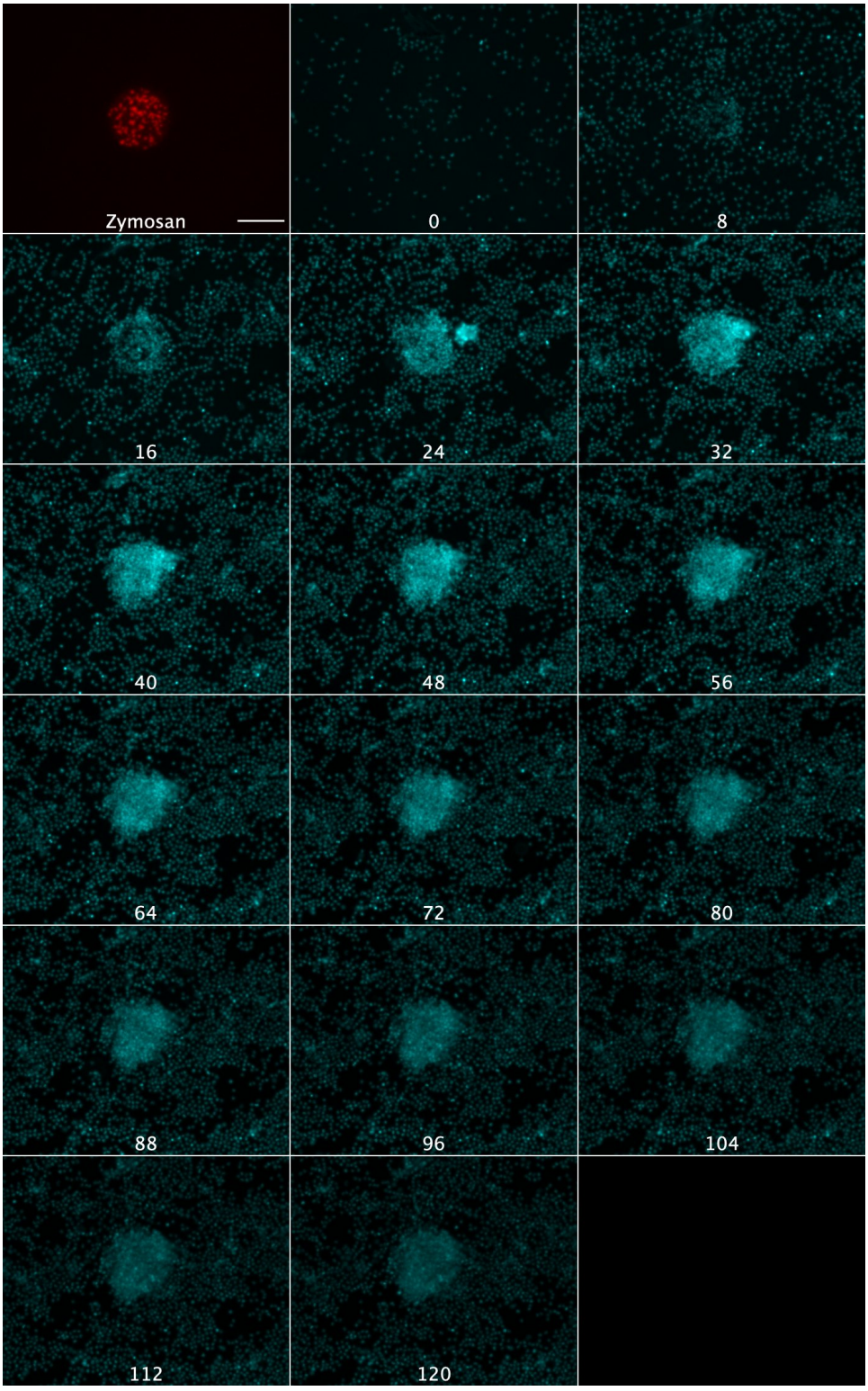

Figure 6.2.2.1 Time lapse movie of neutrophil swarming. 5x10^5 neutrophils stained with Hoechst were placed into wells on a glass slide containing clusters of zymosan. The first panel shows Texas Red stained zymosan cluster. The rest show time lapse images acquired every 8 minutes, for 2 hours showing neutrophil swarms surrounding the zymosan clusters. Scale bar is 100 μm.

Next, I carried out swarming assays comparing neutrophils from old donors (>60) to young donors (<25). In addition, to understand the importance of the lipid mediator LTB4 on neutrophil swarming, 2 further conditions were included that tested the effect of blocking LTB4 production by applying the FLAP inhibitor MK-886 to neutrophils from each of the donors (LTB4 production summarised in Figure 1.4.3). The time lapse images were processed automatedly as detailed in chapter 2.4.6 and the signal intensities were measured for each time point for 10 different zymosan clusters per condition in each well. The graphical representation in Figure 6.2.2.2 A shows the mean fluorescent intensity measurements of the swarms formed around the zymosan clusters in a representative time-lapse experiment. Despite some variability between donors, neutrophils from older donors formed smaller swarms than those from young donors in four of the five experiments performed. As expected, interfering with LTB4 formation decreased swarm formation in neutrophils isolated from young donors, but surprisingly, neutrophils from older donors showed improved swarming in response to MK-886 inhibition.

The area under the curve for these parameters for all five experiments are plotted in Figure 6.2.2.2 B, revealing a statistical difference between neutrophils that were and weren't LTB4 inhibited from old donors. The neutrophil swarms formed from young donors showed the opposite trend, where adding an LTB4 inhibitor decreased the intensity of the swarms. This suggests that neutrophils from younger donors are more reliant on LTB4

during swarming and it may be possible that older donors release excessive amounts of LTB4.

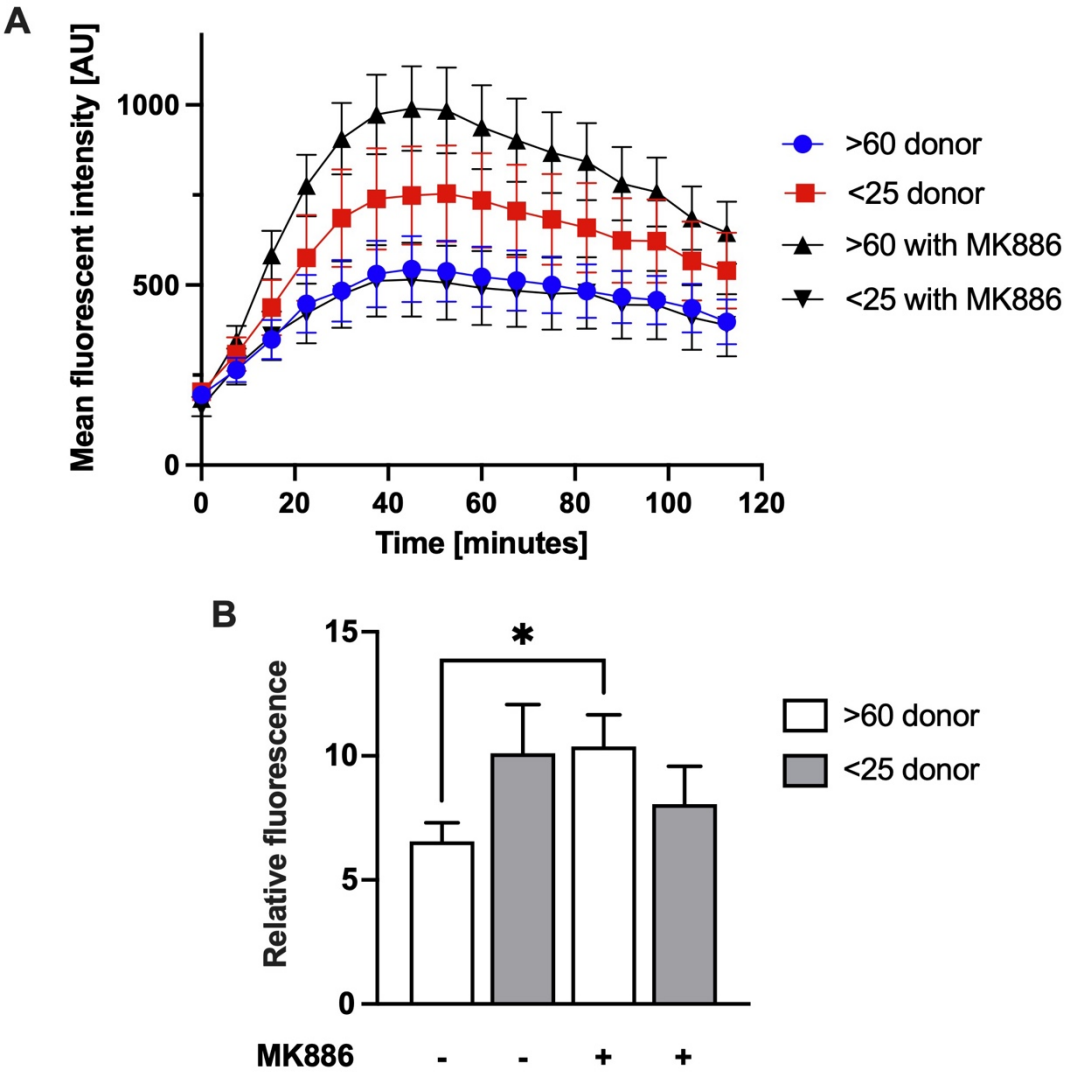

Figure 6.2.2.2 Inhibiting LTB4 significantly improves swarming of neutrophils prepared from elderly but not young donors. $5x10^5$ neutrophils from young and elderly donors were treated or mock treated with the LTB4 inhibitor (5-LO FLAP inhibitor, MK886 at 100 nM) and stained with Hoechst. The cells were then placed into wells on a glass slide containing clusters of zymosan and time lapse images acquired of the swarms formed. The images were analysed in Fiji measuring signal intensity of the swarms. **(A)** A representative graph from one experiment is shown. **(B)** A bar graph of the 5 experiments which were performed on different days with 10 swarms per condition for each; *p* values were determined with RM one-way ANOVA; Error bars show SEM, p=0.0224.

6.2.3 IL-8 production during swarming is decreased in neutrophils from older donors

In parallel to analysing neutrophil swarming in neutrophils isolated from the elderly and young donors, I also quantified cytokines produced by the neutrophils during swarming. A previous study by the Irimia group employed a multiplex quantitative enzyme-linked immunosorbent assay during neutrophil swarming towards zymosan and identified 440 mediators that contribute to the process as well as other swarming specific proteins [224]. Among the 10 proteins found to be released at significantly increased amounts during swarming, I analysed Cathepsin S, PDGF-BB, TIMP-1, Complement Factor D/Adipsin, Galectin-3, and Pentraxin 3 from the supernatants of neutrophils from the young and elderly. In addition, I analysed CXCL8, G-CSF and GM-CSF which were also found to enhance neutrophil swarming in other studies [47, 225]. However, the majority of these analytes were out of range in my analysis, being either too dilute or too concentrated.

The analytes within detection range included IL-8, TIMP-1 and Galectin-3 (Figure 6.2.3). TIMP-1 is a protease inhibitor shown to be important for the interaction of swarms with its local environment by limiting potential tissue damage and protecting healthy tissue [226].

Galectin-3 is an antimicrobial protein against bacteria and fungi [227], which in addition to activating endothelial cells, is known to augment neutrophil motility [228]. Of these, only IL-8 was found to differ between the age groups. The trend obtained with IL-8 measurements is suggestive of decreased IL-8

production in neutrophils from elderly donors during swarming regardless of the addition of the FLAP-inhibitor.

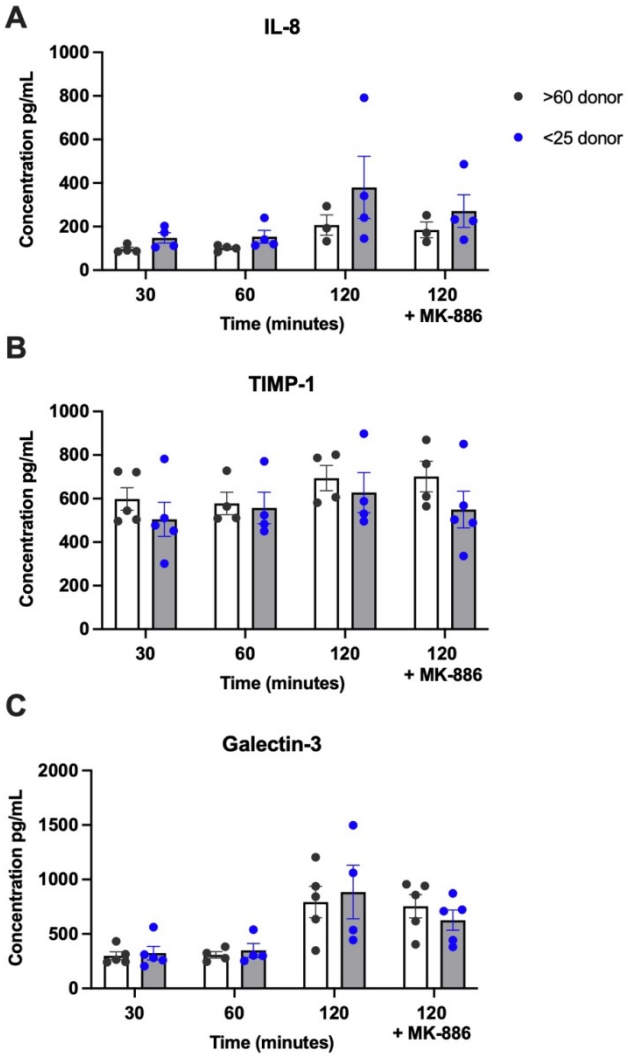

Figure 6.2.3 Neutrophils from old donors release less IL-8 during swarming compared to young donors. A Luminex assay was performed to measure **(A)** IL-8, **(B)** TIMP-1 and **(D)** Galectin-3 release during neutrophil swarming towards zymosan clusters from old and young donors with samples analysed at 30, 60 and 120 minutes after plating neutrophils onto zymosan arrays. The final time point at 120 minutes was also assessed with cells that had been treated with MK-886 (5-LO FLAP inhibitor, 100 nM). Every donor is represented with a symobol and the error bars show SEM. 3 or 4 experiments were analysed for each timepoint, and the p values determined by an ordinary 2-way ANOVA multicomparison post-hoc test, none of the trends reached statistical significance.

6.2.4 Neutrophils from old and young donors are characterised by similar levels of elastase release and ROS production

In paralell I also tested the effects of neutrophil ageing on ROS production and elastase release in response to fMLF stimulation. To my knowledge, there are no recent studies that investigate elastase release in ageing neutrophils. Contrastingly, there have been contradictory findings for ROS production, with some data identifying a decrease in elderly subjects [170, 229, 230] while others reported no difference [168, 231].

Figure 5.2.4 shows graphs of neutrophils that had been primed and mock primed with LPS, with and without fMLF stimulation, of neutrophils from young and elderly donors. No difference was identified for any of the conditions between the ages for either ROS production or elastase release.

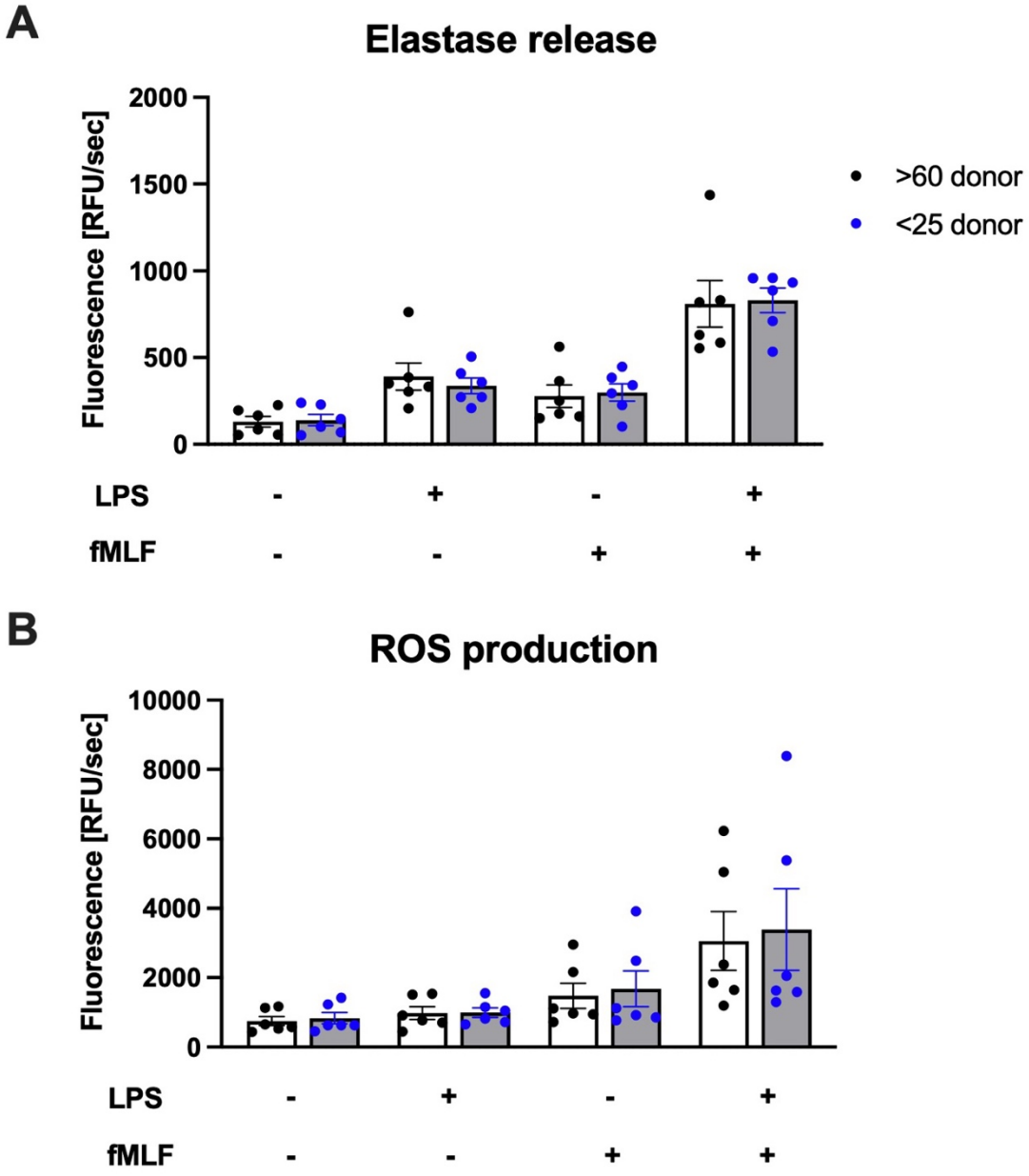

Figure 6.2.4 Old and young donors release and produce similar amounts of elastase and ROS respectively. (A-B) Neutrophils with or without LPS priming (50 ng/ml, O26:B6) were either stimulated or mock stimulated with 0.75 µM fMLF to compare neutrophils from young and old donors, measuring **(A)** elastase release and **(B)** ROS production. 6 experiments were performed for each on separate days and the p values determined by an ordinary 2-way ANOVA multicomparison post-hoc test, none of the trends reached statistical significance, error bars show SEM.

6.3 Discussion

In this chapter I identified a swarming defect in neutrophils from older donors. Intriguingly, the inhibition of the lipid mediator LTB4 by inhibiting Flap, which is required for LTB4 biosynthesis restored the swarming defect to match the swarms observed in neutrophils from young donors. While MK866 is a widely used Flap inhibitor, it would be good to repeat this experiment with an alternative pharmacological tool, such as a selective BLT1 inhibitor, e.g. LY2552837 which also interferes with swarming. Assuming that my intriguing observation would hold true, one possible explanation might lie in the possibility that LTB4 production increases with age as identified in a study on fresh bird blood [**Error! Hyperlink reference not valid.**]. In mice, another study identified that LTB4 release from resident bronchoalveolar macrophages was significantly greater in aged mice in response to A23187 compared to the younger animals [233]. In addition, LTB4 levels were found to increase chronically in several age-related inflammatory diseases in humans such as rheumatoid arthritis [234-237]. Excess LTB4 might saturate the media and make it more difficult for swarms to form. LTB4 would need to be quantified to confirm this hypothesis. The restoration of the swarming defect might be due to other mediators that contribute to swarming e.g. complement factors or chemokines [224] only once LTB4 is inhibited. However, if anything, the trends observed in my cytokine quantification revealed lower concentrations of IL-8 production in the supernatants from old donors.

In addition to the experiments presented here, I also prepared and froze down protease inhibitor treated neutrophil pellets, which I had planned to use to determine SHIP2 expression by Western blot and SHIP2 catalytic activity by a phosphatase activity fluorescence polarisation assay, comparing the young and old donors as previously described (Figure 6.1). However, due to time constraints I could not analyse these samples and instead focused on the swarming assays, the relevant cytokine analysis and measuring elastase release and ROS production. I prioritised those experiments since the swarming assays with the $Ship^{\Delta/\Delta}$ neutrophils had suggested SHIP2 is not likely to be an important regulator of neutrophil swarming (Chapter 4.2.4.2).

For the swarming assays a total of 5 repeats were performed, which is a very small *n* number considering that I was analysing human donors. More repeats would likely make the differences observed between young and old statistically significant, including for cytokine analysis (for which I only analysed 3-4 donors) where there typically is a large degree of variation between donors. In addition, due to lack of donor availability, the elderly donors I used were only >60 years old. To put this into perspective, studies into the effects of immunosenescence commonly use more than 10 repeats, with the elderly donors being >65 years old. Despite these limitations, I did observe a difference between the neutrophils from young and old donors during swarming and a trend towards reduced IL-8 generation. In contrast, neutrophils from the same donors showed no difference in ROS production or elastase release, suggesting that some, but not all functions in the neutrophils from these elderly donors were dysregulated.

7. Final Discussion

7.1 Project overview

The work discussed in this thesis examines the effects of the PI3K pathway on neutrophil chemotaxis and swarming. To address this, my original project focused on the PI3K effector protein ARAP3 since ARAP3 knockout neutrophils in contrast to other PI3K effectors exhibited a chemotaxis defect. Although the chemotaxis defect from ARAP3 knockout neutrophils were severe, it was hypothesized that changes to the activation status by phosphorylation would lead to more subtle changes, resembling the migratory defect observed in neutrophils from elderly donors [122]. Therefore, I aimed to determine the phosphorylation status of ARAP3 comparing samples from young and elderly donors by mass spectrometry. This project was abandoned however after several failed attempts to isolate the protein from neutrophil lysates as detailed in chapter 3.

Previous data from the Vermeren group showed that in contrast to wild-type neutrophils that polarize persistently towards a chemoattractant, ARAP3 deficient neutrophils were unable to do so. In the context of integrin-dependent migration, ARAP3-deficient neutrophils were unable to detach from the substratum and displayed a severe migration defect. In the context of integrin-independent chemotaxis, e.g. when migrating in a collagen matrix, ARAP3-deficient neutrophils still had a directionality defect, and migrated in a meandering fashion. By analysing neutrophils from mice expressing a GFP-PKB-PH construct which translocates to the site of PIP3 production in living

cells [65], these neutrophils were shown to exhibit poor persistency of PIP3 polarisation towards a point source of chemoattractant (fMLF) [91].

ARAP3 binds to PIP3 via its PH domains and is recruited to the plasma membrane in a PI3K-dependent fashion [80, 181]. ARAP3 was shown to form heterodimers in a SAM domain-mediated fashion with the 5' phosphatase SHIP2 [192, 238] which is known to require scaffold proteins for plasma membrane translocation [220, 239]. Chemotaxing neutrophils showed the localisation of GFP-ARAP3 (but not of GFP-R307,8A-ARAP3) at the leading edge [240]. In the context of an artificial PIP3 bead binding assay, SHIP2 was able to bind PIP3 only if present in a heterodimer with an ARAP3 construct [181], leading to the hypothesis that ARAP3 might recruit SHIP2 to the site of PIP3 production in chemotaxing neutrophils. In this way SHIP2 might function in a negative feedback loop, dephosphorylating PIP3 at the leading edge to focus PIP3 polarisation and aid integrin inactivation in the chemotaxing neutrophil, thereby contributing to efficient neutrophil chemotaxis without meandering.

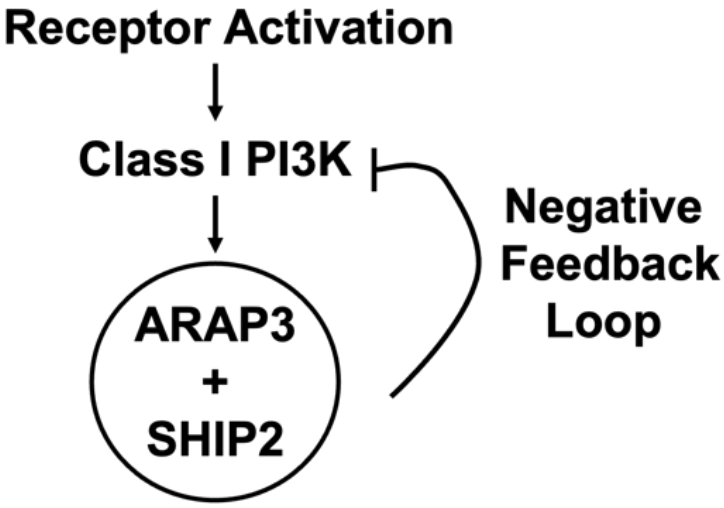

Figure 7.1 Schematic of hypothesised ARAP3 and SHIP2 negative feedback loop.

This was the working hypothesis when I joined the already ongoing SHIP2 project in the Vermeren lab with the aim of determining the function of SHIP2 in neutrophils as laid out in chapters 4 and 5. This project did indeed identify a regulatory function in chemotaxis. However, unlike ARAP3, SHIP2 does not appear to be deeply involved in integrin-dependent processes. Moreover, I observed differences in PI(3,4)P2 on internal membranes rather than the plasma membrane. Finally, unstimulated wild-type and *Arap3* deficient HoxB8 cells that had been transduced with mCherry SHIP2 showed that ARAP3 was not essential for SHIP2 localisation as described in section 5.2.5. It has yet to be determined if the same applies upon chemoattractant stimulation, or if they co-localise at the plasma membrane. Therefore, these experiments do not allow me to exclude that ARAP3 may act as a scaffold to recruit SHIP2 to sites of PIP3 formation in the neutrophil, however altogether my observations make it highly unlikely that SHIP2 holds the explanation for the severe chemotaxis defect of ARAP3-deficient neutrophils. Two scenarios would allow for the initial assumption to be correct after all: (i) SHIP2 is recruited to the plasma membrane where it acts as a scaffold independently of its catalytic activity to regulate integrin-dependent functions. To determine if this is the case, SHIP2-deficient neutrophils would need to be analysed rather than $Ship2^{\Delta/\Delta}$ neutrophils. (ii) Compensatory events perhaps involving another 5-phosphatase, took place that allowed neutrophils to adjust to the lack of SHIP2 catalytic activity. To determine if that is the case, inducible $Ship2^{\Delta/\Delta}$ mice would need to be analysed rather than constitutive mice. In support of this possibility, neutrophils from *Arap3*$^{PH^*/PH^*}$ mice in which ARAP3 was uncoupled from

activation by PI3K/PIP3 by incorporation of the R302,3A point mutation, have a weaker chemotaxis defect than those in which ARAP3-deficiency is recently induced [22, 122]. However, *Arap3*$^{PH*/PH*}$ neutrophils were still characterized by excessive production of ROS and degranulation in response to adhesion-induced stimulation. Such functions were not found to be upregulated in Ship2$^{\Delta/\Delta}$ neutrophils. Therefore, both scenarios are conceivable yet unlikely.

Finally, during my placement at GSK I determined the effects of ageing on neutrophil swarming as explained in chapter 6. I also wanted to investigate if the PI3K pathway was involved in neutrophil swarming. Hence, I planned to carry out SHIP2 phosphatase activity assays, however, due to time constrains I was unable to do so.

7.2 Functions of SHIP2 in neutrophils

In chapter 4, SHIP2 was found to regulate neutrophil chemotaxis, polarisation and adhesion under conditions of flow in vitro. In vivo, SHIP2 was identified to regulate neutrophil recruitment in response to LPS induced acute lung injury and thioglycollate induced peritonitis. These results are congruent with a previous study in SHIP2 depleted U251 glioma cells which showed significantly impaired cell polarisation and migration compared to controls [241]. The same study attributed this to the association of SHIP2 with RhoA since this phenotype could be rescued by adding wild-type SHIP2, but not SHIP2 with a mutation in the RhoA binding site. In addition, they found that SHIP2 depleted cells exhibited impaired PIP3 localisation during polarisation, with PIP3 located throughout the cell periphery. Although PIP3 localisation remains to be determined in $Ship2^{\Delta/\Delta}$ neutrophils, in chapter 5 the regulatory functions of SHIP2 were studied mechanistically and explained by changes to global 3-phosphorylated phosphoinositide species.

As described in sections 1.3.2 and 5.3, many studies have shown that PI3Kγ and δ regulate chemotaxis in vitro and neutrophil recruitment to sites of inflammation in vivo [221-223]. Despite this, the 3-phosphatase PTEN which antagonizes PI3K activity only has a subtle regulatory function in chemotaxis [60]. On the other hand, neutrophils deficient in the 5-phosphatase SHIP1 are extremely adherent and fail to polarize efficiently upon adhesion and hence have impaired chemotaxis [63]. Here I show that in contrast to SHIP1, the loss of SHIP2 catalytic activity impairs chemotactic directionality suggesting that

both SHIP family 5-phosphatases have important, non-redundant regulatory functions in the neutrophil. This is particularly interesting considering the catalytic domains are relatively well conserved, sharing 64.2% sequence identity between the enzymes [70].

It is still possible that SHIP2 could have additional responsibilities in cells that don't express SHIP1. In support of this argument, a study using U87-MG glioblastoma cells (which don't express SHIP1) with antisense oligonucleotide reduced SHIP2 reported increased PKB phosphorylation [242]. This comes in contrast with the PKB analysis in chapter 5 where no change in PKB phosphorylation was observed in $Ship2^{\Delta/\Delta}$ neutrophils with or without stimulation. In addition, transfecting SHIP2 into COS-7 cells and overexpressing SHIP2 in CHO cells were also both reported to cause a decrease in PIP3 production and PKB in response to insulin and EGF stimulation respectively compared to controls [243, 244]. However, our PIP3 measurements in $Ship2^{\Delta/\Delta}$ neutrophils show only a subtle increase after 1 minute of stimulation with fMLF, and we observed no change in PKB phosphorylation under any conditions tested. One possible explanation for this discrepancy might be redundancy and functional compensation by other phosphatases in the neutrophil. Compensation by phosphatases isn't limited to SHIP1, several other 5'phosphatases exist as explained in section 1.2.2 which could be compensating for the lack of SHIP2 catalytic activity [245].

Malek and colleagues showed that the 3-phosphatase PTEN, in addition to dephosphorylating PIP3, also uses PI(3,4)P2 as a substrate in EGF-stimulated

Mcf10 breast cancer cells [215]. Therefore, the upregulation of PTEN activity in SHIP2$^{\Delta/\Delta}$ neutrophils might explain why PI(3,4)P2 differences appeared more prevalent despite only subtle PIP3 differences. To investigate this possibility, I inhibited PTEN in wild-type and Ship2$^{\Delta/\Delta}$ neutrophils and then measured PI(3,4)P2 levels with immunofluorescence as was carried out in section 5.2.3 (data not shown). Unlike the previous observations in Mcf10 breast cancer cells, I found that neutrophils in which PTEN had been inhibited also displayed a drop in PI(3,4)P2 in wild-type cells. In keeping with this assessment, after PTEN inhibition, there was also less PI(3,4)P2 in Ship2$^{\Delta/\Delta}$ neutrophils. This observation suggests that PTEN is unlikely to be involved in using PI(3,4)P2 as a substrate in neutrophils at least under the conditions that were tested here.

Lack of good selectivity is a problem with most phosphatase inhibitors, and this also applies to SF1640 which I employed to inhibit PTEN. While further experiments would need to be performed to confirm this, my observations with this inhibitor suggest that the 3-phosphatase PTEN, although shown to regulate cellular PI(3,4)P2 in EGF-stimulated breast cancer cells, is not likely to function in this capacity in fMLF-stimulated neutrophils. Interestingly, in Mcf10 breast cancer cells, PI(3,4)P2 was found to localise to the plasma membrane, whereas staining in neutrophils as shown in section 5.2.3.1 shows PI(3,4)P2 localisation at endomembranes.

During my time in the lab, I explored several avenues simultaneously, allowing me to prioritize and further investigate what showed most potential. Here I discuss some experiments I had started but due to time constraints or unforeseen circumstances were abandoned, allowing for potential future examination:

PIP3 localisation in WT and Ship2$^{\Delta/\Delta}$ neutrophils

The canonical model for PI3K signalling suggests PI3K activity localized almost exclusively at the plasma membrane [246-248]. Several studies challenge this view by identifying endomembrane and nuclear PIP3 [249, 250]. One example in EGF-stimulated HeLa cells showed that PIP3 generation and AKT phosphorylation were mostly found in confined intracellular membranes in a fashion that was linked to the microtubules [251]. This study showed colocalisation using three different anti-PIP3 antibodies with endosomal markers in HeLa cells which indicated that PIP3 is generated in internal endosomal compartments. It would be interesting to see whether the use of these antibodies also shows internal PIP3 in cell types other than HeLa.

Since we determined very subtle differences in PIP3 production by mass spectrometry between wild-type and Ship2$^{\Delta/\Delta}$ neutrophils, we questioned if the localisation of PIP3 in neutrophils differed between the genotypes. To address this, I stained fMLF stimulated and unstimulated neutrophils for each genotype with anti-PIP3 antibody. Staining primary mouse neutrophils is challenging, yielding a lot of non-specific signal even in unstimulated cells, and more controls would be necessary to draw solid conclusions. However, an initial

scan of all conditions showed PIP3 was mainly found in small intracellular membranes in neutrophils.

The results obtained in these antibody studies stand in contradiction to those performed with lipid biosensors such as [215, 252, 253] which suggest that PIP3 localises to the plasma membrane. If they are indeed found in intracellular membranes, then two reasons might explain the apparent discrepancy in results. First, the biosensor which is always fluorescent may obscure internal signal; and second the biosensor may be picking up PIP3 signal in a biased fashion. The use of a PIP3 smartprobe that only lights up once bound to PIP3 would allow improved detection over these conventional genetically encoded biosensors, and it would be very interesting to develop such reagents in the future.

HoxB8 neutrophils to study PI3K signalling

In my second year, I spent some considerable time culturing HoxB8 cells and introducing a range of genetic modifications. This aim of this was to generate tools that would allow us to visualise SHIP2 signalling in a spatiotemporal fashion in real-time by imaging. To visualise the pools of PIP3 and PIP2, the PI(3,4,5)P3 reporter GFP-PH-GRP1 [254] and the PI(3,4)P2 reporter mCherry-PH-TAPP1 [215] were transduced into WT and Ship2$^{\Delta/\Delta}$ HoxB8 cells. While the mCherry-PH-TAPP1 reporter was successfully transduced from the first try, attempting to transduce the PIP3 reporter proved more challenging. My observations suggested that HoxB8 cells might be more amenable to retroviral transductions (as has been observed with haematopoietic progenitor cells by

others [255]). It is conceivable that abundant reporters might deplete PIP3 which would disrupt the molecular signalling to such an extent that it has lethal effects on the cells. This might be overcome by using less of the reporter, which would, however, result in poorer signal. A potential solution for this scenario could be to use an alternative construct, such as PH-GRP1-mNeonGreen (Dr David Bryant, University of Glasgow, [256]), where less reporter is required since mNeonGreen is about five times brighter than GFP.

This aspect of my work came to an abrupt halt at the start of the pandemic and these transduced clones were either lost or frozen down. After the initial lockdown, access to the laboratory remained restricted, and work had to be performed by individuals in isolation posing limits on the experiments. The following months made cell-based lab work difficult since we had continued restrictions in place to keep building occupancy at an acceptable low density. Therefore, instead of going back to HoxB8 cells, I carried out experiments with primary neutrophils that could be performed in a single day.

One thing that I tried to address using inhibitors was the question of redundancy between SHIP1 and SHIP2. The original rationale had been that if there was considerable redundancy between the two SHIP proteins, comparing the same functions in $Ship2^{\Delta/\Delta}$, SHIP1 inhibited and $Ship2^{\Delta/\Delta}$ SHIP1 inhibited neutrophils would lead to a worse than additive defect in the $Ship2^{\Delta/\Delta}$ SHIP1 inhibited neutrophils. Unfortunately, the SHIP1 inhibitor (3-AC) used was highly toxic to neutrophils and it could not be employed (not shown). I also tried the SHIP2 inhibitor AS1938909, but found it was not very specific, having

the same effects on wild-type and Ship2$^{\Delta/\Delta}$ neutrophils (not shown). To find a way around this, I generated SHIP1 shRNA knockdown HoxB8 progenitors which are also currently frozen down.

I was therefore unable to address potential redundancy between SHIP1 and SHIP2. This is an important question that should be analysed in more depth in the future. As mentioned earlier, in addition to SHIP1/2, there are also a range of other 5-phosphatases [245] which remain less well characterised to date and at least some of which may also be involved in regulating PI3K/PIP3 signalling and chemotaxis in the neutrophil. It will be exciting to follow future developments in this field.

SHIP2 mass spectrometry

In common with many signalling proteins, SHIP2 is subject to regulation by post-translational modifications (PTM). Phosphorylation is a common form of PTM and both serine/threonine and tyrosine residues were reported to be phosphorylated in SHIP2 [257]. A phosphotyrosine blot of HeLa cells plated on a collagen I-coated surface, showed the appearance of SHIP2 phosphorylation within 30 minutes [258]. However, tyrosine phosphorylation was blocked when inhibitors of Src family kinases (SFKs) were added to the plated cells on the collagen I-coated surface, suggesting a role for SFKs in the adhesion dependent tyrosine phosphorylation of SHIP2. Another example is that of human preadipocytes overexpressing a FLAG SHIP2 WT construct, which when stimulated with PDGF for just 5 minutes were found to be threonine phosphorylated by mass spectrometry at T958 in the proline rich

region [259]. Studying the phosphorylation of SHIP2 could prove to be key to understanding its regulation [260, 261]. More specifically, the phosphorylation of Tyr-986 and Tyr-1162 were shown to regulate SHIP2's catalytic activity [262], subcellular localisation [263], interactions with other proteins [264], and mono-ubiquitination [265] as was shown to be the case with SHIP1 [266].

To investigate this in neutrophils, I immunoprecipitated SHIP2 from neutrophil lysates and ran the samples on a gel. To confirm the protein being detected is SHIP2, a different antibody was used for the blot than the one used for immunoprecipitation. Next, silver and Coomassie stained gels were prepared, which showed a detectible band at the expected SHIP2 position. Although no SHIP2 was detected by mass spectrometry, this was only carried out once and a second repeat would have likely led to a different outcome.

7.3 Neutrophil swarming in neutrophils from elderly donors

As reported by the United Nations, there is a constant change in demographics. This means that by the year 2050, it is projected that more people will be above the age of 60 than below the age of 15, forming 22% of the global population [267]. Over the past 30 years in the UK, people aged 90 or above have increased by more than two and a half times [268]. The percentage of people taking prescription medications increases from 19% between the ages of 16-24 to 96% for people above the age of 85 [269], with more than a third of the population above 80 taking 8 or more types of medication [270]. Elderly people are more susceptible to infection and chronic diseases, and with this change in demographics, immunosenescence is becoming a more prevalent issue.

The effects of immunosenescence have been studied on a range of neutrophil effector functions and chemotaxis. Although chemokinesis was reported to remain unaltered in old age [179], chemotaxis is impaired in older subjects [179, 180]. In aged mice, neutrophil in vivo recruitment in response to s.c injection with 100 pg KC was decreased in comparison to the younger mice which remained the case even when KC was injected at a 10-fold higher dose [271]. The same was observed in a model of wound infection, showing delayed wound healing in aged mice.

The coordinated movement of neutrophils in response to infection or inflammation, also known as swarming, is a relatively newer identified

phenomenon and had yet to be investigated in the context of ageing. It is very probable that swarming contributes to the in vivo recruitment defect observed in aged mice. In chapter 6, I employed in vitro swarming assays using human neutrophils from old (>60) and young (<25) donors and identified a trend towards a swarming defect from the elderly donors. Only a small *n*-number was analysed, making it likely that with a larger number of donors this will turn out to be a significant difference. Interestingly, adding the FLAP inhibitor MK886 to inhibit LTB4 production rescued this defect. This is a very exciting observation given that (i) neutrophil recruitment is dysregulated in old age and thought to contribute to excessive inflammation and that (ii) pharmacological targeting of LTB4 generation and receptors is already used in the clinic for a range of conditions (e.g. allergic asthma) and known to be well tolerated. It would be imperative to measure LTB4 production, a critical lipid mediator during swarming, in neutrophils from each age group. Other exciting things to follow up on include analysing chemotaxis/swarming responses to alternative chemokines and cytokines of neutrophils from young and old donors in alternative chemotaxis chambers. In addition, it would be interesting to compare chemokine/chemoattractant receptor expression on neutrophils from the two age groups as well as the receptor signalling in response to stimulation.

References

1. Dancey, J.T., et al., *Neutrophil kinetics in man.* J Clin Invest, 1976. **58**(3): p. 705-15.

2. Rosales, C., *Neutrophil: A Cell with Many Roles in Inflammation or Several Cell Types?* Frontiers in Physiology, 2018. **9**.

3. Ballesteros, I., et al., *Co-option of Neutrophil Fates by Tissue Environments.* Cell, 2020. **183**(5): p. 1282-1297.e18.

4. Lahoz-Beneytez, J., et al., *Human neutrophil kinetics: modeling of stable isotope labeling data supports short blood neutrophil half-lives.* Blood, 2016. **127**(26): p. 3431-8.

5. Pillay, J., et al., *In vivo labeling with 2H2O reveals a human neutrophil lifespan of 5.4 days.* Blood, 2010. **116**(4): p. 625-7.

6. Gordy, C., et al., *Regulation of steady-state neutrophil homeostasis by macrophages.* Blood, 2011. **117**(2): p. 618-29.

7. Mayadas, T.N., X. Cullere, and C.A. Lowell, *The Multifaceted Functions of Neutrophils.* Annual Review of Pathology: Mechanisms of Disease, 2014. **9**(1): p. 181-218.

8. Tecchio, C. and M.A. Cassatella, *Neutrophil-derived chemokines on the road to immunity.* Seminars in Immunology, 2016. **28**(2): p. 119-128.

9. Crainiciuc, G., et al., *Behavioural immune landscapes of inflammation.* Nature, 2022. **601**(7893): p. 415-421.

10. Evrard, M., et al., *Developmental Analysis of Bone Marrow Neutrophils Reveals Populations Specialized in Expansion, Trafficking, and Effector Functions.* Immunity, 2018. **48**(2): p. 364-379.e8.

11. Schulte-Schrepping, J., et al., *Severe COVID-19 Is Marked by a Dysregulated Myeloid Cell Compartment.* Cell, 2020. **182**(6): p. 1419-1440.e23.

12. Greenlee-Wacker, M.C., *Clearance of apoptotic neutrophils and resolution of inflammation.* Immunological Reviews, 2016. **273**(1): p. 357-370.

13. Fox, S., et al., *Neutrophil apoptosis: relevance to the innate immune response and inflammatory disease.* Journal of innate immunity, 2010. **2**(3): p. 216-227.

14. McCracken, J.M. and L.-A.H. Allen, *Regulation of human neutrophil apoptosis and lifespan in health and disease.* Journal of cell death, 2014. **7**: p. 15-23.

15. Liew, P.X. and P. Kubes, *The Neutrophil's Role During Health and Disease.* Physiological Reviews, 2019. **99**(2): p. 1223-1248.

16. Sadik, C.D., N.D. Kim, and A.D. Luster, *Neutrophils cascading their way to inflammation.* Trends in immunology, 2011. **32**(10): p. 452-460.

17. Phillipson, M. and P. Kubes, *The neutrophil in vascular inflammation.* Nature Medicine, 2011. **17**(11): p. 1381-1390.

18. Phillipson , M., et al., *Intraluminal crawling of neutrophils to emigration sites: a molecularly distinct process from adhesion in the recruitment cascade.* Journal of Experimental Medicine, 2006. **203**(12): p. 2569-2575.

19. Caster, D.J., et al., *Re-Examining Neutrophil Participation in GN.* Journal of the American Society of Nephrology, 2017: p. ASN.2016121271.

20. Kolaczkowska, E. and P. Kubes, *Neutrophil recruitment and function in health and inflammation.* Nature Reviews Immunology, 2013. **13**: p. 159-175.

21. Nathan, C., *Neutrophils and immunity: challenges and opportunities.* Nature Reviews Immunology, 2006. **6**(3): p. 173-182.

22. Gambardella, L. and S. Vermeren, *Molecular players in neutrophil chemotaxis—focus on PI3K and small GTPases.* Journal of Leukocyte Biology, 2013. **94**(4): p. 603-612.

23. Nauseef, W.M. and N. Borregaard, *Neutrophils at work.* Nat Immunol, 2014. **15**(7): p. 602-11.

24. Mayadas, T.N., X. Cullere, and C.A. Lowell, *The multifaceted functions of neutrophils.* Annual review of pathology, 2014. **9**: p. 181-218.

25. Segal, A.W., J. Dorling, and S. Coade, *Kinetics of fusion of the cytoplasmic granules with phagocytic vacuoles in human polymorphonuclear leukocytes. Biochemical and morphological studies.* Journal of Cell Biology, 1980. **85**(1): p. 42-59.

26. Underhill, D.M. and A. Ozinsky, *Phagocytosis of microbes: complexity in action.* Annu Rev Immunol, 2002. **20**: p. 825-52.

27. Nordenfelt, P. and H. Tapper, *Phagosome dynamics during phagocytosis by neutrophils.* J Leukoc Biol, 2011. **90**(2): p. 271-84.

28. Faurschou, M. and N. Borregaard, *Neutrophil granules and secretory vesicles in inflammation.* Microbes Infect, 2003. **5**(14): p. 1317-27.

29. Borregaard, N., *Neutrophils, from marrow to microbes.* Immunity, 2010. **33**(5): p. 657-70.

30. Sengeløv, H., L. Kjeldsen, and N. Borregaard, *Control of exocytosis in early neutrophil activation.* J Immunol, 1993. **150**(4): p. 1535-43.

31. Winterbourn, C.C., et al., *Modeling the reactions of superoxide and myeloperoxidase in the neutrophil phagosome: implications for microbial killing.* J Biol Chem, 2006. **281**(52): p. 39860-9.

32. Amulic, B., et al., *Neutrophil Function: From Mechanisms to Disease.* Annual Review of Immunology, 2012. **30**(1): p. 459-489.

33. Papayannopoulos, V., *Neutrophil extracellular traps in immunity and disease.* Nature Reviews Immunology, 2018. **18**(2): p. 134-147.

34. Brinkmann, V., et al., *Neutrophil extracellular traps kill bacteria.* Science, 2004. **303**(5663): p. 1532-5.

35. Balloy, V., et al., *Neutrophil DNA contributes to the antielastase barrier during acute lung inflammation.* Am J Respir Cell Mol Biol, 2003. **28**(6): p. 746-53.

36. Villanueva, E., et al., *Netting neutrophils induce endothelial damage, infiltrate tissues, and expose immunostimulatory molecules in systemic lupus erythematosus.* J Immunol, 2011. **187**(1): p. 538-52.

37. Saffarzadeh, M., et al., *Neutrophil extracellular traps directly induce epithelial and endothelial cell death: a predominant role of histones.* PLoS One, 2012. **7**(2): p. e32366.

38. Papayannopoulos, V., D. Staab, and A. Zychlinsky, *Neutrophil elastase enhances sputum solubilization in cystic fibrosis patients receiving DNase therapy.* PLoS One, 2011. **6**(12): p. e28526.

39. Tanabe, O., et al., *Genomic structure of the murine IL-6 gene. High degree conservation of potential regulatory sequences between mouse and human.* J Immunol, 1988. **141**(11): p. 3875-81.

40. Buchberg, A.M., et al., *A comprehensive genetic map of murine chromosome 11 reveals extensive linkage conservation between mouse and human.* Genetics, 1989. **122**(1): p. 153-61.

41. Schwartz, S., et al., *Human-mouse alignments with BLASTZ.* Genome Res, 2003. **13**(1): p. 103-7.

42. Collins, S.J., et al., *Terminal differentiation of human promyelocytic leukemia cells induced by dimethyl sulfoxide and other polar compounds.* Proceedings of the National Academy of Sciences, 1978. **75**(5): p. 2458-2462.

43. Drexler, H.G., et al., *False leukemia–lymphoma cell lines: an update on over 500 cell lines.* Leukemia, 2003. **17**(2): p. 416-426.

44. Wang, G.G., et al., *Quantitative production of macrophages or neutrophils ex vivo using conditional Hoxb8.* Nature Methods, 2006. **3**(4): p. 287-293.

45. Saul, S., et al., *Signaling and functional competency of neutrophils derived from bone-marrow cells expressing the ER-HOXB8 oncoprotein.* Journal of Leukocyte Biology, 2019. **106**(5): p. 1101-1115.

46. Orosz, A., B. Walzog, and A. Mócsai, *In Vivo Functions of Mouse Neutrophils Derived from HoxB8-Transduced Conditionally Immortalized Myeloid Progenitors.* J Immunol, 2021. **206**(2): p. 432-445.

47. Hopke, A., et al., *Neutrophil swarming delays the growth of clusters of pathogenic fungi.* Nat Commun, 2020. **11**(1): p. 2031.

48. Cohen, J.T., et al., *Engraftment, Fate, and Function of HoxB8-Conditional Neutrophil Progenitors in the Unconditioned Murine Host.* Frontiers in Cell and Developmental Biology, 2022. **10**.

49. Chu, J.Y., et al., *HoxB8 neutrophils replicate Fcγ receptor and integrin-induced neutrophil signaling and functions.* Journal of leukocyte biology, 2019. **105**(1): p. 93-100.

50. Hawkins, P.T., et al., *PI3K Signaling in Neutrophils*, in *Phosphoinositide 3-kinase in Health and Disease: Volume 1*, C. Rommel, B. Vanhaesebroeck, and P.K. Vogt, Editors. 2011, Springer Berlin Heidelberg: Berlin, Heidelberg. p. 183-202.

51. Alliouachene, S., et al., *Inactivation of the Class II PI3K-C2β Potentiates Insulin Signaling and Sensitivity.* Cell Rep, 2015. **13**(9): p. 1881-94.

52. Hervieu, A. and S. Kermorgant, *The Role of PI3K in Met Driven Cancer: A Recap.* Frontiers in Molecular Biosciences, 2018. **5**.

53. Bart Vanhaesebroeck, et al., *Synthesis and Function of 3-Phosphorylated Inositol Lipids.* Annual Review of Biochemistry, 2001. **70**(1): p. 535-602.

54. Mora, A., et al., *PDK1, the master regulator of AGC kinase signal transduction.* Seminars in Cell & Developmental Biology, 2004. **15**(2): p. 161-170.

55. Sarbassov, D.D., et al., *Phosphorylation and Regulation of Akt/PKB by the Rictor-mTOR Complex.* Science, 2005. **307**(5712): p. 1098-1101.

56. Hawkins, P.T. and L.R. Stephens, *Emerging evidence of signalling roles for PI(3,4)P2 in Class I and II PI3K-regulated pathways.* Biochem Soc Trans, 2016. **44**(1): p. 307-14.

57. Cristofano, A.D., et al., *Pten is essential for embryonic development and tumour suppression.* Nature Genetics, 1998. **19**(4): p. 348-355.

58. Helgason, C.D., et al., *Targeted disruption of SHIP leads to hemopoietic perturbations, lung pathology, and a shortened life span.* Genes Dev, 1998. **12**(11): p. 1610-20.

59. Liu, Q., et al., *SHIP is a negative regulator of growth factor receptor-mediated PKB/Akt activation and myeloid cell survival.* Genes Dev, 1999. **13**(7): p. 786-91.

60. Subramanian, K.K., et al., *Tumor suppressor PTEN is a physiologic suppressor of chemoattractant-mediated neutrophil functions.* Blood, 2007. **109**(9): p. 4028-4037.

61. Li, Z., et al., *Regulation of PTEN by Rho small GTPases.* Nature Cell Biology, 2005. **7**(4): p. 399-404.

62. Zhu, D., et al., *Deactivation of phosphatidylinositol 3,4,5-trisphosphate/Akt signaling mediates neutrophil spontaneous death.* Proceedings of the National Academy of Sciences of the United States of America, 2006. **103**(40): p. 14836-14841.

63. Mondal, S., et al., *Phosphoinositide lipid phosphatase SHIP1 and PTEN coordinate to regulate cell migration and adhesion.* Molecular biology of the cell, 2012. **23**(7): p. 1219-1230.

64. Gardai, S., et al., *Activation of SHIP by NADPH oxidase-stimulated Lyn leads to enhanced apoptosis in neutrophils.* J Biol Chem, 2002. **277**(7): p. 5236-46.

65. Nishio, M., et al., *Control of cell polarity and motility by the PtdIns(3,4,5)P3 phosphatase SHIP1.* Nat Cell Biol, 2007. **9**(1): p. 36-44.

66. Eramo, Matthew J. and Christina A. Mitchell, *Regulation of PtdIns(3,4,5)P3/Akt signalling by inositol polyphosphate 5-phosphatases.* Biochemical Society Transactions, 2016. **44**(1): p. 240-252.

67. Thomas, M.P., C. Erneux, and B.V. Potter, *SHIP2: Structure, Function and Inhibition.* Chembiochem, 2017. **18**(3): p. 233-247.

68. Schurmans, S., et al., *The mouse SHIP2 (Inppl1) gene: complementary DNA, genomic structure, promoter analysis, and gene expression in the embryo and adult mouse.* Genomics, 1999. **62**(2): p. 260-71.

69. Raaijmakers, J.H., et al., *The PI3K effector Arap3 interacts with the PI(3,4,5)P3 phosphatase SHIP2 in a SAM domain-dependent manner.* Cell Signal, 2007. **19**(6): p. 1249-57.

70. Erneux, C., et al., *SHIP2 multiple functions: A balance between a negative control of PtdIns(3,4,5)P3 level, a positive control of PtdIns(3,4)P2 production, and intrinsic docking properties.* Journal of Cellular Biochemistry, 2011. **112**(9): p. 2203-2209.

71. Lazar, D.F. and A.R. Saltiel, *Lipid phosphatases as drug discovery targets for type 2 diabetes.* Nature Reviews Drug Discovery, 2006. **5**(4): p. 333-342.

72. Clément, S., et al., *The lipid phosphatase SHIP2 controls insulin sensitivity.* Nature, 2001. **409**(6816): p. 92-97.

73. Sleeman, M.W., et al., *Absence of the lipid phosphatase SHIP2 confers resistance to dietary obesity.* Nat Med, 2005. **11**(2): p. 199-205.

74. Kagawa, S., et al., *Impact of Transgenic Overexpression of SH2-Containing Inositol 5'-Phosphatase 2 on Glucose Metabolism and Insulin Signaling in Mice.* Endocrinology, 2008. **149**(2): p. 642-650.

75. Zhang, G., et al., *Induction of human chronic myeloid leukemia K562 cell apoptosis by virosecurinine and its molecular mechanism.* Molecular medicine reports, 2014. **10**(5): p. 2365-2371.

76. Gumbleton, M., et al., *Dual enhancement of T and NK cell function by pulsatile inhibition of SHIP1 improves antitumor immunity and survival.* Science Signaling, 2017. **10**(500): p. eaam5353.

77. Ye, Y., et al., *Suppression of SHIP2 contributes to tumorigenesis and proliferation of gastric cancer cells via activation of Akt.* Journal of Gastroenterology, 2016. **51**(3): p. 230-240.

78. Suwa, A., T. Kurama, and T. Shimokawa, *SHIP2 and its involvement in various diseases.* Expert Opinion on Therapeutic Targets, 2010. **14**(7): p. 727-737.

79. Dubois, E., et al., *Developmental defects and rescue from glucose intolerance of a catalytically-inactive novel Ship2 mutant mouse.* Cell Signal, 2012. **24**(11): p. 1971-80.

80. Krugmann, S., et al., *Identification of ARAP3, a novel PI3K effector regulating both Arf and Rho GTPases, by selective capture on phosphoinositide affinity matrices.* Mol Cell, 2002. **9**(1): p. 95-108.

81. Fritsch, R., et al., *RAS and RHO families of GTPases directly regulate distinct phosphoinositide 3-kinase isoforms.* Cell, 2013. **153**(5): p. 1050-63.

82. McCormick, B., J.Y. Chu, and S. Vermeren, *Cross-talk between Rho GTPases and PI3K in the neutrophil.* Small GTPases, 2019. **10**(3): p. 187-195.

83. Welch, H.C.E., et al., *P-Rex1 Regulates Neutrophil Function.* Current Biology, 2005. **15**(20): p. 1867-1873.

84. Pan, D., et al., *P-Rex and Vav Rac-GEFs in platelets control leukocyte recruitment to sites of inflammation.* Blood, 2015. **125**(7): p. 1146-58.

85. Lawson, C.D., et al., *P-Rex1 and Vav1 Cooperate in the Regulation of Formyl-Methionyl-Leucyl-Phenylalanine–Dependent Neutrophil Responses.* The Journal of Immunology, 2011. **186**(3): p. 1467-1476.

86. Vermeren, S., U. Karmakar, and A.G. Rossi, *Immune complex-induced neutrophil functions: A focus on cell death.* European Journal of Clinical Investigation, 2018. **48**(S2): p. e12948.

87. Miura, K., et al., *ARAP1: A Point of Convergence for Arf and Rho Signaling.* Molecular Cell, 2002. **9**(1): p. 109-119.

88. Li, Q., et al., *Biochemical and Structural Studies of the Interaction between ARAP1 and CIN85.* Biochemistry, 2018. **57**(14): p. 2132-2139.

89. Krugmann, S., et al., *ARAP3 is essential for formation of lamellipodia after growth factor stimulation.* J Cell Sci, 2006. **119**(Pt 3): p. 425-32.

90. Krugmann, S., et al., *ARAP3 is a PI3K- and rap-regulated GAP for RhoA.* Curr Biol, 2004. **14**(15): p. 1380-4.

91. McCormick, B., et al., *A Negative Feedback Loop Regulates Integrin Inactivation and Promotes Neutrophil Recruitment to Inflammatory Sites.* The Journal of Immunology, 2019. **203**(6): p. 1579-1588.

92. I, S.T., et al., *ARAP3 is transiently tyrosine phosphorylated in cells attaching to fibronectin and inhibits cell spreading in a RhoGAP-dependent manner.* J Cell Sci, 2004. **117**(Pt 25): p. 6071-84.

93. Lokuta, M.A., P.A. Nuzzi, and A. Huttenlocher, *Analysis of neutrophil polarization and chemotaxis.* Methods Mol Biol, 2007. **412**: p. 211-29.

94. Lauffenburger, D.A. and A.F. Horwitz, *Cell migration: a physically integrated molecular process.* Cell, 1996. **84**(3): p. 359-69.

95. Petrie, R.J. and K.M. Yamada, *Multiple mechanisms of 3D migration: the origins of plasticity.* Current Opinion in Cell Biology, 2016. **42**: p. 7-12.

96. Migeotte, I., D. Communi, and M. Parmentier, *Formyl peptide receptors: A promiscuous subfamily of G protein-coupled receptors controlling immune responses.* Cytokine & Growth Factor Reviews, 2006. **17**(6): p. 501-519.

97. Lee, H., P.L. Whitfeld, and C.R. Mackay, *Receptors for complement C5a. The importance of C5aR and the enigmatic role of C5L2.* Immunology & Cell Biology, 2008. **86**(2): p. 153-160.

98. McInnes, I.B., et al., *IL-18 Enhances Collagen-Induced Arthritis.* J Immunol, 2003. **171**: p. 1009-1015.

99. Murphy, P.M., et al., *International Union of Pharmacology. XXII. Nomenclature for Chemokine Receptors.* Pharmacological Reviews, 2000. **52**(1): p. 145-176.

100. Proudfoot, A.E.I., et al., *Glycosaminoglycan binding and oligomerization are essential for the in vivo activity of certain chemokines.* Proceedings of the National Academy of Sciences, 2003. **100**(4): p. 1885-1890.

101. Boff, D., et al., *Neutrophils: Beneficial and Harmful Cells in Septic Arthritis.* International journal of molecular sciences, 2018. **19**(2): p. 468.

102. Venkatakrishnan, A.J., et al., *Molecular signatures of G-protein-coupled receptors.* Nature, 2013. **494**(7436): p. 185-194.

103. Neptune, E.R. and H.R. Bourne, *Receptors induce chemotaxis by releasing the βγ subunit of G_i, not by activating G_q or G_s.* Proceedings of the National Academy of Sciences, 1997. **94**(26): p. 14489-14494.

104. Xu, X., et al., *Ras inhibitor CAPRI enables neutrophil-like cells to chemotax through a higher-concentration range of gradients.* Proceedings of the National Academy of Sciences, 2021. **118**(43): p. e2002162118.

105. Sasaki, A.T., et al., *Localized Ras signaling at the leading edge regulates PI3K, cell polarity, and directional cell movement.* The Journal of cell biology, 2004. **167**(3): p. 505-518.

106. Suire, S., et al., *GPCR activation of Ras and PI3Kγ in neutrophils depends on PLCβ2/β3 and the RasGEF RasGRP4.* The EMBO Journal, 2012. **31**(14): p. 3118-3129.

107. Gambardella, L. and S. Vermeren, *Molecular players in neutrophil chemotaxis--focus on PI3K and small GTPases.* J Leukoc Biol, 2013. **94**(4): p. 603-12.

108. Stephens, L., L. Milne, and P. Hawkins, *Moving towards a Better Understanding of Chemotaxis.* Current Biology, 2008. **18**(11): p. R485-R494.

109. Norton, L., et al., *Localizing the lipid products of PI3Kγ in neutrophils.* Adv Biol Regul, 2016. **60**: p. 36-45.

110. Ferguson, G.J., et al., *PI(3)Kgamma has an important context-dependent role in neutrophil chemokinesis.* Nat Cell Biol, 2007. **9**(1): p. 86-91.

111. Houk, A.R., et al., *Membrane tension maintains cell polarity by confining signals to the leading edge during neutrophil migration.* Cell, 2012. **148**(1-2): p. 175-88.

112. Mócsai, A., B. Walzog, and C.A. Lowell, *Intracellular signalling during neutrophil recruitment.* Cardiovasc Res, 2015. **107**(3): p. 373-85.

113. Weiner, O.D., et al., *A PtdInsP(3)- and Rho GTPase-mediated positive feedback loop regulates neutrophil polarity.* Nature cell biology, 2002. **4**(7): p. 509-513.

114. Li, Z., et al., *Roles of PLC-β2 and -β3 and PI3Kγ in Chemoattractant-Mediated Signal Transduction.* Science, 2000. **287**(5455): p. 1046-1049.

115. Hirsch, E., et al., *Central Role for G Protein-Coupled Phosphoinositide 3-Kinase γ in Inflammation.* Science, 2000. **287**(5455): p. 1049-1053.

116. Sasaki, T., et al., *Function of PI3Kgamma in thymocyte development, T cell activation, and neutrophil migration.* Science, 2000. **287**(5455): p. 1040-6.

117. Suire, S., et al., *Gbetagammas and the Ras binding domain of p110gamma are both important regulators of PI(3)Kgamma signalling in neutrophils.* Nat Cell Biol, 2006. **8**(11): p. 1303-9.

118. Deladeriere, A., et al., *The regulatory subunits of PI3Kγ control distinct neutrophil responses.* Sci Signal, 2015. **8**(360): p. ra8.

119. Walton, G., et al., *LSC 2013 abstract - Abnormal neutrophil migration is a feature of early COPD, present across disease phenotypes and causally related to increased phosphoinositide-3-kinase signalling.* European Respiratory Journal, 2013. **42**(Suppl 57): p. PP125.

120. Sapey, E., et al., *Phosphoinositide 3-kinase inhibition restores neutrophil accuracy in the elderly: toward targeted treatments for immunosenescence.* Blood, 2014. **123**(2): p. 239-248.

121. Michael, M. and S. Vermeren, *A neutrophil-centric view of chemotaxis.* Essays in biochemistry, 2019.

122. Gambardella, L., et al., *The GTPase-activating protein ARAP3 regulates chemotaxis and adhesion-dependent processes in neutrophils.* Blood, 2011. **118**(4): p. 1087-98.

123. Gambardella, L., et al., *Phosphoinositide 3-OH Kinase Regulates Integrin-Dependent Processes in Neutrophils by Signaling through Its Effector ARAP3.* The Journal of Immunology, 2013. **190**(1): p. 381-391.

124. Heit, B., et al., *PTEN functions to 'prioritize' chemotactic cues and prevent 'distraction' in migrating neutrophils.* Nature Immunology, 2008. **9**(7): p. 743-752.

125. Allen, L.-A.H., *Braking neutrophils with PTEN.* Blood, 2007. **109**(9): p. 3620-3621.

126. Kim, H.K., et al., *G-CSF down-regulation of CXCR4 expression identified as a mechanism for mobilization of myeloid cells.* Blood, 2006. **108**(3): p. 812-820.

127. Eash, K.J., et al., *CXCR2 and CXCR4 antagonistically regulate neutrophil trafficking from murine bone marrow.* J Clin Invest, 2010. **120**(7): p. 2423-31.

128. Martin, C., et al., *Chemokines Acting via CXCR2 and CXCR4 Control the Release of Neutrophils from the Bone Marrow and Their Return following Senescence.* Immunity, 2003. **19**(4): p. 583-593.

129. Furze, R.C. and S.M. Rankin, *The role of the bone marrow in neutrophil clearance under homeostatic conditions in the mouse.* The FASEB Journal, 2008. **22**(9): p. 3111-3119.

130. Campbell, J.J., E.F. Foxman, and E.C. Butcher, *Chemoattractant receptor cross talk as a regulatory mechanism in leukocyte adhesion and migration.* Eur J Immunol, 1997. **27**(10): p. 2571-8.

131. Heit , B., et al., *An intracellular signaling hierarchy determines direction of migration in opposing chemotactic gradients.* Journal of Cell Biology, 2002. **159**(1): p. 91-102.

132. Lämmermann, T., et al., *Neutrophil swarms require LTB4 and integrins at sites of cell death in vivo.* Nature, 2013. **498**(7454): p. 371-5.

133. Chtanova, T., et al., *Dynamics of Neutrophil Migration in Lymph Nodes during Infection.* Immunity, 2008. **29**(3): p. 487-496.

134. Lämmermann, T., *In the eye of the neutrophil swarm-navigation signals that bring neutrophils together in inflamed and infected tissues.* J Leukoc Biol, 2016. **100**(1): p. 55-63.

135. Park, S.A., et al., *Real-time dynamics of neutrophil clustering in response to phototoxicity-induced cell death and tissue damage in mouse ear dermis.* Cell Adhesion & Migration, 2018. **12**(5): p. 424-431.

136. Lämmermann, T., et al., *Neutrophil swarms require LTB4 and integrins at sites of cell death in vivo.* Nature, 2013. **498**(7454): p. 371-375.

137. Ng, L.G., et al., *Visualizing the neutrophil response to sterile tissue injury in mouse dermis reveals a three-phase cascade of events.* J Invest Dermatol, 2011. **131**(10): p. 2058-68.

138. Uderhardt, S., et al., *Resident Macrophages Cloak Tissue Microlesions to Prevent Neutrophil-Driven Inflammatory Damage.* Cell, 2019. **177**(3): p. 541-555.e17.

139. Bradley, L.M., et al., *Matrix metalloprotease 9 mediates neutrophil migration into the airways in response to influenza virus-induced toll-like receptor signaling.* PLoS Pathog, 2012. **8**(4): p. e1002641.

140. Kienle, K. and T. Lämmermann, *Neutrophil swarming: an essential process of the neutrophil tissue response.* Immunol Rev, 2016. **273**(1): p. 76-93.

141. Hopke, A. and D. Irimia, *Ex Vivo Human Neutrophil Swarming Against Live Microbial Targets.* Methods Mol Biol, 2020. **2087**: p. 107-116.

142. McDonald, B., et al., *Intravascular Danger Signals Guide Neutrophils to Sites of Sterile Inflammation.* Science, 2010. **330**(6002): p. 362-366.

143. Chou, R.C., et al., *Lipid-cytokine-chemokine cascade drives neutrophil recruitment in a murine model of inflammatory arthritis.* Immunity, 2010. **33**(2): p. 266-78.

144. Kim , N.D., et al., *A unique requirement for the leukotriene B4 receptor BLT1 for neutrophil recruitment in inflammatory arthritis.* Journal of Experimental Medicine, 2006. **203**(4): p. 829-835.

145. Needleman, P., et al., *ARACHIDONIC ACID METABOLISM.* Annual Review of Biochemistry, 1986. **55**(1): p. 69-102.

146. Peters-Golden, M., *Cell biology of the 5-lipoxygenase pathway.* Am J Respir Crit Care Med, 1998. **157**(6 Pt 2): p. S227-31; discussion S231-2, S247-8.

147. Brandt, S.L. and C.H. Serezani, *Too much of a good thing: How modulating LTB(4) actions restore host defense in homeostasis or disease.* Seminars in immunology, 2017. **33**: p. 37-43.

148. Jamieson, T., et al., *The chemokine receptor D6 limits the inflammatory response in vivo.* Nature Immunology, 2005. **6**(4): p. 403-411.

149. Vetrano, S., et al., *The lymphatic system controls intestinal inflammation and inflammation-associated colon cancer through the chemokine decoy receptor D6.* Gut, 2010. **59**(2): p. 197-206.

150. Poon, I.K.H., et al., *Apoptotic cell clearance: basic biology and therapeutic potential.* Nature Reviews Immunology, 2014. **14**(3): p. 166-180.

151. Ji, J. and J. Fan, *Neutrophil in Reverse Migration: Role in Sepsis.* Frontiers in Immunology, 2021. **12**.

152. Colom, B., et al., *Leukotriene B4-Neutrophil Elastase Axis Drives Neutrophil Reverse Transendothelial Cell Migration In Vivo.* Immunity, 2015. **42**(6): p. 1075-1086.

153. Owen-Woods, C., et al., *Local microvascular leakage promotes trafficking of activated neutrophils to remote organs.* J Clin Invest, 2020. **130**(5): p. 2301-2318.

154. Wang, J., et al., *Visualizing the function and fate of neutrophils in sterile injury and repair.* Science, 2017. **358**(6359): p. 111-116.

155. Rink, L. and I. Wessels, *Immunosenescence*, in *Reference Module in Biomedical Sciences*. 2021, Elsevier.

156. Henry, L., *Involution of the human thymus.* The Journal of Pathology and Bacteriology, 1967. **93**(2): p. 661-671.

157. XU, X., et al., *A comprehensive analysis of peripheral blood lymphocytes in healthy aged humans by flow cytometry.* Immunology & Cell Biology, 1993. **71**(6): p. 549-557.

158. Sansoni, P., et al., *Lymphocyte subsets and natural killer cell activity in healthy old people and centenarians [see comments].* Blood, 1993. **82**(9): p. 2767-2773.

159. Ligthart, G.J., et al., *Monoclonal gammopathies in human aging: Increased occurrence with age and correlation with health status.* Mechanisms of Ageing and Development, 1990. **52**(2): p. 235-243.

160. Wlaschek, M., et al., *Connective Tissue and Fibroblast Senescence in Skin Aging.* Journal of Investigative Dermatology, 2021. **141**(4, Supplement): p. 985-992.

161. Bailey, K.L., et al., *Oxidative stress associated with aging activates protein kinase Cε, leading to cilia slowing.* American Journal of Physiology-Lung Cellular and Molecular Physiology, 2018. **315**(5): p. L882-L890.

162. Uciechowski, P. and L. Rink, *Neutrophil, Basophil, and Eosinophil Granulocyte Functions in the Elderly*, in *Handbook of Immunosenescence: Basic Understanding and Clinical Implications*, T. Fulop, et al., Editors. 2018, Springer International Publishing: Cham. p. 1-27.

163. Aiello, A., et al., *Immunosenescence and Its Hallmarks: How to Oppose Aging Strategically? A Review of Potential Options for Therapeutic Intervention.* Frontiers in Immunology, 2019. **10**.

164. Chatta, G.S., et al., *Hematopoietic Progenitors and Aging: Alterations in Granulocytic Precursors and Responsiveness to Recombinant Human G-CSF, GM-CSF, and IL-3.* Journal of Gerontology, 1993. **48**(5): p. M207-M212.

165. Alonso-Fernández, P., et al., *Neutrophils of Centenarians Show Function Levels Similar to Those of Young Adults.* Journal of the American Geriatrics Society, 2008. **56**(12): p. 2244-2251.

166. Mege, J.L., et al., *Phagocytic cell function in aged subjects.* Neurobiology of Aging, 1988. **9**: p. 217-220.

167. Butcher, S.K., et al., *Senescence in innate immune responses: reduced neutrophil phagocytic capacity and CD16 expression in elderly humans.* Journal of Leukocyte Biology, 2001. **70**(6): p. 881-886.

168. Lord, J.M., et al., *Neutrophil ageing and immunesenescence.* Mechanisms of Ageing and Development, 2001. **122**(14): p. 1521-1535.

169. Corberand, J.X., P.F. Laharrague, and G. Fillola, *Neutrophils of healthy aged humans are normal.* Mechanisms of Ageing and Development, 1986. **36**(1): p. 57-63.

170. Braga, P.C., et al., *Influence of age on oxidative bursts (chemiluminescence) of polymorphonuclear neutrophil leukocytes.* Gerontology, 1998. **44**(4): p. 192-7.

171. Fülöp, T., Jr., et al., *Age-dependent alterations of Fc gamma receptor-mediated effector functions of human polymorphonuclear leucocytes.* Clinical and experimental immunology, 1985. **61**(2): p. 425-432.

172. Hazeldine, J., et al., *Impaired neutrophil extracellular trap formation: a novel defect in the innate immune system of aged individuals.* Aging Cell, 2014. **13**(4): p. 690-698.

173. Dransfield, I., S.C. Stocks, and C. Haslett, *Regulation of cell adhesion molecule expression and function associated with neutrophil apoptosis.* Blood, 1995. **85**(11): p. 3264-73.

174. Rynkiewicz, N.K., et al., *Gβγ is a direct regulator of endogenous p101/p110γ and p84/p110γ PI3Kγ complexes in mouse neutrophils.* Science signaling, 2020. **13**(656): p. eaaz4003.

175. IBIDI. Available from: https://ibidi.com/content/310-chemotaxis-assays.

176. Hopke, A. and D. Irimia, *Ex Vivo Human Neutrophil Swarming Against Live Microbial Targets.* Methods in molecular biology (Clifton, N.J.), 2020. **2087**: p. 107-116.

177. Wang, G.G., et al., *Quantitative production of macrophages or neutrophils ex vivo using conditional Hoxb8.* Nat Methods, 2006. **3**(4): p. 287-93.

178. Cepinskas, G., M. Sandig, and P.R. Kvietys, *PAF-induced elastase-dependent neutrophil transendothelial migration is associated with the mobilization of elastase to the neutrophil surface and localization to the migrating front.* J Cell Sci, 1999. **112 (Pt 12)**: p. 1937-45.

179. Wenisch, C., et al., *Effect of age on human neutrophil function.* Journal of Leukocyte Biology, 2000. **67**(1): p. 40-45.

180. Niwa, Y., et al., *Neutrophil chemotaxis, phagocytosis and parameters of reactive oxygen species in human aging: Cross-sectional and longitudinal studies.* Life Sciences, 1989. **44**(22): p. 1655-1664.

181. Craig, H.E., et al., *ARAP3 binding to phosphatidylinositol-(3,4,5)-trisphosphate depends on N-terminal tandem PH domains and adjacent sequences.* Cellular Signalling, 2010. **22**(2): p. 257-264.

182. Stacey, T.T.I., et al., *ARAP3 is transiently tyrosine phosphorylated in cells attaching to fibronectin and inhibits cell spreading in a RhoGAP-dependent manner.* Journal of Cell Science, 2004. **117**(25): p. 6071-6084.

183. *PhosphoSite*. 2022 21/1/2022]; Available from: https://www.phosphosite.org/proteinAction?id=7273&showAllSites=true.

184. Ward, C., et al., *NF-kappaB activation is a critical regulator of human granulocyte apoptosis in vitro.* J Biol Chem, 1999. **274**(7): p. 4309-18.

185. Gilbert, C., E. Rollet-Labelle, and P.H. Naccache, *Preservation of the pattern of tyrosine phosphorylation in human neutrophil lysates. II. A sequential lysis protocol for the analysis of tyrosine phosphorylation-dependent signalling.* Journal of immunological methods, 2002. **261**(1-2): p. 85-101.

186. Tsang, J.L., J.C. Parodo, and J.C. Marshall, *Regulation of apoptosis and priming of neutrophil oxidative burst by diisopropyl fluorophosphate.* Journal of inflammation (London, England), 2010. **7**: p. 32-32.

187. Al-Shami, A., et al., *Preservation of the pattern of tyrosine phosphorylation in human neutrophil lysates.* Journal of Immunological Methods, 1997. **202**(2): p. 183-191.

188. Gilbert, C., E. Rollet-Labelle, and P.H. Naccache, *Preservation of the pattern of tyrosine phosphorylation in human neutrophil lysates. II. A sequential lysis protocol for the analysis of tyrosine phosphorylation-dependent signalling.* J Immunol Methods, 2002. **261**(1-2): p. 85-101.

189. Zhou, M.-j., et al., *Distinct Tyrosine Kinase Activation and Triton X-100 Insolubility upon FcγRII or FcγRIIIB Ligation in Human Polymorphonuclear Leukocytes.: IMPLICATIONS FOR IMMUNE COMPLEX ACTIVATION OF THE RESPIRATORY BURST ⁎.* Journal of Biological Chemistry, 1995. **270**(22): p. 13553-13560.

190. Seng Rong, Y., L. Fumagalli, and G. Berton, *Activation of SRC family kinases in human neutrophils. Evidence that p58c-frg and p53/56lyn redistributed to a Triton X-100-insoluble cytoskeletal fraction, also enriched in the caveolar protein Caveolin, display an enhanced kinase activity.* FEBS Letters, 1996. **380**(1): p. 198-203.

191. Zhou, M. and M.R. Philips, *Nitrogen Cavitation and Differential Centrifugation Allows for Monitoring the Distribution of Peripheral Membrane Proteins in Cultured Cells.* Journal of visualized experiments : JoVE, 2017(126): p. 56037.

192. Raaijmakers, J.H., et al., *The PI3K effector Arap3 interacts with the PI(3,4,5)P3 phosphatase SHIP2 in a SAM domain-dependent manner.* Cellular Signalling, 2007. **19**(6): p. 1249-1257.

193. Mercurio, F.A., et al., *Heterotypic Sam-Sam association between Odin-Sam1 and Arap3-Sam: binding affinity and structural insights.* Chembiochem, 2013. **14**(1): p. 100-6.

194. Di Cristofano, A., et al., *Pten is essential for embryonic development and tumour suppression.* Nat Genet, 1998. **19**(4): p. 348-55.

195. Li, Z., et al., *Regulation of PTEN by Rho small GTPases.* Nat Cell Biol, 2005. **7**(4): p. 399-404.

196. Zhu, Y., et al., *PTEN: a crucial mediator of mitochondria-dependent apoptosis.* Apoptosis, 2006. **11**(2): p. 197-207.

197. Michael, M., et al., *The 5-Phosphatase SHIP2 Promotes Neutrophil Chemotaxis and Recruitment.* Frontiers in Immunology, 2021. **12**.

198. Iglesias, P.A. and P.N. Devreotes, *Navigating through models of chemotaxis.* Curr Opin Cell Biol, 2008. **20**(1): p. 35-40.

199. Calzetti, F., et al., *The importance of being "pure" neutrophils.* J Allergy Clin Immunol, 2017. **139**(1): p. 352-355.e6.

200. Lewis, R.A. and K.F. Austen, *The biologically active leukotrienes. Biosynthesis, metabolism, receptors, functions, and pharmacology.* J Clin Invest, 1984. **73**(4): p. 889-97.

201. Fardin, P., et al., *A biology-driven approach identifies the hypoxia gene signature as a predictor of the outcome of neuroblastoma patients.* Molecular cancer, 2010. **9**: p. 185-185.

202. Marshall, J.G., et al., *Restricted accumulation of phosphatidylinositol 3-kinase products in a plasmalemmal subdomain during Fc gamma receptor-mediated phagocytosis.* The Journal of cell biology, 2001. **153**(7): p. 1369-1380.

203. Crowley, M.T., et al., *A critical role for Syk in signal transduction and phagocytosis mediated by Fcgamma receptors on macrophages.* The Journal of experimental medicine, 1997. **186**(7): p. 1027-1039.

204. Vieira, O.V., et al., *Distinct roles of class I and class III phosphatidylinositol 3-kinases in phagosome formation and maturation.* The Journal of cell biology, 2001. **155**(1): p. 19-25.

205. Ai, J., et al., *The inositol phosphatase SHIP-2 down-regulates FcgammaR-mediated phagocytosis in murine macrophages independently of SHIP-1.* Blood, 2006. **107**(2): p. 813-820.

206. Karmakar, U., et al., *Immune complex-induced apoptosis and concurrent immune complex clearance are anti-inflammatory neutrophil functions.* Cell Death & Disease, 2021. **12**(4): p. 296.

207. Beemiller, P., et al., *A Cdc42 Activation Cycle Coordinated by PI 3-Kinase during Fc Receptor-mediated Phagocytosis.* Molecular Biology of the Cell, 2010. **21**(3): p. 470-480.

208. Alessi, D.R., et al., *Characterization of a 3-phosphoinositide-dependent protein kinase which phosphorylates and activates protein kinase Balpha.* Curr Biol, 1997. **7**(4): p. 261-9.

209. Stephens, L., et al., *Protein kinase B kinases that mediate phosphatidylinositol 3,4,5-trisphosphate-dependent activation of protein kinase B.* Science, 1998. **279**(5351): p. 710-4.

210. Sarbassov, D.D., et al., *Phosphorylation and regulation of Akt/PKB by the rictor-mTOR complex.* Science, 2005. **307**(5712): p. 1098-101.

211. Ebner, M., et al., *PI(3,4,5)P(3) Engagement Restricts Akt Activity to Cellular Membranes.* Mol Cell, 2017. **65**(3): p. 416-431.e6.

212. Stephens, L., et al., *Protein Kinase B Kinases That Mediate Phosphatidylinositol 3,4,5-Trisphosphate-Dependent Activation of Protein Kinase B.* Science, 1998. **279**(5351): p. 710-714.

213. Clark, J., et al., *Quantification of PtdInsP3 molecular species in cells and tissues by mass spectrometry.* Nat Methods, 2011. **8**(3): p. 267-72.

214. JAMES, S.R., et al., *Specific binding of the Akt-1 protein kinase to phosphatidylinositol 3,4,5-trisphosphate without subsequent activation.* Biochemical Journal, 1996. **315**(3): p. 709-713.

215. Malek, M., et al., *PTEN Regulates PI(3,4)P(2) Signaling Downstream of Class I PI3K.* Mol Cell, 2017. **68**(3): p. 566-580.e10.

216. Posor, Y., et al., *Spatiotemporal control of endocytosis by phosphatidylinositol-3,4-bisphosphate.* Nature, 2013. **499**(7457): p. 233-7.

217. Boucrot, E., et al., *Endophilin marks and controls a clathrin-independent endocytic pathway.* Nature, 2015. **517**(7535): p. 460-5.

218. Maekawa, M., et al., *Sequential breakdown of 3-phosphorylated phosphoinositides is essential for the completion of macropinocytosis.* Proc Natl Acad Sci U S A, 2014. **111**(11): p. E978-87.

219. Dyson, J.M., et al., *The SH2-containing inositol polyphosphate 5-phosphatase, SHIP-2, binds filamin and regulates submembraneous actin.* The Journal of cell biology, 2001. **155**(6): p. 1065-1079.

220. Chan Wah Hak, L., et al., *FBP17 and CIP4 recruit SHIP2 and lamellipodin to prime the plasma membrane for fast endophilin-mediated endocytosis.* Nat Cell Biol, 2018. **20**(9): p. 1023-1031.

221. Sadhu, C., et al., *Essential Role of Phosphoinositide 3-Kinase δ in Neutrophil Directional Movement.* The Journal of Immunology, 2003. **170**(5): p. 2647-2654.

222. Martin, K.J., et al., *The role of phosphoinositide 3-kinases in neutrophil migration in 3D collagen gels.* PLoS One, 2015. **10**(2): p. e0116250.

223. Randis, T.M., et al., *Role of PI3Kdelta and PI3Kgamma in inflammatory arthritis and tissue localization of neutrophils.* European journal of immunology, 2008. **38**(5): p. 1215-1224.

224. Reátegui, E., et al., *Microscale arrays for the profiling of start and stop signals coordinating human-neutrophil swarming.* Nature biomedical engineering, 2017. **1**: p. 0094.

225. Young, R.E., et al., *Neutrophil Elastase (NE)-Deficient Mice Demonstrate a Nonredundant Role for NE in Neutrophil Migration, Generation of Proinflammatory Mediators, and Phagocytosis in Response to Zymosan Particles In Vivo.* The Journal of Immunology, 2004. **172**(7): p. 4493-4502.

226. Iyer, R.P., et al., *The history of matrix metalloproteinases: milestones, myths, and misperceptions.* Am J Physiol Heart Circ Physiol, 2012. **303**(8): p. H919-30.

227. Markowska, A.I., F.-T. Liu, and N. Panjwani, *Galectin-3 is an important mediator of VEGF- and bFGF-mediated angiogenic response.* The Journal of experimental medicine, 2010. **207**(9): p. 1981-1993.

228. Bhaumik, P., et al., *Galectin-3 facilitates neutrophil recruitment as an innate immune response to a parasitic protozoa cutaneous infection.* J Immunol, 2013. **190**(2): p. 630-40.

229. Biasi, D., et al., *Neutrophil migration, oxidative metabolism, and adhesion in elderly and young subjects.* Inflammation, 1996. **20**(6): p. 673-81.

230. Tortorella, C., G. Piazzolla, and S. Antonaci, *Neutrophil oxidative metabolism in aged humans: a perspective.* Immunopharmacol Immunotoxicol, 2001. **23**(4): p. 565-72.

231. Butcher, S., H. Chahel, and J.M. Lord, *Ageing and the neutrophil: no appetite for killing?* Immunology, 2000. **100**(4): p. 411-416.

232. Těšický, M., et al., *Longitudinal evidence for immunosenescence and inflammaging in free-living great tits.* Experimental Gerontology, 2021. **154**: p. 111527.

233. Esposito, A.L., et al., *The release of neutrophil chemoattractant activity by bronchoalveolar macrophages from adult and senescent mice.* J Gerontol, 1989. **44**(4): p. B93-9.

234. He, R., Y. Chen, and Q. Cai, *The role of the LTB4-BLT1 axis in health and disease.* Pharmacol Res, 2020. **158**: p. 104857.

235. Chen , M., et al., *Neutrophil-derived leukotriene B4 is required for inflammatory arthritis.* Journal of Experimental Medicine, 2006. **203**(4): p. 837-842.

236. Shao, W.-H., et al., *Targeted Disruption of Leukotriene B₄ Receptors BLT1 and BLT2: A Critical Role for BLT1 in Collagen-Induced Arthritis in Mice.* The Journal of Immunology, 2006. **176**(10): p. 6254-6261.

237. Crooks, S.W. and R.A. Stockley, *Leukotriene B4.* The International Journal of Biochemistry & Cell Biology, 1998. **30**(2): p. 173-178.

238. Leone, M., J. Cellitti, and M. Pellecchia, *The Sam domain of the lipid phosphatase Ship2 adopts a common model to interact with Arap3-Sam and EphA2-Sam.* BMC Structural Biology, 2009. **9**(1): p. 59.

239. Venkatareddy, M., et al., *Nephrin regulates lamellipodia formation by assembling a protein complex that includes Ship2, filamin and lamellipodin.* PloS one, 2011. **6**(12): p. e28710-e28710.

240. Craig, H., *Investigating the interplay between ARAP3 and its regulator phosphoinositide 3'-kinase*. 2010, University of Cambridge.

241. Kato, K., et al., *The inositol 5-phosphatase SHIP2 is an effector of RhoA and is involved in cell polarity and migration.* Mol Biol Cell, 2012. **23**(13): p. 2593-604.

242. Taylor, V., et al., *5′ Phospholipid Phosphatase SHIP-2 Causes Protein Kinase B Inactivation and Cell Cycle Arrest in Glioblastoma Cells.* Molecular and Cellular Biology, 2000. **20**(18): p. 6860-6871.

243. Blero, D., et al., *The SH2 domain containing inositol 5-phosphatase SHIP2 controls phosphatidylinositol 3,4,5-trisphosphate levels in CHO-IR cells stimulated by insulin.* Biochem Biophys Res Commun, 2001. **282**(3): p. 839-43.

244. Pesesse, X., et al., *The Src homology 2 domain containing inositol 5-phosphatase SHIP2 is recruited to the epidermal growth factor (EGF) receptor and dephosphorylates phosphatidylinositol 3,4,5-trisphosphate in EGF-stimulated COS-7 cells.* J Biol Chem, 2001. **276**(30): p. 28348-55.

245. Ramos, A.R., S. Ghosh, and C. Erneux, *The impact of phosphoinositide 5-phosphatases on phosphoinositides in cell function and human disease.* Journal of Lipid Research, 2019. **60**(2): p. 276-286.

246. Varticovski, L., et al., *Activation of phosphatidylinositol 3-kinase in cells expressing abl oncogene variants.* Molecular and Cellular Biology, 1991. **11**(2): p. 1107-1113.

247. Funamoto, S., et al., *Spatial and Temporal Regulation of 3-Phosphoinositides by PI 3-Kinase and PTEN Mediates Chemotaxis.* Cell, 2002. **109**(5): p. 611-623.

248. Stephens, L.R., K.T. Hughes, and R.F. Irvine, *Pathway of phosphatidylinositol(3,4,5)-trisphosphate synthesis in activated neutrophils.* Nature, 1991. **351**(6321): p. 33-9.

249. Lindsay, Y., et al., *Localization of agonist-sensitive PtdIns(3,4,5)P3 reveals a nuclear pool that is insensitive to PTEN expression.* J Cell Sci, 2006. **119**(Pt 24): p. 5160-8.

250. Sato, M., et al., *Production of PtdInsP3 at endomembranes is triggered by receptor endocytosis.* Nat Cell Biol, 2003. **5**(11): p. 1016-22.

251. Thapa, N., et al., *Phosphatidylinositol-3-OH kinase signalling is spatially organized at endosomal compartments by microtubule-associated protein 4.* Nature cell biology, 2020. **22**(11): p. 1357-1370.

252. Matsuoka, S. and M. Ueda, *Mutual inhibition between PTEN and PIP3 generates bistability for polarity in motile cells.* Nature Communications, 2018. **9**(1): p. 4481.

253. Servant, G., et al., *Polarization of chemoattractant receptor signaling during neutrophil chemotaxis.* Science, 2000. **287**(5455): p. 1037-40.

254. Halet, G., P. Viard, and J. Carroll, *Constitutive PtdIns(3,4,5)P3 synthesis promotes the development and survival of early mammalian embryos.* Development, 2008. **135**(3): p. 425-429.

255. Logan, A.C., C. Lutzko, and D.B. Kohn, *Advances in lentiviral vector design for gene-modification of hematopoietic stem cells.* Current Opinion in Biotechnology, 2002. **13**(5): p. 429-436.

256. Nacke, M., et al., *An ARF GTPase module promoting invasion and metastasis through regulating phosphoinositide metabolism.* Nature communications, 2021. **12**(1): p. 1623-1623.

257. PhosphoSitePlus. 2022; Available from: https://www.phosphosite.org/proteinAction.action?id=2588&showAllSites=true.

258. Prasad, N., R.S. Topping, and S.J. Decker, *Src family tyrosine kinases regulate adhesion-dependent tyrosine phosphorylation of 5'-inositol phosphatase SHIP2 during cell attachment and spreading on collagen I.* J Cell Sci, 2002. **115**(Pt 19): p. 3807-15.

259. Artemenko, Y., et al., *Regulation of PDGF-stimulated SHIP2 tyrosine phosphorylation and association with Shc in 3T3-L1 preadipocytes.* J Cell Physiol, 2007. **211**(3): p. 598-607.

260. Habib, T., et al., *Growth Factors and Insulin Stimulate Tyrosine Phosphorylation of the 51C/SHIP2 Protein*.* Journal of Biological Chemistry, 1998. **273**(29): p. 18605-18609.

261. Pesesse, X., et al., *The Src Homology 2 Domain Containing Inositol 5-Phosphatase SHIP2 Is Recruited to the Epidermal Growth Factor (EGF) Receptor and Dephosphorylates Phosphatidylinositol 3,4,5-Trisphosphate in EGF-stimulated COS-7 Cells*.* Journal of Biological Chemistry, 2001. **276**(30): p. 28348-28355.

262. Batty, Ian H., et al., *The control of phosphatidylinositol 3,4-bisphosphate concentrations by activation of the Src homology 2 domain containing inositol polyphosphate 5-phosphatase 2, SHIP2.* Biochemical Journal, 2007. **407**(2): p. 255-266.

263. Deneubourg, L., J.-M. Vanderwinden, and C. Erneux, *Regulation of SHIP2 function through plasma membrane interaction.* Advances in Enzyme Regulation, 2010. **50**(1): p. 262-271.

264. Wisniewski, D., et al., *A novel SH2-containing phosphatidylinositol 3,4,5-trisphosphate 5-phosphatase (SHIP2) is constitutively tyrosine phosphorylated and associated with src homologous and collagen gene (SHC) in chronic myelogenous leukemia progenitor cells.* Blood, 1999. **93**(8): p. 2707-20.

265. De Schutter, J., et al., *SHIP2 (SH2 Domain-containing Inositol Phosphatase 2) SH2 Domain Negatively Controls SHIP2 Monoubiquitination in Response to Epidermal Growth Factor*.* Journal of Biological Chemistry, 2009. **284**(52): p. 36062-36076.

266. Ruschmann, J., et al., *Tyrosine phosphorylation of SHIP promotes its proteasomal degradation.* Exp Hematol, 2010. **38**(5): p. 392-402, 402.e1.

267. McNicoll, G., *World Population Ageing 1950-2050.* Population and Development Review, 2002. **28**: p. 814+.

268. Storey, A. *Estimates of the very old, including centenarians, UK: 2002 to 2020*. 2021.

269. Armstrong, M. 2019; Available from: https://www.statista.com/chart/20056/prescription-medicine-by-age-group-england/.

270. GOV.UK. 2021; Available from: https://www.gov.uk/government/publications/national-overprescribing-review-report.

271. Brubaker, A.L., et al., *Reduced Neutrophil Chemotaxis and Infiltration Contributes to Delayed Resolution of Cutaneous Wound Infection with Advanced Age.* The Journal of Immunology, 2013. **190**(4): p. 1746-1757.

Appendix

Subject: RE: Contact Us Form Submission
Date: Wednesday, 2 February 2022 at 11:32:09 Greenwich Mean Time
From: Portland Press – Production
To: MICHAEL Melina
Attachments: image001.gif, image002.jpg

Dear Melina,

Thank you for your email. Please regard this message as permission to reuse figures from your thesis in an article submission to one of our journals at no charge, subject to the following conditions:

1) Your reproduced figures must cite the article and author, both in the reference list and in the figure legend.
2) Please include a hyperlink to the article on the journal/repository site when referencing/citing the figures.
3) If you modify an original figure in any way, please ensure that it is labelled as a modified version of the original

If you also require a formal licence, please visit copyright.com and make your request following the steps on this site.

Please note that whilst we do not charge for re-using figures in the manner that you are requesting, you may be charged an admin fee of $3.50 USD by the Copyright Clearance Center if you seek permission on copyright.com.

You can find more information on copyright and permissions on our website.

With best wishes,

Shou Hwa Liu | Senior Production Editor
Biochemical Society | **Portland Press**

Mailing address: 1 Naoroji Street, London WC1X 0GB
Registered address: First Floor, 10 Queen Street Place, London EC4R 1BE

shou.liu@portlandpress.com | **biochemistry.org** | **portlandpress.com**
Follow us on Twitter: @BiochemSoc | @PPPublishing

From: noreply@portlandpress.com <noreply@portlandpress.com>
Sent: 01 February 2022 22:16
To: Portland Press – Production <production@portlandpress.com>
Subject: Contact Us Form Submission

A new feedback form has been submitted.

Feedback Form Fields

- First Name: Melina
- Last Name: Michael
- Email Address: Melina.Michael@ed.ac.uk
- Subject: Permission
- I am a librarian: No
- Reason: Other
- Comment: Dear Sir/Madam, I am an author in the following review paper published in Essays in biochemistry: https://doi.org/10.1042/EBC20190011 called 'A neutrophil-centric view of chemotaxis'. I am hoping to include some of the figures I made in my doctoral thesis which I will submit to the University of Edinburgh, which will eventually be publically available. I would be grateful if you could advise if this will be acceptable. Thank you, Melina Michael

frontiers in Immunology

ORIGINAL RESEARCH
published: 19 April 2021
doi: 10.3389/fimmu.2021.671756

The 5-Phosphatase SHIP2 Promotes Neutrophil Chemotaxis and Recruitment

*Melina Michael[1], Barry McCormick[1], Karen E. Anderson[2], Utsa Karmakar[1], Matthieu Vermeren[3], Stéphane Schurmans[4], Augustin Amour[5] and Sonja Vermeren[1]**

[1] Centre for Inflammation Research, Institute for Regeneration and Repair, The University of Edinburgh, Edinburgh, United Kingdom, [2] Signalling Programme, The Babraham Institute, Cambridge, United Kingdom, [3] Centre of Regenerative Medicine, Institute for Regeneration and Repair, The University of Edinburgh, Edinburgh, United Kingdom, [4] Laboratory of Functional Genetics, GIGA Research Centre, University of Liège, Liège, Belgium, [5] Adaptive Immunity Research Unit, GlaxoSmithKline, Stevenage, United Kingdom

OPEN ACCESS

Edited by:
Janos G. Filep, Université de Montréal, Canada

Reviewed by:
Clifford A. Lowell, University of California, San Francisco, United States
Bart Vanhaesebroeck, University College London, United Kingdom

***Correspondence:**
Sonja Vermeren
sonja.vermeren@ed.ac.uk
orcid.org/0000-0002-8460-0884

Specialty section:
This article was submitted to Molecular Innate Immunity, a section of the journal Frontiers in Immunology

Received: *24 February 2021*
Accepted: *30 March 2021*
Published: *19 April 2021*

Citation:
Michael M, McCormick B, Anderson KE, Karmakar U, Vermeren M, Schurmans S, Amour A and Vermeren S (2021) The 5-Phosphatase SHIP2 Promotes Neutrophil Chemotaxis and Recruitment. Front. Immunol. 12:671756. doi: 10.3389/fimmu.2021.671756

Neutrophils, the most abundant circulating leukocytes in humans have key roles in host defense and in the inflammatory response. Agonist-activated phosphoinositide 3-kinases (PI3Ks) are important regulators of many facets of neutrophil biology. PIP3 is subject to dephosphorylation by several 5' phosphatases, including SHIP family phosphatases, which convert the PI3K product and lipid second messenger phosphatidylinositol 3,4,5-trisphosphate (PIP3) into PI(3,4)P2, a lipid second messenger in its own right. In addition to the leukocyte restricted SHIP1, neutrophils express the ubiquitous SHIP2. This study analyzed mice and isolated neutrophils carrying a catalytically inactive SHIP2, identifying an important regulatory function in neutrophil chemotaxis and directionality *in vitro* and in neutrophil recruitment to sites of sterile inflammation *in vivo*, in the absence of major defects of any other neutrophil functions analyzed, including, phagocytosis and the formation of reactive oxygen species. Mechanistically, this is explained by a subtle effect on global 3-phosphorylated phosphoinositide species. This work identifies a non-redundant role for the hitherto overlooked SHIP2 in the regulation of neutrophils, and specifically, neutrophil chemotaxis/trafficking. It completes an emerging wider understanding of the complexity of PI3K signaling in the neutrophil, and the roles played by individual kinases and phosphatases within.

Keywords: neutrophil, chemotaxis, recruitment, PI3K, SHIP2, SHIP1, lipid second messenger

INTRODUCTION

Neutrophils are the most abundant circulating leukocytes in humans. These polymorphonuclear phagocytes provide a first line immune response against infection by invading pathogens and play a key role in the development of the inflammatory response. Neutrophils express a range of G protein coupled chemoattractant/chemokine receptors with the help of which they detect, and quickly react to gradients of chemoattractants, e.g. bacterial peptides. This underpins their ability to leave the blood stream and move directionally (chemotax) towards sources of chemoattractant. Once neutrophils reach the sites of inflammation, they deploy a range of effector functions including

phagocytosis, degranulation, production of reactive oxygen species (ROS), and the release of neutrophil extracellular traps (NETs) to eliminate pathogens (1).

Amongst the proximal enzymes activated downstream of the chemoattractant receptor-ligand interaction is phosphoinositide 3-kinase (PI3K), which generates the lipid second messenger phosphatidylinositol(3,4,5)trisphosphate (PIP3) by phosphorylating the D3 position of the inositol ring of phosphatidylinositol(4,5)bisphosphate (PI(4,5)P2), an integral component of the inner leaflet of the plasma membrane (2). Neutrophils express all four isoforms of agonist-activated PI3K. PIP3 causes the recruitment to the plasma membrane and activation of PI3K effectors, many of which are expressed in the neutrophil (3). The localization of PIP3 at the leading edge is one of the earliest molecular events in neutrophil chemotaxis (4, 5), thought to be important for their ability to polarize and subsequently migrate directionally towards a source of chemoattractant.

PI3K activity is counteracted by phosphatases which hydrolyze the short-lived PIP3. As a major 3-phosphatase, phosphatase and tensin homolog (PTEN) converts PIP3 back to PI(4,5)P2, while the hematopoietic cell-restricted SHIP1 is thought to be a major 5-phosphatase in leukocytes that dephosphorylates PIP3 to form PI(3,4)P2, a lipid second messenger in its own right that shares some effectors with PIP3 (6). Global PTEN-deficiency is embryonic lethal (7), but SHIP1-deficient mice are viable and fertile, however, they exhibit a shortened lifespan that is thought to be due to leukocyte infiltration of the lungs (8, 9). Both PTEN and SHIP1-deficient neutrophils were previously described; PTEN knockout neutrophils are characterized by increased PIP3 (10), enhanced ROS production when stimulated with fMLF, increased ruffling and sensitivity to chemoattractants, a minor directionality defect (11), and a lengthened lifespan (12), while SHIP1 knock-out neutrophils display reduced ROS production (13) and augmented apoptosis (14). SHIP1-deficient neutrophil spread extensively on the substratrum, and in response to chemoattractant stimulation fail to polarize and chemotax efficiently towards a chemoattractant (15).

In addition to SHIP1, neutrophils also express its ubiquitous isozyme, SHIP2, the function of which in the neutrophil remains uncharacterized. In this study, we describe the analysis of neutrophils from a mouse (here called $Ship2^{\Delta/\Delta}$) that carries a small deletion in the SHIP2 catalytic domain which renders it catalytically dead (16). We demonstrate that SHIP2 is an important regulator of neutrophil chemotaxis *in vitro* and of neutrophil recruitment to sites of sterile inflammation *in vivo*, whereas other neutrophil functions remain essentially intact. While we do not detect differential PI3K activity when using PKB phosphorylation as an indirect read-out, PI(3,4)P2 was found to be reduced.

MATERIALS AND METHODS

Unless otherwise specified, materials were acquired from Sigma Aldrich (Gillingham, UK). All reagents were of the lowest available endotoxin level. Tissue culture media and buffers were from Gibco (Thermo Fisher Scientific, Loughborough, UK). Percoll was from GE Healthcare (Amersham, UK).

Antibodies

Anti-HSP90 (clone 3H3C27), anti-SHIP1 (clone PICI-A5), FITC-conjugated rat anti-mouse GR1 (clone RB6-8C5), PE-conjugated rat anti-mouse/human CD11b (clone M1/70), PE/Cy7-conjugated rat anti mouse/human CD45 (clone 30-F11), PerCP/Cy5.5-conjugated rat anti F4/80 (clone BM8), APC-conjugated rat anti-B220 (clone RA3-6B2), PE/Cy7-conjugated rat anti CD3 (clone 17A2) and pacific blue-conjugated rat anti-LY6G (clone 1A8) were from BioLegend (London, UK); anti-PTEN (clone D4.3), anti-PKB (clone 11E7), anti-PKB T308 (clone C25E6) and anti-PKB S473 (clone D9E) were from Cell Signaling Technology (London, UK). Rabbit IgG (I8140) was obtained from Sigma. Anti-SHIP2 (AF5389) and PE-conjugated rat anti-CD64 (clone FAB20741P) were from R&D Systems (Abingdon, UK) and biotinylated anti-PI(3,4)P2 (z-B034) was from Echelon Biosciences (Salt Lake City, UT, USA); streptavidin-AF647, AF488-conjugated phalloidin, AF568-conjugated phalloidin, and secondary antibodies anti-rat AF488, anti-rabbit AF568 and anti-rabbit AF488 were obtained from Thermo Fisher Scientific (Loughborough, UK).

SHIP2 Mouse Model

$Ship2^{\Delta/\Delta}$ mice (16) were housed in individually ventilated cages in a specific opportunistic pathogen-free small animal barrier unit at the University of Edinburgh. After backcrossing for eight generations to C57Bl/6 background, $Ship2^{\Delta/\Delta}$ and wild-type controls were derived by $Ship2^{\Delta/+}$ intercrosses. Sex and age-matched mice were used in experiments. All animal work was approved by the University of Edinburgh Animals Welfare and Ethical Review Body and conducted under the control of the U.K. Home Office (PPL 60/4502 and PFFB 42579).

Neutrophil Preparations

Bone marrow-derived neutrophils were prepared from the tibias and femurs of age and sex-matched mice on a discontinuous percoll gradient as previously described (17), using endotoxin-free reagents throughout. Neutrophil preparations typically reached ~70% purity as assessed by Diff-Quik-stained cytocentrifuge preparations. Unless otherwise stated, experiments were performed in Dulbecco's PBS supplemented with Ca^{2+} and Mg^{2+}, 1g/L glucose and 4mM sodium bicarbonate.

Degranulation

Lactoferrin release was assayed by making use of an antibody directed to human lactoferrin that had previously been shown to cross-react with mouse protein as described (18, 19).

Phagocytosis

0.8 μm diameter latex beads were opsonized with polyclonal rabbit IgG as per manufacturer's instruction. TNF (1000 U/mL) and GM-CSF (100 ng/mL)-primed neutrophils (R&D Research, Abingdon UK) were stimulated with IgG-opsonized latex beads at a ratio of 5:1 for 20 mins at 37°C. Cells were allowed to adhere onto coverslips for 1h on ice and then fixed with 2% ice-cold

paraformaldehyde (PFA) for 10 minutes. Adherent latex beads were labelled with anti-rabbit AF568, prior to cell permeabilization with 0.1% Triton X-100, labelling of all latex beads with anti-rabbit AF488; cells were mounted with ProLong Gold (Thermo Fisher Scientific, Loughborough UK). Cells were viewed using an Evos cell imaging system (Thermo Fisher). The percentage of cells that had internalized beads, and internalized beads/cell were recorded.

Analysis of ROS Production

ROS production was detected indirectly by measuring chemoluminescence production by $5x10^5$ neutrophils/well using luminescence-grade 96-well plates (Nunc, Thermo Fisher Scientific Loughborough, UK) in a Cytation plate reader (BioTek, Swindon, UK) as described (17, 20) with neutrophils incubated with 150μM luminol and 18.75U/ml horseradish peroxidase. Data output was in light units/second.

Chemotaxis

Chemotaxis was analyzed with neutrophils resuspended in HBSS supplemented with 15mM HEPES (pH 7.4) and 0.05% fatty acid and endotoxin-free BSA. For integrin-dependent chemotaxis, neutrophil migration on a glass bridge was monitored by time lapse-imaging for 30 minutes in Dunn chambers (Hawksley, Lancing, UK). Dunn chambers were assembled as previously described (21) with 300nM fMLF as the chemoattractant. For integrin-independent chemotaxis, neutrophils were mixed with a 3D collagen matrix (A1048301, Roche Diagnostics, Mannheim, Germany), which was prepared as per manufacturer's instructions, and left to polymerize in a humidified incubator at 37°C at 5% CO_2 before cells were allowed to migrate towards 300nM fMLF in Chemotaxis μ-slides (Ibidi, Martinsried, Germany). Images were acquired on a Leica IRB inverted microscope with temperature-controlled chamber, automated stage (Prior, Cambridge UK), Orca camera (Hamamatsu, Welwyn Garden City, UK) and Micromanager image acquisition software (Fiji). Paths of individual cells were tracked using the manual tracking plug-in into Image J and tracks analyzed using the Chemotaxis Tool (Ibidi) plug-in into Image J as described (19).

Adhesion Under Laminar Flow

Ibidi $VI^{0.4}$ flow chambers that had been coated with recombinant murine (rm) ICAM-1 (15μg/mL), rmE-selectin (20μg/mL; both Biolegend) and rmCXCL1 (15μg/mL; Biotechne, Minneapolis, MN, USA) were perfused with bone marrow derived neutrophils at 37°C to deliver a constant sheer stress of 1 dyne/cm^2 using a syringe pump (Legato 200; KD Scientific, Holliston, MA, USA) (20). Cell adhesion under flow was recorded by time-lapse imaging (2.5 images/s) for 1 minute at 1, 5, 10 and 15 minutes after starting flow with a x20 phase contract objective using a Leica IRB inverted microscope (Leica, Milton Keynes, UK). Firmly adherent cells were counted using ImageJ.

Reconstitutions

Cohorts of female C57Bl/6 mice were subjected to two doses of irradiation (4.5Gy) 3 hours apart, and reconstituted the next day by tail vein injection of 4 x 10^6 T-cell depleted (CD3ε microbead kit (Militenyi Biotech, Surrey, UK) bone marrow cells from $Ship2^{\Delta/\Delta}$ mice or wild-type littermates. Following irradiation mice were offered enrofloxacin (Bayer, Cambridge, UK) in their drinking water for 4 weeks. Reconstitution of the hematopoietic system in bone marrow chimeras was confirmed by analyzing test bleeds by flow cytometry, comparing ratios of B cells, myeloid cells and neutrophils in chimera to those in wild-type control bloods. Control and $Ship2^{\Delta/\Delta}$ bone marrow cells were equally able to reconstitute irradiated recipients (not shown).

Blood Cell Counts

10-12-week-old control and $Ship2^{\Delta/\Delta}$ littermates were subjected to cardiac puncture under terminal isofluorane anaesthesia with confirmation of death by cervical dislocation. Blood was collected into EDTA-coated vacutainers (Sarstedt, Nümbrecht, Germany). Erythrocyte counts were obtained from an automated Alpha VET cell counter (Nihon Kohden, Surrey, UK); leukocyte markers were labelled and leukocyte numbers obtained by volumetric counting using an Attune NxT flow cytometer (Thermo Fisher).

Models of Acute Sterile Inflammation

To induce thioglycollate peritonitis, mice were intraperitoneally administered 20 ml/kg matured Brewer's thioglycollate (BD Biosciences; Wokingham, UK). LPS-induced acute lung inflammation (ALI) was performed as previously described (20) by administering 1μg *E.coli*-derived LPS (serotype O127: B8, Sigma) in 50μl sterile saline intratracheally. 15 minutes prior to being sacrificed, mice received 3μg PE/Cy7 labelled anti-CD45 in 100μl sterile saline to label all intravascular leukocytes. Lavage cells were labelled with FITC-anti-GR1 and APC-anti-CD11b and analyzed by flow cytometry to calculate total neutrophils numbers ($GR1^{high}$, $CD11b^+$).

Immunoblotting for PI3K Activity

Neutrophils in PBS^{++} were pre-warmed for 5 min at 37°C prior to being stimulated as indicated with fMLF or vehicle for indicated times. Cells were lysed in ice-cold 20mM Tris-HCl pH 7.5, 150mM NaCl, 1mM EDTA, 1mM EGTA, 1% Triton X-100, 2.5mM Na pyrophosphate, 1mM β-glycero-phosphate, 1mM Na orthovanadate, 0.1mM PMSF and 10μg/ml of each antipain, aprotinin, pepstatin A and leupeptin for 5 minutes. Clarified lysates were subjected to SDS-PAGE, and proteins transferred to Immobilon membrane (Merck Millipore, Darmstadt, Germany) and subjected to Western blotting with phosphospecific antibodies directed against PKB as well as a loading control (HSP 90).

PIP3 Measurements

Neutrophils were prepared for PIP3 detection essentially as described (22). Neutrophil aliquots (1 x 10^6 cells in 135 μl) were stimulated with pre-warmed 865 μl fMLF (final concentration 10μM) or vehicle. At specified times 5 ml of ice-cold initial organic mix (CHCL3:MeOH, 1:2 v:v) were added and sampled stored at -80°C until lipid extractions were performed in

the presence of internal standards (d6-C18:0/C20:4-PIP3 (10ng) and –PI(4,5)P2 (100ng)) to correct for any variation in recovery. The analysis of inositol lipids was performed as previously described (22) using a QTRAP 4000 (AB Sciex) mass spectrometer. Data are shown as response ratios, calculated by normalizing the MRM targeted lipid integrated response area to that of a known amount of relevant internal standard. PIP3 response ratios were normalized to PIP2 response ratio to account for any cell input variability.

Immunocytochemistry and Image Acquisition

Neutrophils were allowed to attach onto glass coverslips for 10 minutes prior to being stimulated with fMLP (1 μM final concentration) or vehicle. At indicated times, cells were fixed in 2% paraformaldehyde. $PI(3,4)P_2$ immunostaining was performed essentially as described (23) with 0.5% saponin-permeabilized neutrophils being labelled with a biotin-conjugated primary antibody and streptavidin coupled AF647 as detection reagent. Samples were mounted and 8 images were acquired semi-automatedly using Zen software and a widefield Zeiss Observer with a 20x objective (Zeiss, Oberkochen, Germany); Confocal microscopy was performed using a Leica TCS SP8 microscope with a 60x objective and Lasx image acquisition software. For comparing signal intensities, all settings were kept constant between conditions and experiments.

Image Analysis

Automated image analysis pipelines in CellProfiler (24) were used to determine cell size, brightness and polarization. Briefly, cells were segmented using nuclei (DAPI) and neutrophil-specific GR1 signals. In cells that had been thus identified signal intensity, intensity distribution and cell shape were then measured. Confocal images were processed with FiJi.

Statistical Analysis

Statistical analysis was performed with Graph Pad Prism 8. Where data met the assumptions for parametric tests, two-tailed t-tests, paired t-tests or 2-way ANOVAs with multi-comparison post-hoc tests were performed; otherwise, the non-parametric Mann-Whitney test was applied. For kinetic experiments, the area under the curve was used for analysis. p values < 0.05 were deemed statistically significant.

RESULTS

$Ship2^{\Delta/\Delta}$ mice carry a 57 amino acid deletion in their catalytic domain which renders SHIP2 catalytically dead (16). These mice share their characteristically short faces, small stature and leanness with a previously described SHIP2-deficient mouse (16, 25). We prepared bone marrow derived neutrophils from $Ship2^{\Delta/\Delta}$ mice and matched wild-type controls and compared expression of the PIP3 phosphatases SHIP1, SHIP2 as well as the lipid phosphatase PTEN and the protein kinase PKB (also known as Akt). No differential expression was observed (**Figures 1A–E**). This contrasts with a prior observation in adipose and muscle tissue, where $SHIP2^{\Delta/\Delta}$ protein expression was found to be significantly reduced (16).

Lungs of $Ship2^{\Delta/\Delta}$ Mice Are Not Infiltrated by Leukocytes

$Ship1^{-/-}$ mice were characterized by a substantial increase in circulating myeloid cells in the peripheral blood (8, 9). They developed myeloid cell hyperplasia in the bone marrow and spleen from an early age and developed sterile inflammatory macrophage/neutrophil lung infiltration, which consequently caused >50% to die by only 10 weeks of age (8, 9). In contrast, blood cell counts were not affected in $Ship2^{\Delta/\Delta}$ mice (**Figure 1F**). SHIP2-deficient and $Ship2^{\Delta/\Delta}$ mice survived over 18 months (16, 25). Unchallenged $Ship2^{\Delta/\Delta}$ mice housed in individually ventilated cages in our specific opportunistic pathogen free small animal unit did not display any signs of disease or distress. We used flow cytometry to analyze lung digests from 7-9-month-old mice, noting no obvious immune cell infiltrations in lungs of $Ship2^{\Delta/\Delta}$ mice, nor splenomegaly (**Figure S1**), further supporting the notion that unchallenged $Ship2^{\Delta/\Delta}$ mice are not prone to developing myeloid cell infiltration into their lungs, even at an advancing age.

SHIP2 Regulates *In Vivo* Neutrophil Recruitment to Sites of Inflammation

To determine whether SHIP2 regulates neutrophil recruitment to the lungs upon inflicting an inflammatory challenge, we generated bone marrow chimeras and analyzed neutrophil recruitment in response to LPS-induced acute lung injury (ALI). We recovered a significantly decreased number of $Ship2^{\Delta/\Delta}$ neutrophils compared to wild-type controls from bronchoalveolar lavages (BAL) of these chimeras (**Figure 2A**). In addition to examining BAL fluid, we also determined total lung neutrophil numbers in single cell digests of PBS-perfused lungs by flow cytometry. This identified reduced neutrophil counts in lungs from $Ship2^{\Delta/\Delta}$>wt as opposed to wt>wt bone marrow chimeras (**Figure 2B**). Within the total lung neutrophils, we distinguished between circulating neutrophils that had firmly adhered to the vessel wall or partially transmigrated and those that were truly interstitial by labelling fully or partially intravascular neutrophils with a fluorescently conjugated anti-CD45 antibody delivered intravenously immediately prior to lung perfusion and tissue harvest. We observed fewer interstitial (anti-$CD45^-$) and increased vascular (anti-$CD45^+$) $Ship2^{\Delta/\Delta}$ than wild-type control neutrophils (**Figures 2C, D**).

Neutrophil recruitment can be differentially regulated in a site- and stimulus-specific manner. For this reason, we also analyzed neutrophil recruitment in thioglycollate-induced peritonitis in $Ship2^{\Delta/\Delta}$>wt and wt>wt bone marrow chimeras, again observing a substantial recruitment defect of $Ship2^{\Delta/\Delta}$ neutrophils (**Figure 2E**).

Together, these experiments identified that $Ship2^{\Delta/\Delta}$ neutrophil recruitment to sites of sterile inflammation is impaired, and suggested a reduced ability of $Ship2^{\Delta/\Delta}$ neutrophils to extravasate.

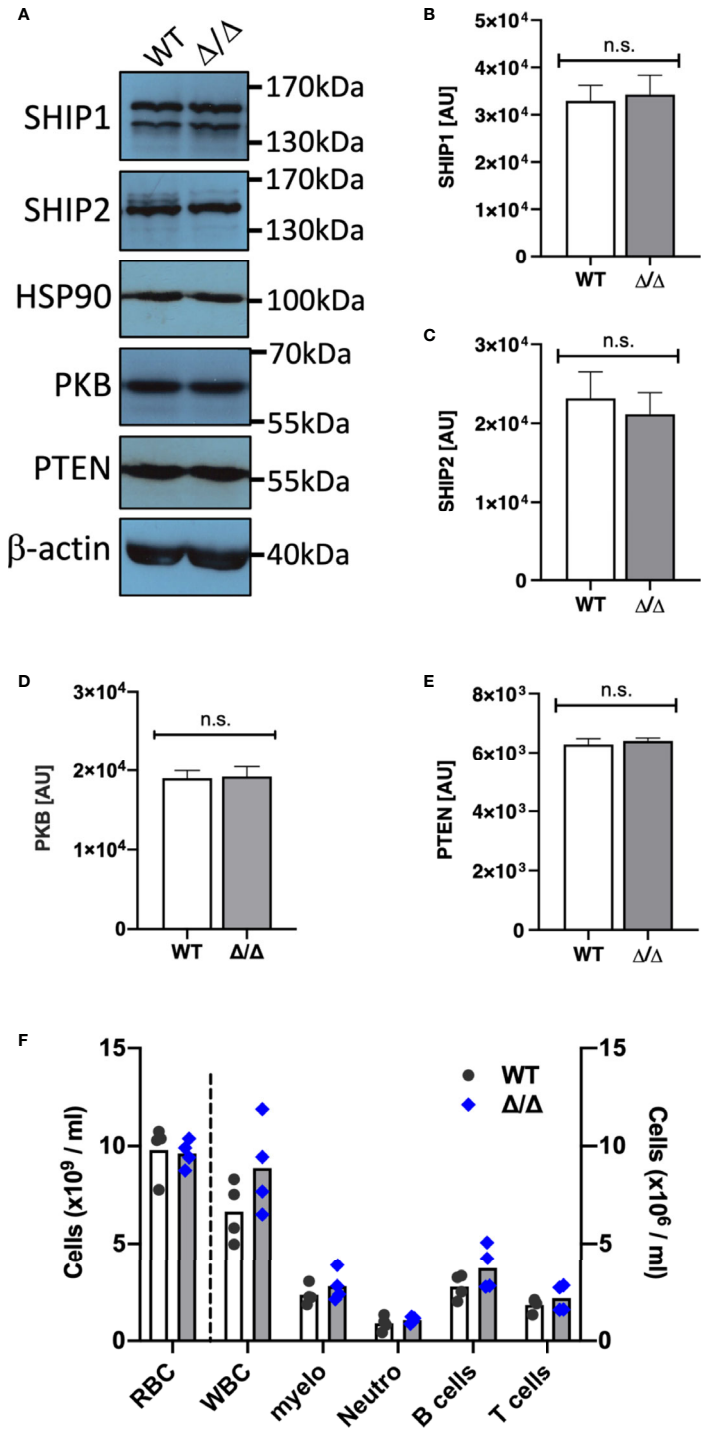

FIGURE 1 | SHIP1/2 and PTEN expression is not affected in Ship2$^{\Delta/\Delta}$ mice. Neutrophils from wild-type (WT) and Ship2$^{\Delta/\Delta}$ (Δ/Δ) mice were tested for SHIP1, SHIP2, PTEN, PKB and loading control (HSP90, β-actin) expression. **(A)** Representative examples and **(B–E)** densitometry of 4 (PTEN, PKB, HSP90) or 5 (SHIP1/2, β-actin) separate experiments performed. Mean ± SEM are presented; AU, arbitrary units. n.s., not significant. **(F)** A comparison of blood cell counts between wild-type and Ship2$^{\Delta/\Delta}$ mice. RBC, red blood cells; WBC, white blood cells; myelo, myeloid cells; neutro, neutrophils. Every symbol represents data obtained from one mouse. *p* values were determined by unpaired two-tailed t tests; differences did not reach significance.

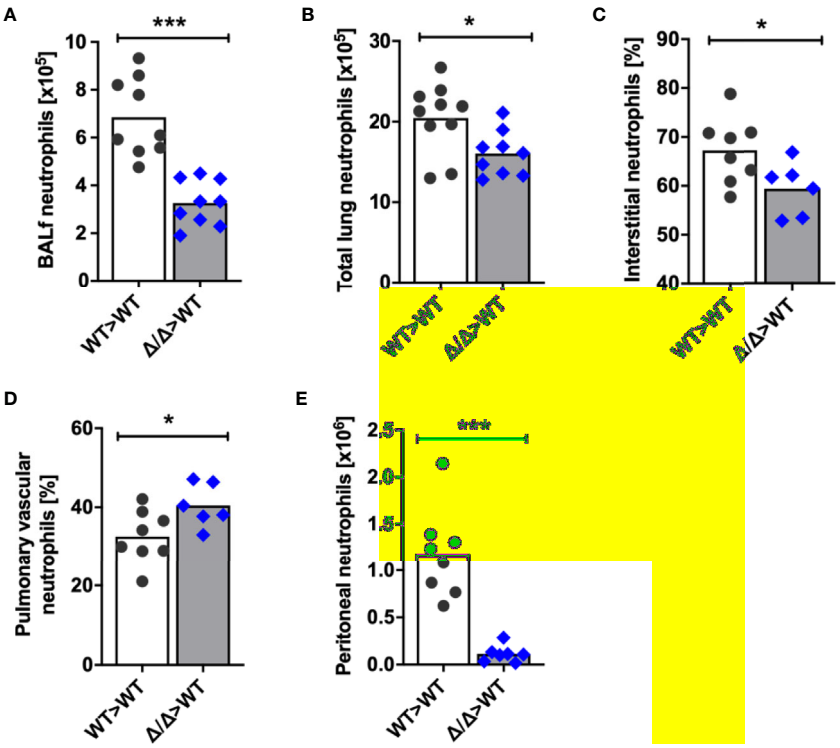

FIGURE 2 | SHIP2 activity is required for neutrophil recruitment to sites of sterile inflammation. **(A–D)** Neutrophil recruitment in acute lung injury (ALI). ALI was induced by administering 1μg LPS in 50μl sterile saline intratracheally into 9 wild-type (WT) and Ship2$^{\Delta/\Delta}$ (Δ/Δ) bone marrow chimeras (generated with 4 bone marrow donors per genotype). Neutrophil numbers retrieved from **(A)** bronchoalveolar lavages and from **(B)** lung digests are plotted. **(C, D)** Chimeras were i.v. administered fluorescently coupled anti-CD45 antibody prior to lavaging of saline-perfused lungs. Single-cell lung digests were then analyzed by flow cytometry. Percentages of **(C)** interstitial CD45 label-negative neutrophils and **(D)** pulmonary intravascular or partially transmigrated CD45 label-positive neutrophils are plotted. **(E)** Neutrophil recruitment in thioglycollate peritonitis. Peritonitis was induced by injecting 20ml/kg thioglycollate-containing broth into 8 wild-type and 7 Ship2$^{\Delta/\Delta}$ bone marrow chimeras; the peritonea were flushed 2.5 hours later. Peritoneal neutrophil numbers are plotted. Experiments were performed on two separate days and results pooled in the graphs shown. Every symbol represents result obtained from one mouse, with means obtained indicated by bars; *p* values were determined by unpaired two-tailed t tests. *$p < 0.05$; ***$p < 0.001$.

SHIP2 Regulates Neutrophil Chemotaxis and Directionality

Given the substantial recruitment defect of Ship2$^{\Delta/\Delta}$ neutrophils *in vivo*, we next examined the involvement of SHIP2 catalytic activity in neutrophil chemotaxis *in vitro*. We allowed wild-type control and Ship2$^{\Delta/\Delta}$ neutrophils to migrate through a linear concentration gradient of fMLF in a 3D collagen matrix. The tracks of individual neutrophils were plotted in spider plots (**Figure 3A**) and parameters of the tracks, including total accumulated and Euclidian distances travelled, velocity and directionality were calculated. This identified that Ship2$^{\Delta/\Delta}$ neutrophils were able to migrate in response to the fMLF stimulation. The Euclidian (i.e. the straight line between the start and end point), but not the total distances covered by Ship2$^{\Delta/\Delta}$ neutrophils were smaller than those of wild-type controls (**Figure 3B**), indicating that directionality, but not the ability to migrate nor the speed of Ship2$^{\Delta/\Delta}$ neutrophils was reduced (**Figures 3C, D**). We concluded that SHIP2 regulates neutrophil chemotaxis.

Migration in a 3D matrix is integrin-independent, whereas migration on glass is dependent upon integrins (17, 26–28). Since SHIP1 regulates integrin-dependent processes including chemotaxis (13, 15), we also analyzed neutrophil chemotaxis in Dunn chambers (29), where neutrophils migrate in a shallow gradient of chemoattractant on a glass bridge (**Figure 3E**). Again, we observed significant chemotaxis defects as indicated by reduced Euclidian distances covered and reduced directionality by Ship2$^{\Delta/\Delta}$ neutrophils compared to controls (**Figures 3F, H**). Interestingly, with Dunn chamber chemotaxis the total accumulated distances travelled and the speed of Ship2$^{\Delta/\Delta}$ neutrophils were also smaller than those of controls (**Figures 3F, G**), suggesting that there may be an additional, integrin-dependent component to the chemotaxis defect conferred by Ship2$^{\Delta/\Delta}$.

In summary, these experiments highlight that SHIP2 is a regulator of neutrophil chemotaxis.

SHIP2 Regulates Firm Adhesion Under Conditions of Flow

To get a better understanding of the extent to which SHIP2 may be required for integrin-dependent neutrophil functions, we next analyzed cell adhesion and spreading. We performed adhesion

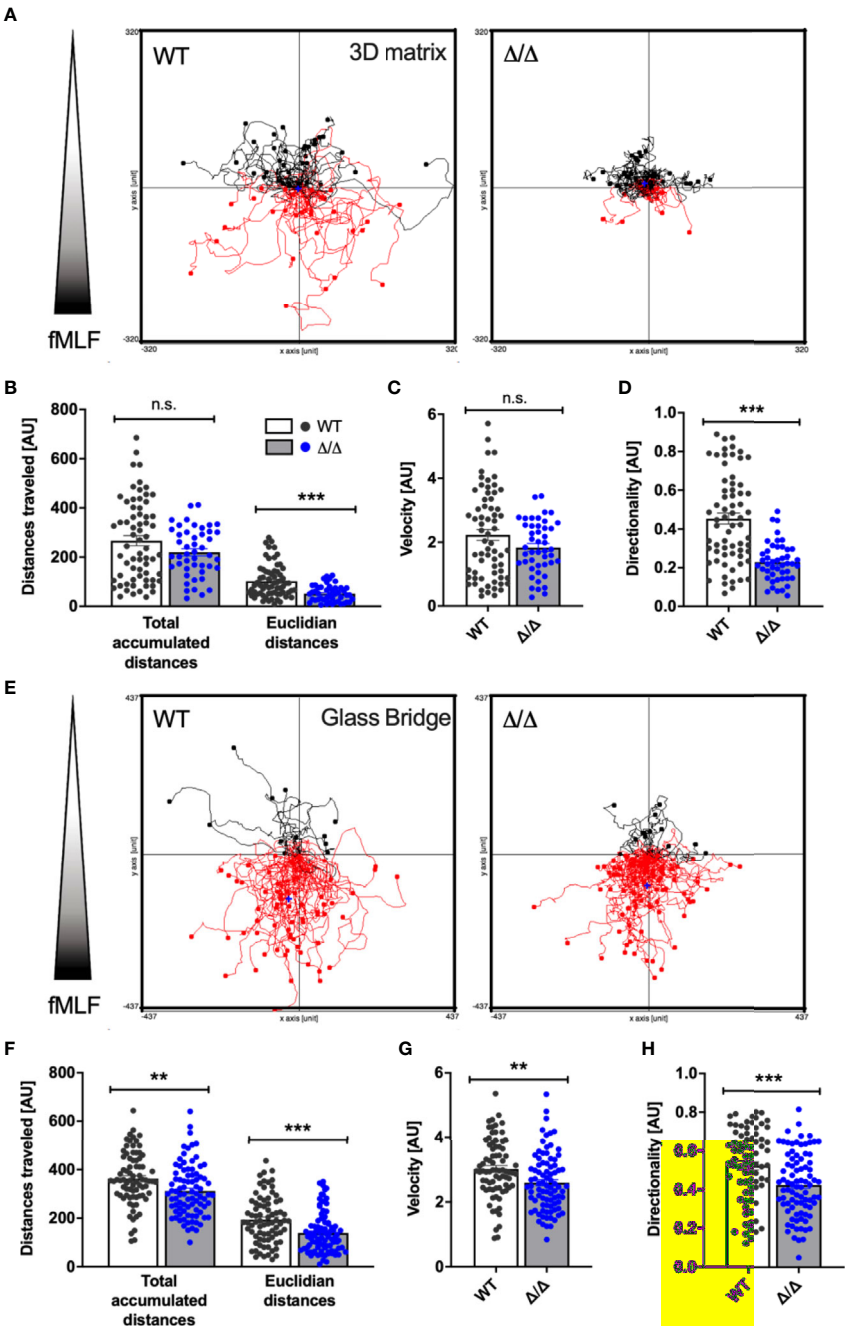

FIGURE 3 | SHIP2 activity is required for chemotactic directionality. Bone marrow-derived wild-type (WT) and Ship2$^{\Delta/\Delta}$ (Δ/Δ) neutrophils were allowed to chemotax towards 300nM fMLF either embedded in a collagen-matrix in Ibidi chemotaxis µ-slides **(A–D)** or in Dunn chemotaxis chambers **(E–H)**. The orientation of the gradient is indicated to the left of spider plots shown in **(A)** and **(E)** Cell migration was recorded by time-lapse imaging, with pooled tracks of individual neutrophils recorded with cells from three separate preparations were plotted as spider plots **(A, E)** and analyzed **(B–D, F–H)** using the Ibidi Chemotaxis tool plug-in into Image J. Accumulated and Euclidean distances **(B, F)**, Velocity **(C, G)** and Directionality **(D, H)** are plotted. *p* values were determined using the Mann-Whitney test. $^{**}p < 0.01$; $^{***}p < 0.001$; n.s., not significant.

assays under static conditions, seeding cells onto glass with or without fMLF stimulation, and measured the area of the fixed, adherent neutrophils. While we did not observe any difference in terms of numbers of cells attached under either condition, the mean area occupied by fMLF-stimulated (but not unstimulated) attached Ship2$^{\Delta/\Delta}$ neutrophils was smaller than that of controls, suggesting a subtle defect in fMLF-induced spreading (**Figure 4A**).

In vivo neutrophils adhere to the vessel wall in the context of blood flow rather than in a static situation. We therefore analyzed neutrophil adhesion of neutrophils to ICAM-1, E-selectin, and CXCL-1 in parallel plate flow chambers. Interestingly and contrasting with the observations in the static adhesion assays, we observed fewer firmly adhering Ship2$^{\Delta/\Delta}$ compared to wild-type control neutrophils (**Figure 4B**). Together these observations suggest that SHIP2 has a subtle regulatory function in neutrophil adhesion and spreading, which becomes more apparent under conditions of flow.

For neutrophils to migrate directionally in a gradient of chemoattractant, they polarize in response to chemoattractant stimulation. To better understand the reason for the observed directionality defect, we compared the abilities of Ship2$^{\Delta/\Delta}$ and wild-type control neutrophils to polarize by analyzing two morphological parameters, compactness and eccentricity in response to uniform fMLF stimulation. According to both parameters, stimulated Ship2$^{\Delta/\Delta}$ neutrophils polarized less efficiently than wild-type controls (**Figures 4D, E**).

SHIP2 Does Not Regulate ROS Production, Degranulation or Phagocytosis

Neutrophils perform a range of effector functions required for killing of pathogens, which include phagocytosis, ROS production and degranulation. We asked whether SHIP2 regulates these functions. Our experiments identified no significant defect in the ability of Ship2$^{\Delta/\Delta}$ neutrophils to phagocytose IgG-opsonized latex beads in terms of the percentage of cells that internalized beads, nor the number of internalized beads (**Figures 5A, B**).

ROS production and degranulation can be induced by stimulating a number of receptors, an effect that can be useful for establishing whether a regulator acts downstream of a particular receptor. We stimulated neutrophils by plating them onto a synthetic multivalent pan-integrin ligand, polyArg-Gly-Lys, which does not depend on co-stimulation of a second receptor (30), and also with fMLF, but did not detect any significant differences in ROS produced, nor lactoferrin

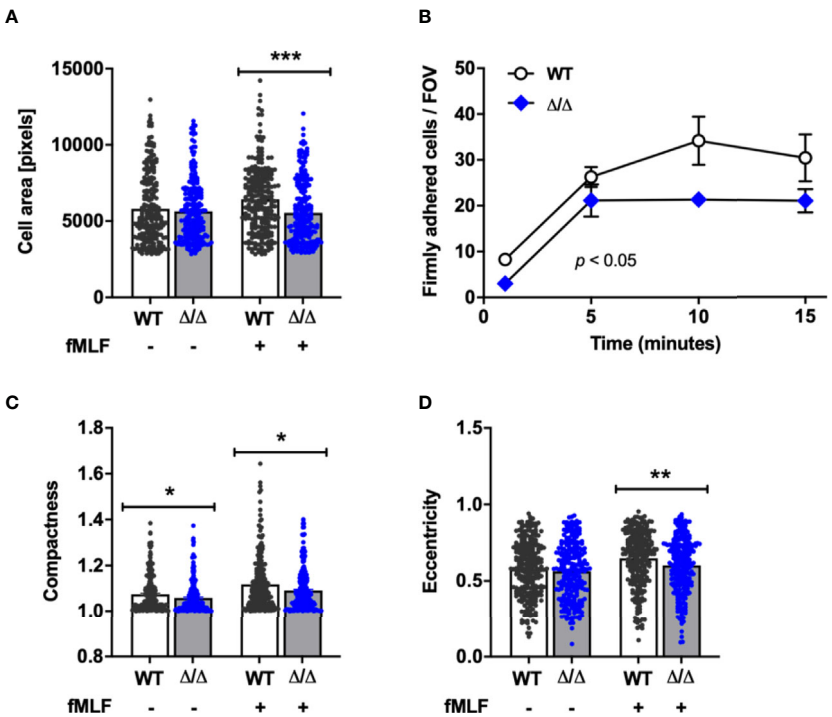

FIGURE 4 | SHIP2 regulates adhesion under flow and chemoattractant induced polarization. Bone marrow derived wild-type (WT) and Ship2$^{\Delta/\Delta}$ (Δ/Δ) neutrophils were prepared and **(A)** plated onto glass coverslips in the presence of absence of 1 μM fMLF for 5 minutes prior to being fixed. The area of GR1-positive cells obtained from 5 separate neutrophil preparations for a total of 240 cells per condition was measured using CellProfiler software. **(B)** Neutrophils were perfused at constant sheer stress through flow chambers coated with ICAM-1, rmE-selectin and rmCXCL1 as detailed in Materials and Methods. The graph shown combined results obtained from a minimum of three separate experiments. **(C, D)** Neutrophils from five separate neutrophil preparations were plated onto glass coverslips in the presence of absence of 1 μM fMLF for 5 minutes prior to being fixed. Compactness **(C)** and eccentricity **(D)** of GR1-positive cells were analyzed by CellProfiler to determine neutrophil polarization according to compactness (**C**; defined as the mean squared distance of the object's pixels from the centroid divided by the area, and where a full circle is attributed a value of 1 and larger values are given to irregular shapes), and eccentricity (**D**; the ratio of the distance between the foci of the ellipse and its major axis length, where 0 is a perfect circle, and 1 represents a straight line). *p* values were determined using the Mann-Whitney test **(A, C, D)** or an unpaired, two-tailed t test of the area under the graphs **(B)**. *$p < 0.05$; **$p < 0.01$; ***$p < 0.001$.

released under any of these conditions (**Figures 5C–G**). Together these results suggest that SHIP2 is not required for the ability of neutrophils to produce ROS or to degranulate in response to stimulation of integrins nor formylated peptide receptors.

SHIP2$^{\Delta/\Delta}$ Has No Major Effect on Agonist-Stimulated PKB Phosphorylation or PIP3 Production

Stimulated and unstimulated neutrophil lysates from SHIP1-deficient mice were characterized by enhanced PKB Thr 308 and Ser 473 phosphorylation attributed to the increased levels of PI (3,4,5)P3 accumulation (9). To test if this holds true for Ship2$^{\Delta/\Delta}$ neutrophils, we carried out Western blots to detect PKB phosphorylation as an indirect measurement of PI3K activity, where it is phosphorylated on Thr 308 by PDK1, a direct effector of PI3K and on Ser 473 indirectly *via* mTORC2 (31–33). We performed an fMLF stimulation timecourse, observing no significant differences in PKB phosphorylation of either residue (**Figures 6A–C**). Having determined an integrin-dependent component with functional assays (**Figures 3** and **4**), we also analyzed PKB phosphorylation upon plating neutrophils onto an integrin ligand (fibrinogen) in the presence or absence of co-stimulation with fMLF, but again observed no significant difference between genotypes (**Figures 6D–F**).

Since PKB can associate with PIP3 or PI(3,4)P2 for phosphorylation (34), analyzing its phosphorylation state may not inform on an altered ratio between PIP3 and PI(3,4)P2. For a direct readout, we therefore repeated the stimulation timecourse, and directly quantified PIP3 in fMLF and mock-stimulated neutrophils using mass spectrometry (35). This revealed that

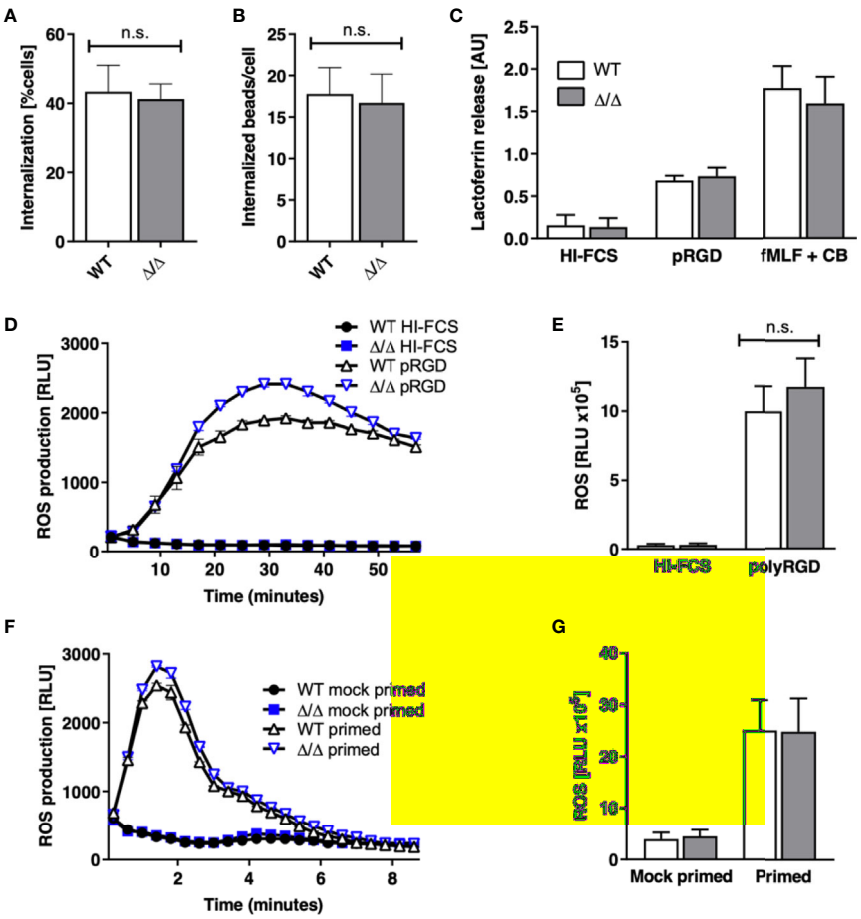

FIGURE 5 | SHIP2 is dispensable for ROS production, degranulation and phagocytosis. Bone marrow derived wild-type (WT) and Ship2$^{\Delta/\Delta}$ (Δ/Δ) neutrophils were assayed for **(A, B)** phagocytosis of rabbit IgG-opsonized latex beads. Results obtained in 5 separate experiments are presented as bar graphs. **(A)** Percentage of cells that had internalized beads; **(B)** average number of beads internalized per cell. **(C)** Degranulation. Cells were stimulated by being plated onto plastic blocked with heat inactivated (HI) FCS or coated with the pan integrin ligand poly-Arg-Gly-Asp (pRGD), or stimulated with fMLF in the presence of cytochalasin B and lactoferrin release was measured by ELISA. Means ± SEM obtained from 4 separate experiments are integrated in this experiment. **(D–G)** ROS production, with neutrophils stimulated by being plated onto integrin ligands **(D, E)** or with the soluble stimulus fMLF **(F, G)**. **(D, F)** Representative experiments and **(E, G)** accumulated light emission (mean ± SEM) from 4 separate experiments are shown. Pairwise comparison between wild-type and Ship2$^{\Delta/\Delta}$ neutrophils were not significant under any of the conditions tested. n.s., not significant.

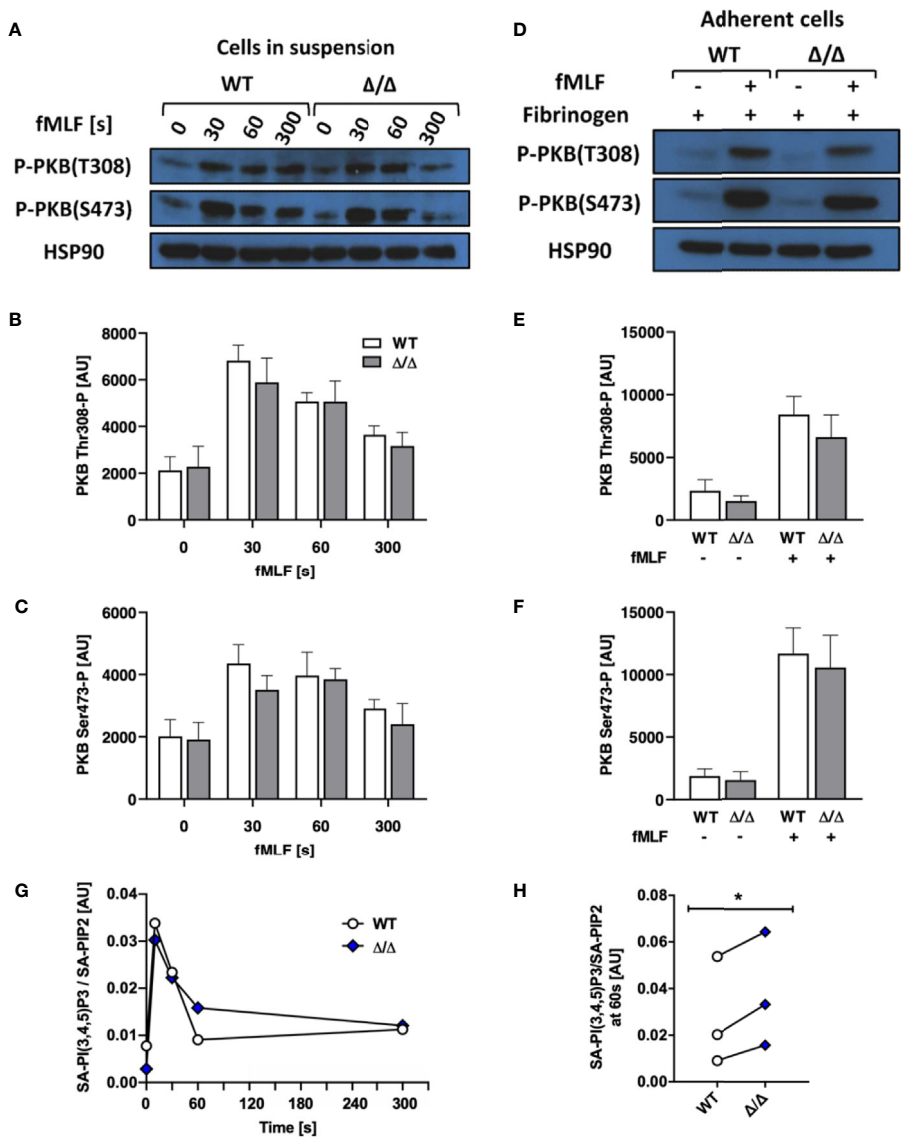

FIGURE 6 | SHIP2$^{\Delta/\Delta}$ has no major effect on agonist-stimulated PKB phosphorylation or PIP3 production. Bone marrow-derived wild-type (WT) and Ship2$^{\Delta/\Delta}$ (Δ/Δ) neutrophils were stimulated and **(A–F)** subjected to analysis of PKB phosphorylation. **(A–C)** Cells in suspension were stimulated with 1 μM fMLF at 37°C for the indicated times or **(D–F)** neutrophils were plated onto 150 μg/mL fibrinogen-coated tissue culture plastic in the presence of absence of 1 μM fMLF at 37°C for 19 minutes and processed for Western blotting. Blots were probed for phospho-PKB Thr 308 and Ser 473 with HSP90 as a loading control. Representative blots are shown **(A, D)** and densitometrical analyses combining 5 **(B, C)** or 4 **(E, F)** separate experiments are plotted (mean ± SEM). **(G, H)** Neutrophils were stimulated with 10 μM fMLF for the indicated times at 37°C, and PIP3 generated was analyzed by mass spectrometry. **(G)** A representative experiment, presenting stearoyl/arachidonyl (SA) PIP3 divided by SA-PIP2. **(H)** At the 60 s timepoint, Ship2$^{\Delta/\Delta}$ neutrophils reproducibly contained subtly increased PIP3. **(G, H)**, Symbols represent individual experiments. Statistical analysis was by 2-way ANOVA with multicomparison post-hoc test **(B, C, E, F)** and a paired t test **(H)**. *$p < 0.05$.

PIP3 in fMLF-stimulated Ship2$^{\Delta/\Delta}$ neutrophils was subtly but significantly increased at one minute after fMLF stimulation compared to wild-type controls (**Figures 6G, H**).

Ship2$^{\Delta/\Delta}$ Neutrophils Contain Less PI(3,4)P2 Than Controls

The functional differences we observed between Ship2$^{\Delta/\Delta}$ and wild-type control neutrophils could be due to the minor change in global PI(3,4,5)P3 that we had observed (**Figure 6H**). Alternatively, it could be due to changes in cellular PI(3,4)P2, a second messenger in its own right. We performed mass spectrometry to measure this minor phosphoinositide species (23), but unfortunately this approach was not sufficiently sensitive to detect changes in PI(3,4)P2 in response to fMLF stimulation even with control mouse neutrophils (data not shown). We therefore resorted to immunofluorescence, making use of a PI(3,4)P2 antibody to analyze this phosphoinositide in adherent neutrophils. We noticed that PI(3,4)P2 predominantly

resided on neutrophil endomembranes, consistent with its function in endocytic processes (36–38). Interestingly, when analyzing fluorescence intensity of control and Ship2$^{\Delta/\Delta}$ neutrophils that had or had not been stimulated with fMLF while being allowed to adhere to glass coverslips, we observed significantly less PI(3,4)P2 signal in Ship2$^{\Delta/\Delta}$ than in wild-type neutrophils under both of these conditions (**Figures 7A, B**). Hence loss of SHIP2 catalytic activity caused reduced cellular PI(3,4)P2 of Ship2$^{\Delta/\Delta}$ neutrophils at least in this context which analyzed adhesion coupled with fMLF stimulation.

DISCUSSION

This study characterized the function of SHIP2 in the neutrophil, analyzing neutrophils isolated, and bone marrow chimeras generated from a mouse carrying a homozygous Ship2$^{\Delta/\Delta}$ that contained a small deletion in the catalytic domain, which rendered SHIP2 catalytically dead. Unlike with Ship2-deficiency, analysis of Ship2$^{\Delta/\Delta}$ neutrophils allowed us to identify neutrophil functions that were dependent on SHIP2 catalytic activity without being confounded by potential scaffold effects, although the major phenotypes of Ship2$^{-/-}$ and Ship2$^{\Delta/\Delta}$ mice were very similar (16, 25). It is possible that compensatory events reduced the severity of the phenotype we observed, and that use of an inducible, rather than a germ-line Cre to generate Ship2$^{\Delta/\Delta}$ mice might have resulted in a more severe phenotype.

Despite these considerations, we identified a clear-cut role for this 5-phosphatase in regulating neutrophil directionality during chemotaxis *in vitro* (**Figure 3**) together with a substantial defect in neutrophil recruitment to sites of sterile inflammation *in vivo* (**Figure 2**). We further observed a defect in firm adhesion under flow with neutrophils that were simultaneously stimulated with immobilized integrin ligand, chemokine and selectin and subtle defects in neutrophil polarization and spreading in response to uniform chemoattractant stimulation (**Figure 4**). In contrast, no significant defects were observed with any other neutrophil functions tested (phagocytosis, degranulation, ROS production; **Figure 5**). Mechanistically, we conclude that the phenotype of Ship2$^{\Delta/\Delta}$ neutrophils is largely due to reduced cellular PI(3,4)P2 (**Figure 7**) rather than globally increased PIP3.

A large body of work has implicated PI3Kγ and δ isoforms in the regulation of neutrophil chemotaxis/chemokinesis *in vitro* and recruitment to inflamed sites *in vivo*, with some later studies suggesting a context-dependent function (4, 5, 39–45). While the 3-phosphatase PTEN appears to have a rather subtle regulatory function in neutrophil chemotaxis (10, 15, 46), neutrophils deficient in the 5-phosphatase SHIP1 are characterized by excessive adhesion and spreading, defects in polarization (when adherent) and chemotaxis *in vitro* as well as hyperactivity in ROS production induced by integrin ligation (13, 15). Our finding of impaired chemotactic directionality caused by loss of SHIP2 catalytic activity complements this and suggests important non-redundant regulatory functions of the two 5-phosphatases in neutrophil chemotaxis and recruitment.

Contrasting with SHIP1-deficient neutrophils, which were characterized by substantially increased PIP3 production (15), there was only a very subtle increase in PIP3 with Ship2$^{\Delta/\Delta}$ neutrophils that had been stimulated for 60s with fMLF (**Figure 6**). Rather we observed substantially reduced intracellular PI(3,4)P2 in cells that were allowed to adhere to glass in the presence and absence of fMLF (**Figure 7**). PI(3,4)P2 at endomembranes has been attributed to Class II PI3K 2a-dependent phosphorylation of PI4P in the context of clathrin-dependent endocytosis (36), but also to 5-dephosphorylation of PIP3 in clathrin-independent endocytic processes, where SHIP2 has been implicated (37, 38, 47). Overall our data suggests distinct

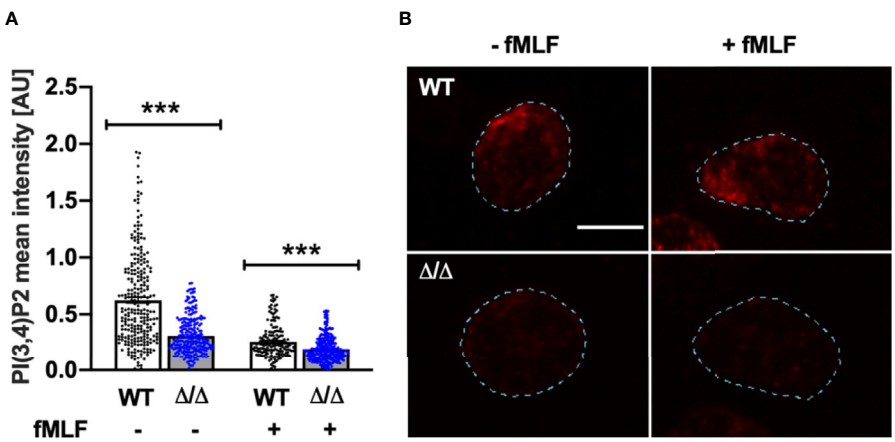

FIGURE 7 | Ship2$^{\Delta/\Delta}$ neutrophils contain less PI(3,4)P2 than controls. Bone marrow-derived wild-type (WT) and Ship2$^{\Delta/\Delta}$ (Δ/Δ) neutrophils were plated onto glass coverslips in the presence or absence of 1 μM fMLF for 5 minutes prior to being fixed and subjected to immunostaining with an anti-PI(3,4)P2 antibody. **(A)** PI(3,4)P2 signal intensity was analyzed automatedly using CellProfiler as detailed in Materials and Methods. The graph presented combines cells from 3 separate experiments for a minimum of 176 cells per condition and data were analyzed with the Mann-Whitney test. ***p <0.001. **(B)** Representative examples of PI(3,4)P2-stained neutrophils for each condition. For ease of viewing, the outline of the cells shown here was traced using FiJi (broken lines). Scale bar, 5 μm.

functions of SHIP1 and SHIP2 in the neutrophil which together control neutrophil chemotaxis and recruitment. Given that variation in housing conditions and microbiota regulate neutrophil production and functions (48) and that discrepancies in experimental conditions can differentially modulate neutrophil activation status, it is possible that a side-by-side comparison of both lines may have unearthed additional features which were missed here.

Still, altogether our work suggests that both SHIP family 5-phosphatases are important regulators of neutrophil functions. Hence SHIP2 specifically regulates chemotactic directionality and neutrophil recruitment to sites of inflammation, while SHIP1 is a regulator of adhesion-dependent neutrophil functions. As our understanding of the wider family of 5-phosphatases grows (49), we will continue to learn how this group of enzymes regulates different facets of neutrophil biology.

DATA AVAILABILITY STATEMENT

The original contributions presented in the study are included in the article/**Supplementary Material**. Further inquiries can be directed to the corresponding author.

ETHICS STATEMENT

The animal study was reviewed and approved by University of Edinburgh Animals Welfare and Ethical Review Body.

AUTHOR CONTRIBUTIONS

MM performed *in vitro* experiments, data analysis, and wrote the paper. BM and UK performed *in vivo* experiments and data analysis. MV helped with image acquisition and analysis. KA performed mass spec and data analysis. SS provided Ship2$^{\Delta/\Delta}$ mice. AA provided resources and supervision. SV conceived the study, performed *in vitro* experiments, data analysis, supervision and wrote the paper. All authors edited and concur with the paper. All authors contributed to the article and approved the submitted version.

FUNDING

MM was funded by a BBSRC iCASE studentship with GSK (BB/R505651/1). BM and SV were funded by the MRC (MR/M023060/1) and UK holds a Versus Arthritis PhD scholarship (21577).

ACKNOWLEDGMENTS

We are indebted to Drs Len Stephens and Phillip Hawkins (The Babraham Institute, Cambridge) for helpful discussions and generously providing resources for the PIP3 measurements by mass spec. We thank Dr Ian Handel (Roslin Institute, University of Edinburgh) for help with statistics and experimental design; we thank Shonna Johnston, Will Ramsey and Mairi Ward for assistance with flow cytometry and members of the Vermeren laboratory for helpful discussions.

SUPPLEMENTARY MATERIAL

The Supplementary Material for this article can be found online at: https://www.frontiersin.org/articles/10.3389/fimmu.2021.671756/full#supplementary-material

REFERENCES

1. Nauseef WM, Borregaard N. Neutrophils at work. *Nat Immunol* (2014) 15 (7):602–11. doi: 10.1038/ni.2921
2. Hawkins PT, Stephens LR. PI3K signalling in inflammation. *Biochim Biophys Acta* (2015) 1851(6):882–97. doi: 10.1016/j.bbalip.2014.12.006
3. Krugmann S, Anderson KE, Ridley SH, Risso N, McGregor A, Coadwell J, et al. Identification of ARAP3, a novel PI3K effector regulating both Arf and Rho GTPases, by selective capture on phosphoinositide affinity matrices. *Mol Cell* (2002) 9(1):95–108. doi: 10.1016/s1097-2765(02)00434-3
4. Gambardella L, Vermeren S. Molecular players in neutrophil chemotaxis–focus on PI3K and small GTPases. *J Leukoc Biol* (2013) 94(4):603–12. doi: 10.1189/jlb.1112564
5. Stephens L, Milne L, Hawkins P. Moving towards a Better Understanding of Chemotaxis. *Curr Biol* (2008) 18(11):R485–94. doi: 10.1016/j.cub.2008.04.048
6. Hawkins PT, Stephens LR. Emerging evidence of signalling roles for PI(3,4)P2 in Class I and II PI3K-regulated pathways. *Biochem Soc Trans* (2016) 44 (1):307–14. doi: 10.1042/bst20150248
7. Cristofano AD, Pesce B, Cordon-Cardo C, Pandolfi PP. Pten is essential for embryonic development and tumour suppression. *Nat Genet* (1998) 19 (4):348–55. doi: 10.1038/1235
8. Helgason CD, Damen JE, Rosten P, Grewal R, Sorensen P, Chappel SM, et al. Targeted disruption of SHIP leads to hemopoietic perturbations, lung pathology, and a shortened life span. *Genes Dev* (1998) 12(11):1610–20. doi: 10.1101/gad.12.11.1610
9. Liu Q, Sasaki T, Kozieradzki I, Wakeham A, Itie A, Dumont DJ, et al. SHIP is a negative regulator of growth factor receptor-mediated PKB/Akt activation and myeloid cell survival. *Genes Dev* (1999) 13(7):786–91. doi: 10.1101/gad.13.7.786
10. Subramanian KK, Jia Y, Zhu D, Simms BT, Jo H, Hattori H, et al. Tumor suppressor PTEN is a physiologic suppressor of chemoattractant-mediated neutrophil functions. *Blood* (2007) 109(9):4028–37. doi: 10.1182/blood-2006-10-055319
11. Li Z, Dong X, Wang Z, Liu W, Deng N, Ding Y, et al. Regulation of PTEN by Rho small GTPases. *Nat Cell Biol* (2005) 7(4):399–404. doi: 10.1038/ncb1236
12. Zhu D, Hattori H, Jo H, Jia Y, Subramanian KK, Loison F, et al. Deactivation of phosphatidylinositol 3,4,5-trisphosphate/Akt signaling mediates neutrophil spontaneous death. *Proc Natl Acad Sci U S A* (2006) 103(40):14836–41. doi: 10.1073/pnas.0605722103
13. Mondal S, Subramanian KK, Sakai J, Bajrami B, Luo HR. Phosphoinositide lipid phosphatase SHIP1 and PTEN coordinate to regulate cell migration and adhesion. *Mol Biol Cell* (2012) 23(7):1219–30. doi: 10.1091/mbc.E11-10-0889
14. Gardai S, Whitlock BB, Helgason C, Ambruso D, Fadok V, Bratton D, et al. Activation of SHIP by NADPH oxidase-stimulated Lyn leads to enhanced apoptosis in neutrophils. *J Biol Chem* (2002) 277(7):5236–46. doi: 10.1074/jbc.M110005200

15. Nishio M, Watanabe K, Sasaki J, Taya C, Takasuga S, Iizuka R, et al. Control of cell polarity and motility by the PtdIns(3,4,5)P3 phosphatase SHIP1. *Nat Cell Biol* (2007) 9(1):36–44. doi: 10.1038/ncb1515
16. Dubois E, Jacoby M, Blockmans M, Pernot E, Schiffmann SN, Foukas LC, et al. Developmental defects and rescue from glucose intolerance of a catalytically-inactive novel Ship2 mutant mouse. *Cell Signal* (2012) 24(11):1971–80. doi: 10.1016/j.cellsig.2012.06.012
17. Gambardella L, Anderson KE, Nussbaum C, Segonds-Pichon A, Margarido T, Norton L, et al. The GTPase-activating protein ARAP3 regulates chemotaxis and adhesion-dependent processes in neutrophils. *Blood* (2011) 118(4):1087–98. doi: 10.1182/blood-2010-10-312959
18. Abdel-Latif D, Steward M, Macdonald DL, Francis GA, Dinauer MC, Lacy P. Rac2 is critical for neutrophil primary granule exocytosis. *Blood* (2004) 104 (3):832–9. doi: 10.1182/blood-2003-07-2624
19. Vermeren S, Miles K, Chu JY, Salter D, Zamoyska R, Gray M. PTPN22 Is a Critical Regulator of Fcγ Receptor–Mediated Neutrophil Activation. *J Immunol* (2016) 197(12):4771-9. doi: 10.4049/jimmunol.1600604
20. McCormick B, Craig HE, Chu JY, Carlin LM, Canel M, Wollweber F, et al. A Negative Feedback Loop Regulates Integrin Inactivation and Promotes Neutrophil Recruitment to Inflammatory Sites. *J Immunol* (2019) 203 (6):1579–88. doi: 10.4049/jimmunol.1900443
21. Wells CM, Ridley AJ. Analysis of cell migration using the Dunn chemotaxis chamber and time-lapse microscopy. *Methods Mol Biol* (2005) 294:31–41. doi: 10.1385/1-59259-860-9:031
22. Rynkiewicz NK, Anderson KE, Suire S, Collins DM, Karanasios E, Vadas O, et al. Gbetagamma is a direct regulator of endogenous p101/p110gamma and p84/p110gamma PI3Kgamma complexes in mouse neutrophils. *Sci Signal* (2020) 13(656):eaaz4003. doi: 10.1126/scisignal.aaz4003
23. Malek M, Kielkowska A, Chessa T, Anderson KE, Barneda D, Pir P, et al. PTEN Regulates PI(3,4)P(2) Signaling Downstream of Class I PI3K. *Mol Cell* (2017) 68(3):566–80.e10. doi: 10.1016/j.molcel.2017.09.024
24. McQuin C, Goodman A, Chernyshev V, Kamentsky L, Cimini BA, Karhohs KW, et al. CellProfiler 3.0: Next-generation image processing for biology. *PloS Biol* (2018) 16(7):e2005970. doi: 10.1371/journal.pbio.2005970
25. Sleeman MW, Wortley KE, Lai K-MV, Gowen LC, Kintner J, Kline WO, et al. Absence of the lipid phosphatase SHIP2 confers resistance to dietary obesity. *Nat Med* (2005) 11(2):199–205. doi: 10.1038/nm1178
26. Lämmermann T, Bader BL, Monkley SJ, Worbs T, Wedlich-Söldner R, Hirsch K, et al. Rapid leukocyte migration by integrin-independent flowing and squeezing. *Nature* (2008) 453(7191):51–5. doi: 10.1038/nature06887
27. Schmalstieg FC, Rudloff HE, Hillman GR, Anderson DC. Two-dimensional and three-dimensional movement of human polymorphonueclear leukocytes: two fundamentally different mechanisms of locomotion. *J Leukoc Biol* (1986) 40(6):677–91. doi: 10.1002/jlb.40.6.677
28. Malawista SE, d. B A. Chevance: Random locomotion and chemotaxis of human blood polymorphonuclear leukocytes (PMN) in the presence of EDTA: PMN in close quarters require neither leukocyte integrins nor external divalent cations. *Proc Natl Acad Sci* (1997) 94(21):11577–82. doi: 10.1073/pnas.94.21.11577
29. Zicha D, Dunn GA, Brown AF. A new direct-viewing chemotaxis chamber. *J Cell Sci* (1991) 99(4):769–75.
30. Mocsai A, Zhou M, Meng F, Tybulewicz VL, Lowell CA. Syk is required for integrin signaling in neutrophils. *Immunity* (2002) 16(4):547–58. doi: 10.1016/s1074-7613(02)00303-5
31. Alessi DR, James SR, Downes CP, Holmes AB, Gaffney PR, Reese CB, et al. Characterization of a 3-phosphoinositide-dependent protein kinase which phosphorylates and activates protein kinase Balpha. *Curr Biol* (1997) 7 (4):261–9. doi: 10.1016/s0960-9822(06)00122-9
32. Stephens L, Anderson K, Stokoe D, Erdjument-Bromage H, Painter GF, Holmes AB, et al. Protein kinase B kinases that mediate phosphatidylinositol 3,4,5-trisphosphate-dependent activation of protein kinase B. *Science* (1998) 279(5351):710–4. doi: 10.1126/science.279.5351.710
33. Sarbassov DD, Guertin DA, Ali SM, Sabatini DM. Phosphorylation and regulation of Akt/PKB by the rictor-mTOR complex. *Science* (2005) 307 (5712):1098–101. doi: 10.1126/science.1106148
34. Ebner M, Lučić I, Leonard TA, Yudushkin I. PI(3,4,5)P(3) Engagement Restricts Akt Activity to Cellular Membranes. *Mol Cell* (2017) 65(3):416–31.e6. doi: 10.1016/j.molcel.2016.12.028
35. Clark J, Anderson KE, Juvin V, Smith TS, Karpe F, Wakelam MJ, et al. Quantification of PtdInsP3 molecular species in cells and tissues by mass spectrometry. *Nat Methods* (2011) 8(3):267–72. doi: 10.1038/nmeth.1564
36. Posor Y, Eichhorn-Gruenig M, Puchkov D, Schöneberg J, Ullrich A, Lampe A, et al. Spatiotemporal control of endocytosis by phosphatidylinositol-3,4-bisphosphate. *Nature* (2013) 499(7457):233–7. doi: 10.1038/nature12360
37. Boucrot E, Ferreira AP, Almeida-Souza L, Debard S, Vallis Y, Howard G, et al. Endophilin marks and controls a clathrin-independent endocytic pathway. *Nature* (2015) 517(7535):460–5. doi: 10.1038/nature14067
38. Maekawa M, Terasaka S, Mochizuki Y, Kawai K, Ikeda Y, Araki N, et al. Sequential breakdown of 3-phosphorylated phosphoinositides is essential for the completion of macropinocytosis. *Proc Natl Acad Sci* (2014) 111(11):E978–87. doi: 10.1073/pnas.1311029111
39. Hirsch E, Katanaev VL, Garlanda C, Azzolino O, Pirola L, Silengo L, et al. Central role for G protein-coupled phosphoinositide 3-kinase gamma in inflammation. *Science* (2000) 287(5455):1049–53. doi: 10.1126/science.287.5455.1049
40. Li Z, Jiang H, Xie W, Zhang Z, Smrcka AV, Wu D. Roles of PLC-beta2 and -beta3 and PI3Kgamma in chemoattractant-mediated signal transduction. *Science* (2000) 287(5455):1046–9. doi: 10.1126/science.287.5455.1046
41. Sasaki T, Irie-Sasaki J, Jones RG, Oliveira-dos-Santos AJ, Stanford WL, Bolon B, et al. Function of PI3Kgamma in thymocyte development, T cell activation, and neutrophil migration. *Science* (2000) 287(5455):1040–6. doi: 10.1126/science.287.5455.1040
42. Ferguson GJ, Milne L, Kulkarni S, Sasaki T, Walker S, Andrews S, et al. PI(3)Kgamma has an important context-dependent role in neutrophil chemokinesis. *Nat Cell Biol* (2007) 9(1):86–91. doi: 10.1038/ncb1517
43. Smith DF, Deem TL, Bruce AC, Reutershan J, Wu D, Ley K. Leukocyte phosphoinositide-3 kinase {gamma} is required for chemokine-induced, sustained adhesion under flow in vivo. *J Leukoc Biol* (2006) 80(6):1491–9. doi: 10.1189/jlb.0306227
44. Sadhu C, Masinovsky B, Dick K, Sowell CG, Staunton DE. Essential Role of Phosphoinositide 3-Kinase δ in Neutrophil Directional Movement. *J Immunol* (2003) 170(5):2647–54. doi: 10.4049/jimmunol.170.5.2647
45. Puri KD, Doggett TA, Huang CY, Douangpanya J, Hayflick JS, Turner M, et al. The role of endothelial PI3Kgamma activity in neutrophil trafficking. *Blood* (2005) 106(1):150–7. doi: 10.1182/blood-2005-01-0023
46. Heit B, Robbins SM, Downey CM, Guan Z, Colarusso P, Miller BJ, et al. PTEN functions to 'prioritize' chemotactic cues and prevent 'distraction' in migrating neutrophils. *Nat Immunol* (2008) 9(7):743–52. doi: 10.1038/ni.1623
47. Chan Wah Hak L, Khan S, Di Meglio I, Law A-L, Lucken-Ardjomande Häsler S, Quintaneiro LM, et al. FBP17 and CIP4 recruit SHIP2 and lamellipodin to prime the plasma membrane for fast endophilin-mediated endocytosis. *Nat Cell Biol* (2018) 20(9):1023–31. doi: 10.1038/s41556-018-0146-8
48. Zhang D, Frenette PS. Cross talk between neutrophils and the microbiota. *Blood* (2019) 133(20):2168–77. doi: 10.1182/blood-2018-11-844555
49. Ramos AR, Ghosh S, Erneux C. The impact of phosphoinositide 5-phosphatases on phosphoinositides in cell function and human disease. *J Lipid Res* (2019) 60(2):276–86. doi: 10.1194/jlr.R087908

Conflict of Interest: AA is employed by GlaxoSmithKline.

The remaining authors declare that the research was conducted in the absence of any commercial or financial relationships that could be construed as a potential conflict of interest.